Characterizing the Roles of Myoregulin and Dwarf Open Reading Frame in Regulating Calcium Homeostasis in Muscle

by

Emma Sara Juracic

A thesis
presented to the University of Waterloo
in fulfillment of the
thesis requirement for the degree of
Doctor of Philosophy
in
Kinesiology

Waterloo, Ontario, Canada, 2024

© Emma Sara Juracic 2024

Examining Committee Membership

The following served on the Examining Committee for this thesis. The decision of the Examining Committee is by majority vote.

External Examiner	Name: Dr. Robert Grange, PhD Title: Professor, Assistant Department Head, Department of Human Nutrition, Foods, and Exercise, Virginia Tech
Supervisor	Name: Dr. A. Russell Tupling, PhD Title: Professor, Chair, Department of Kinesiology, University of Waterloo
Internal Members	Name: Dr. Robin Duncan, PhD Title: Associate Professor, Department of Kinesiology, University of Waterloo
	Name: Dr. Joe Quadrilatero, PhD Title: Associate Professor, Department of Kinesiology, University of Waterloo
Internal-External Member	Name: Dr. David Spafford, PhD Title: Associate Professor, Department of Biology, University of Waterloo

Author's Declaration

I hereby declare that I am the sole author of this thesis. This is a true copy of the thesis, including any required final revisions, as accepted by my examiners.

I understand that my thesis may be made electronically available to the public.

Abstract

The sarco(endo)plasmic reticulum Ca^{2+}-ATPases (SERCAs) are responsible for inducing muscle relaxation and are integral to the maintenance of intracellular calcium (Ca^{2+}) homeostasis. As such, their activity is modulated by multiple regulatory proteins. Two well-characterized regulators of SERCAs are the homologous proteins sarcolipin (SLN) and phospholamban (PLN), which act to reduce the pump's Ca^{2+} affinity/maximal activity. Though PLN and SLN share structural and functional homology, they exhibit distinct and diverse biological roles. It is well established that through their interaction with the SERCA pumps, both proteins are key regulators of muscle contraction/relaxation and both confer protection to the pump under times of cellular stress. However, SLN but not PLN, increases the amount of energy required by SERCA pumps, making SLN a key modulator of skeletal muscle energy metabolism, and protective against diet-induced obesity. Moreover, SLN plays a critical role in activating calcium signaling pathways that control adaptations in muscle mass and fiber type under conditions of muscle overload, disuse and disease. Myoregulin (MLN) and dwarf open reading frame (DWORF) are newly discovered protein regulators of SERCAs that share extensive sequence homology with SLN and PLN, and physically interact with the pump to regulate Ca^{2+}-handling in muscle. Our understanding of these new regulators is still in its infancy. MLN has been shown to exert an inhibitory role similar to that of PLN and SLN by lowering SERCA Ca^{2+} affinity. Meanwhile, DWORF has been shown to act as a positive regulator of the pump both by removing the inhibition incurred by SLN, PLN and MLN and by directly stimulating SERCA Ca^{2+} affinity and/or maximal activity.

While MLN and DWORF have emerged as key regulators of Ca^{2+} homeostasis and muscle contractility, it is unknown whether MLN and DWORF share similar roles to PLN and SLN and/or offer their own distinct and diverse physiological roles. It is well established that SERCAs are

highly susceptible to damage and inactivation by high levels of oxidative stress and that their function is commonly impaired under conditions of muscle overload, disuse and disease. Thus, it is imperative to determine whether MLN and DWORF can protect the SERCA pumps from cellular stress. Furthermore, SLN's ability to uncouple SERCA Ca^{2+} transport from ATP hydrolysis, and in doing so, alter SERCAs' Ca^{2+} transport efficiency, is a vital mechanism underlying energy metabolism in skeletal muscle. Investigating whether MLN and DWORF can also contribute to muscle based adaptive thermogenesis by altering SERCA efficiency could offer new avenues for investigating whole body and muscle based metabolism. Finally, these four regulatory proteins appear to share overlap in their expression patterns, therefore, understanding whether the expression pattern of these two newly discovered proteins is altered by the absence of SLN and/or PLN would offer valuable insight into governance of intracellular Ca^{2+} homeostasis. To that end, the primary objectives for this thesis were to: 1) investigate whether the interaction between MLN:SERCA and DWORF:SERCA can protect the pump from damage during times of cellular stress, such as the thermal instability caused by heat shock; 2) determine whether MLN and/or DWORF were able to alter SERCA Ca^{2+} pumping efficiency; and 3) examine the potential compensatory changes in expression by evaluating MLN and DWORF gene and protein expression in *Sln*$^{-/-}$, *Pln*$^{-/-}$, and *Sln*$^{-/-}$/*Pln*$^{-/-}$ mice.

To address the first objective, HEK-293 cells were transfected for cDNA encoding SERCA1a or SERCA2a alone (20 ug) and co-transfected for cDNA encoding SERCA1a or SERCA2a (10 ug) at a molar ratio of 1:1 to those encoding MLN or DWORF (10 ug) with a total plasmid DNA of 20 µg. To induce heat stress (HS), prior to harvesting half of the cells from the groups were exposed to 40°C for one hour (HS) while the other half of the cells remained incubated at 37°C to be used as controls (CTL). Effects of HS on Ca^{2+}-dependent SERCA activity was

evaluated on crude cell homogenate over Ca^{2+} concentrations ranging from *p*Ca 6.85 to 4.80 in the presence of the Ca^{2+} ionophore A23187 using a Ca^{2+}-dependent, enzyme-linked spectrophotometric plate reader assay. Furthermore, effects of HS on the oxidation and nitrosylation of the SERCA protein were determined by western blotting on crude cell homogenate to assess oxidation by measuring protein carbonyls and nitrosylation by measuring nitrotyrosine formation. HS treatment of cells transfected with SERCA1a and SERCA2a alone significantly reduced maximal activity of both isoforms ($p < 0.05$) and resulted in stark elevations in both oxidation ($p < 0.05$) and nitrosylation ($p < 0.05$) of the pumps compared to CTL. In contrast, exposure of cells co-transfected with SERCA1a and MLN or DWORF and cells co-transfected with SERCA2a and MLN or DWORF to HS maintained maximal activity at levels resembling that of CTL ($p > 0.05$) and prevented SERCA oxidation ($p > 0.05$) and nitrosylation ($p > 0.05$), again keeping levels comparable to CTL. The results of this thesis are indicative of MLN and DWORF stabilizing SERCA structure and function during cellular stress by preserving maximal pump activity of both SERCA isoforms while minimizing oxidation and nitrosylation of the pump in the face of HS.

To investigate the second objective, HEK-293 cells were transfected for cDNA encoding SERCA1a or SERCA2a alone (20 ug) and co-transfected for cDNA encoding SERCA1a or SERCA2a (10 ug) at a molar ratio of 1:1 to those encoding MLN or DWORF (10 ug) with a total plasmid DNA of 20 µg. Both Ca^{2+} uptake and Ca^{2+}-ATPase activity were measured on crude cell homogenate prepared from the transfected cells. Ca^{2+}-dependent SERCA activity was assessed over Ca^{2+} concentrations ranging from pCa 6.85 to 4.80 in presence and absence of the Ca^{2+} ionophore A23187 using a spectrophotometric plate reader assay. SERCA-mediated Ca^{2+} uptake was measured in the presence and absence of the precipitating anion, oxalate, using the fluorescent

dye Indo-1 and spectrofluorometric plate reader assay. SERCA coupling ratio was calculated by dividing Ca^{2+} uptake by Ca^{2+}-ATPase rates across different pCa values. The ionophore ratio was determined at each pCa to provides an additional way of assessing SERCA efficiency and was calculated by dividing SERCA activity measured in the presence of the ionophore by SERCA activity measured in the absence of the ionophore. In both the presence ($p < 0.05$) and absence of ionophore ($p < 0.05$), MLN significantly depressed the maximal rate of ATP consumption (V_{max}) and SERCA's Ca^{2+} affinity. Moreover, in both the presence ($p < 0.05$) and absence of oxalate ($p < 0.05$), MLN was shown to reduce SERCA Ca^{2+} uptake. However, MLN did not affect the Ca^{2+}/ATP coupling ratio of SERCA1a and SERCA2a pumps at maximal (presence of ionophore/oxalate) and physiological (absence of ionophore/oxalate) conditions. Nor did MLN alter the ionophore ratio at each pCa. Thus, MLN does not have a bearing on SERCA pumping efficiency and is unlikely to contribute to muscle based energy expenditure.

When examined in both the presence ($p > 0.05$) and absence ($p > 0.05$) of a Ca^{2+} gradient, DWORF had no bearing on the apparent affinity of SERCA1a and SERCA2a for Ca^{2+}, no effect on maximal SERCA activity, no impact on the rate of SERCA-mediated Ca^{2+} uptake and did not alter the apparent coupling ratio or ionophore ratio, as no difference was observed between cells transfected with SERCA1a alone and those co-transfected with SERCA1a and DWORF or for cells transfected with SERCA2a alone and those co-transfected with SERCA2a and DWORF for any of these measures. Furthermore, no significant differences in Ca^{2+} affinity and maximal activity were observed in cells that were transfected with either SERCA isoform alone or co-transfected with DWORF (1:3) in either maximal ($p > 0.05$) or physiological ($p > 0.05$) conditions. Interestingly, DWORF was shown to increase SERCA apparent affinity for Ca^{2+}, maximal SERCA activity and the rate of SERCA-mediated Ca^{2+} uptake in both the presence ($p < 0.05$) and absence

($p < 0.05$) of a Ca^{2+} gradient in cells co-transfected with SERCA1a or SERCA2a and DWORF at a molar ratio of 1:5. However, despite the activation of SERCA observed with a five-fold overexpression of DWORF, the apparent coupling ratio and ionophore ratio remained unaltered, therefore indicating that DWORF does not influence SERCA pumping efficiency.

Lastly, to evaluate the third objective, western blotting was performed on soleus, left ventricle and atrial muscle isolated from 4-6-month-old male and female wild type mice and compared to single knockout ($Sln^{-/-}$ and $Pln^{-/-}$) mice and double knockout ($Sln^{-/-}/Pln^{-/-}$) mice to examine if ablation of one or two SERCA regulatory protein(s) would result in compensatory changes in the expression of other SERCA regulatory proteins. In the $Pln^{-/-}$ genotype, no change in MLN or DWORF protein expression was detected with the ablation of PLN in both soleus ($p > 0.05$) and left ventricle ($p > 0.05$) muscle in either male nor female mice. Likewise, the $Sln^{-/-}$ genotype revealed no change in MLN or DWORF protein expression in the absence of SLN in both soleus ($p > 0.05$) and atrial ($p > 0.05$) muscle in either sex. Similarly, in the $Sln^{-/-}/Pln^{-/-}$ model, the results for both proteins in both sexes matched what was observed in the single knockout models, as the ablation of both SLN and PLN did not result in any significant changes in the expression of MLN and DWORF ($p > 0.05$). To compliment the protein expression analysis, real-time PCR (qPCR) was performed on SOL and LV muscles from the same WT and knockout male and female mice to investigate potential changes in *Mln* and *Dworf* gene expression in the presence and absence of *Sln* and *Pln* expression individually and dual ablation. Gene expression of *Mln* was only altered in left ventricle tissue of female DKO, showing an elevation relative to WT ($p < 0.05$). The change in gene expression was generally unaltered in skeletal muscle tissue, with only soleus of male $Sln^{-/-}$ mice showing a significant elevation in *Dworf* expression ($p < 0.05$). In contrast, cardiac tissue exhibited a more complicated story: left ventricle tissue of male and female $Pln^{-/-}$

mice showed either a trending increase ($p > 0.05$) or significant increase ($p < 0.05$), respectively. Similarly, atria of *Sln*$^{-/-}$ male mice exhibited a trending increase in *Dworf* expression ($p > 0.05$), whereas, atria of *Sln*$^{-/-}$ female mice exhibited a significant decrease ($p < 0.05$). Finally, left ventricle and atrial tissue of both male and female *Sln*$^{-/-}$/*Pln*$^{-/-}$ mice displayed a significant decline in *Dworf* expression ($p < 0.05$).

Overall, this thesis has revealed that i) similar to SLN and PLN, MLN and DWORF stabilize SERCA structure and function during cellular stress; ii) like PLN, MLN negatively regulates SERCA kinetics without altering transport efficiency; iii) unlike any other known regulator, DWORF positively modulates the pump by enhancing SERCA apparent Ca^{2+} affinity, maximal activity and the rate of Ca^{2+} uptake without changing SERCA pumping efficiency; and iv) under basal conditions, the protein expression levels of MLN and DWORF are not altered by the presence/absence of either PLN and SLN alone or the presence/absence of both PLN and SLN together.

Acknowledgements

Thank you to my supervisor, Dr. Russ Tupling, for taking a chance on me. Russ, you have helped shape me into the scientist I am today, and have made me a better person in the process. When asked about my future, my answer is and always will be: "I want to be Russ when I grow up". From your love of science and the way it comes through in a five-minute conversation or a fifty-minute lecture to the way that you run your lab and inspire your students. I have had the privilege of being part of a very special lab in a very special department. Thank you for your unwavering support, guidance and immense patience. Thank you for easing my anxieties and telling me that it will all work out (especially when I didn't want to hear it) because it always did. I hope to inspire others the way you have inspired me.

Thank you to the members of my thesis committee, Dr. Robin Duncan, Dr. Joe Quadrilatero, Dr. David Spafford, and Dr. Robert Grange for your helpful insights and interesting discussions on my thesis research. A special thank you to Dr. Robin Duncan, who has served on every committee and as a reference for every scholarship since I started graduate school, eight years ago.

Thank you to Dr. Anthony Gramolini and Allen Teng for providing the PEI transfection solution and transfection protocol. A special thank you to Allen for his willingness to hop on a call and help me through the problems that arose as I was troubleshooting Studies I and II.

Thank you to Dr. Val Fajardo and Jessica Braun for letting me run my uptake analysis at Brock. In all honesty, even if I could have run it at UW, I still would have made the trek to Brock for the beers and conversation!

Thank you to Mai Harris, Adi Brahmbhatt, Michelle Tomczewski and John Chan for all of your hard work on this thesis.

Thank you to Dr. Eric Bombardier for continuing to mentor me despite moving on from the department. Eric, you were one of the main reasons I wanted to do a PhD and your mentorship and guidance were driving factors in me staying to do one at UW. I am beyond grateful that I could still count on you despite our working relationship ending too soon.

To my friends, both in and out of grad school, who at this point have become more like family, I am so very, very grateful for you. It feels like it all ended too early and I was too worried about finishing this thesis to really appreciate all of the time we had together. The coffee runs, the conversations on the 4th floor, the shifts at CIF, the nights at 44A. I wish I could sit back and watch a montage of it now that we've all moved on. You kept me going when I thought I couldn't.

Thank you Kevin, for being cool as a cucumber. The last two years of my PhD have been tumultuous and starting my PDF while still wrapping up my thesis has been difficult, but you just have this ability to put me at ease and lighten the mood. No matter what is happening, I just can't help but be happy when I'm around you. Thank you for making me smile so big and so much that my cheeks hurt. I cannot begin to tell you how much your love and support has meant to me.

If Chris Stapleton's "Millionaire" was written about familial love, it would be about my little family. Mama and Tata, I've spent a long time thinking about what I will write here and even now, there is nothing I can say that will adequately express the magnitude of my gratitude for everything that you've done for Emanuel, Borna and me. All I have ever wanted to do is to make you proud and honor the sacrifices that you've made for us. I hope that the work I have done here, to obtain this PhD, is everything you had hoped for when you brought us to Canada. Emanuel and Borna, thank you for your support, but more than anything, thank you for the comedic relief. I'm sad to say I have not found a cure (nor was I ever looking for one).

In the words of Snoop Dogg, "Last but not least, I want to thank me. I want to thank me for believing in me. I want to thank me for doing all this hard work. I want to thank me for never quitting". Thank you, 2018 Emma, for being naïve enough to pursue a doctorate, for having your head in the clouds and dreaming big. Thank you, 2021-2023 Emma, for your resilience, thank you for showing up when it was the last thing you wanted to do, thank you for not giving up when it would have been the easier option.

Dedication

This thesis is dedicated to my mother, Marina Juracic.

"Gde ja stadoh - ti ćeš poći
Što ne mogoh - ti ćeš moći
Kud ja nisam - ti ćeš doći
Što ja počeh - ti produži"

"From where I stopped – you will continue
What I couldn't do – you will
Where I couldn't go – you will
What I started – you will continue"

Table of Contents

Examining Committee Membership ii

Author's Declaration iii

Abstract iv

Acknowledgments x

Dedication xii

List of Figures xvi

List of Tables xx

List of Abbreviations xxi

Chapter 1 – Review of the Literature and Statement of the Problem 1

1.0 Introduction 2

1.1 Excitation-Contraction Coupling in Skeletal Muscle 5

1.2 The Structure and Function of the SERCA Protein 8

1.3.1 Phospholamban Structure and Interaction with SERCA 15

1.3.2 Phospholamban Protects the SERCA Pump from Cellular Stress 17

1.3.3 Phospholamban Expression Profile and Role in Cardiac Muscle 18

1.3.4 Characterization of Phospholamban in Skeletal Muscle (Muscle Metabolism, SERCA Protection and SERCA Superinhibition) 19

1.4.1 Comparison of Sarcolipin and Phospholamban Structure: Similarities and Differences 24

1.4.2 Mechanism of Interaction between Sarcolipin and SERCA 27

1.4.3 Expression Profile of Sarcolipin 29

1.4.4 Sarcolipin's Role in Adaptive Muscle Remodeling 31

1.4.5 Sarcolipin's Role in Conditions of Muscle Disease, Disuse and Injury 33

1.4.6 Sarcolipin Uncouples the SERCA pump to Drive Adaptive Thermogenesis 35

1.4.7 Sarcolipin Protects the SERCA Pump from Cellular Stress 37

1.5 The Emergence of New SERCA Regulatory Proteins 39

1.5.1 Myoregulin Discovery and Comparison of Structure Relative to Sarcolipin and Phospholamban 39

1.5.2 Expression Pattern of Myoregulin 41

1.5.3 Myoregulin's Interaction with SERCA 42

1.5.4 Dwarf Open Reading Frame Discovery and Comparison of Structure Relative to Sarcolipin and Phospholamban 43

1.5.5 Dwarf Open Reading Frame Directly Activates the SERCA Pump and the Discrepancies Underlying the Mechanism of this 44
1.5.6 Relationship between Dwarf Open Reading Frame and Phospholamban 47
1.5.7 Role of Dwarf Open Reading Frame in Cardiac Muscle 48
1.5.8 Role of Dwarf Open Reading Frame in Skeletal Muscle 49
1.5.9 Summary of Literature and Gaps Therein 50
1.6 Statement of the Problem 54

Chapter 2 – Methodology 55
2.1 Culture and Co-transfection of HEK-293 Cells 56
2.2 Preparation of Cell Homogenate 57
2.3.1 Ca^{2+} Dependent Ca^{2+}- ATPase Activity 57
2.3.2 Ca^{2+} Dependent Ca^{2+}- Uptake Activity 59
2.4.1 Carbonyl Formation in SERCA1/2a 60
2.4.2 Nitrotyrosine Levels in SERCA1/2a 61
2.5.1 Crude Cell Homogenate Western Blot Analysis 62
2.5.2 Mouse Muscle Homogenate Western Blot Analysis 63
2.6.1 *Pln*$^{-/-}$ Line 64
2.6.2 *Sln*$^{-/-}$ Line 65
2.6.3 *Pln*$^{-/-}$/*Sln*$^{-/-}$ Line 66
2.7 Tissue Collection 66
2.8 RNA Extraction, Reverse Transcription (RT) and Real-Time (q) PCR 67
2.9 Statistical Analyses 68

Chapter 3 – Thesis Study I: Investigating if the interaction between MLN:SERCA and DWORF:SERCA Can Protect the SERCA pump from Oxidative/Thermal Damage 69
3.1 Study Objectives and Hypotheses 70
3.2 Study Design 72
3.3.1 SERCA Isoform and Regulator Transfection Verification 73
3.3.2 MLN Preserves SERCA Function and Prevents Carbonylation/Nitrosylation following Heat Stress 75
3.3.3 DWORF Obstructs SERCA Carbonylation/Nitrosylation following Heat Stress to Maintain SERCA Function 80
3.4 Discussion 85
3.5 Conclusion 93

Chapter 4 – Thesis Study II: Assessing if MLN and/or DWORF Can Alter the SERCA Coupling Ratio 94
4.1 Study Objectives and Hypotheses 95

4.2 Study Design 97
4.3.1 MLN is Not an Uncoupler of SERCA Ca^{2+} Transport and ATP Hydrolysis 98
4.3.2 DWORF Does Not Uncouple of SERCA Ca^{2+} Transport from ATP Hydrolysis 106
4.3.3 DWORF is a Direct Activator of SERCA but Does Not Alter SERCA Efficiency 111
4.4 Discussion 119
4.5 Conclusion 127

Chapter 5 – Thesis Study III: Assessing Potential Compensatory Changes in SERCA Regulatory Expression 128
5.1 Study Objectives and Hypotheses 129
5.2 Study Design 130
5.3.1 MLN and DWORF protein expression is not altered by the absence of PLN while *Dworf* mRNA expression shows differences with PLN ablation 131
5.3.2. Ablation of SLN does not affect MLN and DWORF protein content but does alter mRNA expression 137
5.3.3. Knock-Out of both PLN and SLN had no bearing on MLN and DWORF protein content but did alter mRNA expression 142
5.4 Discussion 147
5.5 Conclusions 154

Chapter Six – Thesis Summary, Integrated Discussion, and Future Perspectives 155
6.1 Thesis Summary 157
6.2 Integrated Discussion & Future Directions 164

References 169

Appendix A 179

Appendix B 185

List of Figures

Chapter 1

Fig. 1.0.1: Gene Sequence Homology of SERCA Regulatory Proteins

Fig. 1.2.1: Representative Figure of SERCA-mediated Ca^{2+} Transport

Fig. 1.2.2: Representation of the Alternate Reactions Occurring During SERCA-Mediated Ca^{2+} Transport

Fig. 1.3.4.1: Visual Summary of the Physiological Role of PLN in Muscle

Fig. 1.4.1.1: PLN & SLN Domain Comparison Summary

Fig. 1.4.7.1: Visual Summary of the Different Roles Exerted by the Interaction between SLN and SERCA

Chapter 3

Fig. 3.2.1: Schematic of Study Design for Thesis Study I.

Fig. 3.3.1.1: SERCA Isoform and Regulator Transfection Verification.

Fig 3.3.2.1: MLN Preserves SERCA1a Function and Prevents SERCA1a Oxidation & Nitrosylation following Heat Stress.

Fig 3.3.2.2: MLN Protects SERCA2a Function and Impedes Oxidation & Nitrosylation following Heat Stress.

Fig 3.3.3.1: DWORF Prevents Oxidation & Nitrosylation following Heat Stress to Conserve SERCA1a Maximal Activity.

Fig 3.3.3.2. DWORF Protects SERCA2a Function and Impedes Oxidation & Nitrosylation following Heat Stress.

Chapter 4

Fig. 4.2.1: Schematic of Study Design for Thesis Study II.

Fig. 4.3.1.1: MLN lowered SERCA1a V_{max} and reduced the rate of Ca^{2+} uptake but did not alter Ca^{2+} pumping efficiency under Physiological Conditions.

Fig. 4.3.1.2: MLN lowered SERCA1a V_{max} and reduced the rate of Ca^{2+} uptake but did not alter Ca^{2+} pumping efficiency under Maximal Conditions.

Fig. 4.3.1.3: Ionophore ratios of cells transfected with S1a and co-transfected with S1a and MLN.

Fig. 4.3.1.4: SERCA1a and MLN protein expression in HEK-293 crude homogenate.

Fig. 4.3.1.5: MLN lowered SERCA2a V_{max} and reduced the rate of Ca^{2+} uptake but did not alter Ca^{2+} pumping efficiency under Physiological Conditions.

Fig. 4.3.1.6: MLN lowered SERCA2a V_{max} and reduced the rate of Ca^{2+} uptake but did not alter Ca^{2+} pumping efficiency under Maximal Conditions.

Fig. 4.3.1.7: Ionophore ratios of cells transfected with S2a and co-transfected with S2a and MLN.

Fig. 4.3.1.8: SERCA2a and MLN protein expression in HEK-293 crude homogenate.

Fig. 4.3.2.1: DWORF did not alter SERCA1a kinetics or Ca^{2+} pumping efficiency under Physiological Conditions.

Fig. 4.3.2.2: DWORF did not alter SERCA1a kinetics or Ca^{2+} pumping efficiency under Maximal Conditions.

Fig. 4.3.2.3: Ionophore ratios of cells transfected with S1a and co-transfected with S1a and DWORF.

Fig. 4.3.2.4: SERCA1a and DWORF protein expression in HEK-293 crude homogenate.

Fig. 4.3.2.5: DWORF did not alter SERCA2a kinetics or Ca^{2+} pumping efficiency under Physiological Conditions.

Fig. 4.3.2.6: DWORF did not alter SERCA2a kinetics or Ca^{2+} pumping efficiency under Maximal Conditions.

Fig. 4.3.2.7: Ionophore ratios of cells transfected with S1a and co-transfected with S1a and DWORF.

Fig. 4.3.2.8: SERCA2a and DWORF protein expression in HEK-293 crude homogenate.

Fig. 4.3.3.1: DWORF did not alter SERCA1a kinetics under Physiological nor Maximal Conditions.

Fig. 4.3.3.2: DWORF did not alter SERCA2a kinetics under Physiological nor Maximal Conditions.

Fig. 4.3.3.3: DWORF directly activated SERCA1a but did not alter Ca^{2+} pumping efficiency under Physiological Conditions.

Fig. 4.3.3.4: DWORF directly activated SERCA1a but did not alter Ca^{2+} pumping efficiency under Maximal Conditions.

Fig. 4.3.3.5: Ionophore ratios of cells transfected with S1a and co-transfected with S1a and DWORF (1:5).

Fig. 4.3.3.6: DWORF directly activated SERCA2a but did not alter Ca^{2+} pumping efficiency under Physiological Conditions.

Fig. 4.3.3.7: DWORF directly activated SERCA1a but did not alter Ca^{2+} pumping efficiency under Maximal Conditions.

Fig. 4.3.3.8: Ionophore ratios of cells transfected with S2a and co-transfected with S2a and DWORF (1:5).

Fig. 4.3.3.9: SERCA1a/2a and DWORF protein expression in HEK-293 crude homogenate.

Chapter 5

Fig. 5.2.1: Schematic of Study Design for Thesis Study III.

Fig. 5.3.1.1: MLN and DWORF protein expression in $Pln^{+/+}$ and $Pln^{-/-}$ male mice.

Fig. 5.3.1.2: MLN and DWORF protein expression in $Pln^{+/+}$ and $Pln^{-/-}$ female mice.

Fig. 5.3.1.3: *Mln* and *Dworf* mRNA expression in $Pln^{+/+}$ and $Pln^{-/-}$ male mice.

Fig. 5.3.1.4: *Mln* and *Dworf* mRNA expression in $Pln^{+/+}$ and $Pln^{-/-}$ female mice.

Fig. 5.3.2.1: MLN and DWORF protein expression in $Sln^{+/+}$ and $Sln^{-/-}$ male mice.

Fig. 5.3.2.2: MLN and DWORF protein expression in $Sln^{+/+}$ and $Sln^{-/-}$ female mice.

Fig. 5.3.2.3: *Mln* and *Dworf* mRNA expression in $Sln^{+/+}$ and $Sln^{-/-}$ male mice.

Fig. 5.3.2.4: *Mln* and *Dworf* mRNA expression in $Sln^{+/+}$ and $Sln^{-/-}$ female mice.

Fig. 5.3.3.1: MLN and DWORF protein expression in $Sln^{+/+}/Pln^{+/+}$ and $Sln^{-/-}/Pln^{-/-}$ male mice.

Fig. 5.3.3.2: MLN and DWORF protein expression in $Sln^{+/+}/Pln^{+/+}$ and $Sln^{-/-}/Pln^{-/-}$ female mice.

Fig. 5.3.3.3: *Mln* and *Dworf* mRNA expression in $Sln^{+/+}/Pln^{+/+}$ and $Sln^{-/-}/Pln^{-/-}$ male mice.

Fig. 5.3.3.4: *Mln* and *Dworf* mRNA expression in $Sln^{+/+}/Pln^{+/+}$ and $Sln^{-/-}/Pln^{-/-}$ female mice.

Chapter 6

Fig. 6.1.1: Visual Summary of the Physiological Role of MLN in Muscle

Fig. 6.1.2: Visual Summary of the Physiological Role of DWORF in Muscle

Appendix B

Fig. B.1: DWORF protein expression is reduced in soleus of Pln^{OE} male mice.

Fig. B.2: Strain differences in SLN expression in murine soleus.

Fig. B.3: Tissue distribution of MLN protein content in $Sln^{+/+}/Pln^{+/+}$ male mice.

Fig. B.4: Tissue distribution of DWORF protein content in $Sln^{+/+}/Pln^{+/+}$ male mice.

List of Tables

Chapter 3

Table 3.3.2.1. Maximal SERCA activity (V_{Max}; μmol/g prot/ min) of cells transfected with SERCA alone and of cells co-transfected with MLN (n = 3/group) measured either under CTL (37°C) or HS (40°C) conditions.

Table 3.3.3.1. Maximal SERCA activity (V_{Max}; μmol/g prot/ min) of cells transfected with SERCA alone and of cells co-transfected with DWORF (n = 3/group) measured either under CTL (37°C) or HS (40°C) conditions.

Chapter 4

Table 4.3.1.1. Ca^{2+} affinity (i.e. pCa_{50}: pCa at half maximal ATPase activity) of cells transfected with SERCA alone and of cells co-transfected with MLN (n = 3/group) measured in the presence (i.e. maximal conditions) and absence (i.e. physiological conditions) of the Ca^{2+}-specific ionophore A23187.

Table 4.3.3.1. Ca^{2+} affinity (i.e. pCa_{50}: pCa at half maximal ATPase activity) of cells transfected with SERCA alone and of cells co-transfected with DWORF (n = 3/group) measured in the presence (i.e. maximal conditions) and absence (i.e. physiological conditions) of the Ca^{2+}-specific ionophore A23187.

Chapter 6

Table 6.1.1: Summary of key findings and novel contributions

Appendix A

Table A.1: Upregulation of SLN expression across different models of skeletal muscle disease, disuse, and injury.

Table A.2: Comparison of Key Parameters in Studies Evaluating the Interaction of SERCA with DWORF and its Effect

Table A.3: *Mln* and *Dworf* primer sequences for qPCR analysis

Table A.4. Primer sequences for genotyping of wild-type (WT) phospholamban (PLN), sarcolipin (SLN), or corresponding targeted knock-out sequences.

Table A.5. Western blotting details. Samples were transferred to either polyvinylidene difluoride (PVDF) or nitrocellulose (NC) membranes. Antibody incubations occurred at room temperature (RT) or overnight (ON).

List of Abbreviations

ADP - Adenosine diphosphate
ALN - Another-regulin
ATP – Adenosine triphosphate
Ca^{2+} - Calcium
$[Ca^{2+}]_i$ - Intracellular Ca^{2+} concentration
$[Ca^{2+}]_f$ - Free Ca^{2+} concentration
CaMK – Ca^{2+}/calmodulin-dependent protein kinase
Cn – Calcineurin
CNM – Centronuclear myopathy
DGC - Dystroglycan complex
DHPR - Dihydropyridine receptors
DKO – Sarcolipin/Phospholamban double knock-out mice
DMD - Duchenne muscular dystrophy
DWORF – Dwarf Open Reading Frame
Dworf$^{-/-}$ - Dwarf open reading frame deficient mice
ECC - Excitation-contraction coupling
EDL - Extensor digitors longus
ELN – Endoregulin
FRET - Fluorescence resonance energy transfer
GFP – Green fluorescent protein
HEK-293 – Human embryonic kidney 293 cells
HFD – High-fat diet
HS – Heat Shock
HSP70 - Heat shock protein 70
K_{ca} – SERCA apparent affinity for calcium
KO – Knock-out
LV – Left ventricle
mdx - Murine model of Duchenne muscular dystrophy
MHC – Myosin heavy chain
Mg^{2+} - Magnesium
MLN – Myoregulin
Mln$^{-/-}$ - Myoregulin deficient mice
NFAT - Nuclear factor of activated T-cells
NKA - Na^+/K^+-ATPase
pCa - $-\log_{10}([Ca^{2+}]_f)$
pCa_{50} - Ca^{2+} affinity; pCa value at half maximal ATPase activity
PKA – Protein kinase A
PLN – Phospholamban
Pln$^{-/-}$ - Phospholamban deficient mice
Pln^{OE} - Phospholamban overexpressing mice
PMSF - phenylmethylsulfonyl fluoride buffer
ROS - Reactive oxygen species
RNS - Reactive nitrogen species
RyR - Ryanodine receptor

SERCA - Sarco(endo)plasmic reticulum Ca^{2+}-ATPase
SLN – Sarcolipin
Sln$^{-/-}$ - Sarcolipin deficient mice
Sln^{OE} - Sarcolipin overexpressing mice
SOL - Soleus
SR - Sarco(endo)plasmic reticulum
TM - transmembrane
V_{max} - Maximum velocity
WT – wild-type

CHAPTER 1

Review of the Literature and Statement of the Problem

1.0 Introduction

The physiological role of the interactions between the sarco(endo)plasmic reticulum Ca^{2+} - ATPase (SERCA) and its two best known regulators, phospholamban (PLN) and sarcolipin (SLN), have been extensively investigated and well understood. The regulatory function exerted by SLN allows for the uncoupling of energy consumption (ATP hydrolysis) from Ca^{2+} transport, thus enabling a "futile Ca^{2+} - cycling mechanism" to occur. This mechanism has been implicated in the ability of skeletal muscle to contribute to whole body metabolism and energy expenditure and has served as an avenue to investigate obesity and type II diabetes [1-5]. Apart from exerting a direct effect on the SERCA pump, SLN has been shown to participate in the NFAT-calcineurin-utrophin signalling cascade. In this regard, SLN mediates the ability of the muscle fibre to respond to intracellular Ca^{2+} - signalling and promote oxidative fibre characteristics or aid in skeletal muscle regeneration following injury [6-8]. Though SLN and PLN share considerable gene sequence homology, the regulatory function of PLN differs from that of SLN, particularly in cardiac muscle where the PLN protein is crucial to normal contractile function [9, 10]. PLN modulates SERCA function by impairing access of Ca^{2+} ions to their Ca^{2+} binding site on the SERCA protein. In doing so, PLN assists to maintain basal intracellular Ca^{2+} concentrations while protecting the Ca^{2+} binding site from physiological stressors such as reactive oxygen/nitrogen species (ROS/RNS) [11]. This protective role of PLN proves to be very important in the context of skeletal muscle myopathies in which the SERCA protein is highly susceptible to oxidative damage. Recently, a myriad of new SERCA regulatory proteins have been discovered in both muscle and nonmuscle cell types [12, 13]. The muscle cell type proteins include myoregulin (MLN) and dwarf open reading frame (DWORF), whereas the nonmuscle proteins have been identified as endoregulin (ELN) and another-regulin (ALN). The discovery of these proteins was

facilitated by the level of gene sequence conservation and homology between these proteins and PLN/SLN, the "original" SERCA regulatory proteins [12, 13]. The murine sequence alignment is visualized below in Figure 1 with emphasis placed on the residues in the transmembrane domain that are shared between each protein; those highlighted in blue represent identically conserved residues with those in green representing weakly similar residues.

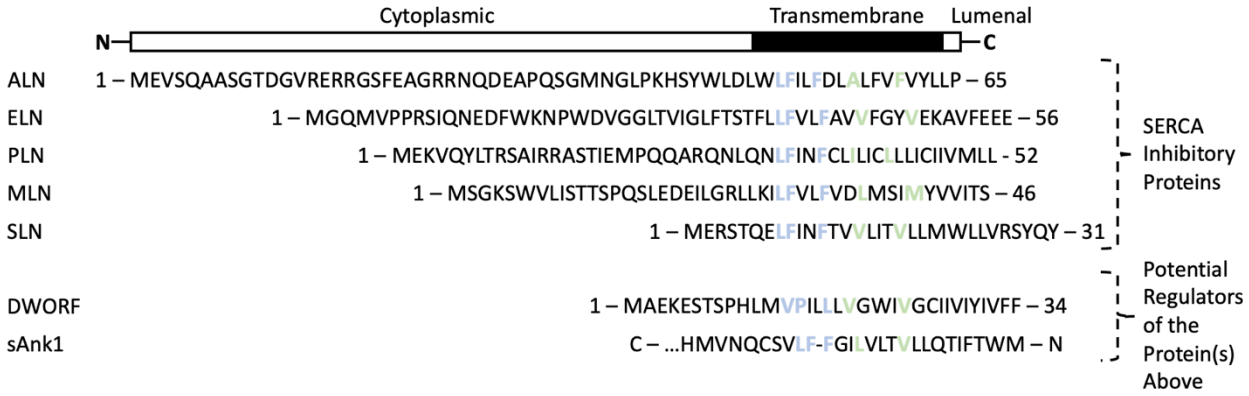


Fig. 1.0.1: Gene Sequence Homology of SERCA Regulatory Proteins.
The SERCA regulatory proteins share significant sequence homology in their transmembrane region which allows these proteins to interact with the SERCA pump and exert their inhibitory effect. Adapted from Anderson, DM. et al (2017). Widespread control of calcium signaling by a family of SERCA-inhibiting micropeptides. Sci Signal.; 9(457): ra119.doi:10.1126/scisignal.aaj1460.

Investigations into the physiological role of these proteins has focused primarily on MLN and DWORF and since our group focuses exclusively on SERCA regulation in skeletal and cardiac muscle, these are the proteins that will be examined in the remainder of this document. Briefly, MLN mRNA expression has been identified in all skeletal muscle, with the greatest degree of expression present in glycolytic muscle fibres, such as the quadriceps, plantaris and gastrocnemius. GFP fluorescence and confocal microscopy have revealed that the MLN protein co-localizes primarily with the SERCA1a isoform, where it appears to exert an inhibitory effect similar to that of PLN and SLN as directly determined via a Ca^{2+} dependent Ca^{2+} - ATPase assay in HEK293 co-expressing both SERCA and MLN [12, 13]. On the other hand, DWORF protein expression has

been identified solely in the heart (specifically the left ventricle) and oxidative muscle fibres such as the soleus. Contrary to the proteins discussed to this point, DWORF was orginially discovered to act on SERCA to enhance function as opposed to repressing it and to do so by displacing SLN, PLN and MLN from the pump. In this regard, the DWORF protein *itself* would not directly improve SERCA function but would exert a regulatory role by modulating the effect of the inhibitory proteins interacting directly with SERCA [12, 13]. However, subsequent studies have revealed a potential role of DWORF in directly activating the pump, either by acting on SERCA's affinity for Ca^{2+} or the pump's maximal activity. The advent of these newly discovered proteins offers much potential to further our understanding of skeletal muscle excitation-contraction and the factors governing intracellular Ca^{2+} homeostasis. The questions pertinent here revolve around three fundamental questions:

1) Can the interaction between MLN:SERCA and DWORF:SERCA protect the pump from damage during times of cellular stress,

2) Are MLN and/or DWORF able to alter SERCA Ca^{2+} pumping efficiency;

3) Is there potential redundancy in SERCA regulation by evaluating MLN and DWORF protein expression and interaction in *Sln*$^{-/-}$, *Pln*$^{-/-}$, and *Sln*$^{-/-}$/*Pln*$^{-/-}$ mice.

The resolution of these questions will be the main objective of this thesis.

1.1 Excitation-Contraction Coupling in Skeletal Muscle

Calcium (Ca^{2+}) is regarded as a universal intracellular messenger that is essential for nearly all aspects of cell life [14-16]. Conceptually, its action is relatively simple: at basal levels, the intracellular Ca^{2+} concentration ($[Ca^{2+}]_i$) is maintained below 100 nM, however, a rise in this concentration to 1000 nM (or greater) triggers cellular activation through the induction of numerous second messenger pathways [14, 15]. The maintenance of a low resting $[Ca^{2+}]$ is critical to normal cell function, and as such, Ca^{2+} levels are tightly controlled [16]. In skeletal muscle specifically, this regulation is achieved primarily by the SR, as well as, by key contributions from sarcolemmal proteins, cytoplasmic buffers and mitochondria [17-19]. The SR is an intracellular tubular network, that while analogous to the endoplasmic reticulum, functions as the dynamic Ca^{2+} regulator in muscle and serves to provide automatic feedback control for altering and maintaining both cytosolic and luminal $[Ca^{2+}]$ [17-19]. It accomplishes this through the collective effort of three major classes of Ca^{2+} - regulating proteins: luminal calcium binding proteins (calsequestrin), Ca^{2+} - release channels (ryanodine receptor; RyR), and the SERCA Ca^{2+} - reuptake pumps [17-19].

With the SR being so intrinsically tied to Ca^{2+} homeostasis, it comes as no surprise that it is pivotal in the induction of both muscle contraction, otherwise known as excitation-contraction coupling (ECC), and muscle relaxation [20]. The sequence of events that initiate skeletal muscle contraction begin with an action potential propagating along the plasma membrane, and depolarizing the transverse-tubule system, where the electrical stimulus is detected by the dihydropyridine receptors (DHPRs) and converted to a chemical one through an allosteric interaction with RyR, that triggers the release of Ca^{2+} [21]. The transient elevation in $[Ca^{2+}]_i$ binds to troponin C, causing a conformational change that removes the inhibitory action of tropomyosin

and enables the formation of cross bridges between actin and myosin in order to generate force [21]. Subsequently, muscle relaxation is elicited by the active transport of Ca^{2+} from the cytosol to the SR lumen by SERCA, in order to restore the luminal SR Ca^{2+} stores for ensuing contractions and to return cytosolic $[Ca^{2+}]_i$ to basal levels [21]. SERCA activity is not limited to SR re-filling. The SERCA pumps are additionally vital in maintaining resting $[Ca^{2+}]_i$ under basal conditions by counteracting passive Ca^{2+} leak either through RyR or the pumps themselves, thus keeping a tight control of Ca^{2+} levels.

The molecular diversity of these Ca^{2+} - regulatory proteins govern basal $[Ca^{2+}]_i$, as well as, contraction and relaxation properties of different muscle fibre types [22, 23]. Slow twitch muscle fibres (fibres expressing slow or type I myosin) exhibit higher resting $[Ca^{2+}]_i$ compared to fast twitch fibres (fibres expressing fast or type II myosin) [24-26]. Additionally, this is accompanied by complete saturation of the luminal SR Ca^{2+} store, whereas, fast twitch fibre SR content is only 35% of its capacity at basal levels [24]. This is directly related to the variable density of protein expression between fibre types. Fast twitch muscle fibres express 3-5-fold greater DHPR and RyR content, thus facilitating an accelerated Ca^{2+} release [22, 24, 27]. Moreover, these fibres exhibit a 5-7-fold greater density of SERCA, which ensures faster and more efficient Ca^{2+} clearance [24, 28]. Lastly, fast twitch fibres express increased calsequestrin content that enables a greater luminal SR Ca^{2+} capacity [24, 28, 29]. Consequentially, the Ca^{2+} transient in fast twitch muscle fibres is greater and shorter compared to slow twitch fibres and this results in faster contraction kinetics and greater force production [24]. These characteristics not only highlight the differences in muscle fibre composition, but the diverse effects that could be imposed by the dysregulation of Ca^{2+} - handling proteins.

The concerted action of multiple Ca^{2+} - regulating proteins required for the maintenance of skeletal muscle Ca^{2+} homeostasis necessitates varying degrees of ATP consumption and individual contribution to energy expenditure. For instance, in the process isometric contraction, the contributions of the myosin ATPase, SERCA, and Na+/K+-ATPase are estimated to range from ~65-80%, 10-25%, and 5-10% towards ATP consumption, respectively (18). Even at resting conditions, SERCA remains active in an effort to maintain $[Ca^{2+}]_i$ as the pumps counteract the natural leak of Ca^{2+} that occurs through RyRs and the SERCA pumps themselves. Discussed in further detail in the section below, our group has highlighted SERCA's significant contribution to maintaining resting $[Ca^{2+}]_i$ in skeletal muscle and has established SERCA as a control point for energy balance regulation. While the processes of muscle contraction, relaxation, and resetting of ion gradients inevitably dictate skeletal muscle energy metabolism, mounting evidence indicates that the energy consumed by SERCA is a dynamically regulated process which can be modulated by the interaction between SERCA and its regulatory proteins.

1.2 The Structure and Function of the SERCA Protein

SERCAs are 110-kDa integral membrane transporter proteins embedded within the SR that consist of a single polypeptide chain which arranges into the transmembrane and cytosolic regions [30]. The transmembrane region is composed of 10 α-helices (M1-M10) of differing lengths and properties, in which SERCA's two Ca^{2+} binding sites reside within helices M2, M4, M6 and M9 [30, 31]. Crystal structure analysis has demonstrated that these two Ca^{2+} binding sites are located adjacent to each other and near the cytoplasmic surface of the lipid layer. In fact, the Ca^{2+} binding sites are only accessible from the cytoplasmic side of the SR, thus prohibiting the binding of luminal Ca^{2+} [18, 32]. The transmembrane region is connected to the large cytosolic headpiece, consisting of three domains: the ATP or nucleotide binding domain; the phosphorylation domain which is phosphorylated by the γ-phosphate of ATP at a conserved aspartate residue; and the actuator domain which is integral to the de-phosphorylation event, as assisted by a conserved glutamate [30, 31]. Phosphorylation of the SERCA protein, due to binding of ATP, induces a conformational change of the transmembrane helices that transfers bound Ca^{2+} from the cytoplasm to the SR lumen [18]. SERCA belongs to the P-type ATPase (P-ATPase) superfamily of ion transporters due to its α-helical structure, its ability to catalyze ATP and its ability to undergo a reversible conformational shift between two states, denoted E_1 and E_2 [18, 33]. The SERCA family itself is encoded by the *ATP2A1-3* genes which are located on 3 different chromosomes and code for the expression of SERCA1, SERCA2 and SERCA3 isoforms respectively, with further isoform diversity occurring through alternative splicing [33]. These isoforms are highly conserved, retaining 75% structural homology despite differences in species-specific and muscle-specific expression [33]. The SERCA isoform variants of particular interest in muscle health and disease are SERCA1a and SERCA2a. SERCA1a is the primary isoform in adult fast-twitch skeletal muscle

and has been demonstrated to have a vital role in skeletal muscle development [33]. In contrast, SERCA2a is predominantly expressed in cardiac muscle and slow-twitch skeletal muscle [33]. Additional SERCA isoform variants include SERCA2b, which is expressed at low levels in all tissues, and SERCA3, which is expressed in numerous non-muscle tissues [18].

SERCAs use the free energy released from the hydrolysis of ATP to transport Ca^{2+} ions from the cytosol into the lumen of the SR; and as such, are major regulators of $[Ca^{2+}]_i$ [34]. As visualized in the schematic below, SERCA – mediated Ca^{2+} transport necessitates multiple steps and conformational changes to the pump [18]. Transport begins with the SERCA pump in its E_1 conformational state and the binding of Ca^{2+} to its high-affinity sites on the cytoplasmic face of the transmembrane domain [35]. The binding of cytosolic Ca^{2+} to its designated site induces the autophosphorylation of Asp351 (an amino acid residue located within SERCA's phosphorylation domain) by ATP [36]. In doing so, this elicits the formation of a high-energy phospho-protein intermediate [37] (Figure 2; reactions 1-2). With this change in phosphorylative state, SERCAs transition into their low-energy phospho-protein E_2 state, in which the two Ca^{2+} binding sites face the SR lumen and exhibit reduced Ca^{2+} affinity. This encourages the dissociation of Ca^{2+} ions from the pump causing them to enter the SR lumen [37] (Figure 2; reaction 3-4). Departure of the two Ca^{2+} ions initiates the exchange of the inorganic phosphate contained on Asp351 for H_2O and with this, SERCAs transition back to their E_1 state [37], completing the catalytic cycle (Figure 2; reactions 5-6). Under optimal conditions, the pump can transport two molecules of Ca^{2+} at the expense of one ATP molecule [18, 34]. However, this ratio is subject to change depending on a number of factors including: $[Ca^{2+}]_i$, ATP level, pH, ADP and inorganic phosphate level. These factors can have an influence on SERCA Ca^{2+} affinity, ATP binding and subsequent hydrolysis, phosphorylation of the pump, and the return of the pump to the E_1 conformation. Each of these

factors listed above cause the process of SERCA-mediated Ca^{2+} transport to become less energetically efficient and this can modulate both muscle and whole body metabolism.

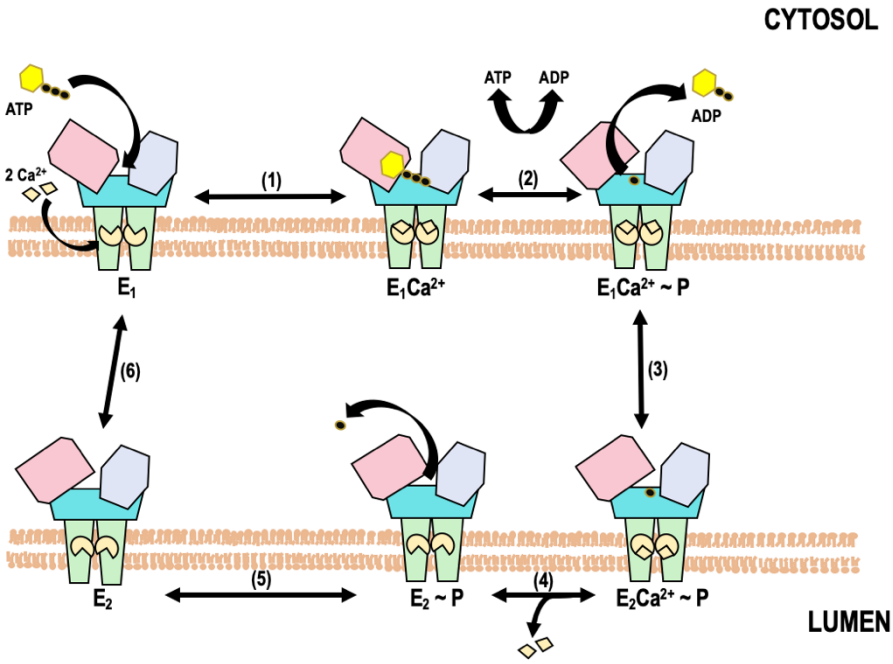


Fig. 1.2.1: Representative Figure of SERCA-mediated Ca^{2+} Transport
Schematic representation of the catalytic cycle of SERCA as it transports Ca^{2+} from the cytosol to the lumen of the sarcoplasmic reticulum and the conformational changes that enable it to do so (reactions 1-6). Briefly, transport begins with the SERCA pump in its E_1 conformational state with ATP bound to the ATP binding site in the nucleotide binding domain and the binding of Ca^{2+} to its high-affinity sites on the cytoplasmic face of the transmembrane domain. Occupation of these sites induces ATP hydrolysis and this triggers SERCA phosphorylation and a change in conformation to the E_2 state. This state exhibits reduced Ca^{2+} affinity and thus Ca^{2+} dissociates from the pump and enters the SR lumen. Under optimal conditions, the pump can transport two molecules of Ca^{2+} at the expense of one ATP molecule. Adapted from Gamu, D., et al (2020). The Sarcoplasmic Reticulum and SERCA: A Nexus for Muscular Adaptive Thermogenesis**.** Appl Physiol Nutr Metab. 45(1):1-10. doi: 10.1139/apnm-2019-0067.

The alternate reactions that allow for SERCA to exhibit such a significant influence on energy metabolism are represented in red in Figure 3 below and warrant further elaboration. Under conditions of high luminal $[Ca^{2+}]_f$ (which can occur during rest or relaxation), Ca^{2+} ions are capable of binding to their designated sites on the E_2 conformation of the pump, or if already bound, are capable of remaining bound to the E_2 conformational state. Consequently, as the SERCA pumps transition to their E_1 conformation, these ions are translocated back into the

cytosol. In this situation, Ca^{2+} transport and ATP synthesis are uncoupled, as the expulsion of luminal Ca^{2+} ions takes place without the concomitant synthesis of ATP. This is referred to as uncoupled Ca^{2+} efflux or passive leak [38, 39] (Figure 3; reactions 7-9). Additionally, high luminal $[Ca^{2+}]_f$ can slow the rate at which SERCAs transition from the E_1 to E_2 conformational states. This subsequently increases the number of pumps paused in the Ca^{2+}-bound E_1 conformation and stimulates the cleavage of P*i* without the resultant translocation of Ca^{2+} ions. In this case, the utilization of ATP is uncoupled from the transport of Ca^{2+} ions – this is referred to as uncoupled ATPase activity [38, 39] (Figure 3; reaction 10). In the last alternate scenario pictured below, Ca^{2+} ions may dissociate from the pump during its transition from the E_1 to E_2 state, following ATP hydrolysis but prior to translocation to the SR lumen – termed, slippage [11] (Figure 3; reaction 11). Interestingly, this reaction has been shown to be regulated by the physical interaction between SERCA and SLN (discussed in Section 1.4) [1-5]. These alternate reactions share a common feature in that they result in the activation of SERCA activity which necessitates the continual consumption of ATP to maintain basal Ca^{2+} homeostasis, resultantly, these reactions cause a reduction in SERCA pumping efficiency, or a lowering of the theoretical optimal coupling ratio of 2 Ca^{2+}:1 ATP. Excitingly, these alternate reactions are encouraged by the large SR gradient which favors the efflux of Ca^{2+} ions, thus, implying that there may be a constant requirement to pump Ca^{2+} across the SR, even at rest. Indeed, our group has demonstrated that the consumption of ATP by SERCAs comprises a large proportion of the resting (i.e. non-contracting) energy expenditure of skeletal muscle [40-43]. The indirect calorimetry of intact mouse skeletal muscles was used to determine the contribution of SERCA-mediated Ca^{2+} transport to resting energy expenditure [43]. In this study, SERCA activity was indirectly inhibited via prevention of SR Ca^{2+} release from the RyR by exposing muscles to high cellular Mg^{2+}. This Mg^{2+} treatment resulted in

a reduction of O_2 consumption in both slow- and fast-twitch muscles by ~42-48% relative to their basal rates [43] – this decline is representative of the specific contribution of SERCA-mediated Ca^{2+} transport to basal energy expenditure. Extrapolating this contribution to the whole-body level, SERCA activity potentially may account for ~12-15% of whole-body basal energy expenditure and ~15-20% of total daily energy expenditure in adult man [43].

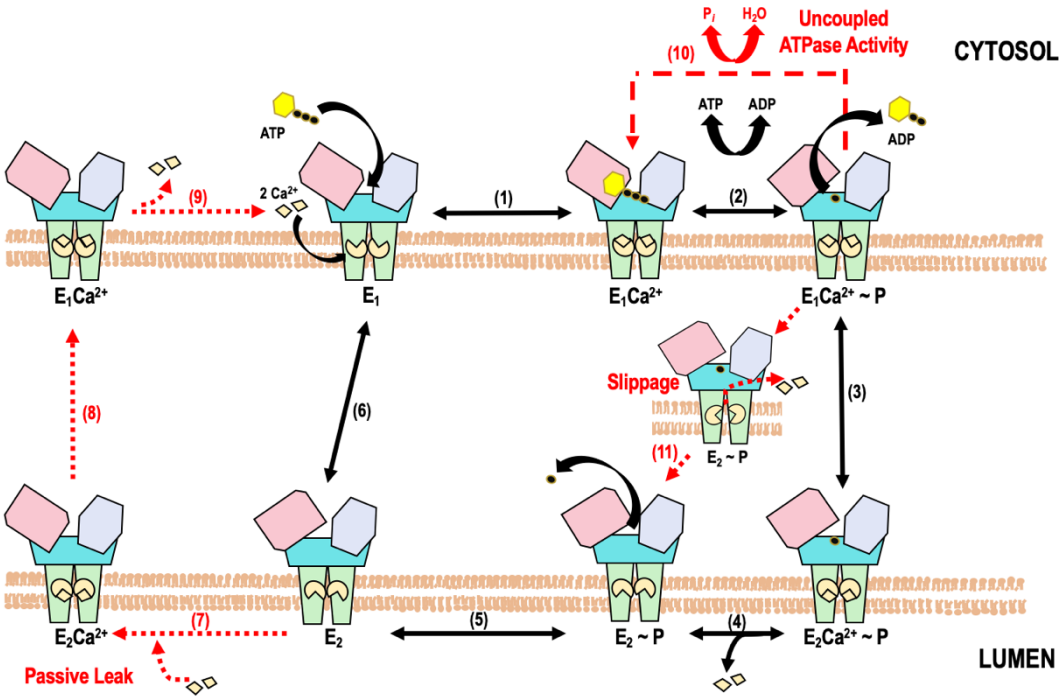


Fig. 1.2.2: Representation of the Alternate Reactions Occurring During SERCA-Mediated Ca^{2+} Transport
In conditions of high luminal [Ca^{2+}], a process known as passive leak may occur (reactions 7-9), in which one or two luminal Ca^{2+} ions remain bound to the E_2 state and are transported out to the cytosol during SERCA transition to the E_1 conformation. Moreover, high luminal [Ca^{2+}] can also induce uncoupled ATPase activity (reaction 10), as it promotes the release of P_i without the transport of Ca^{2+}. Slippage, as represented by reaction 11, involves the dissociation of one or two Ca^{2+} ions from SERCA during the E_1 to E_2 transition. Reactions 7-9, 10 and 11 are examples of alternate reactions which can act to reduce SERCA's theoretical optimal coupling ratio as they induce a greater demand for SERCA ATP consumption to maintain a basal cytosolic [Ca^{2+}]. Adapted from Gamu, D., et al (2020). The Sarcoplasmic Reticulum and SERCA: A Nexus for Muscular Adaptive Thermogenesis**.** Appl Physiol Nutr Metab. 45(1):1-10. doi: 10.1139/apnm-2019-0067.

While the alterations to SERCA activity listed above are necessary for muscle health and function, oxidation, a form of post-translational modification to the SERCA pump has the potential to impede SERCA and disrupt cellular Ca^{2+}-handling [44-50]. In fact, dysregulation of Ca^{2+}-

homeostasis is a common feature in most, if not all, skeletal muscle myopathies, with impairments in SERCA function a frequent underlying characteristic and/or consequence [7, 8, 51-58]. SERCAs are redox-sensitive proteins that exhibit a high vulnerability to oxidative damage and inactivation. The quaternary structures of both SERCA1 and SERCA2 isoforms are comprised of a considerable number of cysteine (Cys) residues (24 and 26 residues, respectively) [44-50, 59]. Generally, proteins designed for residence on a plasma membrane consist of a greater amount of Cys residues due to their ability to form inter- and intra-chain disulfide bonds with other Cys residues to confer structural stability. Unfortunately, the thiol groups required to produce disulfide bonds are highly reactive with reactive oxygen/nitrogen species (ROS/RNS) [60]. As such, these residues (and consequently the SERCA protein) are highly susceptible to modification incurred by exposure to oxidative stress, including oxidation, nitrosylation, S –glutathiolation of protein thiols, and Tyr nitration. Targeting cysteine residues for oxidation can structurally alter the pump to induce impairments that cannot be overcome and result in loss of function because these alterations reduce maximal SERCA activity when localized to the Ca^{2+}-binding and ATP-binding domains, consequently changing SERCA enzyme kinetics. Interestingly, our group and others have demonstrated that protein-protein interactions can stabilize SERCA and offer protection against the many forms of oxidative stress [11, 44, 51, 61]. One such protein-protein interaction is that of the chaperone protein, heat shock protein 70 (HSP70) and SERCA [44, 51, 61]. In examining the protective effects of HSP70 on both SERCA1a and SERCA2a isoforms, HEK – 293 cells were cotransfected with cDNA encoding human HSP70 and either rabbit SERCA1a or SERCA2a, respectfully, and exposed to 37°C and 41°C for various incubation times [61]. Co-immunopreciptation revealed a physical interaction between HSP70 and both isoforms that protected against their thermal inactivation [61]. The protein-protein interaction maintained

maximal SERCA activity and prevented SERCA nitrosylation and carbonyl formation [61]. Moreover, Sections 1.3 and 1.4 below will involve a discussion on our finding that the interaction of SERCA with both SLN and PLN, respectively, confers similar protection to the pump.

In maintaining the Ca^{2+} homeostasis required to preserve muscle health, SERCA activity serves to facilitate muscle relaxation by depressing $[Ca^{2+}]_i$ while simultaneously restoring a SR Ca^{2+} load necessary for subsequent muscle contractions. In doing so, SERCA exhibits a substantial role in regulating muscular and whole body energy expenditure and so is a source of dynamic regulation by numerous factors including: alternate reactions, post-translational modifications and several protein regulators. Of these regulators, the two best understood are the functionally homologous SR integral membrane proteins mentioned previously: PLN and SLN [62]. While the main function of these proteins is to regulate SERCA mediated Ca^{2+} transport, small differences in their structural homology allow each protein to exert different effects on SERCA activity, intracellular Ca^{2+} signalling, muscle health and function and whole body metabolism.

1.3.1 Phospholamban Structure and Interaction with SERCA

PLN is a 52-amino acid monomeric protein composed of a long hydrophilic, NH_2-terminal, cytoplasmic domain and a short hydrophobic, transmembrane, COOH-terminal domain [62-64]. Its quaternary structure is organized into three domains: cytosolic domain Ia (amino acids 1-20) that houses the phosphorylation sites Ser^{16} and Thr^{17}; cytosolic domain Ib (amino acids 21-30); and transmembrane domain II (amino acids 31-52) [65]. Within cardiac and oxidative skeletal muscle, in its unphosphorylated state, PLN physically interacts with SERCA to reduce its apparent Ca^{2+} affinity, while exhibiting little to no effect on the V_{max} measured at saturating $[Ca^{2+}]$ [64, 66]. The inhibitory effect of PLN on SERCA function can be observed as a rightward shift in the Ca^{2+} curve of enzyme activation and has been documented in SR vesicles prepared from all mammalian species examined to date, including murine, canine and human samples [62-64, 66]. PLN monomers have been observed to oligomerize into noninhibitory homopentamers, however, the function of these homopentamers is not yet understood [64, 66]. Conditions of high $[Ca^{2+}]_i$ or adrenergic stimulation will induce phosphorylation of PLN, as cAMP-dependent protein kinase A will target Ser^{16} and Ca^{2+}/calmodulin-dependent kinase II will target Thr^{17} to relieve the inhibition [64, 66, 67].

The interaction between SERCA and PLN has been shown to occur at three sites:

i) a cytoplasmic interaction site produced by charged and hydrophobic amino acids in PLN cytosolic domain Ia and by amino acids Lys-Asp-Asp-Lys-Pro-Val402 in SERCA2a [68-70]

ii) a cytoplasmic interaction site, formed by the PLN cytosolic domain Ib [68-70]

iii) the SERCA transmembrane domain; and the PLN transmembrane domain II/SERCA transmembrane helix M6 interaction site [68-70]

These interaction sites are highly conserved between SERCA1 and SERCA2 isoforms, and as such, SERCA1 and SERCA2 co-expression with PLN in COS-1 cells has demonstrated an identical reduction in Ca^{2+} affinity in the presence of PLN [64].

Studies examining how PLN exerts its inhibitory effect on SERCA have been conflicting. It has been suggested that the binding of PLN to SERCA renders the pump catalytically inactive and that PLN dissociation is required for activation [66, 68, 71-73]. Conversely, other studies suggest that PLN is a subunit of SERCA and as such remains bound to the pump throughout the catalytic cycle [66, 74-76]. Recently, Akin & Jones (2012) have confirmed that PLN exclusively binds to the E_2 SERCA conformation (specifically, residues Gln^{23} to Leu^{52} interact with the groove formed between transmembrane helices M2, M4, M6 and M9 of the pump) and that PLN competes with Ca^{2+} for binding to the pump by stabilizing SERCA in the E_2 state and thus inhibiting the formation of the E_1 conformation [66, 71]. Due to this, at low [Ca^{2+}], SERCA is essentially catalytically inactive, however, increases in the [Ca^{2+}] completely inhibit the interaction between PLN and SERCA (as the binding of Ca^{2+} to SERCA closes the groove with which PLN interacts) and induces a conformational change to the E_1 state [66, 71]. This seems to suggest that PLN dissociation from the pump is required for catalytic activation and subsequent Ca^{2+} transport. Indeed, this is corroborated by increases in Ca^{2+}-ATPase activity and Ca^{2+} uptake in the absence of PLN interaction with SERCA [66]. However, this does not explain the effects of PLN phosphorylation on this interaction. MacLennan and his team have been instrumental in advancing our understanding of this and have demonstrated that while the physical interaction between PLN and SERCA is dissociated by elevations in [Ca^{2+}], PLN phosphorylation relieves the inhibitory interaction without physical dissociation of the two proteins [68-71]. According to their model, the transmembrane domain remains tethered to SERCA, while the cytoplasmic domain exists in

an equilibrium between three different conformational states: a stable inhibitory T state, an intermediate excited R state, and an uninhibitory B state [68-71]. PLN phosphorylation shifts the equilibrium towards the B state, thus relieving inhibition, while maintaining physical interaction between the pump and its regulatory protein [68-71]. NMR spectroscopy in combination with mutant PLN studies have corroborated this model and have illustrated that the phosphorylation of PLN disrupts only the functional interaction while leaving the physical interaction intact [68-71].

1.3.2 Phospholamban Protects the SERCA Pump from Cellular Stress

Preserving this physical interaction between SERCA and PLN in the face of PLN phosphorylation is a vital component to the newly discovered role of PLN in maintaining $[Ca^{2+}]_i$ homeostasis. In addition to the regulatory effect exerted by the PLN protein, recent research from our lab has demonstrated that the physical interaction between PLN and SERCA serves to protect the pump from oxidative stress [11]. SERCA2a activity in the presence and absence of PLN expression in HEK-293 cells which were heat shocked to invoke elevations in reactive oxygen/nitrogen species (ROS/RNS) were used to evaluate the potential ability of PLN to modulate SERCA oxidation. While the temperature (37°C vs 40°C) did not affect the expression of PLN in cells transfected with SERCA2a and PLN, we did observe stark differences in maximal SERCA2a activity in the absence of PLN expression compared to its presence. The expression of PLN had no effect on SERCA carbonyl group content and/or nitrotyrosine levels at 37^oC, whereas, the increase to 40°C resulted in significant increases in carbonyl formation and nitrotyrosine levels in SERCA2a in the absence of PLN. These results are indicative of the interaction between SERCA and PLN being protective in nature during heat stress to negate thermal inactivation of SERCA2a and thus preserve maximal activity [11]. Further validation of the protective role served by the

interaction of SERCA and PLN came from the use of a PLN mutant that cannot bind to SERCA2a. When exposed to identical heat shock treatment, our group has demonstrated that only PLN and not mutant PLN (N34A), can form a protective interaction with SERCA2a to prevent carbonyl and nitrotyrosine formation and thus preserve SERCA maximal activity [11]. As previously mentioned, PLN interacts with SERCA within the TM groove surrounded by TM helices M2, M4, M6 and M9 [68, 69, 77-79]. However, this interaction is reliant upon the Asn^{34} residue of the PLN monomer, as it is responsible for generating the critical contacts with residues in these TM helices. Therefore, a mutation of this residue impedes the interaction between SERCA and PLN and results in loss of both the ability of PLN to exert an inhibitory function [66, 80] and to stabilize SERCA structure and function during heat shock. Furthermore, overexpression of mutant PLN (N34A) under conditions of heat shock prohibited only carbonyl but not nitrotyrosine formation, thus implying that protective nature of the interaction between PLN and SERCA is specific to preserving thermal stability of SERCA2a by preventing Tyr nitration.

1.3.3 Phospholamban Expression Profile and Role in Cardiac Muscle

In human cardiac muscle, PLN is predominately expressed in the ventricle where it regulates the activity of SERCA2a, whereas, in human skeletal muscle, PLN has been shown to regulate both SERCA1a and SERCA2a, with a preference for SERCA2a [9, 10]. In murine muscle, PLN content is significantly reduced when compared to human levels, however, the expression pattern is similar, as PLN has been found in both the left ventricle and slow twitch muscles, such as the soleus [81]. The regulatory role of PLN in cardiac tissue has been extensively investigated. In the heart, the physiological role of SERCA2a is to modulate the rate of clearance of cytosolic Ca^{2+} and the capacity of the luminal SR Ca^{2+} load, and as such, is crucial in cardiac relaxation and

contraction [65, 82, 83]. PLN acts as the intersection point between two signal transduction pathways: the β - adrenergic signalling pathway (that allows for protein phosphorylation) and the Ca^{2+} - signalling pathway (that initiates contraction), through which it can modulate SERCA2a activity, therefore regulating cardiac relaxation and contraction [65]. In murine models, the absence of PLN in cardiac tissue resulted in a linear increase in SERCA affinity for Ca^{2+}, as well as, linear increases in contractile properties (such as myocyte cell shortening, contraction rate and re-lengthening) and improved relaxation rates [65]. In fact, PLN ablation mimicked the maximal stimulation contraction and relaxation rates of wild-type hearts [65]. Conversely, overexpression of PLN in murine cardiac tissue resulted in reduced rates of contraction and relaxation, as well as, decreases in the amplitude of the Ca^{2+} signal and an extended decay of the Ca^{2+} transient [65].

1.3.4 Characterization of Phospholamban in Skeletal Muscle (Muscle Metabolism, SERCA Protection and SERCA Superinhibition)

A characterization of PLN in skeletal muscle is currently underway, with our lab at the forefront. We have explicitly shown that PLN is expressed in mouse soleus muscle, where it exerts an inhibitory effect on both SERCA1a and SERCA2a [9]. We have examined the impact of PLN deletion on muscle health and showed that in its absence, gross muscle mass, fiber-type distribution, and fibre size were unaffected [9]. Furthermore, we have investigated role of PLN in energy metabolism and obesity, as well as, in skeletal muscle diseases that stem from abnormal Ca^{2+} - handling, such as Duchenne Muscular Dystrophy (DMD). While SLN promotes slippage of Ca^{2+} ions from the pump and as such augments the energy consumption needed to restore cytosolic $[Ca^{2+}]_i$ [1-5] (discussed below), we have shown that unlike SLN, PLN does not promote SERCA inefficiency. *Pln*$^{-/-}$ mice exhibit similar SERCA pumping efficiency to that of WT littermates, indicating that PLN does not uncouple SERCA mediated Ca^{2+} uptake from ATP hydrolysis in

oxidative muscle [84]. Consequently, *Pln*$^{-/-}$ mice showed no differences in whole-body metabolic rate, metabolic efficiency, glucose tolerance, fat pad mass and adiposity compared to WT following 8 weeks of high-fat feeding (42% kcal from fat) – suggesting that PLN is not involved in adaptive muscle-induced thermogenesis [84]. Interestingly, the physical interaction between SERCA and PLN is *reduced* by caloric surfeit, as there was a significant decline in PLN content in the soleus of high-fat fed WT mice compared to chow-fed controls, as well as, a tendency of high-fat feeding to increase the non-inhibitory phosphorylated form of PLN [84]. This divergence in function between SLN and PLN can be attributed to their respective cytosolic NH_2 – terminal regions and to distinct differences in their physical interaction with the SERCA pump, which will be discussed further in Section 1.4.1.

In corroboration of protective role offered by the interaction between PLN and SERCA, we have shown that the absence of PLN in the murine *mdx* model of DMD worsens the disease phenotype [85]. DMD is inherited as a recessive X-linked disorder, affecting predominately males and resulting in fatal weakening and wasting of skeletal, respiratory and cardiac muscles [86]. It is caused by an absence of the dystrophin protein, primarily due to out-of-frame deletions within the large dystrophin gene, or less commonly due to nonsense mutations [87]. The absence of dystrophin results in impairments in the formation of the dystroglycan complex (DGC) and thus a loss of the critical link between the submembrane cytoskeleton and components of the extracellular matrix [88-91]. Consequently, this functionally alters the architecture of the sarcolemmal membrane and the incurred membrane instability has been reported to contribute to the increased sarcolemmal permeability to extracellular Ca^{2+} [88]. The subsequent dysregulation of Ca^{2+} homeostasis in the dystrophic environment results in the induction of numerous degradative pathways that lead to successive cycles of muscle fibre degeneration and regeneration, chronic

inflammation, fibrosis and eventual muscle cell necrosis [88, 90]. Based on previous studies showing that targeted therapy to improve SERCA function is a proven strategy to alleviate DMD in *mdx* mice, we originally hypothesized that the ablation of PLN would restore SERCA activity and thus alleviate DMD pathology in *mdx* mice. Unexpectedly, PLN ablation in the *mdx* mouse model resulted in: 1) a potential maladaptive transition to a fast fibre type that is more susceptible to damage; 2) further reductions in the ability to generate force compared to *mdx/Pln*$^{+/+}$ mice; 3) impairments in SERCA Ca^{2+} uptake when compared to *mdx/Pln*$^{+/+}$ mice; and 4) drastic elevations in detrimental SERCA oxidative post-translational modifications [85].

The depressed rates of SERCA mediated Ca^{2+} uptake observed in the *mdx* phenotype in the absence of PLN can be attributed to both a decline in SERCA expression and to increased SERCA susceptibility to damage in the dystrophic environment as evident by greater SERCA nitrosylation [85]. Both muscles examined in this study exhibited an increase in PLN content in *mdx/Pln*$^{+/+}$ relative to WT. The fact that PLN is upregulated in this *mdx/Pln*$^{+/+}$ model and that there is a worsening of the overall myopathy, muscle weakness and SERCA impairment in the absence of PLN suggests that PLN is required in dystrophic muscle to protect SERCA from damage [85]. Based on the three sites of physical interaction between PLN and SERCA, it would be expected that the transmembrane domain (which houses SERCA's two Ca^{2+} binding sites in helices M2, M4, M6 and M9) would be afforded structural and functional protection by PLN during times of stress [18, 30-32, 64]. Indeed, this is corroborated by the fact that *mdx/Pln*$^{-/-}$ muscle experienced a stark increase in the nitrosylation of both SERCA isoforms compared to both WT and *mdx/Pln*$^{+/+}$ [85]. While SERCA damage and subsequent dysregulation is an expected hallmark of the aberrant Ca^{2+} handling observed in this myopathy, the fact that the absence of PLN exacerbated SERCA susceptibility to oxidative stress is a clear indication of the protection offered by the interaction

between SERCA and its regulatory protein. Furthermore, the results of this study demonstrate that this protection is specific to SERCA's two Ca^{2+} binding sites. *mdx/Pln*$^{-/-}$ muscle exhibited a drastic impairment in Ca^{2+} uptake without an accompanying change in ATPase activity, indicating that Ca^{2+} uptake and ATP hydrolysis of the pumps had become severely uncoupled. With PLN ablation, the Ca^{2+} binding domain became vulnerable to damage resulting in impairments in Ca^{2+} uptake, whereas, the ATP binding domain, and thus ATP binding and hydrolysis by the pump, remained unaffected.

While the above discussion demonstrated the importance of PLN expression in skeletal muscle myopathies, the *Pln*^{OE} mouse line offers the opposite scenario – a myopathy resulting from *Pln* overexpression. Centronuclear myopathy (CNM) presents as a congenital myopathy, histopathologically characterized by three key features: centrally located nuclei, central aggregation of oxidative activity, and type I fiber predominance and hypotrophy. *Pln*^{OE} muscle is marked by a 6- to 7-fold overexpression of PLN [55]. The consequent $[Ca^{2+}]_i$ overload induces impairments in SERCA function, made evident by marked reductions in rates of Ca^{2+} uptake, maximal ATPase activity and the apparent affinity of SERCA for Ca^{2+}. Furthermore, this dysregulation in SERCA function may be responsible for the manifestation of centrally located nuclei, central aggregation of oxidative activity, type I fiber predominance and hypotrophy, progressive fibrosis and muscle weakness (the hallmarks of CNM) in soleus and gluteus minimus muscles from the *Pln*^{OE} mice [55]. What's more, in examining muscle biopsies from three human CNM patients, our group has shown increases in both total and monomeric PLN content and a significant reduction in SERCA activity and compared with five healthy subjects [55]. Fascinatingly, this discovery also offers a new avenue of potential pharmaceutical treatments. We have additionally demonstrated that administration of formoterol causes improvements in SERCA

activity and, ultimately, ameliorates the histopathological features of CNM (unpublished). Formoterol is a β-agonist which activates protein kinase A (PKA), this increases phosphorylation of PLN at Ser16 causing it to dissociate from SERCA, thus increasing SR Ca^{2+} uptake. Expectedly, western blotting revealed a reduction in monomeric PLN ($p < 0.05$) and an increase in phospho-PLN ($p < 0.05$) following administration. Additionally, treatment resulted in reductions in centralized nucleation and type I fibre proportions, as well as, increased type I fibre cross-sectional area (CSA) in soleus muscle of *Pln*^{OE} mice. While β_2-adrenoceptor activation improved two of three histological features of CNM in this *Pln*^{OE} mouse model (as it did not alter aggregations of oxidative activity in soleus), the role of PLN and the therapeutic effects of β-agonists in CNM treatment is of value to investigate further. The *Pln*^{OE} mouse is also a novel animal model to examine the dynamic relationship between SERCA, PLN and DWORF – which will be discussed further in Section 1.5.7

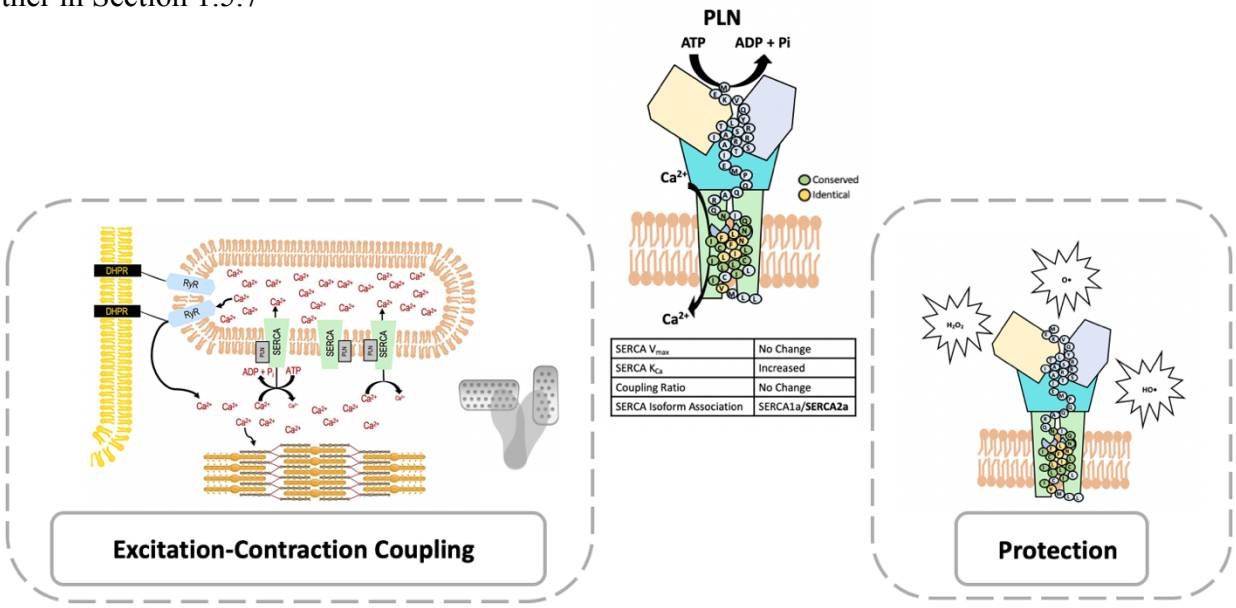


Fig. 1.3.4.1: Visual Summary of the Physiological Role of PLN in Muscle
A graphical summary of the text above, showing the role of PLN in acting as a "brake" to inhibit SERCA function during basal/resting conditions (when the transport of Ca^{2+} to the SR lumen is not required). Rising intracellular [Ca^{2+}] or adrenergic stimulation removes the brake (PLN) from SERCA to allow for rapid sequestering of Ca^{2+} into the SR to restore intracellular [Ca^{2+}] homeostasis and allow for subsequent muscle contractions. Additionally, the physical interaction between PLN and SERCA protects the pump from damage incurred by cellular stress pathways and preserves maximal activity of the pump.

1.4.1 Comparison of Sarcolipin and Phospholamban Structure: Similarities and Differences

SLN is a 31-amino acid type I, integral membrane protein in which residues 1–7 form an unstructured N-terminal/cytosolic domain, residues 8-26 comprise the transmembrane (TM) α-helix domain and residues 27–31 form a highly-conserved C-terminal/luminal domain [30, 92, 93]. A structural comparison of SLN and PLN highlights the significant degree of homology observed predominately in the TM domain. While slightly smaller in length, the SLN TM domain is composed of 19 residues, of which, 8 are identical and 8 are highly conserved compared to the corresponding residues in the TM domain of PLN. This extensive homology in the TM region is critical for SLN and PLN localization and interaction with SERCA, as both proteins share a common binding site within SERCA transmembrane helices M2, M4, M6 and M9 [30, 92, 93]. Mutagenesis studies in the SERCA TM region have demonstrated that the interaction between SERCA and both SLN *and* PLN occurs in the same groove with both regulatory proteins cross-linking to SERCA at Cys-318 and Val-89 in the TM region [93]. However, these same studies additionally showed that SLN and PLN interact with a different set of amino acid residues within this TM groove, as certain SERCA TM mutations had different effects on the binding characteristics of each protein to SERCA [93]. The differences in the amino acid composition of the cytosolic and luminal domains account for the structural changes that provide these peptides with their own unique functional properties. The relatively short SLN cytosolic domain is poorly conserved and varies among species: rodent SLN exhibits a 2ERSTQE sequence compared to the 2ERSTRE sequence in rabbit and the 2GINTRE sequence in primates [30, 92]. As previously mentioned, PLN's longer cytosolic domain is divided into cytosolic domain Ia (amino acids 1-20) and cytosolic domain Ib (amino acids 21-30) and is the location of two out of three interaction sites between PLN and SERCA [68-70]. In contrast, the relevance of SLN's counterpart domain

has not been well defined but appears to be functional as opposed to solely interactional. The highly conserved Thr5 residue, has been proposed to be a putative phosphorylation site – phosphorylation at Thr5 of SLN could act as the site of reversible alleviation of SLN inhibition of SERCA, in a similar fashion as for PLN [30, 94, 95]. This proposition has been verified by multiple groups which have demonstrated that this residue can be acted upon by CaMKII and that subsequent SERCA activity was increased; however, evidence for such phosphorylation is lacking *in vivo* and the relevance of Thr5 phosphorylation to SLN function remains unknown [30, 94, 95]. Recently, Sahoo and colleagues [92] have employed domain swapping and mutagenesis techniques to show that the cytosolic domain is vital for SLN's uncoupling capabilities and thus for its role in skeletal muscle thermogenesis (as discussed below). Their results were twofold: 1) truncation of the SLN protein via deletion of the N-terminus caused SLN to lose sensitivity to changes in $[Ca^{2+}]_i$ and negated SLN's effect on SERCA function; and 2) replacement of the SLN's cytosolic domain with that of PLN allowed the chimeric SLN protein to retain its regulatory role however it abolished the ability to uncouple ATP hydrolysis from Ca^{2+} transport [92]. Taken together, this implies that the cytosolic domain is responsible for conferring SLN's uncoupling properties.

Further differentiating the two SERCA regulatory proteins are their respective luminal domains. SLN exhibits a unique RSYQY sequence which extends into the lumen of the SR, whereas, the last three residues of PLN continue as a part of the TM domain and as such PLN does not display a tail sequence [30, 63, 96]. Solid-state NMR and alanine mutagenesis studies have illustrated that the luminal tail of SLN (driven predominately by the two aromatic residues Tyr^{29} and Tyr^{31}) is required for its interaction with SERCA [30, 62, 97, 98]. In addition to this critical interaction site, functional studies in co-reconstituted proteoliposomes have shown that the luminal

domain is responsible for conferring SLN's inhibitory properties [63]. Alanine mutagenesis studies targeting the luminal tail have identified Arg^{27} and Tyr^{31} as the two residues required for SLN's effect on SERCA's apparent Ca^{2+} affinity, and furthermore, have shown that Tyr^{31} is essential for altering SERCA maximal activity [30, 63, 92] (further discussed below). Mutation of either of these residues resulted in a lack of SERCA inhibition by SLN. Once again, domain swapping techniques were effective in establishing the properties of the luminal tail. The addition of SLN's luminal domain to PLN (either to the full-length PLN protein or as a replacement for the last three residues which protrude into the lumen) resulted in a synergistic effect on PLN inhibitory function, causing superinhibition of SERCA activity in a fashion similar to that elicited by the ternary SERCA-PLN-SLN complex in the atria [30, 63, 92]. Based on the structural differences discussed above, it comes as no surprise that the role of SLN in regulating calcium homeostasis is quite distinct from that of PLN. While both proteins can be viewed as SERCA inhibitors and Ca^{2+} affinity modulators, SLN serves the additional role of a SERCA uncoupler.

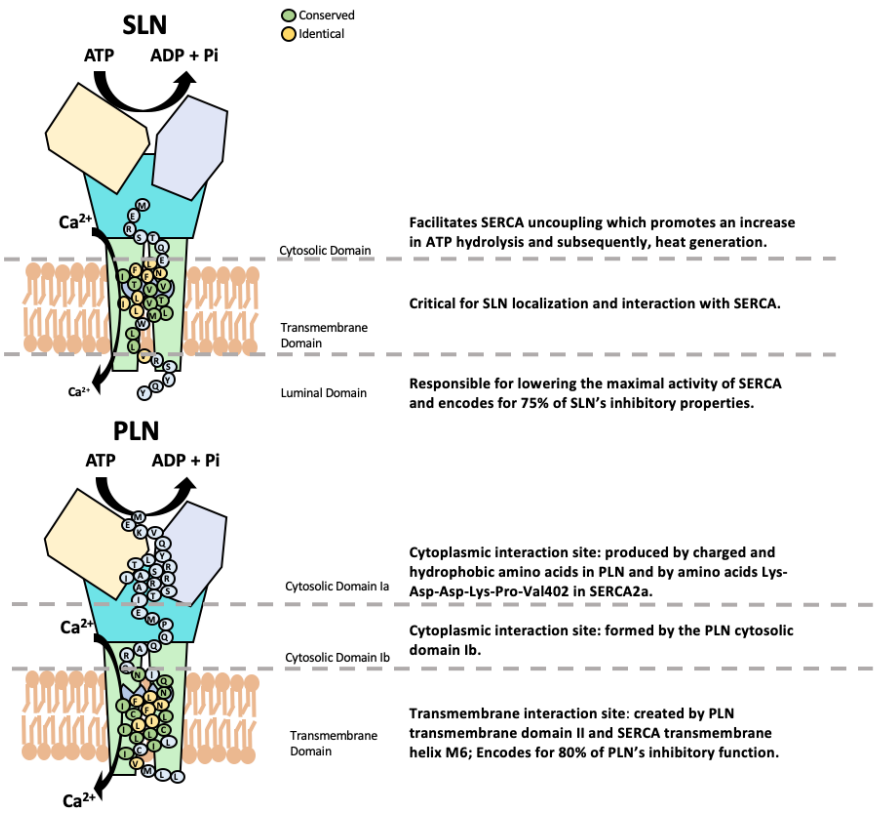


Fig. 1.4.1.1: PLN & SLN Domain Comparison Summary
A visual depiction of the comparison in domains between SLN and PLN. Conserved and identical amino acids are highlighted in green and yellow, respectively, and are located in the transmembrane domain which interacts with the SERCA pumps (the region of greatest sequence homology). Differences in the cytosolic and luminal domains confer the unique properties of each regulatory protein.

1.4.2 Mechanism of Interaction between Sarcolipin and SERCA

Discerning the mechanism of interaction between SLN and SERCA initially posed a challenge due to its small size and highly hydrophobic nature, as well as, the assumption that SLN inhibits SERCA in a fashion similar to PLN [30, 93]. However, the co-expression of SLN and SERCA in HEK cell culture and the subsequent isolation of the protein-expressing microsomes has shown that SLN inhibition is distinct from PLN in the following manner:

i) SLN can remain bound to SERCA in the presence of high Ca^{2+};

ii) The interaction between SLN and SERCA persists throughout the kinetic cycle

Using chemical cross-linking strategies, Sahoo and colleagues (2013) have demonstrated that cytosolic [Ca^{2+}] levels (ranging between 5 – 100 uM) do not induce dissociation of SLN from the SERCA pump [93]. In contrast, the interaction between PLN and SERCA is abolished at [Ca^{2+}] greater than 1 uM. Expectedly, SLN is maximally bound to SERCA in the absence of Ca^{2+}, however, the interaction persists even in the face of high [Ca^{2+}] (100 uM) at both the N terminus and at the C terminus cross-linking sites, albeit at a reduced level [93]. This is in part possible because SLN can interact with SERCA even after occupation of both Ca^{2+} binding sites and in fact, SLN and Ca^{2+} ions compete for and can simultaneously bind to SERCA. These unique properties, specific to only SLN, are enabled by the fact that SLN remains bound to the various kinetic steps of the SERCA protein as it undergoes its aforementioned catalytic cycle [30, 93]. Referring to Figure 1.2.1 in Section 1.2, chemical cross-linking studies have shown that SLN can crosslink to SERCA in its Ca^{2+} free E_1 state and that this interaction is maintained during binding of both Ca^{2+} and ATP as the pump transitions to E_1Ca^{2+} and to $E_1Ca^{2+} \sim P$ as ATP is subsequently hydrolyzed [30, 93]. With the release of Ca^{2+} ions into the lumen of the SR, SLN remains bound to the pump during the transition to its Ca^{2+} free $E_2 \sim P$ state. Finally, SLN can crosslink to SERCA in the Ca^{2+} free E_2 state, with the addition of ATP significantly strengthening the interaction. This strongly suggests that SLN occupies SERCA throughout its entire catalytic cycle, whereas, the interaction between PLN and SERCA is limited to its Ca^{2+} free E_2 state [30, 93].

The inhibitory effects of both SERCA regulators on the pump's kinetic activity can be observed as rightward shifts in the Ca^{2+} curve of enzyme activation, representative of an increased Ca^{2+} requirement to reach half-maximal rates of SERCA Ca^{2+} uptake. Several gain- and loss-of-function studies employing reconstituted liposomes, heterologous cell-expression systems, and transgenic animal models have consistently demonstrated that both regulatory proteins reduce

SERCA's affinity for Ca^{2+} [12, 55, 63, 70, 79, 81, 92, 97, 99-102]. However, the *in vitro* models have shown discrepant results concerning SLN's ability to alter the maximal rate (V_{max}) of Ca^{2+}-induced Ca^{2+}-uptake. Odermatt et al., (1998) initially reported that the co-expression of SLN and SERCA1 in HEK-293 cells caused a reduction in Ca^{2+} affinity, as well as, an increase in the maximal rate (V_{max}) of Ca^{2+}-induced Ca^{2+}-uptake [97]. However, subsequent studies by this same group showed a lack of impact of SLN on both SERCA1a and SERCA2a V_{max}, despite reductions in the Ca^{2+} affinity of both isoforms [103], a finding that has been recently corroborated by Anderson et al., (2015) [12]. Opposing these studies are findings determined by Sahoo and associates. With the use of similar methods, Sahoo et al., (2013) reported that SLN reduced the V_{max} of Ca^{2+}-uptake but did not alter SERCA's Ca^{2+} affinity [93]. Likewise, Sahoo et al., (2015) found that SLN had no impact on the kinetic parameters of Ca^{2+}-dependent ATP hydrolysis of SERCA1, despite causing a reduction in the V_{max} of Ca^{2+}-uptake [92]. Conversely, studies employing rodent models have shown better consistency in establishing that SLN causes a reduction in cardiac [104-106] and skeletal muscle [100, 107] contractility, which is attributed to a depression in SERCA's Ca^{2+} affinity and consequently, a slowing of the rate of SR Ca^{2+}-uptake, however, these studies offered no evidence to suggest SLN alters SERCA V_{max}.

1.4.3 Expression Profile of Sarcolipin

The expression pattern of SLN in muscle tissue is complementary to that of PLN [10]. In the human and rodent heart, SLN is abundant in the atria where it regulates SERCA2a activity [108]. In human skeletal muscle, SLN is expressed in fast-twitch fibres where it has been shown to interact with both SERCA1a and SERCA2a, with a preference for regulating SERCA1a [9]. The expression of SLN is upregulated in rodent embryonic and neonatal skeletal tissue [108, 109],

whereas, in adult rodent skeletal muscle, SLN protein expression has been reported in slow-oxidative muscles such as the soleus, red gastrocnemius and diaphragm, as well as, in fast-glycolytic muscles including the extensor digitorum longus – albeit at far lower levels compared to larger mammals [110-112]. The degree of SLN expression appears to display a phenotypic pattern, with greater protein expression predominantly in oxidative muscle, particularly the soleus muscle where both SERCA1a and SERCA2a are expressed [110-112]. Tupling et al. (2002) first assessed the physiological function of SLN, using intramuscular injection and electro-transfer of plasmid cDNA to over-express NF-SLN in rat soleus [107]. This ectopic over-expression resulted reduced peak twitch and tetanic force production *in situ*, along with slowed rates of contraction and relaxation. These findings were attributed to a reduction in the rate of SERCA Ca^{2+} uptake and reduction in SR Ca^{2+} store of postnuclear homogenates with SLN overexpression [107]. The advent of the SLN knock-out mouse ($Sln^{-/-}$) has been instrumental in evaluating physiological levels of SLN protein expression and the role of SLN on SERCA and muscle function. Using this model, Tupling et al (2011) demonstrated that $Sln^{-/-}$ slow-twitch skeletal muscle exhibit increased SERCA activity rates and increased contractile kinetics, including faster muscle relaxation rates [100]. This has proven consistent in cardiac tissue as well, where the loss of SLN has been shown to enhance SERCA-mediated Ca^{2+} transport and atrial contractility [104], whereas, the over-expression of NF-SLN resulted in impairments in Ca^{2+} transport and cardiac contractility [105]. Rodent studies have consistently shown that SLN is a dynamic regulator of SERCA activity in both cardiac and skeletal muscle and as such has a role in modulating muscle function. Recently, our group has investigated this role further and has discovered that SLN is a key player in a signalling cascade responsible for mediating adaptive muscle remodeling [8].

1.4.4 Sarcolipin's Role in Adaptive Muscle Remodeling

Studies employing the SLN overexpression (Sln^{OE}) model have illustrated that the unique ability of SLN to remain bound to SERCA throughout its kinetic cycle and in the face of high $[Ca^{2+}]_i$ allows SLN to modify cytosolic Ca^{2+} transients and activate Ca^{2+}-dependent signaling pathways which mediate an oxidative muscle phenotype [110]. This model, in which SLN is expressed at high levels in both fast- and slow-twitch skeletal muscle, is associated with greater skeletal muscle oxidative capacity that translates to significant improvements in exercise endurance and fatigue resistance [110]. The physiological relevance of greater SLN content is observed during skeletal muscle development and in instances of skeletal muscle disease, disuse and injury. Early neonatal stages of rodent skeletal muscle development are associated with a severalfold upregulation of SLN content in both fast and slow twitch muscles. The height of this upregulation occurs around birth and persists for approximately two weeks postnatally at which point SLN expression is downregulated in mature glycolytic muscles, remaining present only in oxidative muscles [110]. Greater SLN content during this time is required to regulate mitochondrial biogenesis and promote oxidative metabolism, as its absence results in reduced fatty acid oxidation, decreased mitochondrial DNA content, and altered mitochondrial morphology concomitant with increased levels of glycolytic enzymes indicative of a dependence on glycolytic metabolism [110]. In fact, the overexpression of SLN in adult glycolytic rodent muscle is associated with a greater reliance on oxidative metabolism as evidenced by increased expression of proteins involved in fatty acid transport and mitochondrial enzymes involved in fatty acid oxidation, indicative of a shift in substrate utilization causing greater fatty acid oxidation [110].

The promotion of an oxidative phenotype is reliant on the activation of the Ca^{2+}-dependent CAMKII and calcineurin (Cn)/ nuclear factor activating T-cell (NFAT) signalling pathways. *Sln*^{OE} tissue exhibit an increase in the expression of CamkII, Cn and their respective downstream targets, as well as, increased Cn phosphatase activity [110]. Interestingly, these changes were abolished in *Sln*$^{-/-}$ tissue, thus suggesting that the uncoupling of SERCA from Ca^{2+} transport and the ensuing prolonged cytosolic Ca^{2+} transient can activate Ca^{2+}-dependent signaling pathways which mediate oxidative metabolism and mitochondrial biogenesis [110]. The interaction between SLN and the Cn signalling pathway has been a recent focal point in our lab. Cn is a serine/threonine phosphatase that has proven to be important in the promotion of a slow-oxidative fiber phenotype and in the maintenance of skeletal muscle mass [113]. Activation is induced by sustained low-amplitude elevations in intracellular Ca^{2+} which cause Cn to act on and dephosphorylate the NFAT family of transcription factors, consisting of isoforms NFATc1-4 and NFAT5 [113]. These heavily phosphorylated proteins reside in the cytoplasm, however, their dephosphorylation exposes a nuclear localization signal which stimulates their translocation to the nucleus where they act as transcription factors [113]. The activation of Cn and dephosphorylation of NFATc1 is of particular interest, as it is the primary transcription factor in the promotion of myosin heavy chain I (MHCI) and it acts to increase the expression of stabilin-2, phosphatidylserine receptor that mediates myoblast fusion, myofiber size, and muscle mass [113, 114].

Our group employed the overloaded plantaris and unloaded/tenotomized soleus muscle model to alter $[Ca^{2+}]_i$ and subsequent activation of Ca^{2+} signalling pathways in order to investigate the relationship between SLN and Cn signalling [6]. The WT overloaded plantaris exhibited myofiber hypertrophy, increased fiber number, and a fast-to-slow fiber type shift which were accompanied by the ectopic expression of SLN, increased NFAT dephosphorylation, elevated

stabilin-2 protein content and reduced SERCA activity. On the other hand, the WT tenotomized soleus experienced myofiber atrophy, decreased fiber number, and a slow-to-fast fiber type shift along with a stark increase in SLN protein content, increased calcineurin signaling and reduced SERCA activity. In both models, the absence of SLN resulted in enhanced SERCA activity and impaired calcineurin signaling [6]. Consequentially, *Sln*$^{-/-}$ overloaded plantaris myofibers failed to hypertrophy and transition to a slow-oxidative phenotype and *Sln*$^{-/-}$ unloaded soleus muscles exhibited greater reductions in fiber size and number and an accelerated slow-to-fast fiber type shift. These results add further support to the role SLN plays in mediating an oxidative phenotype and directly implicate the SLN/SERCA interaction in modulating [Ca^{2+}] to augment Cn signaling to drive adaptive muscle remodeling which could have important implications for other muscle diseases and conditions [6].

1.4.5 Sarcolipin's Role in Conditions of Muscle Disease, Disuse and Injury

Indeed, it is recognized that SLN is upregulated under conditions of muscle disease, disuse, and injury in a manner which is proportional to disease severity (the extent of this upregulation and the breadth of models in which this occurs is highlighted in **Table A.1** in **Appendix A**). Recently, our lab examined the *Pln*^{OE} model of CMN [55] (mentioned previously at the end of Section 1.3.4) and generated a *mdx/Sln*$^{-/-}$ model [8] to determine the physiological role of this upregulation and its relation to the Cn-signalling pathway. We have shown that the expression of SLN is upregulated 7-9-fold in the soleus and gluteus minimus muscles from *Pln*^{OE} mice compared to WT. Additionally, as an adaptive response to *Pln* overexpression and the concomitant reduction in type I fibre cross-sectional area, *Pln*^{OE} mice have been observed employ the Cn signalling

pathway to undergo type II fibre hypertrophy and a fast-to-slow fiber type transition [55]. Ablation of *Sln* resulted in blunted Cn signalling as indicated by greater levels of phosphorylated NFAT and decreased expression of stabilin-2 which caused a lack of type II fibre hypertrophy and failure to transition to a slow fibre population. This in turn, exacerbated the Pln^{OE} induced myopathy as evident by greater impairments in *in vitro* soleus force production and a decline in muscle mass relative to body weight [55]. Collectively, this would imply that the SLN upregulation in the Pln^{OE} mouse is critical to the activation of the Cn-signalling pathway and mediating adaptive muscle remodeling [55]. Consistent with these findings are the results from our examination of the *mdx/Sln*$^{-/-}$ mouse model, where there has been a reported 5-fold upregulation of SLN expression in soleus muscle [8]. In muscular dystrophy, Cn-signalling is required to mediate the increased expression of transcriptional regulators of adaptive responses in order to combat disease progression, including promoting the expression of the dystrophin homolog, utrophin and PGC-1α [115-117]. In fact, activation of Cn has been shown to alleviate the *mdx* pathology [115], whereas, impairments in this signalling cascade have resulted in a worsening of the dystrophic phenotype in *mdx* mice [117]. The deletion of *Sln* blunted Cn-signalling as evident by reductions in utrophin, stabilin-2 and calcineurin expression. Consequently, *mdx/Sln*$^{-/-}$ muscles contained smaller myofibres, experienced a maladaptive slow-to-fast fibre-type switch (that corresponded with reduced expression of mitochondrial proteins) and displayed a worsened dystrophic pathology (with greater myofibre degeneration and a reduction in *in vitro* soleus force production compared with *mdx* muscles) [8]. Taken together, the findings from the three separate models of myopathy highlighted here clearly demonstrate that the role of SLN in the promotion of Cn signaling is critical for the activation of muscle growth/remodeling and counteracts disease pathology.

1.4.6 Sarcolipin Uncouples the SERCA pump to Drive Adaptive Thermogenesis

The powerful role that the SLN/SERCA interaction plays is not limited solely to the promotion of healthy muscle function, growth and remodeling. In fact, it is well established that the interaction between SLN/SERCA is an integral control point of muscular and whole-body adaptive thermogenesis [1-3, 31]. Studies conducted on isolated SR vesicles by deMeis and others have demonstrated that the uncoupling of SERCA ATP hydrolysis from Ca^{2+} transport results in the production of heat [5, 39]. As previously mentioned, SLN has been shown to uncouple SERCA Ca^{2+} transport from ATP hydrolysis, resulting in futile cycling of SERCA which causes an increase in ATP consumption and heat production. This SLN-mediated uncoupling of SERCA is attributed both to SLN's cytosolic N-terminal domain (as explained above, truncation of this domain results in a loss of both inhibitory and uncoupling properties) and to SLN's ability to remain associated with the pump throughout the course of its catalytic cycle, even in the face of elevated [Ca^{2+}] [30, 92, 93]. *In vitro* studies have employed reconstituted lipid vesicles in order to experimentally alter the molar ratio of SLN to SERCA and have shown that an increase in this ratio caused a significant reduction in vesicular Ca^{2+} accumulation without an effect on SERCA ATP consumption while additionally increasing the amount of heat released per mol of ATP hydrolyzed by SERCA during Ca^{2+} pumping [4, 5]. This uncoupling of SERCA Ca^{2+} transport from ATP hydrolysis was attributed to SLN's ability to promote "slippage" of Ca^{2+} ions from the SERCA pump as it moves through its catalytic cycle (referred to as alternate reaction 11 in Figure 2) [4, 5]. Our group has used the *Sln*$^{-/-}$ mouse as an *in vivo* model to investigate SLN's ability to facilitate SERCA uncoupling and has shown that endogenous levels of skeletal muscle SLN do indeed cause an uncoupling of SERCA [3]. SR vesicles derived from oxidative limb muscles of *Sln*$^{-/-}$ mice

exhibited a greater SERCA apparent coupling ratio (i.e. Ca^{2+} transported:ATP hydrolyzed) relative to WT controls. The higher coupling ratio in *Sln*$^{-/-}$ mice was the result of lower Ca^{2+} ATPase activity, indicating that in the absence of SLN, SERCA consumes less energy to establish a given Ca^{2+} gradient across the SR, making it energetically more efficient. As such, the contribution of SERCA activity to resting energy expenditure of isolated *Sln*$^{-/-}$ muscle was ~13% lower compared to WT muscle [3]. Moreover, our group and others have shown that *Sln*$^{-/-}$ mice expend less energy during sub-maximal treadmill exercise and are unable to maintain body temperature following acute cold-exposure implying that the uncoupling of SERCA function by SLN can occur during exercise and shivering thermogenesis [1, 2, 93]. Overall, these studies illustrate that an added physiological implication of the SLN/SERCA interaction is that more ATP is required to transport Ca^{2+} ions across the SR, regardless of if the muscle is at rest or in use. Not surprisingly, multiple groups including our own, have shown that *Sln*$^{-/-}$ mice are prone to developing diet-induced obesity due to more efficient SERCA metabolism [1, 2, 118-120], whereas, mice over-expressing SLN are resistant to diet-induced obesity because of greater SLN mediated energy expenditure [121]. At the whole-body level, increasing the energetic efficiency of SERCA results in a predisposition to diet-induced obesity, as *Sln*$^{-/-}$ mice became more obese than WT littermates following an eight-week high-fat diet [1, 2]. Interestingly, in WT counterparts, SLN expression is upregulated in response to diet-induced obesity within slow-oxidative muscle of WT mice, suggesting SLN is recruited to increase the energy demand of SERCA Ca^{2+} pumping to regulate body mass and metabolism [1, 2]. In agreement with this, *Sln*^{OE} mice are hyper-metabolic at thermoneutrality and subsequently resistant to diet-induced obesity, with these mice exhibiting markedly less weight gain and a maintenance of a healthy metabolic profile compared to WT mice [121]. Additionally, these mice exhibited a higher metabolic rate compared to controls and their muscles showed

enhanced oxidative capacity which was accompanied by increased mitochondrial biogenesis and fatty acid transport protein expression [121].

1.4.7 Sarcolipin Protects the SERCA Pump from Cellular Stress

Lastly, the physical interaction between SLN and SERCA has been discovered to afford protection of the pump and preserve its maximal activity. In the protection study outlined in Section 1.3.2, SLN was evaluated in the same fashion as PLN and was found to mirror PLN with its cytoprotective properties [11]. Heat shock treatment of HEK-293 cells expressing SERCA in the presence and absence of SLN showed significant increases in carbonyl formation and nitrotyrosine levels in SERCA2a and consequentially a dramatic decline (-25-35%) in maximal SERCA2a activity, in the absence of SLN [11]. Moreover, endogenous levels of SLN expression in diaphragm muscle were shown to preserve maximal SERCA activity following heat shock treatment, indicating that the ablation of SLN increases susceptibility of the pumps to thermal inactivation [11]. It is clear from the extensive research conducted that while PLN and SLN do share similarities in their ability to inhibit SERCA, it is the differences in their structure and thus interactions with SERCA that allow each protein to exert distinct and unique physiological functions. With the discovery of new SERCA regulatory proteins, it is of great interest to determine the similarities and differences in their interaction with SERCA to evaluate new unique roles and potential redundancies between the proteins.

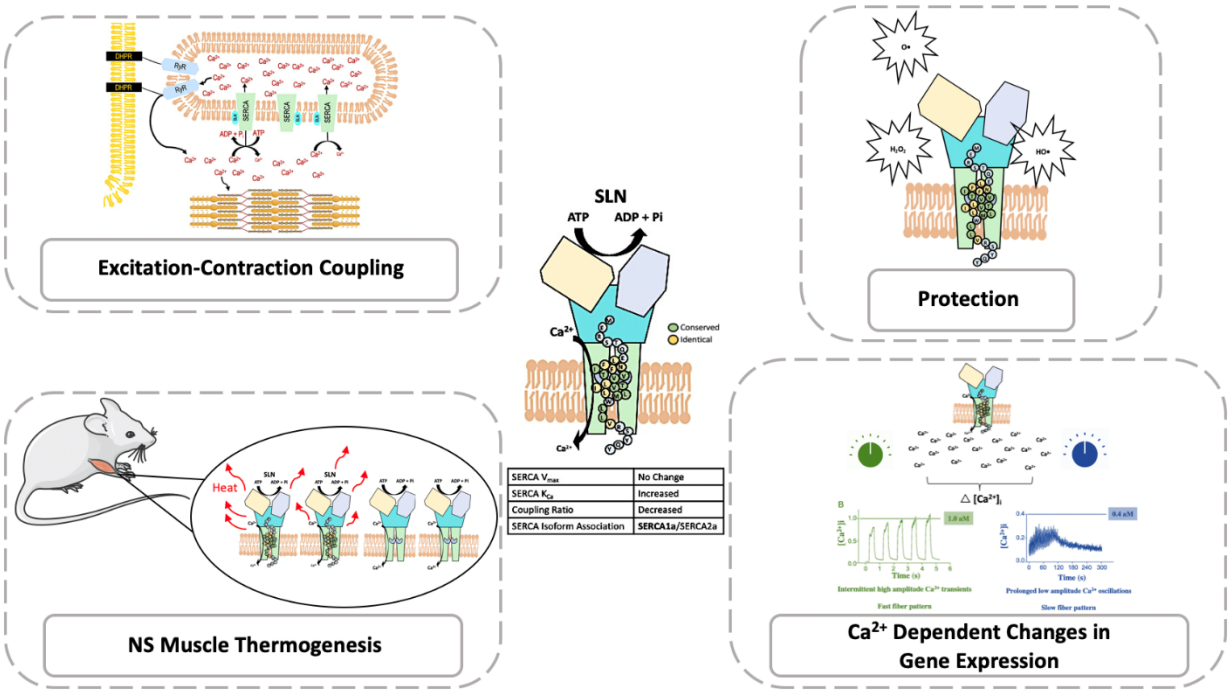


Fig. 1.4.7.1: Visual Summary of the Different Roles Exerted by the Interaction between SLN and SERCA
A graphical summary of the text above, illustrating the diverse biological roles of SLN in acting as a key regulator of muscle contraction and relaxation; a key modulator of skeletal muscle energy metabolism by increasing the energy requirement of the SERCA pumps to transport Ca^{2+}; a critical "dial" in altering the amount of Ca^{2+} transported by the pump to activate calcium signaling pathways that control adaptations in muscle mass and fiber type under conditions of muscle overload, disuse and disease; and a protector of the pump during times of cellular stress.

1.5 The Emergence of New SERCA Regulatory Proteins

The previous two sections have sought to comprehensively illustrate the complex yet distinct behavior of the two best understood SERCA regulators and the ensuing roles both proteins play in muscle function and metabolism. That being said, the advent of new SERCA regulatory proteins provides a new and exciting avenue of research aimed at understanding SERCA regulation and Ca^{2+} homeostasis. The two newly discovered proteins discussed below appear to exhibit a considerable degree of gene sequence conservation and homology, similar/complementary expression patterns, and the ability to modulate SERCA activity (both directly and indirectly). Given the extensive knowledge garnered on the roles of SLN and PLN in muscle Ca^{2+}-handling, there is still much research to be conducted on the physiological role of both MLN and DWORF, however, more pertinent to this thesis is if these proteins are able to interact and regulate SERCA activity in a fashion that is similar to that of SLN and PLN.

1.5.1 Myoregulin Discovery and Comparison of Structure Relative to Sarcolipin and Phospholamban

The MLN micropeptide was discovered as a functional small open reading frame during an analysis of an annotated skeletal muscle-specific long noncoding RNA [12]. It was found to localize with the SERCA pump (and the other regulatory proteins) via electroporation of a plasmid encoding GFP fused to MLN (GFP-MLN) into the flexor digitorum brevis muscle of adult mice. Subsequent confocal microscopy allowed for the simultaneous detection of GFP-MLN fluorescence which overlapped with the localization of an mCherry-SERCA1 fusion protein within the SR, a pattern consistent with the localization of GFP-PLN and GFP-SLN fusion proteins [12]. Coimmunoprecipitation western blotting verified the MLN:SERCA interaction, which was

expectedly abolished when shared residues with PLN and SLN were mutated, thus indicating a high conservation of sequence homology in the transmembrane domain [12].

MLN is a 46-amino acid, type II integral membrane protein which forms a single-pass transmembrane alpha helix composed of 19 N-terminal/cytosolic amino acid residues, 24 luminal residues and 3 C-terminal/luminal residues. N-terminal residues 5–10 are predicted to fold into a small beta sheet, while, the half extending into the C-terminal domain is predicted to contain the transmembrane alpha helix [12]. MLN shares a high degree of sequence homology with PLN and SLN, particularly in the transmembrane domain. This is to be expected as both PLN and SLN share a common interaction point with SERCA in the membrane of the SR in a groove formed by SERCA helices M2, M6, and M9. Not surprisingly, structural modeling comparison of transmembrane helices of the three proteins has shown that all three assemble into alpha helical structures with residues arranged in a similar spatial pattern [12]. In agreement with this, automated protein docking of the transmembrane model of MLN with the crystal structure of SERCA revealed that MLN aligned in the same groove that is occupied by PLN and SLN. However, MLN and PLN diverge from SLN in their N-terminal domains and additional secondary structures other than their transmembrane alpha helices. MLN and PLN have a more extensive N-terminal domain which encodes a beta sheet and alpha helix, respectively. As previously discussed, PLN's cytosolic domain is critical in facilitating its interaction with SERCA and the phosphorylation of residues at this domain diminishes the ability of PLN to modulate SERCA activity [12]. The N-terminal sequence of MLN offers similar potential as a regulatory domain through phosphorylation, as this sequence contains multiple serine and threonine residues. Finally, an examination of MLN's luminal domain in comparison to those of PLN and SLN reveals that MLN more similarly mirrors PLN as it does not possess SLN's signature RSYQY sequence which

extends into the lumen of the SR [12]. Overall, based on the stronger structural resemblance to PLN, it would be expected that MLN's interaction with SERCA would yield more similar effects to PLN than to that of SLN.

1.5.2 Expression Pattern of Myoregulin

The expression pattern of MLN shares some overlap but is predominately broader than the other regulatory proteins. During embryogenesis, MLN is expressed in the myotomal compartment of the somites, the anlagen of skeletal muscle. During fetal and adult stages, MLN has been reported to be robustly expressed in all murine skeletal muscles but is not detectable in cardiac or smooth muscles, appearing to follow the expression pattern of SERCA1. MLN transcripts have also been detected in C2C12 myoblasts and myotubes, but not in 10T1/2 fibroblasts [12]. Recall from Section 1.2 that PLN is mainly expressed in the ventricle where it regulates the activity of SERCA2a, whereas, in skeletal muscle, PLN is primarily in expressed in oxidative muscle where it has been shown to regulate both SERCA1a and SERCA2a, with a preference for SERCA2a [9]. Meanwhile, the expression of SLN is upregulated in rodent embryonic and neonatal skeletal tissue, whereas, in adult rodent skeletal muscle, SLN protein expression has been reported in both oxidative and glycolytic muscles, with greater protein expression predominantly in oxidative muscle, where both SERCA1a and SERCA2a are expressed [110]. This would imply that the expression of MLN would overlap with both SLN and PLN in oxidative muscle of adult rodents, whereas, SLN expression would coincide with the expression of MLN in fetal skeletal muscles and adult rodent oxidative and glycolytic muscles.

1.5.3 Myoregulin's Interaction with SERCA

The physiological function of MLN was assessed via Ca^{2+}-dependent Ca^{2+}-ATPase activity performed on homogenates prepared from HEK293 cells expressing SERCA1 alone or with MLN, SLN, or PLN respectively [12]. Expectedly, the effect of MLN on SERCA function and Ca^{2+} handling was similar to that of PLN and SLN, with all three proteins causing a significant reduction in the rate of Ca^{2+} uptake, measured as an increase in K_{Ca}. Additionally, perhaps more in line with the role of PLN, MLN was not shown to have an impact on V_{max} under any conditions tested [12]. In agreement with this, an examination of SR Ca^{2+} levels in primary myoblasts isolated from hindlimb muscles of *Mln*$^{-/-}$ (MLN knockout) versus WT littermates demonstrated that myoblasts obtained from of *Mln*$^{-/-}$ tissue exhibited significantly increased SR Ca^{2+} levels compared to WT myoblasts. This increase was not accompanied by changes in the expression of RYR1 nor SERCA1 and is thus consistent with the notion that MLN is an inhibitor of SERCA activity [12]. Furthermore, these *Mln*$^{-/-}$ mice were subjected to a regimen of forced treadmill running to exhaustion to investigate the potential role of MLN in regulating skeletal muscle performance. While *Mln*$^{-/-}$ mice did exhibit an overall increase in performance as indicated by a longer average running time and consequently an overall increase in distance ran, there were no accompanying histological differences in fibre type or myofiber size from glycolytic nor oxidative muscles when compared to between WT [12].

1.5.4 Dwarf Open Reading Frame Discovery and Comparison of Structure Relative to Sarcolipin and Phospholamban

The same group credited with the discovery of MLN has also been instrumental in the detection and study of DWORF, another SERCA regulatory protein [13]. DWORF is a 34-amino acid single pass transmembrane protein that was discovered in the same fashion as MLN [13]. Comparatively, DWORF shares the least sequence homology with the currently identified regulatory proteins [13]. Analysis of the quaternary structure is currently ongoing; similar to PLN and SLN, DWORF is subdivided into three distinct domains: a dynamic N-terminal domain, an amphipathic juxtamembrane helix, and a hydrophobic TM domain C-terminal helix. However, while PLN and SLN are composed of continuous transmembrane helices (residues ~ 24–48 and ~1–31, respectively), the DWORF transmembrane domain appears to be discontinuous, with a kink induced by Pro^{15}, separating the two helical domains [122, 123]. With DWORF being shown to have the highest affinity for conformations of SERCA that prevail at high calcium, it has been proposed that DWORF's juxtamembrane domain interacts with SERCA's M4 helix of SERCA's M2-M4-M6-M9 binding groove [124]. With M4 undergoing the most substantial movements throughout SERCA's catalytic cycle [125, 126], the hypothesis is that the kink could allow DWORF to better accommodate the structural transitions of the complex or even promote active states. Indeed, structural and functional data have shown that that Pro^{15} (and the induced kink) are critical for DWORF's interaction with and activating effect on SERCA (both indirectly and directly) [122, 123, 127].

Subcellular localization of DWORF to the SR membrane was determined via electroporation of a GFP–DWORF expression vector into the flexor digitorum brevis muscle of the mouse foot [13]. Subsequent multiphoton excitation microscopy revealed DWORF distribution

specific to the SR where it overlapped with mCherry-SERCA1, GFP-SLN, and GFP-PLN. Tissue distribution of DWORF was assessed via Northern blot analysis for mRNA expression, quantitative reverse transcription polymerase chain reaction (qRT-PCR) for RNA expression and western blotting for protein expression. All three methods determined that the expression of DWORF is limited to cardiac ventricle muscle and slow-oxidative skeletal muscle, including the soleus and diaphragm [13].

1.5.5 Dwarf Open Reading Frame Directly Activates the SERCA Pump and the Discrepancies Underlying the Mechanism of this Interaction

The interaction between DWORF and SERCA was confirmed in COS7 cells which underwent co-transfection with GFP (control) or GFP-DWORF and Myc-tagged SERCA [13]. Co-immunoprecipitation revealed that all isoforms of SERCA associated with the DWORF protein. Surprisingly, in similar experiments in which SERCA was co-transfected in the presence of DWORF in addition to the other regulatory proteins, the binding of DWORF and PLN, SLN, or MLN to SERCA was shown to be mutually exclusive, indicating that DWORF affects complex formation between SERCA and PLN, SLN, and MLN [13]. This is not the case with SLN and PLN as it has been shown that these two proteins can simultaneously bind to and interact with SERCA. In doing so, PLN and SLN form a superinhibitory binary complex that leads to drastic reductions in SERCA affinity for Ca^{2+} and in maximal rates of ATP hydrolysis and Ca^{2+}-uptake [106]. The ability of SLN and PLN to form such a complex with MLN has not yet been evaluated. Consequentially, further experimentation discovered that co-expression of DWORF alone with SERCA2a in COS7 cells had no bearing on SERCA's apparent affinity for Ca^{2+} and overall SERCA function [13]. However, the co-expression of DWORF and PLN, SLN or MLN,

respectively, with SERCA2a relieved the inhibition by these regulatory proteins in a dose-dependent manner. In order to combat the inhibitory function of PLN, SLN, or MLN on SERCA activity, threefold overexpression of DWORF was required to return SERCA activity to basal levels [13]. As such, the implication of these results is that the role of DWORF differs from that of the other regulatory proteins as DWORF does not *directly* regulate SERCA function but rather, acts as a non-inhibitory competitor that displaces the interaction between inhibitory regulators and SERCA in order to re-establish SERCA's Ca^{2+} affinity.

A subsequent study by Li *et al.* employed a combination of a cell-based FRET biosensor system and SERCA functional measurements to validate that DWORF does compete with and reverse PLN inhibition of the SERCA pump but challenged the proposed indirect mechanism of activation [127]. In accordance with initial reports, DWORF was determined to bind directly to SERCA2a and with the pump displaying a higher apparent affinity for DWORF than for PLN, DWORF effectively competed with PLN for SERCA2a binding [13, 127]. However, even in the absence of PLN, the interaction between DWORF and SERCA2a persisted and in fact, DWORF was shown to directly increased the Ca^{2+}– ATPase activity of SERCA at subsaturating Ca^{2+} levels by increasing SERCA's apparent Ca^{2+} affinity [127]. Work conducted by Fisher *et al* corroborated that DWORF does act directly on SERCA, however, not to enhance calcium affinity but rather, to increase SERCA maximal activity (V_{max}) [123]. At near equimolar ratio (~1–2 DWORF per SERCA), DWORF was shown to act as a direct activator by increasing the V_{max} of SERCA by 1.7-fold [123] – a magnitude comparable to that of the small-molecule activator of SERCA, CDN1163 (~1.5-fold; [128]). Improved SERCA V_{max} in the presence of DWORF was accompanied by increased SERCA-mediated Ca^{2+} uptake rates and an enlarged maximum SR calcium load. However, a significant effect of DWORF on the apparent Ca^{2+} affinity of SERCA

was not observed, nor was competitive displacement of PLN from SERCA [123]. The novel mechanistic insight provided by this study was that DWORF and PLN bind to SERCA in a calcium-dependent manner, with PLN binding more avidly to SERCA at low cytoplasmic [Ca^{2+}] and DWORF showing greater binding affinity under conditions of high [Ca^{2+}] [123]. This has been investigated further to reveal that DWORF and PLN bind to different intermediate states of SERCA as it moves through its enzymatic Ca^{2+} transport cycle [124]. PLN shows the highest affinity for SERCA in its E1-ATP state, which prevails at low [Ca^{2+}] and DWORF shows the highest affinity for SERCA in its E1P and E2P states, which dominate at high [Ca^{2+}] [124]. This would suggest that PLN and DWORF engage in a dynamic competition to inhibit SERCA at low cytoplasmic [Ca^{2+}] and stimulate SERCA during elevations in cytoplasmic [Ca^{2+}] [123].

Under the experimental conditions employed by Reddy *et al.*, which relied on oriented sample solid-state NMR (OS-ssNMR) and dynamic refinement in explicit membranes to determine the structure and membrane architecture of DWORF in lipid bilayers, DWORF was found to both reduce SERCA's Ca^{2+} affinity and increase SERCA's V_{max} [122]. SERCA's apparent Ca^{2+} affinity was decreased to a degree less than that of PLN but greater than SLN, while SERCA's V_{max} was enhanced to a magnitude significantly greater than both PLN and SLN. It would appear from the work done by this group that the stimulatory effect on V_{max} compensates for the K_{Ca} shift to enhance SERCA activity at high Ca^{2+} concentrations [122]. The stimulatory V_{max} effect is consistent with the results produced by Fisher *et al*, especially at higher [Ca^{2+}], however, the discrepancies in K_{ca} are interesting [122, 123]. Moreover, this dual mechanism of action appears to be dependent on the kink induced by Pro^{15}, as a mutation in this residue abolished the stimulatory effect on V_{max} without effecting DWORF's inhibition of SERCA's apparent calcium affinity [122].

The current literature which has investigated the mechanism underlying DWORF's interaction with and direct activation of SERCA is summarized in Table A.2 in Appendix A. The discrepancies between these studies can be attributed to differences in DWORF:SERCA stoichiometry, whether an animal-based, cell-based or reconstituted lipid system had been employed, the cell lines used, the presence of protein tags, and/or variations in reconstitution protocols which could affect lipid:protein ratios [13, 122, 123, 127]. Such discrepancies are not uncommon in studies investigating the SERCA regulators. Recall from Section 1.4.2 that there are inconsistences in the literature regarding whether SLN is able to alter SERCA V_{max}, with certain cell-based studies showing that SLN increases V_{max} and others showing that SLN doesn't have a bearing on this parameter [97]. While the studies discussed in this section are not cohesive in their findings, they have shed valuable insight and are consistent with showing that DWORF does interact with SERCA, that the affinity of this interaction is Ca^{2+}-dependent (with higher [Ca^{2+}] driving a stronger interaction between the two proteins) and that the kink induced by Pro^{15} is essential to DWORF's regulation of SERCA.

1.5.6 Relationship between Dwarf Open Reading Frame and Phospholamban

The relationship between DWORF and PLN is one of particular interest, especially in cardiac tissue [13, 129, 130]. The co-expression of SERCA2a with various ratios of DWORF and PLN in COS7 cells and subsequent co-immunoprecipitation have indicated that DWORF and PLN have similar binding affinities for SERCA [13]. In fact, fluorescence resonance energy transfer (FRET) imaging in live cell membranes has determined that SERCA exhibits a greater apparent affinity for DWORF than PLN [13]. Furthermore, mutations of residues known to interact with PLN on the M6 transmembrane helix of SERCA1 resulted in an impairment in SERCA interaction

with DWORF which was comparable to the weakened interaction of SERCA with PLN, thus implying that both peptides bind to similar regions of the SERCA pump [13].

1.5.7 Role of Dwarf Open Reading Frame in Cardiac Muscle

In vivo investigations into the role of DWORF in cardiac and skeletal muscle were achieved via $Dworf^{-/-}$ and $Dworf^{OE}$ transgenic mouse models [129]. The overexpression of DWORF in adult cardiomyocytes resulted in an elevation in the peak Ca^{2+} transient amplitude and a larger SR Ca^{2+} load, as well as, a decline in the time constant of cytosolic Ca^{2+} decay during each cycle of contraction-relaxation. These improvements in cardiac function were not accompanied by changes in protein expression of SERCA or other Ca^{2+} handling proteins, suggesting that DWORF is the driving force behind the increase in SERCA activity [129]. Indeed, the cellular phenotype induced by $Dworf^{OE}$ in cardiac muscle is analogous to that observed in $Pln^{-/-}$ mice. Collectively, this would imply that DWORF acts on SERCA activity by competing for and displacing PLN from the pump in order to relieve the inhibitory effects. With that in mind, researchers examined the potential role of DWORF in the pathophysiology of dilated cardiomyopathy [129]. As mentioned in Section 1.3.3, mammalian heart failure is accompanied by a reduction in expression of SERCA2a with no change in PLN content – this alters the PLN:SERCA2a ratio and creates a model of PLN superinhibition [65]. Through the employment of a transgenic mouse model of induced overexpression of both PLN and DWORF ($Pln^{OE}/Dworf^{OE}$), Makarewich, et al. demonstrated that isolated adult cardiomyocytes exhibited a complete amelioration of the impairments in Ca^{2+} handling associated with PLN overexpression [129]. SERCA activity assays performed on $Pln^{OE}/Dworf^{OE}$ cardiac homogenates showed a recovery in activity that mirrored that observed in $Dworf^{OE}$ mice. This suggests that the superinhibition of SERCA caused by PLN overexpression

can be completely nullified in the presence of DWORF overexpression [129]. Moreover, Western blotting confirmed that this improvement in SERCA function occurred without significant differences in protein or RNA expression levels of any of the major Ca^{2+}-handling proteins. While the endogenous protein content of DWORF in mammalian heart failure has currently not been investigated, the research highlighted here provides more than sufficient evidence that achieving improvements in SERCA function by targeting DWORF could represent a clinically relevant approach [129].

1.5.8 Role of Dwarf Open Reading Frame in Skeletal Muscle

Lastly, the role of DWORF in skeletal muscle Ca^{2+} homeostasis was determined through an examination of *Dworf*$^{-/-}$ vs WT soleus muscle, as this muscle exhibits the most abundant endogenous expression of the DWORF protein [13]. SERCA activity assays performed on soleus homogenates revealed a decrease in the apparent affinity of SERCA for Ca^{2+} in *Dworf*$^{-/-}$ tissue as compared to WT. However, this did not translate to an effect on contractile function as no differences in peak muscle force and in rates of relaxation rates at low, non-tetanic stimulation frequencies were observed [13]. Considering the work conducted in COS7 cells explained above, showing that DWORF alone does not directly affect SERCA's apparent affinity for Ca^{2+} and overall SERCA function, the change in affinity in muscle homogenate is surprising. Though, it could potentially be explained by greater binding of the other SERCA regulatory proteins in the absence of DWORF-mediated regulation [13]. There remains work to be done to establish the role of DWORF in muscle Ca^{2+}-handling, however, this protein offers much exciting potential. Recall from Sections 1.3.4 and 1.4.5 that the overexpression of PLN in skeletal muscle results in the onset of CMN. With DWORF overexpression in cardiac tissue successfully combating the

superinhibition caused by heightened PLN inhibition, it stands to serve that a similar effect could be observed in skeletal muscle of Pln^{OE} mice. While this hypothesis will not be examined in this thesis, it does provide further support of the complexity of SERCA and consequentially Ca^{2+}-regulation. Indeed, with the discovery of these newly identified micropeptides and the potential for even more to be unearthed, the SERCA regulatory complex is beginning to resemble that of the Na^{+}/K^{+}-ATPase (NKA), a related ion transporter which shares extensive structural homology with the SERCA pump, as both are members of the II class of P– type ATPases and share ~65% protein sequence similarity [131, 132]. The NKA has been shown to be associated with numerous tissue specific and species-specific regulatory peptides and it stands to reason that SERCA could exhibit a similar need for a multitude of regulators [131, 132]. The differential expression of diverse micropeptides may function to precisely tune the activity of ion transporter isoforms to the needs of myocytes and the muscle itself. Thus, understanding peptide-transporter regulatory interactions, as well as, the interactions between the regulatory proteins themselves is relevant to not only our understanding of healthy muscle function but to disease prevention and treatment.

1.5.9 Summary of Literature and Gaps Therein

To summarize, currently MLN expression has been identified in all skeletal muscle, with the greatest degree present in glycolytic muscle fibres, and it has been shown that MLN co-localizes primarily with the SERCA1a isoform, where it appears to exert an inhibitory effect similar to that of PLN and SLN [13]. Likewise, the same research group has proven that DWORF protein expression has been identified solely in the left ventricle of the heart and oxidative muscle fibres where it acts to enhance SERCA function by displacing SLN, PLN and MLN from the pump [13]. However, there has been no validation or further investigations into MLN in the literature

outside of the research group which identified it. Furthermore, this group was unable to directly blot for MLN in both their cell model and transgenic animal model. These researchers employed a N-terminal HA-tagged MLN fusion protein (HA-MLN) and a C-terminal FLAG-tagged MLN fusion protein (FLAG-MLN) in their cell model and subsequently blotted for the HA/FLAG-tags in order to determine MLN expression. Meanwhile, their transgenic *Mln*$^{-/-}$ mouse model was confirmed through southern blot analysis and real-time PCR which demonstrated an absence of the MLN transcript [13]. While these are valid measures, it is concerning that there has been no *direct* measure of MLN protein identification and expression. The expression pattern of SLN, PLN and MLN reported were determined via real-time PCR and RNA sequencing analysis, however, these measures were unable to detect expression of PLN in any skeletal muscle and showed an abundance of PLN expression in cardiac atria – which our group and others have proven to be inaccurate [13]. Similarly, these measures failed to identify SLN expression in both glycolytic and oxidative hind limb skeletal muscle. This is not the case for the DWORF protein, as researchers have confirmed expression at the mRNA, RNA and protein levels [13]. It will be imperative to validate the presence and expression of these proteins, especially MLN, in our cell and animal models in order to understand their role in SERCA regulation.

With these regulatory proteins reportedly sharing such a high degree of sequence homology and possessing common interaction sites with SERCA, it is of interest to evaluate the similarities and differences in their respective interactions and the subsequent effect on Ca^{2+}-handling. As highlighted in the previous sections, while PLN and SLN share extensive sequence homology, their interaction with SERCA and physiological roles are considerably distinct. The commonalities in structure enable both regulatory proteins to be key modulators of skeletal muscle contraction and relaxation and to prevent oxidation and nitrosylation of SERCA in order to preserve SERCA

function during cellular stress. With SLN remaining bound to SERCA throughout its catalytic cycle, it allows for more of a fine tuning of $[Ca^{2+}]_i$, in doing so, it assists to facilitate the maintenance of $[Ca^{2+}]_i$ (spatially and temporally) in a manner that would drive a slow fibre pattern and oxidative phenotype in muscle. Moreover, because SLN is altering the amount of Ca^{2+} ions transported without affecting the energy requirement, it is inducing inefficiency of the pump and modulating skeletal muscle energy metabolism. With SERCA playing such an integral and dynamic role in skeletal muscle Ca^{2+} homeostasis, and its regulatory proteins playing such important and diverse roles, evaluating if MLN and DWORF can uncouple Ca^{2+} transport from ATP hydrolysis and consequentially contribute to $[Ca^{2+}]_i$ signalling pathways and alter energy expenditure will prove to be invaluable, particularly because MLN is expressed across all muscle types. Given that MLN shares a higher degree of sequence homology with PLN and lacks SLN's signature cytosolic domain (that is responsible for conferring SLN's uncoupling capabilities [92]), it is unlikely that MLN shares the ability to uncouple SERCA. On the other hand, DWORF shares the least sequence homology, however, DWORF shows the highest affinity for SERCA in its E1P and E2P states, which dominate at high $[Ca^{2+}]$, a characteristic shared with SLN which could confer some sort of ability to fine tune Ca^{2+} transport in a manner similar to SLN.

Moreover, it is unknown from previous studies whether MLN and/or DWORF can protect the SERCA pump from thermal instability during times of cellular stress, such as the thermal instability caused by heat shock. Given the degree of sequence homology and the overlap of interaction sites with the pump, it stands to reason that the interaction of MLN and DWORF with SERCA is similar enough to confer protection and preservation of maximal energy. Of potentially greater interest are differences in protection as a result of dissimilarities in sequence and interaction of MLN and DWORF with SERCA. In the protection study completed by Fu and associates, SLN

and PLN were shown to prevent both carbonyl and nitrotyrosine formation, however, a mutation in PLN that altered its interaction with SERCA also changed the protection that was conferred. With a weakened interaction between SERCA and mutant PLN, carbonyl but not nitrotyrosine modification of the pump was prevented [11]. Likewise, the differences in the strength and specific amino acid sites of interaction between SERCA and MLN/DWORF could result in unique protective properties.

Multiple groups, including our own, have employed single knockout ($Sln^{-/-}$ and $Pln^{-/-}$) mice and double knockout ($Sln^{-/-}/Pln^{-/-}$) mice to investigate the physiological roles of SLN and PLN with great success (as explained in Sections 1.3 and 1.4), therefore, it is unclear whether the expression profile of MLN and DWORF are altered in the presence and absence of either and/or both proteins. With the single knockout ($Sln^{-/-}$ and $Pln^{-/-}$) and double knockout ($Sln^{-/-}/Pln^{-/-}$) mouse models available to us, it is of great interest to explore if the regulatory proteins work in concert to modulate SERCA function, especially in muscle in which all four proteins could be expressed, such as the soleus. While differences in regulatory protein structure and consequentially distinctions in the physiological role exerted by each protein can explain the profound physiological effects observed in the single knockout studies, ultimately the role of these regulatory proteins is to modulate SERCA, therefore, understanding if the regulatory proteins are acting independently or are redundant in some capacity is relevant to not only our understanding of healthy muscle function but to disease prevention and treatment.

1.6 Statement of the Problem:

The primary objectives for this thesis are to: 1) investigate whether the interaction between MLN:SERCA and DWORF:SERCA can protect the pump from damage during times of cellular stress, such as the thermal instability caused by heat shock; 2) determine whether MLN and/or DWORF are able to alter SERCA Ca^{2+} pumping efficiency; and 3) examine the potential redundancy in SERCA regulation by evaluating MLN and DWORF protein expression and interaction in *Sln*$^{-/-}$, *Pln*$^{-/-}$, and *Sln*$^{-/-}$/*Pln*$^{-/-}$ mice.

CHAPTER 2

Methodology

2.1 Culture and Co-transfection of HEK-293 Cells

All cells were maintained at 37°C, with the addition of 5% CO2. Human embryonic kidney (HEK-293) cells were cultured in 15 cm tissue culture-treated dishes in Dulbecco's Modified Eagle's Medium (DMEM) containing 10% fetal bovine serum (FBS) and 1% penicillin-streptomycin.

The culture of HEK-293 cells and their co-transfection with cDNAs was conducted according to the protocol described in earlier publications [80, 133-136]. cDNAs encoding rabbit SERCA1a, rabbit SERCA2a [80], mouse MLN and mouse DWORF [97] were used in these experiments. Plasmid DNAs were purified by using Qiagen columns (Mississauga, Ontario, Canada) and were subsequently co-transfected into HEK-293 cells using the polyethylenimine (PEI) reagent at a molar ratio of 1:1 for cDNA encoding SERCA1/2a to those encoding MLN or DWORF with a total plasmid DNA of 20 μg (S1a (10 μg)/MLN (10 μg) or S1a (10 μg)/DWORF (10 μg); S2a (10 μg)/MLN (10 μg) or S2a (10 μg)/DWORF (10 μg)). Cells transfected with the same amount of cDNA encoding SERCA1/2a were used as controls (S1a (20 μg) & S2a (20 μg)).

For heat shock treatment, 23 h following transfection, half of the plates from each group was incubated at 40°C for one hour before harvesting (HS) (n=3/group). The other half of the plates were incubated at 37°C for the full 24 hours to be used as controls (CTL) (n=3/group).

For ratio experiments, HEK-293 cells were transfected using the PEI reagent at a molar ratio of 1:1, 1:3 and 1:5 for cDNA encoding SERCA1/2a to those encoding DWORF with a total plasmid DNA of 20 μg. For the 1:1 molar ratio: S1a (10 μg)/DWORF (10 μg) and S2a (10 μg)/DWORF (10 μg)). For the 1:3 molar ratio: S1a (5 μg)/DWORF (15 μg) and S2a (5 μg)/DWORF (15 μg)). Lastly for the 1:5 molar ratio: S1a (3.4 μg)/DWORF (16.6 μg) and S2a (3.4

μg)/DWORF (16.6 μg)). Cells transfected with the following amount of cDNA encoding SERCA1/2a were used as controls: (S1a (20 μg) & S2a (20 μg)).

2.2 Preparation of Cell Homogenate

Crude cell homogenate were isolated from harvested HEK-293 cells, frozen in liquid nitrogen and stored at -80 °C as described previously [135]. Cells were harvested 24 hours after transfection in an ice-cold solution of PBS (137 mM NaCl, 10 mM phosphate, 2.7 mM KCl, pH 7.4) containing 5 mM EDTA. In order to obtain the appropriate amount of crude cell homogenate, 5 plates were pooled during harvest, for an n = 3/group. The cells were pelleted by centrifugation at 3000 g for 5 min at 4 °C and washed twice in ice-cold PBS alone. After removal of the supernatants, the cells were resuspended in homogenization buffer containing 250 mM sucrose, 5 mM HEPES, 0.2 mM PMSF and 0.2% NaN_3, homogenized on ice and stored at -80 °C. Total protein concentration was measured by the method of Lowry, as modified by Schacterle and Pollock [137]

2.3 SERCA Measurements

2.3.1 Ca^{2+} Dependent Ca^{2+}- ATPase Activity

Ca^{2+} dependent Ca^{2+}-ATPase activity (μmol ATP/g protein/minute) was measured in crude cell homogenates using an NADH-linked spectrophotometric assay as previously described by our group [138]. ATPase buffer (pH: 7.0) contained in mM: 200 KCl, 20 HEPES, 10 NaN3, 1 EGTA, 15 MgCl2 (Sigma-Aldrich), 10 phosphoenolpyruvate (BioVectra, Charlottetown, PE, Canada), and 5 ATP (Sigma-Aldrich). Following the addition (18 U/mL) of the auxiliary enzymes lactate dehydrogenase (Sigma-Aldrich, product #: L2625-25KU) and pyruvate kinase (Sigma-Aldrich, product #: 10 128 163 001), crude cell homogenates were added to the reaction cocktail, which was then partitioned into 12 Eppendorf tubes containing incrementally greater volumes of $CaCl_2$,

giving free Ca^{2+} concentrations ($[Ca^{2+}]_f$) ranging from pCa (i.e. –log10[Ca2+]*f*) 6.85 – 4.80. Parallel reactions were run for each sample in the presence (1 μM) and absence of the Ca^{2+}-specific ionophore A23187 (Sigma-Aldrich, product #: C7522) within the reaction mixture. In the absence of the Ca^{2+} ionophore, vesicular Ca^{2+} accumulates and can induce back-inhibition of SERCA pumping (123), which more closely mimics the physiological condition of intact muscle. An additional tube (pCa: 4.5) contained 0.12 mM of the highly specific SERCA inhibitor cyclopiazonic acid (CPA; Sigma-Aldrich, product #: C1530), which was used to determine background activity and subtracted from each reaction mixture. Duplicates (100 μl) from each reaction tube were added to a clear round-bottom 96-well plate, and reactions were started by the addition of 0.3 mM NADH (Sigma-Aldrich, product #: 12166339), after which the decreasing rate of NADH absorbance at 340 nm was read for 30 min at 37°C.

To determine the exact $[Ca^{2+}]_f$ present in each reaction well, 1.2 μM of the Ca^{2+}- sensitive ratiometric dye Indo-1 (Biotium, Freemont, CA) was added to the reaction cocktail and partitioned into opaque Eppendorf tubes as above. Two additional tubes containing either zero $CaCl_2$ or 100 mM $CaCl_2$ were included as minimum and maximum measurements, respectively. Triplicates (100 μl) of each reaction tube were added to an opaque 96-well plate and incubated in the dark for 30 min at 37°C, and were read at an excitation wavelength of 355 nm using a fluorometric plate reader. Due to its peak absorbance wavelength and fluorescent properties, NADH was omitted from the reaction mixture. The emission maxima for the Ca^{2+}-free (G) and Ca^{2+}-bound (F) states of Indo-1 were measured at 485 nm and 405 nm, respectively, and the ratio (R) of F to G was used to calculate $[Ca^{2+}]_f$ according to the following equation (124):

Equation 1: $$[Ca^{2+}]_f = K_d \bullet (G_{max}/G_{min})\,(R - R_{min})/(R_{max} - R)$$

where K_d (250 nM) is the equilibrium constant for the interaction between Indo-1 and Ca^{2+} in homogenate (124), G_{max} is the maximum value of G (i.e. zero $CaCl_2$ well), G_{min} is the minimum value of G upon the addition of 100 mM $CaCl_2$ (i.e. max Ca^{2+} well), R_{min} is the minimum value of R (i.e. zero $CaCl_2$ well) and R_{max} is the maximum value of R upon the addition of 100 mM $CaCl_2$ (i.e. max Ca^{2+} well).

Activity curves were plotted as ATPase rate against pCa values using non-linear regression (GraphPad Prism software). The apparent Ca^{2+} affinity (i.e. K_{Ca}: pCa value at half-maximal ATPase activity) was calculated using the sigmoidal dose-response equation:

Equation 2: $$Y = Y_{bot} + (Y_{top} - Y_{bot}) / (1 + {}^{(LogCa50 - x)} * n_H)$$

where Y_{bot} is the value at the bottom of the plateau, Y_{top} is the value at the top of the plateau, $LogCa_{50}$ is the logarithm of pCa_{50} and n_H is the Hill coefficient.

The experimental data was normalized for corresponding protein content as determined by the method of Lowry, as modified by Schacterle and Pollock [137] [133]. The values for maximal SERCA activity (V_{max}) were taken directly from the experimental data.

2.3.2 Ca^{2+}-Dependent Ca^{2+}-Uptake Activity

Ca^{2+}-dependent Ca^{2+}-uptake rate (μmol Ca^{2+}/g protein/minute) was measured in crude cell homogenates in both the presence and absence of the precipitating anion oxalate. Similar to the absence of ionophore described above, the removal of oxalate from the assay more closely resembles the physiological condition of intact muscle as it allows vesicular Ca^{2+} to accumulate and induce back-inhibition of SERCA pumping [23]. Rates of Ca^{2+}-uptake were measured using the Ca^{2+}-sensitive fluorescent dye Indo-1 as previously described [138], but fitted onto a 96-well plate [135, 139]. As described above, $[Ca^{2+}]_f$ measurements are based on the difference in Ca^{2+}

bound Indo-1 (F) and Ca^{2+} free Indo-1 (G) complexes which have emission wavelengths of 405 and 485 nm upon excitation with a 355 nm wavelength, respectively.

Crude cell homogenates, along with Indo-1 (2 μM), were added to Ca^{2+} uptake buffer (200 mM KCl, 20 mM HEPES, 10 mM NaN3, 5 lM N,N,N0,N0-tetrakis(2-pyridylmethyl)ethylenediamine, 15 mM MgCl2, pH 7.0) along with Indo-1 (4 lM final concentration; 57180, Sigma-Aldrich). Samples were plated in duplicate and Ca^{2+} uptake was initiated with ATP (10 mM final concentration). A Molecular Devices M2 plate reader was used to kinetically (shaking the wells prior to each read) measure fluorescence of Ca^{2+}-bound Indo-1 (405 nm emission) and Ca^{2+}-free Indo-1 (485 nm emission) upon excitation at 355 nm at 37 °C. Once the reaction had plateaued (i.e. vesicles filled), 10 μl of EGTA (50 mM) and 80 μl of $CaCl_2$ (100 mM) were added to achieve maximally free and Ca^{2+}-bound states of Indo-1, respectively. **Equation 2** (above) was used to determine change in $[Ca^{2+}]_f$ by time (i.e. Ca^{2+}-uptake rate), after which curves were smoothed over 21 points using a Savitsky-Goloay algorithm, with all rates then normalized to total protein content. Ca^{2+}- uptake rates were measured using linear regression ±100 nM at the following $[Ca^{2+}]_f$: 1000 nM (pCa 6.00) and 500 nM (pCa 6.30). The apparent coupling ratio of SERCA was determined by dividing each Ca^{2+}-dependent uptake rate by the Ca^{2+}-dependent ATPase rate under each condition (i.e. presence/absence of Ca^{2+} gradient).

2.4 Measurements of Oxidative Stress

2.4.1 Carbonyl Formation in SERCA1/2a

Oxidation of SERCA1/2a was assessed by measuring protein carbonyls in SERCA1/2a as described previously [140]. SERCA1/2a protein was immunopreciptated with anti-SERCA1a and anti-SERCA2a monoclonal anti-body, respectfully. The washed beads were treated with 10 μl of

5% SDS. After derivatization with 20 µl of 10 mM 2,4-dinitrophenylhydrazine (2,4-DNPH) in 2M HCl at room temperature for 15 minutes, samples were neutralized by adding 20 µl of 2 M Tris base, 30% (V/V) glycerol and diluted in 30 µl of 2 x SDS-PAGE gel loading buffer. The samples were subsequently separated in a gradient polyacrylamide gel of 10% by SDS-PAGE. After blocking, carbonyl was detected with mouse anti-DNP monoclonal antibody at 1:20000 and HRP-conjugated goat anti-mouse IgG at 1:5000 in TBST containing 0.2% BSA for 1 hour at room temperature [141]. SERCA1/2a protein in the immunoprecipated samples was quantified through Western blotting and used to normalize the carbonyl values. The Chemidoc MP colorimetric imaging system (BioRad, Hercules, CA, USA) was used to detect proteins of interest. Meanwhile quantification and analysis of relative protein content using bands from chemiluminescent imaging and Ponceau staining, was done on ImageLab software (Version 6.0.1, BioRad, Hercules, USA) to determine relative carbonyl levels.

2.4.2 Nitrotyrosine Levels in SERCA1/2a

Nitrosylation of SERCA1/2a was assessed by measuring nitrosylation formation in SERCA1/2a as described previously [140]. SERCA1/2a protein was immunopreciptated with anti-SERCA1a and anti-SERCA2a monoclonal anti-body, respectfully. The washed beads were treated with 10 µl of 5% SDS. After derivatization with 20 µl of 10 mM 2,4-dinitrophenylhydrazine (2,4-DNPH) in 2M HCl at room temperature for 15 minutes, samples were neutralized by adding 20 µl of 2 M Tris base, 30% (V/V) glycerol and diluted in 30 µl of 2 x SDS-PAGE gel loading buffer. Samples were separated in a gradient polyacrylamide gel of 10% by SDS-PAGE and transferred to PVDF membranes. After blocking in 5% skim milk in TBST at 4°C overnight, nitrotyrosine was detected with mouse anti-nitrotyrosine monoclonal antibody at

1:1500 and HRP-conjugated goat anti-mouse IgG at 1:2000 for 1 h at room temperature. SERCA1a/2a protein in the immunoprecipated samples were quantified through Western blotting and used to normalize the nitrotyrosine values. The Chemidoc MP colorimetric imaging system (BioRad, Hercules, CA, USA) was used to detect proteins of interest. Meanwhile quantification and analysis of relative protein content using bands from chemiluminescent imaging, was done on ImageLab software (Version 6.0.1, BioRad, Hercules, USA) to determine relative nitrotyrosine levels.

2.5 Western Blot Analysis

2.5.1 Crude Cell Homogenate

The protein expression levels of SERCA1a, SERCA2a, MLN and DWORF in HEK-293 cells were detected and quantified with standard Western blotting. 10 ul of 0.5% Triton X-100 was added to each sample of crude cell homogenate, following which, the samples were solubilized in a 1x solubilizing buffer (0.1% 2-Mercaptoethanol, 0.0005% Bromophenol blue, 10% Glycerol, 2% SDS, and 63 mM Tris-HCl (pH 6.8)) and denatured by heating to 95°C for 5 minutes prior to separation by SDS-PAGE. Upon electrophoresis, the separated proteins were transferred onto polyvinylidene difluoride (PVDF) membrane (SERCA1a, SERCA2a, MLN and DWORF) with transfer buffer (25 mM glycine, 192 mM Tris base, 20% methanol, 0.1% [w/v] SDS). The membranes were then incubated in blocking solution (TBST buffer: 20mM Tris base, 137 mM NaCl, and 0.1% (v/v) Tween 20, pH 7.5, with 5% [w/v] non-fat dry milk (SERCA1a, SERCA2a and DWORF) or with 5% bovine serum albumin (BSA) (MLN). Proteins were immunoprobed with the corresponding primary antibodies for SERCA1a ((A52) monoclonal antibody acquired as a generous gift from Dr. David MacLennan (University of Toronto)); SERCA2a ((2A7-A1, product no.: MA3–919) monoclonal mouse antibody acquired from Thermo Fisher Scientific);

DWORF monoclonal rabbit antibody acquired as a generous gift from Dr. Eric Olsen (University of Texas Southwestern); and MLN (polyclonal rabbit antibody #2211 acquired from Lampire Biological Laboratories). Subsequently, the proteins were immunoprobed with horseradish peroxidase-conjugated secondary antibodies: goat anti-mouse IgG (SERCA1a and SERCA2a) and goat anti-rabbit IgG (MLN and DWORF), which were obtained from Santa Cruz Biotechnology. Luminata Forte^{TM} was used to detect SERCA1a, SERCA2a, and DWORF, whereas, SuperSignal West Femto^{TM} substrate (Pierce, Thermo Fisher Scientific Inc) will be used to detect MLN. The Chemidoc MP colorimetric imaging system (BioRad, Hercules, CA, USA) was used to detect proteins of interest. Meanwhile quantification and analysis of relative protein content using bands from chemiluminescent imaging and Ponceau staining, was done on ImageLab software (Version 6.0.1, BioRad, Hercules, USA). All values were normalized to protein content as determined from Ponceau staining. All primary, secondary, and detection conditions for each protein are outlined in **Appendix A** (**Table A.5**).

2.5.2 Mouse Muscle Homogenate

The protein expression levels of SLN, PLN, MLN and DWORF in mouse soleus, left ventricle and atria were detected and quantified with standard Western blotting. Upon excision, the muscle samples were detendonized and weighed to determine muscle mass. These samples were then homogenized 1:10 (w/v) in ice-cold homogenizing buffer (250 mM sucrose, 5 mM HEPES, 0.2 mM PMSF and 0.2% [w/v] NaN_3) using a glass homogenizer and stored at -80°C. Subsequently, these muscle homogenates were solubilized in a 1x solubilizing buffer (0.1% 2-Mercaptoethanol, 0.0005% Bromophenol blue, 10% Glycerol, 2% SDS, and 63 mM Tris-HCl (pH 6.8)) and the proteins were separated by SDS-PAGE. Upon electrophoresis, the separated proteins were transferred onto polyvinylidene difluoride (PVDF) membrane (PLN, MLN and DWORF)

and nitrocellulose membrane (SLN) with transfer buffer (25 mM glycine, 192 mM Tris base, 20% methanol, 0.1% [w/v] SDS). The membranes were then incubated in blocking solution (TBST buffer: 20mM Tris base, 137 mM NaCl, and 0.1% (v/v) Tween 20, pH 7.5, with 5% [w/v] non-fat dry milk (PLN and DWORF) or with 5% bovine serum albumin (BSA) (SLN and MLN). Proteins were immunoprobed with the corresponding primary antibodies for PLN ((MA3-922) monoclonal mouse antibody acquired from Pierce Antibodies); SLN ((ABT13) polyclonal rabbit antibody acquired from Sigma-Aldrich); DWORF monoclonal rabbit antibody acquired as a generous gift from Dr. Eric Olsen (University of Texas Southwestern); and MLN (polyclonal rabbit antibody #2211 acquired from Lampire Biological Laboratories). Subsequently, the proteins were immunoprobed with horseradish peroxidase-conjugated secondary antibodies: goat anti-mouse IgG (PLN) and goat anti-rabbit IgG (SLN, MLN and DWORF), which were obtained from Santa Cruz Biotechnology. Luminata Forte™ was used to detect PLN and DWORF, whereas, SuperSignal West Femto™ substrate (Pierce, Thermo Fisher Scientific Inc) was used to detect SLN and MLN. The Chemidoc MP colorimetric imaging system (BioRad, Hercules, CA, USA) was used to detect proteins of interest. Meanwhile quantification and analysis of relative protein content using bands from chemiluminescent imaging and Ponceau staining, was done on ImageLab software (Version 6.0.1, BioRad, Hercules, USA). All values were normalized to protein content as determined from Ponceau staining. All primary, secondary, and detection conditions for each protein are outlined in **Appendix A** (**Table A.5**).

2.6 Experimental Animals and Genotyping

2.6.1 *Pln*$^{-/-}$ Line

Heterozygous breeding pairs (i.e. *Pln*$^{+/-}$, strain genetic background: mix of C57BL/6, C3H, and 129S2/SvPas) were purchased from Mutant Mouse Regional Resource Centers (MMRRC;

strain name: STOCK Plntm1Egk/Mmmh, stock number: 000027-MU) and used to establish a *Pln*$^{-/-}$ colony at the University of Waterloo. Animals were group housed at room temperature (~22°C) under a 12:12-hr reverse light/dark cycle, and given ad libitum access to standard rodent chow (8640 Teklad 22/5 Rodent Diet, Teklad Diets, Madison, WI) and water. Genotyping of experimental animals was done according to MMRRC instructions by digesting ear clippings using the protocol outlined in Appendix A and appropriate forward and reverse primers (**Appendix A: Table A.4**). All experiments were conducted using 4-6 month old homozygous male and female PLN knock-out (*Pln*$^{-/-}$) and WT (*Pln*$^{+/+}$) littermate controls. Studies were approved by the University of Waterloo Animal Care Committee and carried out in accordance with the Canadian Council on Animal Care.

2.6.2 *Sln*$^{-/-}$ Line

Transgenic mice lacking sarcolipin (*Sln*$^{-/-}$) were generously donated by Drs. David MacLennen and Anthony Gramolini (University of Toronto) and used to establish a breeding colony at the University of Waterloo. *Sln*$^{-/-}$ mice were crossbred with C57BL/6J mice to generate heterozygous *Sln*$^{-/-}$ breeding pairs. Breeding pairs yielded homozygous sarcolipin knockout (*Sln*$^{-/-}$), heterozygous (*Sln*$^{+/-}$) and homozygous wild type (*Sln*$^{+/+}$) mice. Animals were group housed at room temperature (~22°C) under a 12:12-hr reverse light/dark cycle, and given ad libitum access to standard rodent chow (8640 Teklad 22/5 Rodent Diet, Teklad Diets, Madison, WI) and water. Genotyping of experimental animals was done according to MMRRC instructions by digesting ear clippings using the protocol outlined in Appendix A and appropriate forward and reverse primers (Appendix A: Table A.4). All experiments were conducted using 4-6 month old homozygous male and female SLN knock-out (*Sln*$^{-/-}$) and WT (*Sln*$^{+/+}$) littermate controls. Studies were approved by

the University of Waterloo Animal Care Committee and carried out in accordance with the Canadian Council on Animal Care.

2.6.3 *Pln*$^{-/-}$/*Sln*$^{-/-}$ Line

Generation of DKO mice was achieved by crossing heterozygous mice of each colony (i.e. *Sln*$^{+/-}$ and *Pln*$^{+/-}$). This strategy yielded homozygous founder WT (i.e. *Sln*$^{+/+}$/*Pln*$^{+/+}$) and DKO (i.e. *Sln*$^{-/-}$/*Pln*$^{-/-}$) mice, which were then used to establish separate WT and DKO lines. Animals were group housed at room temperature (~22°C) under a 12:12-hr reverse light/dark cycle, and given ad libitum access to standard rodent chow (8640 Teklad 22/5 Rodent Diet, Teklad Diets, Madison, WI) and water. All experiments were conducted using 4-6 month old male and female mice and were approved by the University of Waterloo Animal Care Committee and carried out in accordance with the Canadian Council on Animal Care.

2.7 Tissue Collection

All chemicals were purchased from BioShop Canada Inc. (Burlington, ON, Canada) unless indicated otherwise. Animals (4-6 month old) were euthanized by cervical dislocation and muscles were excised, cleaned of connective and extraneous tissue, and placed in ice-cold phenylmethylsulfonyl fluoride (PMSF; Sigma-Aldrich, Oakville, ON, Canada) buffer (pH: 7.5). PMSF buffer contained in mM: 250 sucrose, 5 HEPES, 0.2 PMSF, and 0.2% (w/v) NaN3 (Fisher Scientific, Fair Lawn, NJ). Due to tissue requirements for the RT-qPCR and western blotting (described below), atria from 2-3 animals of each genotype were pooled together (n = 3/genotype). SOL, LV and atria muscles were either homogenized 1:10 (w/v) in ice-cold PMSF buffer using a glass-on-glass Dounce homogenizer after which aliquots were frozen in liquid nitrogen or immediately flash frozen in liquid nitrogen and stored at -80°C until needed.

2.8 RNA Extraction, Reverse Transcription (RT) and Real-Time (q) PCR

Total RNA was isolated from mouse skeletal muscle using TRIzol® Reagent (1 mL/≤100 mg tissue) using a glass homogenizer. Samples were then incubated at room temperature for 5 minutes, followed by the addition of chloroform (20% of TRIzol® volume) with vigorous shaking for 15-20 seconds, incubation at room temperature for 2 minutes, and centrifugation at 12,000 x g for 15 minutes at 4°C. The upper aqueous phase of each sample was removed and mixed with isopropanol (50% of initial volume of TRIzol®), and incubated at room temperature for 10 minutes to precipitate the RNA. Samples were then be centrifuged at 12,000 x g for 10 minutes at 4°C, pelleting the RNA. The supernatant was discarded and the pellet washed in 1 mL of 75% ethanol-25% DEPC-ddH2O, centrifuged at 7,500 x g for 5 minutes at 4°C, then air-dried for 5-10 minutes prior to suspension in 20-50 μL DEPC- ddH2O. The samples were then be incubated at 58°C for 10 minutes to facilitate solubilisation, and stored long-term at -80°C. RNA samples were quantified using a Nanodrop 2000 Spectrophotometer and samples were adjusted to 2 μg/μL.

cDNA was synthesized from 1 μg of RNA by oligo(dT) priming using a High-Capacity cDNA Reverse Transcription Kit according to the manufacturer's protocol (Thermo Scientific). Briefly, 1 μg of RNA was mixed with 10 μL of a reverse-transcription master mix with pre-added RNAse inhibitors (2 μL of 10X RT Buffer, 0.8 μL of dNTP mix (100 mM), 2 μL of RT Random Primers (oliogoDT), 1 μL of Reverse Transcriptase, 4.2 μL of ddH2O). Samples were then incubated in a thermocycler at 25°C for 10 minutes, followed by 37°C for 120 minutes, then finally 85°C for 5 minutes. cDNA was stored long term at -20°C.

For real-time PCR assays (qPCR), 1 μL of cDNA was added to a 96-well plate pre-loaded in each well containing 5 μL of SYBR™ Green (BioRad) Master Mix, 6.67 μM of each forward-

and reverse-primer (pre-diluted to 100 μM stock, 1 μL of each added), and 3 μL of ddH2O. Thermal cycling conditions were 95°C for 2 minutes, followed by 40 cycles at 95°C for 10 seconds, then 60°C for 20 seconds. At the end of the cycling protocol, a melt curve analysis was run to ensure primer specificity for the intended product of interest. Gene expression levels were calculated using the $2^{-\Delta\Delta C}$t method, expressing results normalized to *18S*, and relative to expression in control samples. A list of primer sequences used for qPCR analysis is found in Table A.3 in Appendix A.

2.9 Statistical Analyses

For Thesis Study I: Two-way ANOVA was used to assess the two main effects of HS and presence/absence of MLN or DWORF on each SERCA isoform. Statistical significance was set to p value ≤ 0.05 and when appropriate Tukey's post hoc test was used to determine where specific differences lie.

For Thesis Study II: 2-tailed Student's T-tests (independent samples) were used to assess the main effect of the presence and absence of either MLN and DWORF compared to SERCA1a/2a alone on SERCA K_{Ca} and V_{max}. Statistical significance was set to p value ≤ 0.05 and when appropriate Tukey's post hoc was used test to determine where specific differences lie.

For Thesis Study III: 2-tailed Student's T-tests (independent samples) were used to assess the main effect of genotype on each MLN and DWORF expression, respectfully. Statistical significance was set to p value ≤ 0.05 and when appropriate Tukey's post hoc test was used to determine where specific differences lie.

Chapter 3

Thesis Study I: Investigating if the interaction between MLN:SERCA and DWORF:SERCA Can Protect the SERCA pump from Oxidative/Thermal Damage

3.1 Study Objectives and Hypotheses

Study I focused on whether the physical interaction between SERCA and MLN and DWORF were sufficient to prevent damage under conditions of cellular stress. To determine if the interactions between MLN:SERCA and DWORF:SERCA protect the SERCA pump from oxidative/thermal damage, the effects of heat stress (40°C for 1 hour) on SERCA structure and function were compared between HEK-293 cells co-transfected with cDNA encoding SERCA1a/2a or with SERCA1a/2a and either MLN or DWORF. Unstressed cells that were incubated at 37°C were used as controls. Analyses was carried out on crude cell homogenate that was harvested immediately following heat stress. MLN:SERCA and DWORF:SERCA interactions were assessed using co-immunoprecipitation and Western blotting. SERCA protein oxidation and tyrosine nitration were assessed by immunoblotting with anti-dinitrophenyl (detects carbonyl formation) and anti-nitrotyrosine antibodies, respectively. To determine whether MLN and/or DWORF can protect against thermal inactivation of SERCA activity, measurements of SERCA ATPase activity were assessed at 37°C by using a spectrophotometric assay.

Objectives:

1. To determine if the interaction between MLN and SERCA can preserve maximal SERCA1a/SERCA2a activity following heat stress
2. To determine if the interaction between MLN and SERCA can prevent carbonyl and nitrotyrosine formation following heat stress
3. To determine if the interaction between DWORF and SERCA can preserve maximal SERCA1a/SERCA2a activity following heat stress
4. To determine if the interaction between DWORF and SERCA can prevent carbonyl and nitrotyrosine formation following heat stress

Hypotheses:

.

1. Based on the degree of sequence homology and similarities in interaction sites with SERCA, it is hypothesized that MLN will preserve maximal SERCA1a/SERCA2a activity following heat stress and prevent the formation of carbonyl and nitrotyrosine modifications
2. Based on the degree of sequence homology and similarities in interaction sites with SERCA, it is hypothesized that DWORF will preserve maximal SERCA1a/SERCA2a activity following heat stress and prevent the formation of carbonyl and nitrotyrosine modifications

3.2 Study Design

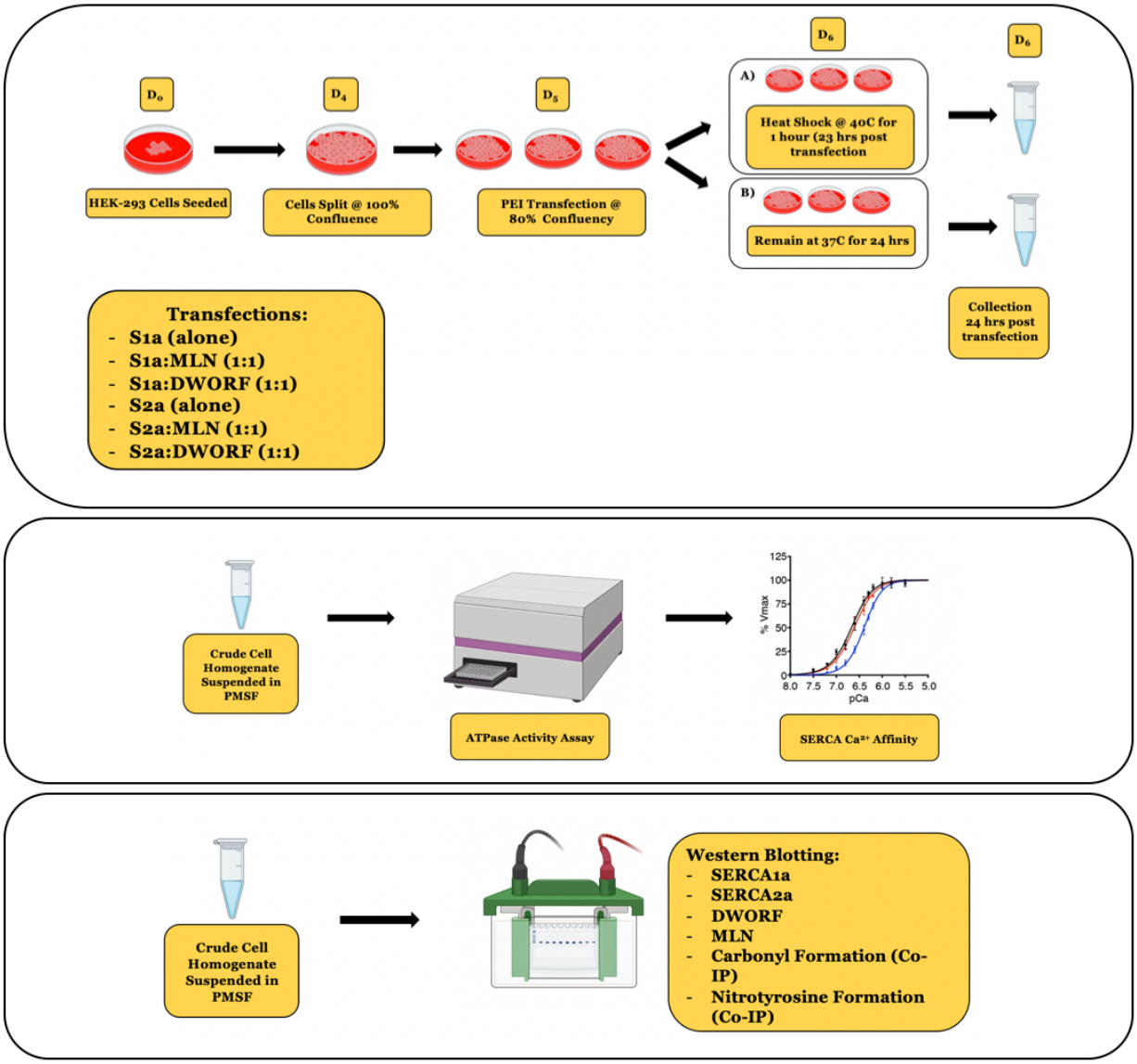


Fig. 3.2.1: Schematic of Study Design for Thesis Study I

3.3 Results

3.3.1 SERCA Isoform and Regulator Transfection Verification

HEK-293 cells transfected for cDNA encoding SERCA1a or SERCA2a alone (20 ug) and co-transfected for cDNA encoding SERCA1a or SERCA2a (10 ug) at a molar ratio of 1:1 to those encoding MLN or DWORF (10 ug) with a total plasmid DNA of 20 µg. Successful transfection of both SERCA isoforms individually and with each respective regulatory protein was validated via western blotting conducted on crude cell homogenate to evaluate the expression of S1a, S2a, MLN and DWORF.

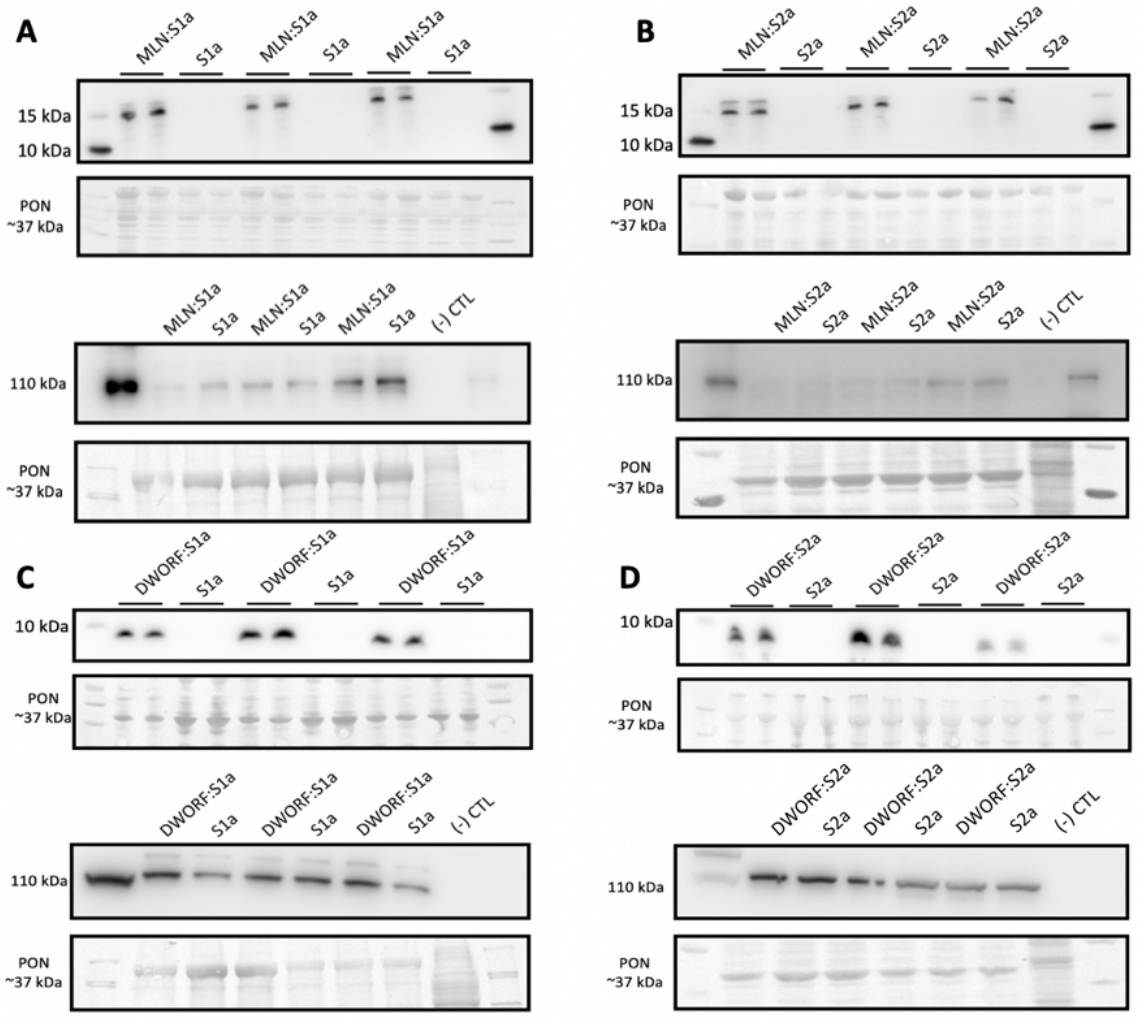


Fig. 3.3.1.1: SERCA Isoform and Regulator Transfection Verification. Western blotting was performed on crude cell homogenates isolated from HEK-293 cells transfected with cDNA encoding SERCA1a/2a alone (20 ug) and co-transfected for cDNA encoding SERCA1a/2a (10 ug) at a molar ratio of 1:1 to those encoding MLN (10 ug) or DWORF (10 ug) with a total plasmid DNA of 20 µg, (n = 3/group). Proteins were separated by SDS-PAGE on a 7.5% gel (SERCA1a/2a) and 13% gel (MLN and DWORF), transferred to a PVDF membrane, and proteins were immunoprobed with the corresponding primary antibodies for SERCA1a (A52); SERCA2a (2A7-A1); DWORF (generous gift from Dr. Eric Olsen (University of Texas Southwestern)); and MLN (2211). Equal protein was confirmed using Ponceau S staining. ***A,*** confirmation of successful transfection of S1a & MLN. ***B,*** confirmation of successful transfection of S2a & MLN. ***C,*** confirmation of successful transfection of S1a & DWORF. ***D,*** confirmation of successful transfection of S2a & DWORF.

3.3.2 MLN Preserves SERCA Function and Prevents Carbonylation/Nitrosylation following Heat Stress

HEK-293 cells transfected for cDNA encoding SERCA1a alone (20 ug) and co-transfected for cDNA encoding SERCA1a (10 ug) at a molar ratio of 1:1 to those encoding MLN (10 ug) with a total plasmid DNA of 20 µg. To induce heat stress (HS), at 23 h post transfection, half of the cells from the groups were incubated at 40°C for one hour prior to harvesting (HS) and the other half of the cells remained incubated at 37°C to be used as controls (CTL). Effects of HS on Ca^{2+}-dependent SERCA1a activity was evaluated on crude cell homogenate over Ca^{2+} concentrations ranging from pCa 6.85 to 4.80 in the presence of the Ca^{2+} ionophore A23187 using a Ca^{2+}-dependent, enzyme-linked spectrophotometric plate reader assay as described in 2.3.1. Exposure of cells expressing SERCA1a alone to heat stress resulted in a significant depression in maximal SERCA1a activity (Fig. 3.3.2.1 A, $p = 0.0018$). In contrast, HS treatment of cells co-transfected with SERCA1a and MLN appeared to spare the pump from damage, maintaining maximal SERCA1a activity at levels resembling the CTL group (Fig. 3.3.2.1 B, $p = 0.346$). Indeed, western blotting on crude cell homogenate to assess SERCA1a oxidation by measuring protein carbonyls in SERCA1a (as described in 2.4.1) demonstrated significant elevations in carbonyl formation following HS treatment only in cells transfected with SERCA1a alone ($p = 0.0023$), with cells co-transfected with SERCA1a and MLN showing minimal carbonylation formation following HS, comparable to that of the CTL groups (Fig. 3.3.2.1 D, $p = 0.291$). Furthermore, western blotting on crude cell homogenate to determine nitrosylation of the SERCA1a protein (as described in 2.4.2) showed stark elevations in nitrotyrosine formation in cells subjected to HS treatment that were transfected with SERCA1a alone ($p = 0.0038$) but not in those that were transfected with both SERCA1a and MLN (Fig. 3.3.2.1 C, $p = 0.311$). Overall, the co-transfection of SERCA1a

with MLN preserved maximal pump activity while minimizing oxidation and nitrosylation of the pump in the face of HS.

This protective effect of MLN's interaction with the pump was subsequently evaluated with the SERCA2a isoform, employing the same HS treatment as described above. HEK-293 cells transfected for cDNA encoding SERCA2a alone (20 ug) and co-transfected for cDNA encoding SERCA2a (10 ug) at a molar ratio of 1:1 to those encoding MLN (10 ug) with a total plasmid DNA of 20 µg. The effects of HS on Ca^{2+}-dependent SERCA2a activity was evaluated on crude cell homogenate over Ca^{2+} concentrations ranging from pCa 6.85 to 4.80 in the presence of the Ca^{2+} ionophore A23187 using a Ca^{2+}-dependent, enzyme-linked spectrophotometric plate reader assay as described in 2.3.1. The protection conferred by the interaction between MLN and SERCA1a translated to similar findings when examining it's co-transfection with the SERCA2a isoform. Subjecting cells expressing SERCA2a alone to the HS treatment resulted in a significant reduction in maximal SERCA2a activity (Fig. 3.3.2.2 A, $p = 0.0021$). Whereas, HS treatment of cells co-transfected with SERCA2a and MLN preserved maximal SERCA2a activity, maintaining activity at a level similar to the CTL group (Fig. 3.3.2.2 B, $p = 0.325$). Concomitantly, the exposure of cells expressing SERCA2a alone to the HS treatment resulted in significant increases in both carbonylation and nitrosylation of the SERCA2a protein. Western blotting on crude cell homogenate to evaluate protein carbonyls in SERCA2a and nitrosylation of the SERCA2a protein (as described in 2.4.1 and 2.4.2) demonstrated significant elevations in both carbonyl (Fig. 3.3.2.2 D, $p = 0.0047$) and nitrotyrosine (Fig. 3.3.2.2 C, $p = 0.0039$) formation following HS treatment only in cells transfected with SERCA2a alone, but not in those expressing both SERCA2a and MLN, with cells co-transfected with SERCA2a and MLN showing minimal oxidation ($p = 0.209$) and nitrosylation ($p = 0.197$) of the pump following HS, comparable to that of the CTL groups. It

is evident that MLN's interaction with both SERCA1a and SERCA2a isoforms in protective in nature under instances of cellular stress, such as those imposed by HS treatment.

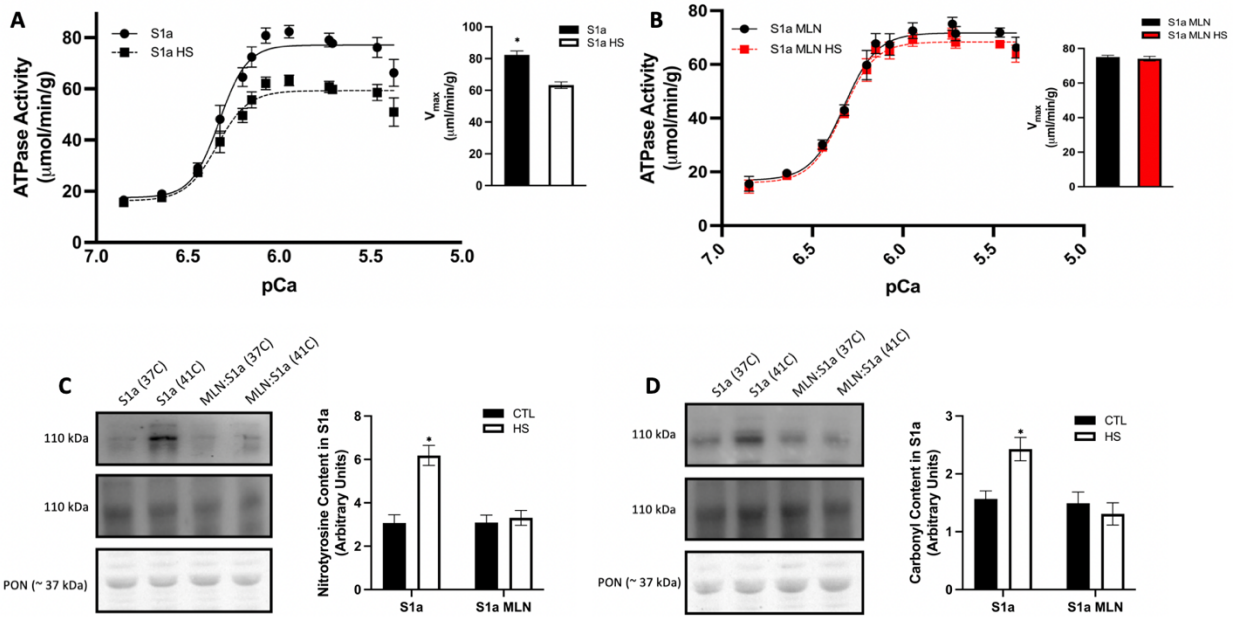


Fig. 3.3.2.1: MLN Preserves SERCA1a Function and Prevents SERCA1a Oxidation & Nitrosylation following Heat Stress. HEK-293 cells were transfected with cDNA encoding SERCA1a alone (20 ug) and co-transfected for cDNA encoding SERCA1a (10 ug) at a molar ratio of 1:1 to those encoding MLN (10 ug) with a total plasmid DNA of 20 µg. At 23 h after transfection, half of the cells from the groups were incubated at 40°C for one hour before harvesting (HS) and the other half of the cells remained incubated at 37°C to be used as controls (CTL). SERCA1a activity in the crude cell homogenate was measured at 37°C using a spectrophotometric assay. ***A,*** effects of heat stress on Ca^{2+}-dependent SERCA1a activity in cells that were transfected with SERCA1a alone and effects of HS on maximal SERCA1a activity. ***B,*** effects of heat stress on Ca^{2+}-dependent SERCA1a activity in cells that were co-transfected with SERCA1a and MLN and effects of MLN on maximal SERCA1a activity following heat stress. SERCA1a was immunoprecipitated from the crude cell homogenate with SERCA1a antibody, precipitates were separated by SDS-PAGE on a 10% gel, transferred to a PVDF membrane and then carbonyls in SERCA1a were detected using anti-DNP antibody and nitrotyrosine levels in SERCA1a were detected using anti-nitrotyrosine antibody and normalized to the levels of SERA1a in the immunoprecipitation products. ***C,*** effects of MLN on nitrotyrosine formation in SERCA1a following heat stress. *Lane 1*, S1a at 37°C; *Lane 2,* S1a at 40°C; *Lane 3,* S1a:MLN at 37°C; *Lane 4*, S1a:MLN at 40°C. ***D,*** effects of MLN on carbonyl formation in SERCA1a following heat stress. *Lane 1*, S1a at 37°C; *Lane 2,* S1a at 40°C; *Lane 3,* S1a:MLN at 37°C; *Lane 4*, S1a:MLN at 40°C. Values are means ± SE, n = 3/group. *, $p < 0.05$ *versus* CTL.

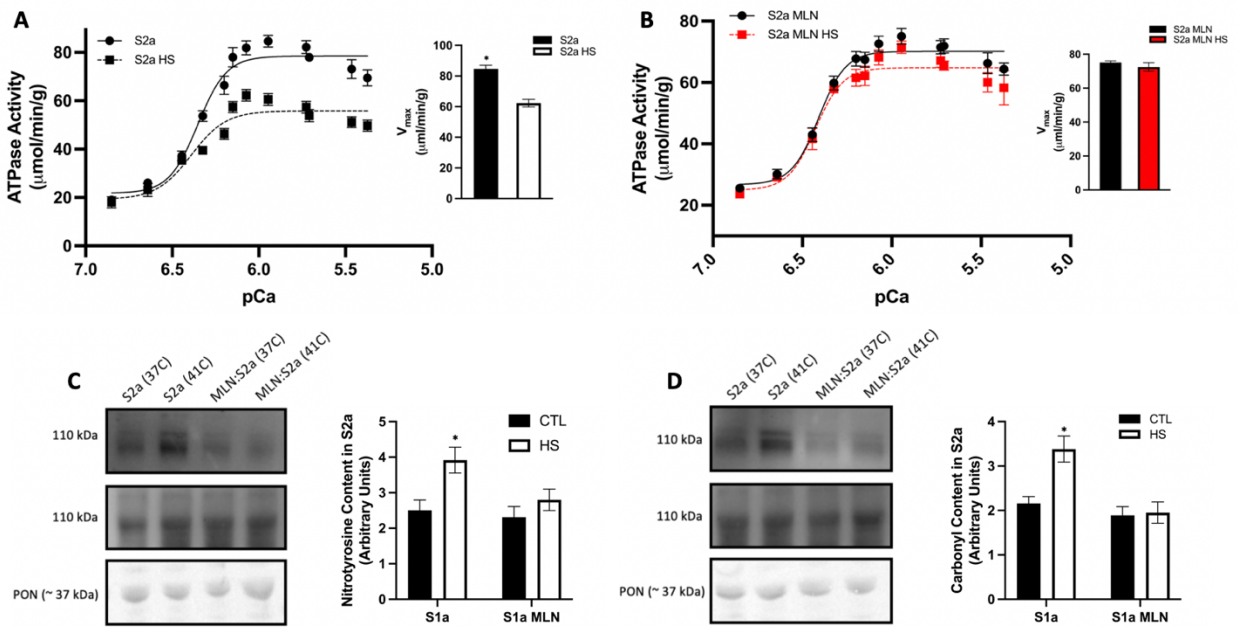


Fig. 3.3.2.2: MLN Protects SERCA2a Function and Impedes Oxidation & Nitrosylation following Heat Stress. HEK-293 cells were transfected with cDNA encoding SERCA2a alone (20 ug) and co-transfected for cDNA encoding SERCA2a (10 ug) at a molar ratio of 1:1 to those encoding MLN (10 ug) with a total plasmid DNA of 20 µg. At 23 h after transfection, half of the cells from the groups were incubated at 40°C for one hour before harvesting (HS) and the other half of the cells remained incubated at 37°C to be used as controls (CTL). SERCA2a activity in the crude cell homogenate was measured at 37°C using a spectrophotometric assay. ***A,*** effects of heat stress on Ca^{2+}-dependent SERCA2a activity in cells that were transfected with SERCA2a alone and effects of HS on maximal SERCA2a activity. ***B,*** effects of heat stress on Ca^{2+}-dependent SERCA2a activity in cells that were co-transfected with SERCA2a and MLN and effects of MLN on maximal SERCA2a activity follwing heat stress. SERCA2a was immunoprecipitated from the crude cell homogenate with SERCA2a antibody, precipitates were separated by SDS-PAGE on a 10% gel, transferred to a PVDF membrane and then carbonyls in SERCA2a were detected using anti-DNP antibody and nitrotyrosine levels in SERCA2a were detected using anti-nitrotyrosine antibody and normalized to the levels of SERA2a in the immunoprecipitation products. ***C,*** effects of MLN on nitrotyrosine formation in SERCA2a following heat stress. *Lane 1*, S2a at 37°C; *Lane 2,* S2a at 40°C; *Lane 3,* S2a:MLN at 37°C; *Lane 4*, S2a:MLN at 40°C. ***D,*** effects of MLN on carbonyl formation in SERCA2a following heat stress. *Lane 1*, S2a at 37°C; *Lane 2,* S2a at 40°C; *Lane 3,* S2a:MLN at 37°C; *Lane 4*, S2a:MLN at 40°C. Values are means ± SE, n = 3/group. *, $p < 0.05$ *versus* CTL.

Table 3.3.2.1. Maximal SERCA activity (V_{Max}; µmol/g prot/ min) of cells transfected with SERCA alone and of cells co-transfected with MLN (n = 3/group) measured either under CTL (37°C) or HS (40°C) conditions.

SERCA1a		
	V_{Max}	
Condition	SERCA1a alone	SERCA1a:MLN
CTL (37°C)	83.65 ± 2.461	73.06 ± 1.045$^{\#}$
HS (40°C)	63.28 ± 2.067	72.13 ± 0.944*
SERCA2a		
	V_{Max}	
Condition	SERCA2a alone	SERCA2a:MLN
CTL (37°C)	83.41 ± 2.479	72.36 ± 1.039$^{\#}$
HS (40°C)	61.86 ± 1.113	71.47 ± 0.957*

*, $p < 0.05$ *versus* CTL
$^{\#}$, $p < 0.05$ *versus* SERCA alone

3.3.3 DWORF Obstructs SERCA Carbonylation/Nitrosylation following Heat Stress to Maintain SERCA Function

HEK-293 cells were transfected with cDNA encoding SERCA1a alone (20 μg) and co-transfected with cDNA encoding SERCA1a (10 μg) at a molar ratio of 1:1 to those encoding DWORF (10 μg), resulting in a total plasmid DNA amount of 20 μg. To invoke HS, 23 hours post-transfection, half of the cells from each group were incubated at 40°C for one hour before harvesting (HS), while the other half remained incubated at 37°C to serve as controls (CTL). The impact of HS on Ca^{2+}-dependent SERCA1a activity was assessed on crude cell homogenate over a range of Ca^{2+} concentrations, from pCa 6.85 to 4.80, in the presence of the Ca^{2+} ionophore A23187, by employing a Ca^{2+}-dependent, enzyme-linked spectrophotometric plate reader assay (as described in 2.3.1). HS treatment of cells expressing SERCA1a alone led to a significant decline in maximal SERCA1a activity (Fig. 3.3.3.1 A, $p = 0.0041$). Whereas, the effects of HS exposure on the maximal activity of the pump were counteracted in cells co-transfected with SERCA1a and DWORF, as the expression of DWORF preserved maximal SERCA1a activity, maintaining it at levels similar to the CTL group (Fig. 3.3.3.1 B, $p = 0.548$).

Subsequent western blotting on crude cell homogenate was performed to assess SERCA1a oxidation by measuring protein carbonyls in SERCA1a (as described in section 2.4.1) and showed a significant elevation in carbonyl formation following HS treatment only in cells transfected with SERCA1a alone ($p = 0.018$). Contrastly, following HS treatment cells co-transfected with SERCA1a and DWORF exhibited minimal carbonylation, resembling levels comparable to the CTL groups (Fig. 3.3.3.1 D, $p = 0.331$). Moreover, western blotting on crude cell homogenate was conducted to assess nitrosylation of the SERCA1a protein (as described in section 2.4.2) and revealed substantial increases in nitrotyrosine formation in cells subjected to HS treatment that

were transfected with SERCA1a alone (0.012), but not in those co-transfected with both SERCA1a and DWORF (Fig. 3.3.3.1 C, $p = 0.283$).

The protection conferred by DWORF's interaction with the pump was next assessed with the SERCA2a isoform, employing the same HS treatment as described above. HEK-293 cells were transfected with cDNA encoding SERCA2a alone (20 μg) and co-transfected with cDNA encoding SERCA2a (10 μg) at a molar ratio of 1:1 to those encoding DWORF (10 μg), resulting in a total plasmid DNA amount of 20 μg. The effects of HS on Ca^{2+}-dependent SERCA2a activity were examined in crude cell homogenate over a range of Ca^{2+} concentrations, from pCa 6.85 to 4.80, in the presence of the Ca^{2+} ionophore A23187, using the same Ca^{2+}-dependent enzyme-linked spectrophotometric plate reader assay (described in section 2.3.1). The protective effect observed in the interaction between DWORF and SERCA1a was shown to extend to the SERCA2a isoform. HS treatment of cells expressing SERCA2a alone revealed a significant decrease in maximal SERCA2a activity (Fig. 3.3.3.2 A, $p = 0.00137$). Conversely, exposing cells co-transfected with SERCA2a and DWORF to HS treatment conserved maximal SERCA2a activity, presevering it at a level similar to the CTL group (Fig. 3.3.3.2 B, $p = 0.179$). Synchronously, the exposure of cells expressing SERCA2a alone to HS treatment resulted in a significant rise in both oxidation and nitrosylation of the SERCA2a protein. Western blotting on crude cell homogenate (as described in sections 2.4.1 and 2.4.2), was carried out to evaluate protein carbonyls in SERCA2a (as a measure of oxidation) and nitrosylation of the SERCA2a protein. Significant increases in both carbonyl ($p = 0.013$) and nitrotyrosine ($p = 0.027$) formation following HS treatment were observed only in cells transfected with SERCA2a alone, but not in those expressing both SERCA2a and DWORF. In comparison, the cells that were co-transfected with SERCA2a and DWORF exhibited minimal oxidation (Fig. 3.3.3.2 D, $p = 0.165$) and nitrosylation (Fig. 3.3.3.2 C,

p = 0.203) of the pump following HS, comparable to that of the CTL groups. Similar to what was observed with MLN, the results outlined here are indicative of a protein-protein interaction that conveys protection under conditions of cellular stress, such as those induced by HS treatment.

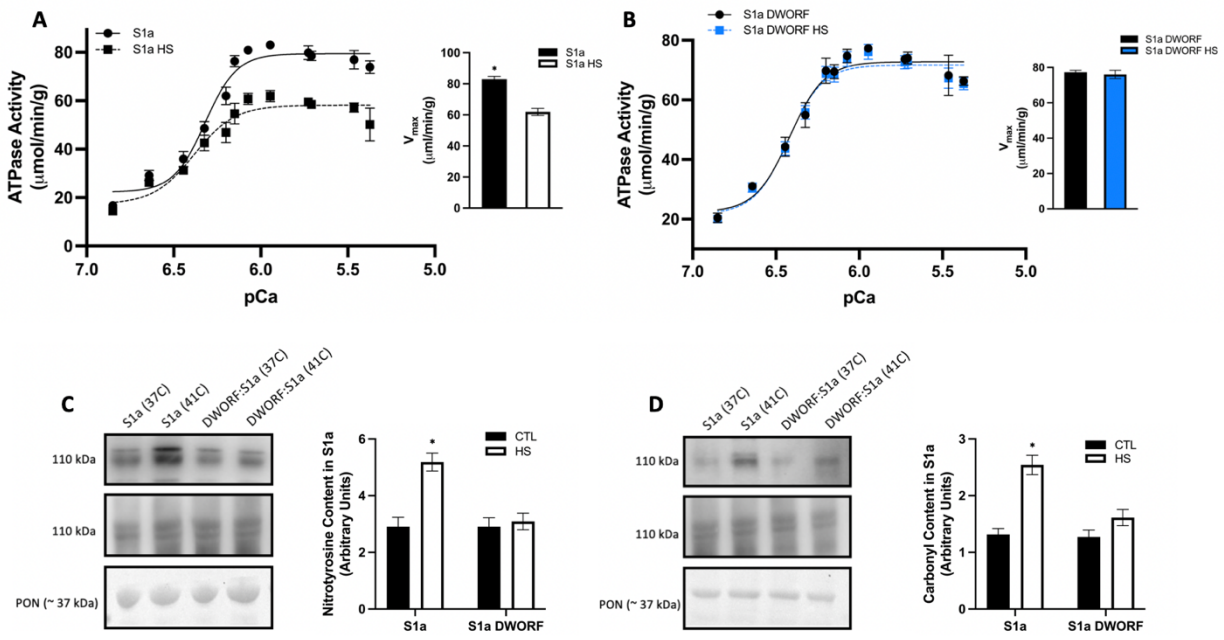


Fig. 3.3.3.1: DWORF Prevents Oxidation & Nitrosylation following Heat Stress to Conserve SERCA1a Maximal Activity. HEK-293 cells were transfected with cDNA encoding SERCA1a alone (20 ug) and co-transfected for cDNA encoding SERCA1a (10 ug) at a molar ratio of 1:1 to those encoding DWORF (10 ug) with a total plasmid DNA of 20 µg. At 23 h after transfection, half of the cells from the groups were incubated at 40°C for one hour before harvesting (HS) and the other half of the cells remained incubated at 37°C to be used as controls (CTL). SERCA1a activity in the crude cell homogenate was measured at 37°C using a spectrophotometric assay. ***A***, effects of heat stress on Ca^{2+}-dependent SERCA1a activity in cells that were transfected with SERCA1a alone and effects of HS on maximal SERCA1a activity. ***B,*** effects of heat stress on Ca^{2+}-dependent SERCA1a activity in cells that were co-transfected with SERCA1a and DWORF and effects of DWORF on maximal SERCA1a activity follwing heat stress. SERCA1a was immunoprecipitated from the crude cell homogenate with SERCA1a antibody, precipitates were separated by SDS-PAGE on a 10% gel, transferred to a PVDF membrane and then carbonyls in SERCA1a were detected using anti-DNP antibody and nitrotyrosine levels in SERCA1a were detected using anti-nitrotyrosine antibody and normalized to the levels of SERAC1a in the immunoprecipitation products. ***C,*** effects of DWORF on nitrotyrosine formation in SERCA1a following heat stress. *Lane 1*, S1a at 37°C; *Lane 2,* S1a at 40°C; *Lane 3,* S1a:DWORF at 37°C; *Lane 4*, S1a:DWORF at 40°C. ***D,*** effects of DWORF on carbonyl formation in SERCA1a following heat stress. *Lane 1*, S1a at 37°C; *Lane 2,* S1a at 40°C; *Lane 3,* S1a:DWORF at 37°C; *Lane 4*, S1a:DWORF at 40°C. Values are means ± SE, n = 3/group. *, $p < 0.05$ *versus* CTL.

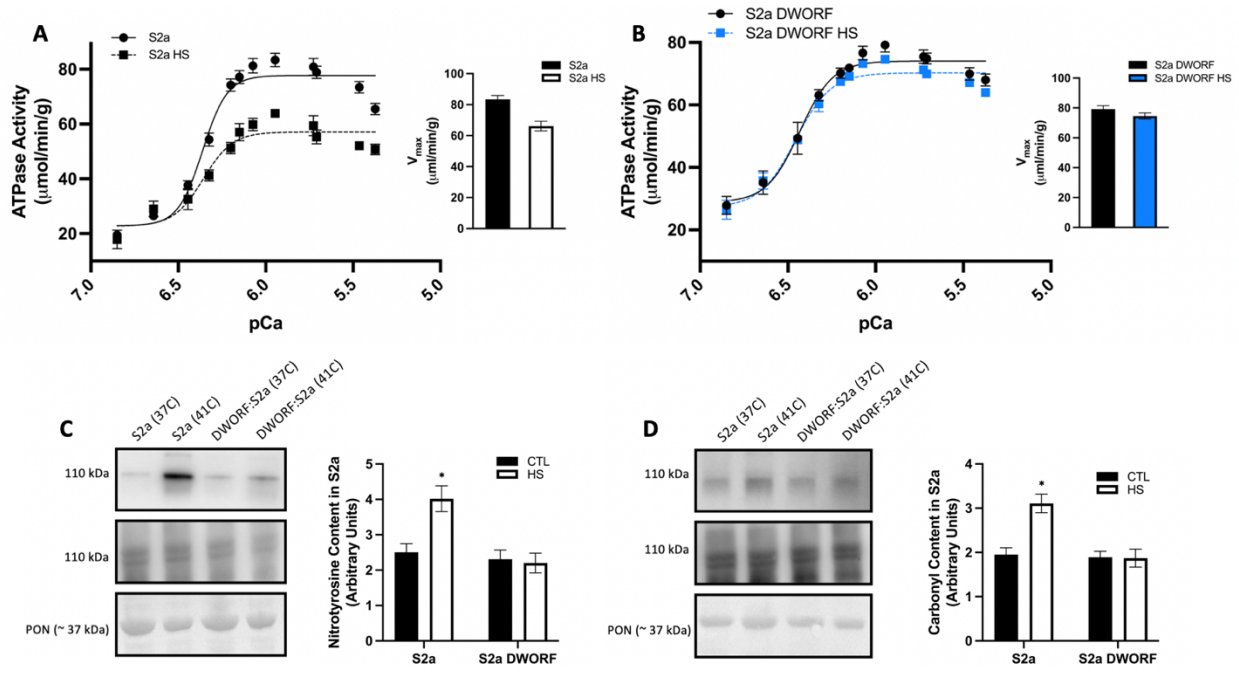


Fig 3.3.3.2. DWORF Protects SERCA2a Function and Impedes Oxidation & Nitrosylation following Heat Stress. HEK-293 cells were transfected with cDNA encoding SERCA2a alone (20 ug) and co-transfected for cDNA encoding SERCA2a (10 ug) at a molar ratio of 1:1 to those encoding DWORF (10 ug) with a total plasmid DNA of 20 µg. At 23 h after transfection, half of the cells from the groups were incubated at 40°C for one hour before harvesting (HS) and the other half of the cells remained incubated at 37°C to be used as controls (CTL). SERCA2a activity in the crude cell homogenate was measured at 37°C using a spectrophotometric assay. ***A***, effects of heat stress on Ca^{2+}-dependent SERCA2a activity in cells that were transfected with SERCA2a alone and effects of HS on maximal SERCA2a activity. ***B,*** effects of heat stress on Ca^{2+}-dependent SERCA2a activity in cells that were co-transfected with SERCA2a and DWORF and effects of DWORF on maximal SERCA2a activity follwing heat stress. SERCA2a was immunoprecipitated from the crude cell homogenate with SERCA2a antibody, precipitates were separated by SDS-PAGE on a 10% gel, transferred to a PVDF membrane and then carbonyls in SERCA2a were detected using anti-DNP antibody and nitrotyrosine levels in SERCA2a were detected using anti-nitrotyrosine antibody and normalized to the levels of SERCA2a in the immunoprecipitation products. ***C,*** effects of DWORF on nitrotyrosine formation in SERCA2a following heat stress. *Lane 1*, S2a at 37°C; *Lane 2,* S2a at 40°C; *Lane 3,* S2a:DWORF at 37°C; *Lane 4*, S2a:DWORF at 40°C. ***D,*** effects of DWORF on carbonyl formation in SERCA2a following heat stress. *Lane 1*, S2a at 37°C; *Lane 2,* S2a at 40°C; *Lane 3,* S2a:DWORF at 37°C; *Lane 4*, S2a:DWORF at 40°C. Values are means ± SE, n = 3/group. *, $p < 0.05$ *versus* CTL.

Table 3.3.3.1. Maximal SERCA activity (V_{Max}; μmol/g prot/ min) of cells transfected with SERCA alone and of cells co-transfected with DWORF (n = 3/group) measured either under CTL (37°C) or HS (40°C) conditions.

SERCA1a		
	V_{Max}	
Condition	SERCA1a alone	SERCA1a:DWORF
CTL (37°C)	83.06 ± 1.708	81.31 ± 1.077
HS (40°C)	61.95 ± 2.299	80.09 ± 0.975*
SERCA2a		
	V_{Max}	
Condition	SERCA2a alone	SERCA2a:DWORF
CTL (37°C)	84.63 ± 3.245	81.22 ± 2.262
HS (40°C)	66.19 ± 1.141	80.31 ± 1.271*

*, $p < 0.05$ *versus* CTL

3.4 Discussion

SERCAs are redox-sensitive proteins that exhibit a high vulnerability to oxidative damage and inactivation, so much so, that the modification of a single cysteine residue is sufficient for the alteration of activity [18, 44-46]. It is well documented that both SERCA1 and SERCA2 are highly susceptible to damage incurred by exposure to oxidative stress, due to the considerable number of cysteine residues (24 and 26 Cys residues, respectively) which comprise the proteins [44-46]. Oxidative stress can include oxidation, nitrosylation, S –glutathiolation of protein thiols, and Tyr nitration and can structurally alter the pump to induce impairments that cannot be overcome and result in the loss of function [44-46]. As such, SERCA function is commonly impaired across a myriad of different myopathies, particularly dystrophies, where SERCAs have proven very susceptible to nitrosylation; which alters SERCA enzyme kinetics by modifying the Ca^{2+}-binding and ATP-binding domains and consequentially reducing maximal SERCA activity and rates of SERCA-mediated Ca^{2+} uptake [51, 52, 58, 142]. Our lab and others have demonstrated that protein-protein interactions can stabilize SERCA and offer protection against the many forms of oxidative stress [44]. As explained in Section 1.2, one such protein-protein interaction is that of the chaperone protein, HSP70 and SERCA [44, 51], which was shown to maintain maximal SERCA activity and prevent SERCA nitrosylation and carbonyl formation following exposure to HS conditions. Indeed, the two avenues explored to protect the pumps in the dystrophic environment have been SERCA overexpression [54, 56] and SERCA stabilization via HSP70 [51]. Both of which acted to successfully mitigate Ca^{2+} dysregulation and, consequently, have been shown to alleviate the dystrophic phenotype by lowering several disease markers, including centrally localized nuclei, muscle fibrosis, serum creatine kinase levels, mitochondrial swelling and calpain activation [54, 56].

However, in the cell model, functional protection of SERCA by HSP70 was lost with progressively greater severity of HS and exposure time [44]. Suggesting that another region on SERCAs (such as the Ca^{2+} binding or transmembrane (TM) domain) may not be able to form an interaction with HSP70, and is exposed to modification under conditions of heightened HS, resulting in inactivation [44]. This underscores the importance of discovering that PLN and SLN confer protection to SERCAs, as outlined in sections 1.3.2 (PLN) and 1.4.7 (SLN). Briefly, SLN and PLN share extensive homology in the TM region and exhibit a shared common binding site within SERCA transmembrane helices M2, M4, M6 and M9 [30, 92, 93]. When exposed to HS conditions, both peptides conserved SERCA thermal stability, serving to maintain maximal activity and prevent detrimental modifications of the SERCA protein [11]. Moreover, disruption of PLN's interaction with the TM region abolished its ability to stabilize SERCA structure and function during HS [11]. Indeed, unpublished work from our lab confirms that PLN plays a critical role in protecting SERCA function in the dystrophic environment as it's ablation in the *mdx* model worsens the myopathy [85].

The work described here, builds upon previous publications, and is the first to examine whether MLN and DWORF, two SR proteins that physically interact with the pump and bare structural resemblance to SLN and PLN, are capable of protecting the pump under conditions of cellular stress. MLN shares a high degree of sequence homology with PLN and SLN, particularly in the transmembrane domain, where it has been shown to interact in the same groove that is occupied by PLN and SLN [12]. Conversely, while DWORF shares the least sequence homology among the four regulatory proteins, it also forms a strong connection with M4 and M6 helices of SERCA's M2, M4, M6, M9 Ca^{2+} binding groove [124]. As hypothesized, in the absence of MLN and DWORF, the maximal catalytic activity of both SERCA isoforms expressed in HEK-293 cells

declined following exposure to HS, which is consistent with findings from similar studies on SERCA1a [44, 143, 144] and SERCA2a [61]. Furthermore, in agreement with our previous studies [61], inactivation of SERCAs coincided with increased carbonyl and nitrotyrosine modification of SERCAs as revealed by Western blotting. The co-expression of the SERCAs with both MLN and DWORF, respectively, prevented thermal inactivation of SERCA1a and SERCA2a, maintaining maximal activity and averting oxidation/nitrosylation in the face of HS treatment. This would imply that the interaction between SERCA and these two newly discovered regulatory proteins is protective in nature, shielding residues that are critical for SERCA function from modifications provoked by HS conditions.

Exposure of HEK-293 cells that expressed SERCA only to HS reduced maximal activity by ~24% (S1a) and ~26% (S2a), compared to those co-transfected with SERCA and MLN, where the difference in SERCA maximal activity between the CTL and HS conditions was negligible. Moreover, the protection conferred by MLN was not isoform specific, both SERCA1a and SERCA2a were afforded similar stabilization during HS, with the activity of both isoforms conserved at ~98% relative to CTL. Interestingly, MLN did exert an inhibitory role, significantly reducing maximal activity of both isoforms to a similar extent (~13.5% S1a and ~13.8% S2a). The importance of this in regard to cellular Ca^{2+} homoeostasis will be discussed further in Chapter 4 below, however, it is indicative of consistency across studies. Likewise, the absence of DWORF resulted in a depression of maximal activity by ~25% (S1a) and ~22% (S2a) following exposure to HS, whereas, the presence of DWORF preserved maximal activity at ~98% for both isoforms, again, without showing a preference for one isoform over another. The degree of HS induced SERCA damage in this study is comparable to our previous study [11], as is the extent of protection offered by the regulatory proteins, however, what could not be evaluated in this study is whether

the this protection is TM-specific. The Fu *et al* study investigating the cytoprotective capacities of PLN and SLN employed a mutant PLN (N34A) that lacked residue Asn^{34} which abolished the critical contact formed with SERCA residues in the TM helices [11]. The inability of PLN to interact with SERCA's TM region eliminated its protective effects and moreover, overexpression of N34A prevented only carbonyl formation but not nitrotyrosine formation during HS [11]. Topology modelling and sequence alignment have proposed that the equivalents to Asn^{34} in PLN are Asn^{11} in SLN, Arg^{24} in MLN and Pro^{15} in DWORF [145]. HS exposure of cells co-transfected with the SERCAs and mutant variants of MLN (targeting Arg^{24} and other residues that form critical contacts with SERCA) would allow us to discern the mechanistic basis underlying MLN protection and identify potential differences in the protection conferred between isoforms and compared to the other regulators. Likewise, the exposure of cells co-transfected with the SERCAs and mutant variants of DWORF (targeting Pro^{15} and other residues that form critical contacts with SERCA) to HS conditions would offer a similar important mechanistic understanding. Interestingly, the aforementioned N34A mutation of PLN caused not only loss of its ability to stabilize SERCA structure and function during HS [11], but also loss of PLN inhibitory function [79, 80]. Therefore, mutagenesis studies with the aim of investigating the residues involved in SERCA interaction and the inherent differences in this interaction between the regulatory proteins would not only serve to better our understanding of the protection conferred by the four regulatory proteins discussed in this thesis but their regulatory functions as well.

An additional avenue for future studies to pursue is to evaluate if endogenous MLN and DWORF expression can stabilize the pump. The Fu *et al* study revealed that the ablation of PLN in mouse cardiac tissue and the ablation of SLN in mouse diaphragm tissue augmented SERCA susceptibility to thermal inactivation [11]. Mouse cardiac and diaphragm represent tissues which

contain a relatively high endogenous expression of PLN [81] and SLN [146], respectfully. In contrast, in response to the same HS condition, maximal SERCA activity was reduced in preparations from rat white gastrocnemius [147, 148], a muscle without detectable endogenous SLN protein [100, 146]. Therefore, while this study does prove that the interaction between the SERCAs and MLN and DWORF is protective in nature under conditions of cellular stress, the next step is to determine whether this protection is conferred in a physiological setting with endogenous expression levels. The MLN gene is reportedly expressed in all murine skeletal muscle [12] and we have detected the protein in murine soleus and cardiac tissue (**Appendix B**: **Figure B.3**). If the protein is expressed across all skeletal muscle and is expressed at high enough levels, it would provide the potential for unprecedented SERCA protection. Comparatively, protein expression of DWORF reportedly mirrors that of PLN, with murine soleus tissue exhibiting the most abundant endogenous expression of the DWORF protein (**Appendix B**: **Figure B.4**) [13]. With all four regulatory proteins showing abundant endogenous expression in murine soleus, this raises an interesting scenario, in which multiple regulatory proteins are expressed and vying for interaction with SERCA. While it is well established that SLN and PLN have different SERCA isoform preferences [9] it is speculated that MLN expresses a preference for SERCA1a [12] while DWORF prefers SERCA2a [13], however, this has yet to be conclusively proven. Moreover, PLN and DWORF have been shown to engage in a dynamic dance as they regulate SERCA activity. Recall from Section 1.5.5 that PLN shows the highest affinity for SERCA in its E1-ATP state, which prevails at low [Ca^{2+}] and DWORF shows the highest affinity for SERCA in its E1P and E2P states, which dominate at high [Ca^{2+}] [124]. With PLN and DWORF engaging in a dynamic competition to inhibit SERCA at low cytoplasmic [Ca^{2+}] and stimulate SERCA during elevations in cytoplasmic [Ca^{2+}] [123], could the same relationship be extended to SERCA protection, with

PLN stabilizing the pump at low cytoplasmic [Ca^{2+}] and DWORF stabilizing the pump during elevations in cytoplasmic [Ca^{2+}]. On the other hand, PLN does form a more extensive interaction with the TM-region of the SERCA protein, could this make it the preferred regulatory protein under conditions of cellular stress. Indeed, despite DWORF protein expression in murine cardiac and soleus muscle, the ablation of PLN in mouse cardiac tissue heightened SERCA susceptibility to thermal inactivation [11] and ablation of PLN in the *mdx* murine model worsened the dystrophic myopathy in soleus tissue [85]. While the expression of DWORF in the preceding studies was not evaluated, DWORF protein expression was shown to be significantly lower in WT 5-6 month old mice compared to Pln^{OE} littermates (**Appendix B, Fig. B.1**). The novelty of this observation is twofold, it shows that DWORF expression can be responsive to changes in PLN expression and that surprisingly, the expression of DWORF is lower in this diseased state. Given the ability of DWORF to displace PLN from the pump and remove its inhibition, it would be expected that DWORF content would be elevated as a countermeasure to protect against PLN overexpression. In fact, as discussed in Section 1.5.7, the superinhibition of SERCA and the resultant myopathy caused by PLN overexpression can be completely reversed with DWORF overexpression [129]. It has been well documented that PLN is a component of a multimeric complex in cardiac tissue, interacting with proteins including protein phosphatase 1 (PP1), HSP20 and HAX-1, to exerts an effect on both SERCA activity and Ca^{2+} homeostasis [65, 149]. It could very well be the case that the four regulatory proteins discussed in this thesis are involved in a similar complex in skeletal muscle, working together to stabilize SERCA structure and function while simultaneously regulating the pump's activity.

If endogenous expression levels of MLN and DWORF are sufficient to confer protection during HS, the next step in establishing MLN and DWORF as cytoprotective proteins would be to

assess their inducibility under conditions of cellular stress. A very important characteristic of HSP70 is that it presents with an immediate response and a delayed response to cellular stress. HSP70 mobilizes to interact with and repair damaged/unfolded proteins concurrently to acting on the nucleus to stimulate HSP70 upregulation [150-152]. To that end, recent unpublished work from the Tupling lab has shown that like HSP70, PLN and SLN protein expression may also be inducible in the face of HS exposure. In a mild acute stress model, endogenous SLN protein was upregulated in rat male soleus tissue and exogenous PLN protein was upregulated in rat male white gastrocnemius tissue in response to *in vivo* heat stress [153]. It will be important to take the MLN and DWORF cytoprotection story even further and to establish whether these two regulatory proteins can also function as stress induced proteins and which muscles are the recipients are this protection.

The final novel contribution of this study has been the development of a western blotting protocol to precisely detect MLN protein. Previous studies had relied on MLN gene expression in lieu of protein expression in murine models and determined potential protein expression via detection of protein tags attached to MLN protein in cell based models. This is the first study to date to specifically identify and detect purified MLN protein that has been collected from HEK-293 cells transfected with MLN cDNA [12]. It was difficult to conclusively identify MLN protein in murine skeletal muscle in prior troubleshooting efforts without MLN knockout tissue to serve as a negative control. Here, cells that were co-transfected with SERCA and MLN served as positive controls while cells that were transfected with SERCA alone served as negative controls. Fig. 3.3.1.1 clearly demonstrates presence and absence of MLN protein in our positive and negative controls, respectively. Interestingly, MLN is detected between 10 – 15 kDa while the remaining regulatory proteins are detected below 10 kDa, at ~ 6 kDa. Further validation of MLN protein

expression in murine cardiac and skeletal muscle will be discussed in Chapter 5 below, including the protein load and western conditions required to detect MLN in cardiac tissue and various oxidative and glycolytic skeletal muscle tissue.

3.5 Conclusion

In summary, the major novel findings of this study were that both MLN and DWORF, two SR integral membrane proteins that structurally resemble SLN and PLN, prevent thermal inactivation of SERCA1a and SERCA2a. This protection is likely conferred through stabilizing physical interactions that prevent oxidation and nitrosylation of SERCA molecules. SERCA residues that are critical for function and are modified by HS must be involved in the protective interaction with MLN and DWORF. These findings suggest that these SERCA-binding proteins may play a crucial role in protecting cellular Ca^{2+} homeostasis. Future studies should examine if endogenous levels of MLN and DWORF protein content can contribute to the preservation of SERCA activity *in vivo* and consequentially, protect cardiac and skeletal muscle function under conditions of chronic oxidative stress and disease.

Chapter 4

Thesis Study II: Assessing if MLN and/or DWORF Can Alter the SERCA Coupling Ratio

4.1 Study Objectives and Hypotheses

The focus of Study II was to determine if the interactions between MLN:SERCA and DWORF:SERCA alters the SERCA transport efficiency. HEK-293 cells were co-transfected with cDNA encoding SERCA1a/2a or with SERCA1a/2a and either MLN or DWORF and both Ca^{2+} uptake and Ca^{2+}-ATPase activity (Ca^{2+}/ATP coupling ratio of SERCA pumps) were measured on crude cell homogenate prepared from the transfected cells. Ca^{2+}-dependent SERCA activity was assessed over Ca^{2+} concentrations ranging from pCa 6.85 to 4.80 in presence and absence of the Ca^{2+} ionophore A23187 using a spectrophotometric plate reader assay. SERCA-mediated Ca^{2+} uptake was measured in the presence and absence of the precipitating anion, oxalate, using the fluorescent dye Indo-1 and a spectrofluorometetric plate reader assay. SERCA coupling ratio was be calculated by dividing Ca^{2+} uptake by Ca^{2+}-ATPase rates across different pCa values. The ionophore ratio was determined at each pCa to provide an additional way of assessing SERCA efficiency and was calculated by dividing SERCA activity measured in the presence of the ionophore by SERCA activity measured in the absence of the ionophore. A lower ionophore ratio indicates more inefficient SR Ca^{2+} transport and storage [3].

Objectives:

1. To determine if SERCA:MLN and SERCA:DWORF interaction alters the SERCA coupling ratio and/or the ionophore ratio.

Hypotheses:

1. Based on the sequence homology and protein structure of MLN, it is hypothesized that it will *not* cause uncoupling of Ca^{2+} transport from ATP hydrolysis or alter the ionophore ratio.

2. Based on the sequence homology and protein structure of DWORF, it is hypothesized that it will *not* cause uncoupling of Ca^{2+} transport from ATP hydrolysis or alter the ionophore ratio.

4.2 Study Design

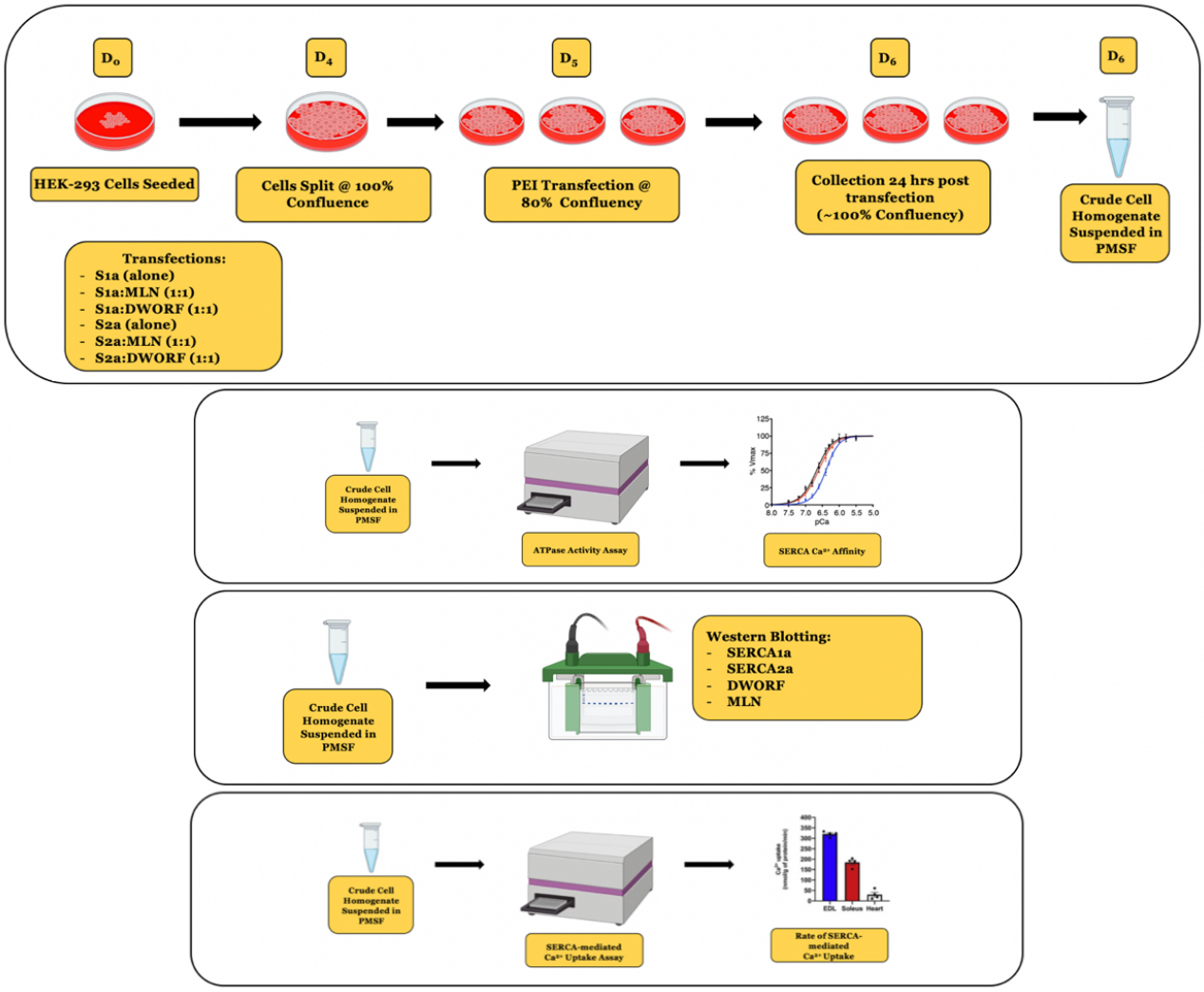


Fig. 4.2.1: Schematic of Study Design for Thesis Study II

4.3 Results

4.3.1 MLN is Not an Uncoupler of SERCA Ca^{2+} Transport and ATP Hydrolysis

HEK-293 cells were transfected for cDNA encoding SERCA1a or SERCA2a alone (20 ug) and co-transfected for cDNA encoding SERCA1a or SERCA2a (10 ug) at a molar ratio of 1:1 to those encoding MLN (10 ug) with a total plasmid DNA of 20 µg. Successful transfection of each isoform individually and in combination with MLN was validated via western blotting for the expression of SERCA1a (Fig. 4.3.1.3), SERCA2a (Fig. 4.3.1.6) and MLN.

Measurements of Ca^{2+}-ATPase activity in crude cell homogenates were made with and without the Ca^{2+} ionophore A23187 (as outlined in section 2.3.1). In the presence of the ionophore, there is no Ca^{2+} gradient across the SR membrane, providing a measure of SERCA activity under maximal (non-limiting conditions) conditions. In the absence of the ionophore, Ca^{2+} accumulates inside the SR vesicle and causes back-inhibition of SERCA pumps, providing a condition more relevant to the physiological system found in skeletal muscle. When assessed in the both the presence (Fig. 4.3.1.2 A) and absence (Fig. 4.3.1.1 A) of a Ca^{2+} gradient, there was a decrease in the apparent affinity of SERCA1a for Ca^{2+} in the cells co-transfected with SERCA1a and MLN compared to cells transfected with SERCA1a only. This was indicated by a significant increase in the pCa_{50} (Table 4.3.1.1.) and a corresponding rightward shift in plots of the Ca^{2+} dependence of Ca^{2+}-ATPase activity. Furthermore, in the both presence ($p = 0.028$) and absence ($p = 0.015$) of the Ca^{2+} ionophore, maximal SERCA1a activity (V_{Max}; µmol/g prot/ min) was significantly lowered in cells co-transfected with SERCA1a and MLN compared to cells transfected with SERCA1a only.

Measurements of SERCA-mediated Ca^{2+} uptake rates in crude cell homogenates were conducted with and without the Ca^{2+} precipitating anion, oxalate (as outlined in section 2.3.2).

Similar to the role of ionophore described above, the presence of the oxalate allows for a measure of SERCA-mediated Ca^{2+} uptake under maximal (non-limiting conditions) conditions, whereas, the removal of oxalate from the assay more closely resembles the physiological condition of intact muscle as it allows for the accumulation of vesicular Ca^{2+} which induces back-inhibition of SERCA pumping. Evaluations of SERCA-mediated Ca^{2+} uptake under both maximal (Fig. 4.3.1.2 B, $p = 0.011$) and physiological (Fig. 4.3.1.1 B, $p = 0.031$) conditions revealed significant depressions in the rate of Ca^{2+} uptake in the cells co-transfected with SERCA1a and MLN compared to cells transfected with SERCA1a only.

The Ca^{2+} transport efficiency of the SERCA1a pump was assessed by calculating the apparent coupling ratio (Ca^{2+} uptake/Ca^{2+}-ATPase activity) in the absence of oxalate and ionophore at a pCa of 6.00 (Fig. 4.3.1.1 C, $p = 0.269$) and in the presence of oxalate and ionophore at pCa 6.00 and 6.30 (Fig. 4.3.1.2 C, $p = 0.290$). No differences in the apparent coupling ratio were identified across pCa values or assay conditions in cells transfected with SERCA1a alone and in those co-transfected with SERCA1a and MLN. Furthermore, the ionophore ratio was determined at each pCa to provide an additional method of assessing SERCA efficiency and was calculated by dividing maximal SERCA activity measured in the presence of the ionophore by maximal SERCA activity measured in the absence of the ionophore. A lower ionophore ratio would have been indicative of more inefficient SR Ca^{2+} transport and storage [3], however, the ionophore ratio was not different in cells transfected with SERCA1a alone compared to those co-transfected with SERCA1a and MLN (Fig. 4.3.1.3).

Measurements of Ca^{2+}-ATPase activity and SERCA-mediated Ca^{2+} uptake in crude cell homogenates were subsequently repeated to evaluate the effect of MLN on SERCA2a kinetics and transport efficiency. As expected, the results were consistent between the SERCA isoforms. When

assessed in the both the presence (Fig. 4.3.1.5 A) and absence (Fig. 4.3.1.4 A) of a Ca^{2+} gradient, there was a decrease in the apparent affinity of SERCA2a for Ca^{2+} in the cells co-transfected with SERCA2a and MLN compared to cells transfected with SERCA2a only. Again, this was indicated by a significant increase in the pCa_{50} (Table 4.3.1.1) and a corresponding rightward shift in plots of the Ca^{2+} dependence of Ca^{2+}-ATPase activity. Moreover, in both the presence ($p = 0.012$) and absence ($p = 0.028$) of the Ca^{2+} ionophore, maximal SERCA2a activity was significantly lowered in cells co-transfected with SERCA2a and MLN compared to cells transfected with SERCA2a only. The rate of SERCA-mediated Ca^{2+} uptake determined both in the presence (Fig. 4.3.1.5 B, 0.041) and absence (Fig. 4.3.1.4 B, $p = 0.033$) of oxalate showed a reduction in the rate of Ca^{2+} uptake in the cells co-transfected with SERCA2a and MLN compared to cells transfected with SERCA2a only. Lastly, the apparent coupling ratio was evaluated in the absence of oxalate and ionophore at a pCa of 6.00 (Fig. 4.3.1.4 C, $p = 0.437$) and in the presence of oxalate and ionophore at pCa 6.00 and 6.30 (Fig. 4.3.1.5 C, $p = 0.365$). No differences in the apparent coupling ratio nor ionophore ratio (Fig. 4.3.1.7) were identified across pCa values or assay conditions in cells transfected with SERCA2a alone and in those co-transfected with SERCA2a and MLN.

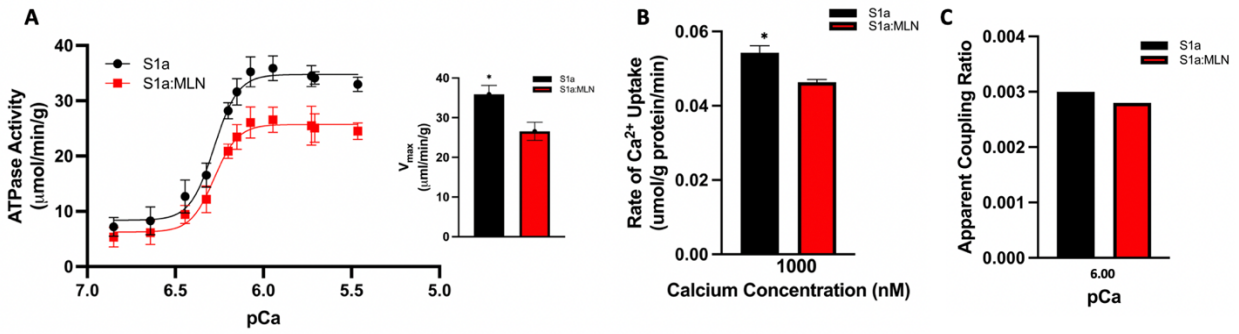


Fig. 4.3.1.1: MLN lowered SERCA1a V_{max} and reduced the rate of Ca^{2+} uptake but did not alter Ca^{2+} pumping efficiency under Physiological Conditions. Ca^{2+} - ATPase activity **(A)** was assessed on crude cell homogenates isolated from HEK-293 cells transfected with either SERCA1a alone or cotransfected with SERCA1a and MLN (n = 3 per group) over [Ca^{2+}] ranging from *p*Ca 6.80 to *p*Ca 4.80 to obtain V_{max} and $K_{Ca.}$, and demonstrated significant differences in these measures between the two experimental groups. The rate of Ca^{2+} - uptake **(B)** was assessed on crude cell homogenates isolated from HEK-293 cells transfected with either SERCA1a alone or cotransfected with SERCA1a and MLN (n = 3 per group) and was significantly depressed in the presence of MLN compared to SERCA1a alone at a [Ca^{2+}] of 1000 nM. SERCA efficiency **(C)** was calculated by dividing Ca^{2+} uptake rates by Ca^{2+} ATPase rates and defined as an apparent coupling ratio, measured in the absence of oxalate and the Ca^{2+} specific ionophore A23187 during Ca^{2+} uptake and Ca^{2+} ATPase measurements, it showed no differences between groups. * indicates a significant difference from S1a alone ($p < 0.05$)

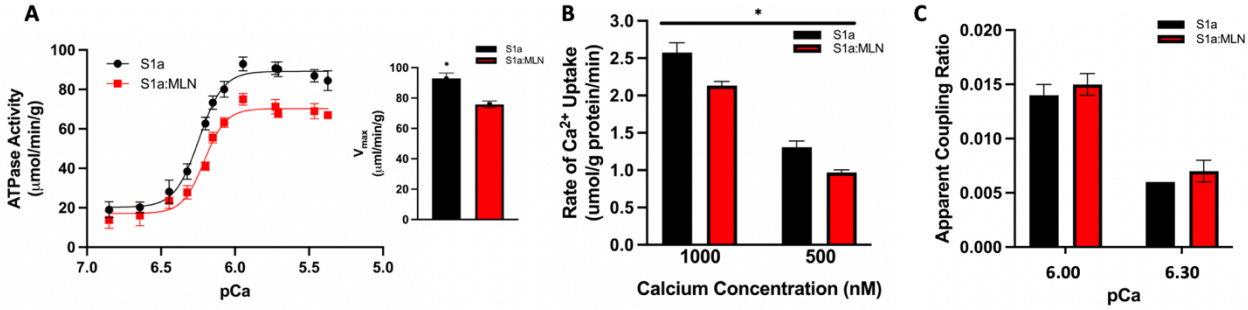


Fig. 4.3.1.2: MLN lowered SERCA1a V_{max} and reduced the rate of Ca^{2+} uptake but did not alter Ca^{2+} pumping efficiency under Maximal Conditions. Ca^{2+} - ATPase activity **(A)** was assessed on crude cell homogenates isolated from HEK-293 cells transfected with either SERCA1a alone or cotransfected with SERCA1a and MLN (n = 3 per group) over [Ca^{2+}] ranging from *p*Ca 6.80 to *p*Ca 4.80 to obtain V_{max}, and demonstrated significant differences in these measures between the two experimental groups. The rate of Ca^{2+} - uptake **(B)** was assessed on crude cell homogenates isolated from HEK-293 cells transfected with either SERCA1a alone or cotransfected with SERCA1a and MLN (n = 3 per group) and was significantly depressed in the presence of MLN compared to SERCA1a alone over [Ca^{2+}] ranging from 500 nM to 1000 nM. SERCA efficiency **(C)** was calculated by dividing Ca^{2+} uptake rates by Ca^{2+} ATPase rates and defined as an apparent coupling ratio, measured in the presence of oxalate and the Ca^{2+} specific ionophore A23187 during Ca^{2+} uptake and Ca^{2+} ATPase measurements, it showed no differences between groups. * indicates a significant difference from S1a alone ($p < 0.05$).

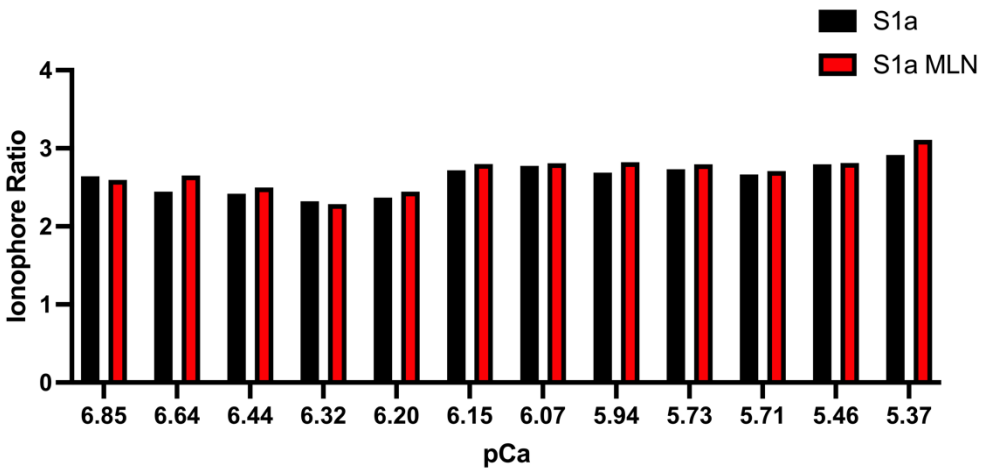


Fig. 4.3.1.3: Ionophore ratios of cells transfected with S1a and co-transfected with S1a and MLN. Ionophore ratios were calculated at each pCa to provide an additional method of assessing SERCA efficiency and were calculated by dividing SERCA activity measured in the presence of the ionophore by SERCA activity measured in the absence of the ionophore.

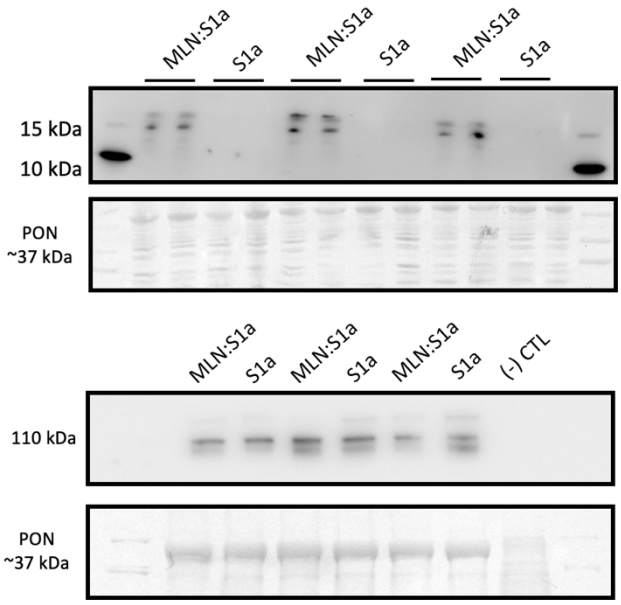


Fig. 4.3.1.4: SERCA1a and MLN protein expression in HEK-293 crude homogenate. Western blotting was performed on crude cell homogenates isolated from HEK-293 cells transfected with either SERCA1a alone or cotransfected with SERCA1a and MLN (n = 3 per group). Proteins were separated by SDS-PAGE on a 7.5% gel (SERCA1a) and 13% gel (MLN), transferred to a PVDF membrane, and proteins were immunoprobed with the corresponding primary antibodies for SERCA1a (A52) and MLN (2211). Equal protein was confirmed using Ponceau S staining.

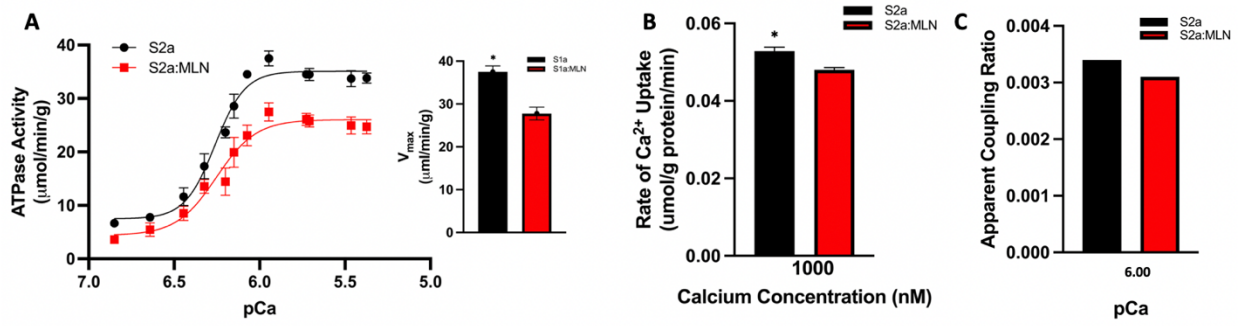


Fig. 4.3.1.5: MLN lowered SERCA2a V_{max} and reduced the rate of Ca^{2+} uptake but did not alter Ca^{2+} pumping efficiency under Physiological Conditions. Ca^{2+} - ATPase activity **(A)** was assessed on crude cell homogenates isolated from HEK-293 cells transfected with either SERCA1a alone or cotransfected with SERCA1a and MLN (n = 3 per group) over [Ca^{2+}] ranging from *p*Ca 6.80 to *p*Ca 4.80 to obtain V_{max} and $K_{Ca.}$, and demonstrated significant differences in these measures between the two experimental groups. The rate of Ca^{2+} - uptake **(B)** was assessed on crude cell homogenates isolated from HEK-293 cells transfected with either SERCA1a alone or cotransfected with SERCA1a and MLN (n = 3 per group) and was significantly depressed in the presence of MLN compared to SERCA1a alone at a [Ca^{2+}] of 1000 nM. SERCA efficiency **(C)** was calculated by dividing Ca^{2+} uptake rates by Ca^{2+} ATPase rates and defined as an apparent coupling ratio, measured in the absence of oxalate and the Ca^{2+} specific ionophore A23187 during Ca^{2+} uptake and Ca^{2+} ATPase measurements, it showed no differences between groups. * indicates a significant difference from S2a alone ($p < 0.05$)

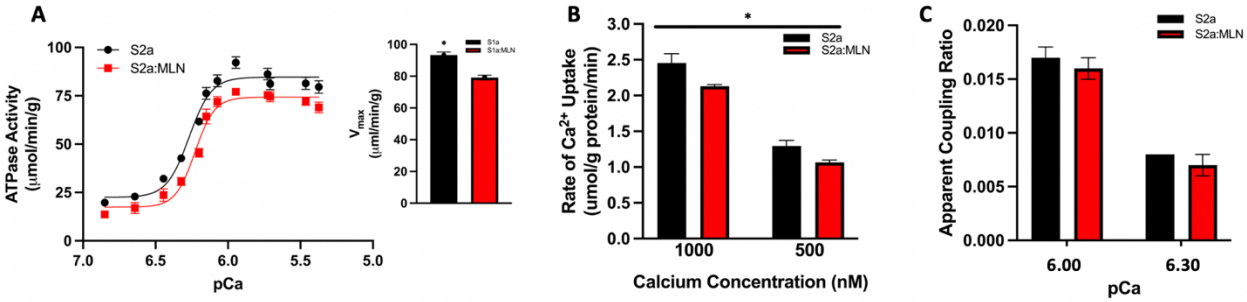


Fig. 4.3.1.6: MLN lowered SERCA2a V_{max} and reduced the rate of Ca^{2+} uptake but did not alter Ca^{2+} pumping efficiency under Maximal Conditions. Ca^{2+} - ATPase activity **(A)** was assessed on crude cell homogenates isolated from HEK-293 cells transfected with either SERCA1a alone or cotransfected with SERCA1a and MLN (n = 3 per group) over [Ca^{2+}] ranging from *p*Ca 6.80 to *p*Ca 4.80 to obtain V_{max}, and demonstrated significant differences in these measures between the two experimental groups. The rate of Ca^{2+} - uptake **(B)** was assessed on crude cell homogenates isolated from HEK-293 cells transfected with either SERCA1a alone or cotransfected with SERCA1a and MLN (n = 3 per group) and was significantly depressed in the presence of MLN compared to SERCA1a alone over [Ca^{2+}] ranging from 500 nM to 1000 nM. SERCA efficiency **(C)** was calculated by dividing Ca^{2+} uptake rates by Ca^{2+} ATPase rates and defined as an apparent coupling ratio, measured in the presence of oxalate and the Ca^{2+} specific ionophore A23187 during Ca^{2+} uptake and Ca^{2+} ATPase measurements, it showed no differences between groups. * indicates a significant difference from S2a alone ($p < 0.05$).

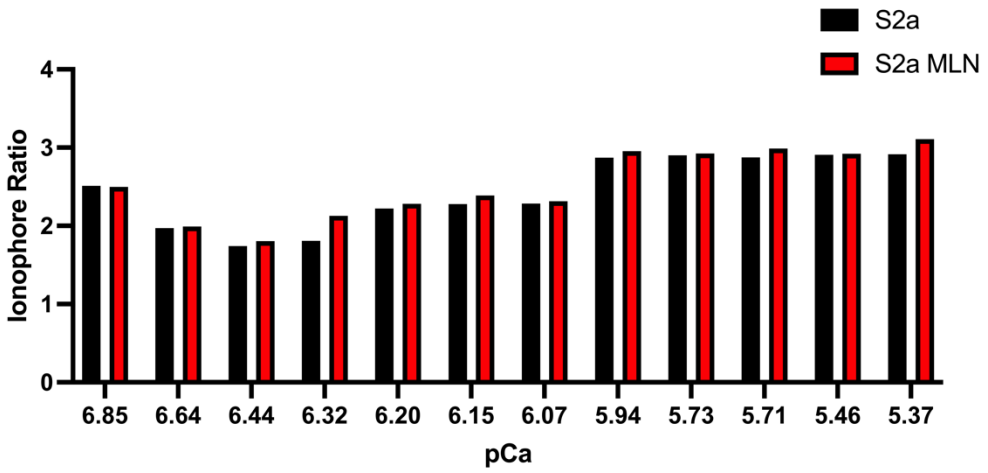


Fig. 4.3.1.7: Ionophore ratios of cells transfected with S2a and co-transfected with S2a and MLN. Ionophore ratios were calculated at each pCa to provide an additional method of assessing SERCA efficiency and were calculated by dividing SERCA activity measured in the presence of the ionophore by SERCA activity measured in the absence of the ionophore.

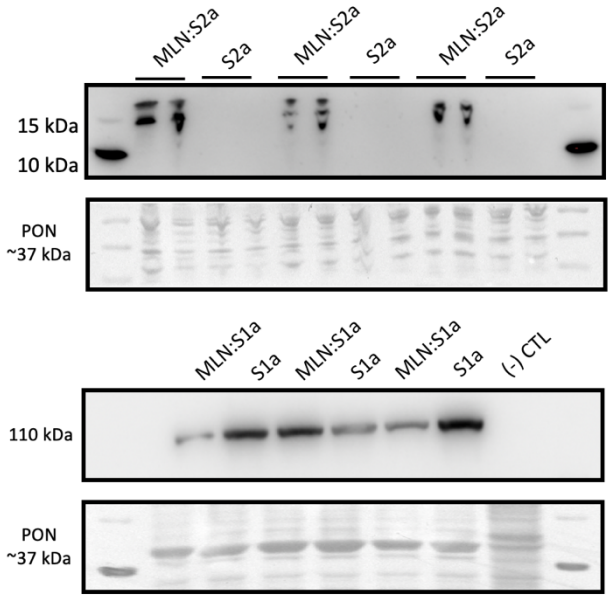


Fig. 4.3.1.8: SERCA2a and MLN protein expression in HEK-293 crude homogenate. Western blotting was performed on crude cell homogenates isolated from HEK-293 cells transfected with either SERCA2a alone or cotransfected with SERCA1a and MLN (n = 3 per group). Proteins were separated by SDS-PAGE on a 7.5% gel (SERCA2a) and 13% gel (MLN), transferred to a PVDF membrane, and proteins were immunoprobed with the corresponding primary antibodies for SERCA2a (2A7-A1) and MLN (2211). Equal protein was confirmed using Ponceau S staining.

Table 4.3.1.1. Ca^{2+} affinity (i.e. pCa_{50}: pCa at half maximal ATPase activity) of cells transfected with SERCA alone and of cells co-transfected with MLN (n = 3/group) measured in the presence (i.e. maximal conditions) and absence (i.e. physiological conditions) of the Ca^{2+}-specific ionophore A23187.

SERCA1a		
	pCa_{50}	
Condition	SERCA1a alone	SERCA1a:MLN
Maximal	6.243 ± 0.01	6.208 ± 0.02*
Physiological	6.280 ± 0.01	6.252 ± 0.01*
SERCA2a		
	pCa_{50}	
Condition	SERCA2a alone	SERCA2a:MLN
Maximal	6.268 ± 0.02	6.228 ± 0.01*
Physiological	6.261 ± 0.02	6.244 ± 0.02*

*, $p < 0.05$ *versus* SERCA1a/2s alone

4.3.2 DWORF Does Not Uncouple of SERCA Ca^{2+} Transport from ATP Hydrolysis

HEK-293 cells were transfected for cDNA encoding SERCA1a or SERCA2a alone (20 ug) and co-transfected for cDNA encoding SERCA1a or SERCA2a (10 ug) at a molar ratio of 1:1 to those encoding DWORF (10 ug) with a total plasmid DNA of 20 μg. Successful transfection of each isoform individually and in combination with DWORF was validated via western blotting for the expression of SERCA1a, SERCA2a and DWORF.

Measurements of Ca^{2+}-ATPase activity and SERCA-mediated Ca^{2+} uptake in crude cell homogenates were conducted as described above to determine the effect of DWORF on SERCA1a kinetics and transport efficiency. When examined in both the presence (Fig. 4.3.2.2, $p = 0.632$) and absence (Fig. 4.3.2.1, $p = 0.479$) of a Ca^{2+} gradient, DWORF had no bearing on the apparent affinity of SERCA1a for Ca^{2+} (Table 4.3.3.1.), no effect on maximal SERCA1a activity, no impact on the rate of SERCA-mediated Ca^{2+} uptake and did not alter the apparent coupling ratio or ionophore ratio, as no difference was observed between cells transfected with SERCA1a alone and those co-transfected with SERCA1a and DWORF for any of these measures. Likewise, the co-transfection of DWORF with SERCA2a yielded similar results. When examined in both the presence (Fig. 4.3.2.5, $p = 0.550$) and absence (Fig. 4.3.2.4, $p = 0.373$) of a Ca^{2+} gradient, DWORF had no bearing on the apparent affinity of SERCA2a for Ca^{2+} (Table 4.3.3.1.), no effect on maximal SERCA2a activity, no impact on the rate of SERCA-mediated Ca^{2+} uptake and did not alter the apparent coupling ratio or ionophore, as no difference was observed between cells transfected with SERCA2a alone and those co-transfected with SERCA2a and DWORF for any of these measures.

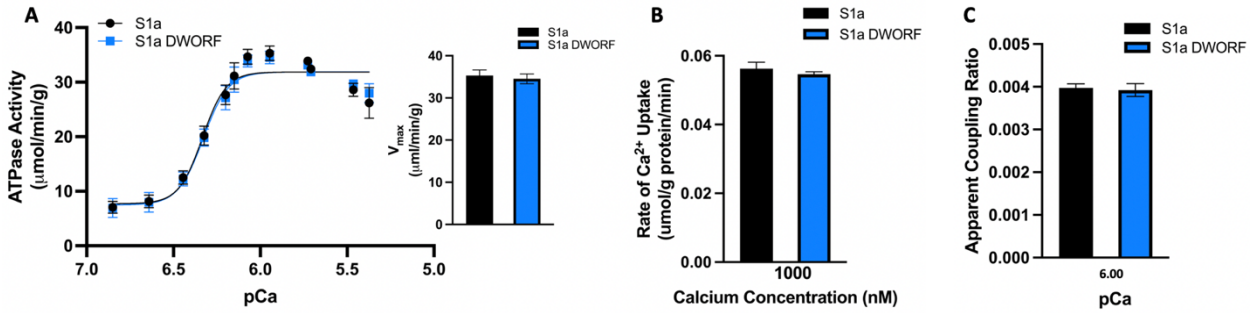


Fig. 4.3.2.1: DWORF did not alter SERCA1a kinetics or Ca^{2+} pumping efficiency under Physiological Conditions. Ca^{2+} - ATPase activity **(A)** was assessed on crude cell homogenates isolated from HEK-293 cells transfected with either SERCA1a alone or cotransfected with SERCA1a and DWORF (n = 3 per group) over [Ca^{2+}] ranging from *p*Ca 6.80 to *p*Ca 4.80 to obtain V_{max} and $K_{Ca\cdot}$, and demonstrated no differences in these measures between the two experimental groups. The rate of Ca^{2+} - uptake **(B)** was assessed on crude cell homogenates isolated from HEK-293 cells transfected with either SERCA1a alone or cotransfected with SERCA1a and DWORF (n = 3 per group) and was unaltered in the presence of DWORF compared to SERCA1a alone at a [Ca^{2+}] of 1000 nM. SERCA efficiency **(C)** was calculated by dividing Ca^{2+} uptake rates by Ca^{2+} ATPase rates and defined as an apparent coupling ratio, measured in the absence of oxalate and the Ca^{2+} specific ionophore A23187 during Ca^{2+} uptake and Ca^{2+} ATPase measurements, it showed no differences between groups. * indicates a significant difference from S1a alone ($p < 0.05$)

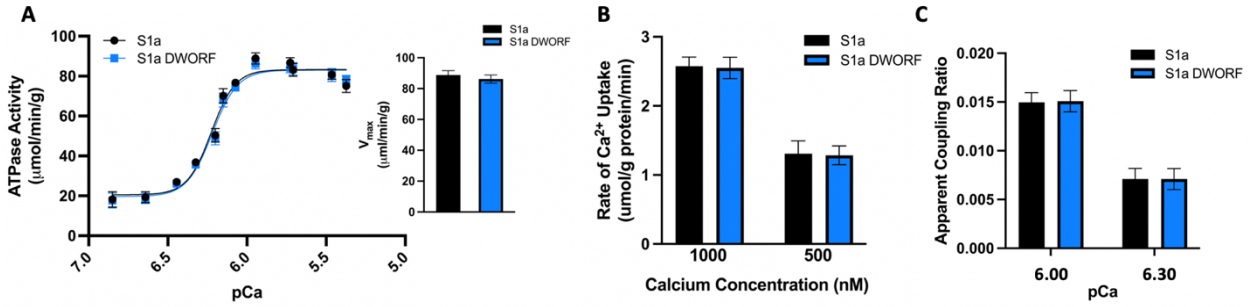


Fig. 4.3.2.2: DWORF did not alter SERCA1a kinetics or Ca^{2+} pumping efficiency under Maximal Conditions. Ca^{2+} - ATPase activity **(A)** was assessed on crude cell homogenates isolated from HEK-293 cells transfected with either SERCA1a alone or cotransfected with SERCA1a and DWORF (n = 3 per group) over [Ca^{2+}] ranging from *p*Ca 6.80 to *p*Ca 4.80 to obtain V_{max} and $K_{Ca\cdot}$, and demonstrated no differences in these measures between the two experimental groups. The rate of Ca^{2+} - uptake **(B)** was assessed on crude cell homogenates isolated from HEK-293 cells transfected with either SERCA1a alone or cotransfected with SERCA1a and DWORF (n = 3 per group) and was unaltered in the presence of DWORF compared to SERCA1a alone at a [Ca^{2+}] of 500 nM and 1000 nM. SERCA efficiency **(C)** was calculated by dividing Ca^{2+} uptake rates by Ca^{2+} ATPase rates and defined as an apparent coupling ratio, measured in the presence of oxalate and the Ca^{2+} specific ionophore A23187 during Ca^{2+} uptake and Ca^{2+} ATPase measurements, it showed no differences between groups. * indicates a significant difference from S1a alone ($p < 0.05$)

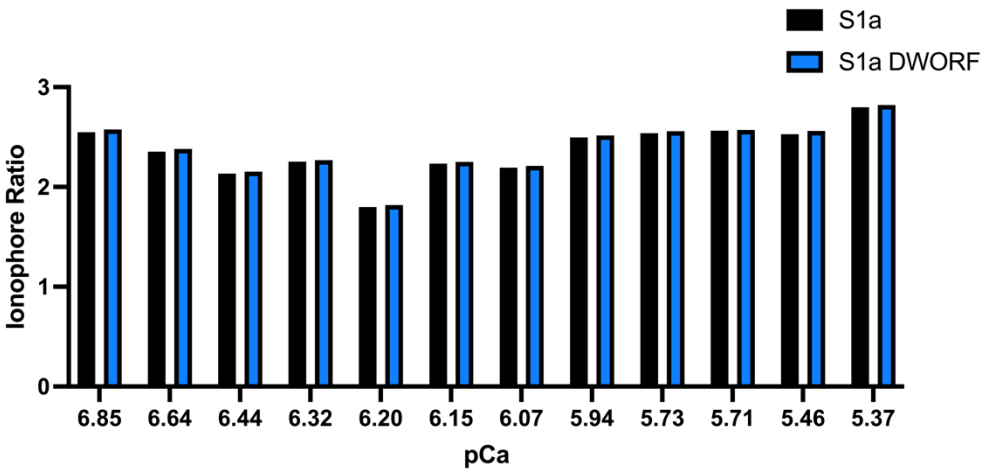


Fig. 4.3.2.3: Ionophore ratios of cells transfected with S1a and co-transfected with S1a and DWORF. Ionophore ratios were calculated at each pCa to provide an additional method of assessing SERCA efficiency and were calculated by dividing SERCA activity measured in the presence of the ionophore by SERCA activity measured in the absence of the ionophore.

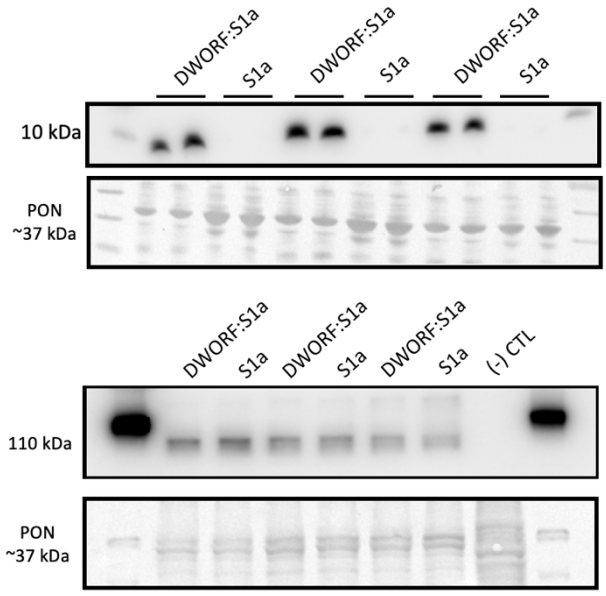


Fig. 4.3.2.4: SERCA1a and DWORF protein expression in HEK-293 crude homogenate. Western blotting was performed on crude cell homogenates isolated from HEK-293 cells transfected with either SERCA1a alone or cotransfected with SERCA1a and DWORF (n = 3 per group). Proteins were separated by SDS-PAGE on a 7.5% gel (SERCA1a) and 13% gel (DWORF), transferred to a PVDF membrane, and proteins were immunoprobed with the corresponding primary antibodies for SERCA1a (A52) and DWORF (generous gift from Dr. Eric Olsen (University of Texas Southwestern). Equal protein was confirmed using Ponceau S staining.

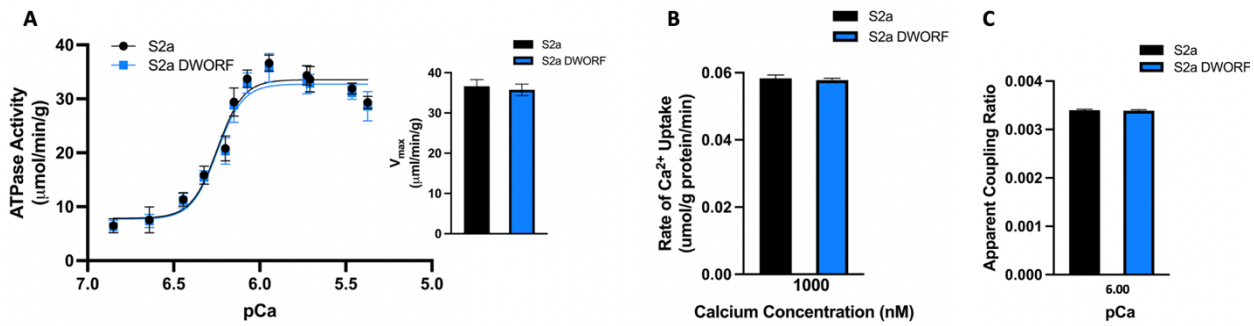


Fig. 4.3.2.5: DWORF did not alter SERCA2a kinetics or Ca^{2+} pumping efficiency under Physiological Conditions. Ca^{2+} - ATPase activity **(A)** was assessed on crude cell homogenates isolated from HEK-293 cells transfected with either SERCA2a alone or cotransfected with SERCA2a and DWORF (n = 3 per group) over [Ca^{2+}] ranging from *p*Ca 6.80 to *p*Ca 4.80 to obtain V_{max} and K_{Ca}., and demonstrated no differences in these measures between the two experimental groups. The rate of Ca^{2+} - uptake **(B)** was assessed on crude cell homogenates isolated from HEK-293 cells transfected with either SERCA2a alone or cotransfected with SERCA2a and DWORF (n = 3 per group) and was unaltered in the presence of DWORF compared to SERCA2a alone at a [Ca^{2+}] of 1000 nM. SERCA efficiency **(C)** was calculated by dividing Ca^{2+} uptake rates by Ca^{2+} ATPase rates and defined as an apparent coupling ratio, measured in the absence of oxalate and the Ca^{2+} specific ionophore A23187 during Ca^{2+} uptake and Ca^{2+} ATPase measurements, it showed no differences between groups. * indicates a significant difference from S2a alone ($p < 0.05$)

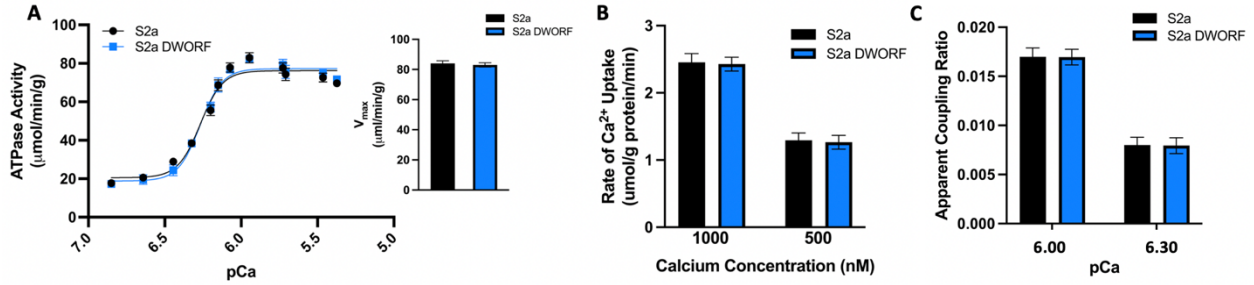


Fig. 4.3.2.6: DWORF did not alter SERCA2a kinetics or Ca^{2+} pumping efficiency under Maximal Conditions. Ca^{2+} - ATPase activity **(A)** was assessed on crude cell homogenates isolated from HEK-293 cells transfected with either SERCA2a alone or cotransfected with SERCA2a and DWORF (n = 3 per group) over [Ca^{2+}] ranging from *p*Ca 6.80 to *p*Ca 4.80 to obtain V_{max} and K_{Ca}., and demonstrated no differences in these measures between the two experimental groups. The rate of Ca^{2+} - uptake **(B)** was assessed on crude cell homogenates isolated from HEK-293 cells transfected with either SERCA2a alone or cotransfected with SERCA2a and DWORF (n = 3 per group) and was unaltered in the presence of DWORF compared to SERCA2a alone at a [Ca^{2+}] of 500 nM and 1000 nM. SERCA efficiency **(C)** was calculated by dividing Ca^{2+} uptake rates by Ca^{2+} ATPase rates and defined as an apparent coupling ratio, measured in the presence of oxalate and the Ca^{2+} specific ionophore A23187 during Ca^{2+} uptake and Ca^{2+} ATPase measurements, it showed no differences between groups. * indicates a significant difference from S2a alone ($p < 0.05$)

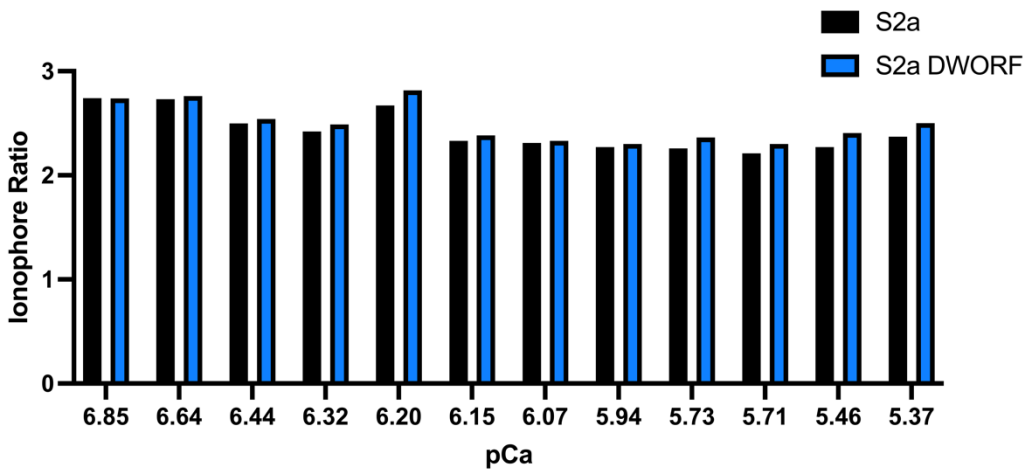


Fig. 4.3.2.7: Ionophore ratios of cells transfected with S2a and co-transfected with S2a and DWORF. Ionophore ratios were calculated at each pCa to provide an additional method of assessing SERCA efficiency and were calculated by dividing SERCA activity measured in the presence of the ionophore by SERCA activity measured in the absence of the ionophore.

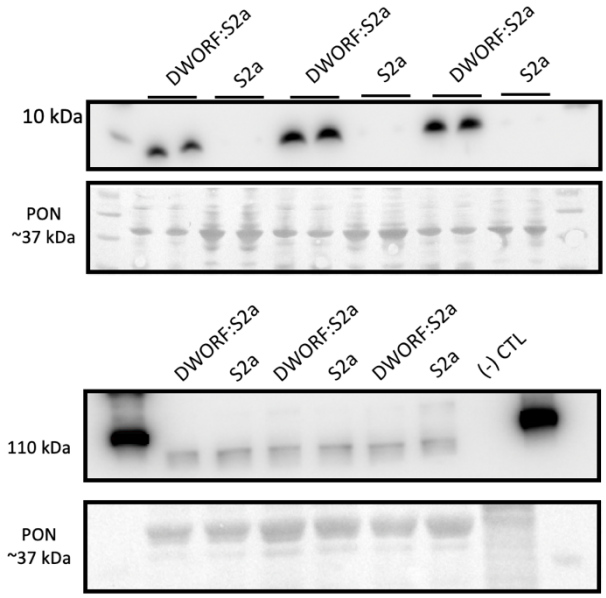


Fig. 4.3.2.8: SERCA2a and DWORF protein expression in HEK-293 crude homogenate. Western blotting was performed on crude cell homogenates isolated from HEK-293 cells transfected with either SERCA2a alone or cotransfected with SERCA2a and DWORF (n = 3 per group). Proteins were separated by SDS-PAGE on a 7.5% gel (SERCA2a) and 13% gel (DWORF), transferred to a PVDF membrane, and proteins were immunoprobed with the corresponding primary antibodies for SERCA2a (2A7-A1) and DWORF (generous gift from Dr. Eric Olsen (University of Texas Southwestern)). Equal protein was confirmed using Ponceau S staining.

4.3.3 DWORF is a Direct Activator of SERCA but Does Not Alter SERCA Efficiency

The lack of a direct effect of DWORF on SERCA kinetics is both consistent and inconsistent with current literature, with discrepancies existing in whether DWORF activates SERCA directly and the mechanism of activation employed, by acting on the pump's affinity for Ca^{2+} or the pump's maximal activity. Therefore, the interaction between DWORF and SERCA was investigated further, by examining the impact of three-fold and five-fold overexpression of DWORF on SERCA kinetics and transport efficiency.

HEK-293 cells were transfected for cDNA encoding SERCA1a or SERCA2a alone (20 ug) and co-transfected for cDNA encoding SERCA1a or SERCA2a (5 ug) at a molar ratio of 1:3 to those encoding DWORF (15 ug) with a total plasmid DNA of 20 µg. Successful transfection of each isoform individually and in combination with DWORF was validated via western blotting for the expression of SERCA1a, SERCA2a and DWORF (Fig. 4.3.3.7).

Measurements of Ca^{2+}-ATPase activity in crude cell homogenates were conducted under maximal (ie. the presence of ionophore) and physiological (ie. the absence of ionophore) conditions to evaluate the effect of the 1:3 transfection ratio on SERCA1a (Fig. 4.3.3.1) and SERCA2a (Fig. 4.3.3.2) kinetics. While no significant differences in Ca^{2+} affinity and maximal activity were observed in cells that were transfected with either SERCA isoform alone or co-transfected with DWORF (1:3) in either condition, both isoforms showed a leftward (albeit non-significant) shift in plots of the Ca^{2+} dependence of Ca^{2+}-ATPase activity – results that are more in line with current literature illustrating the ability of DWORF to act as a positive regulator of SERCA activity (Table 4.3.3.1.).

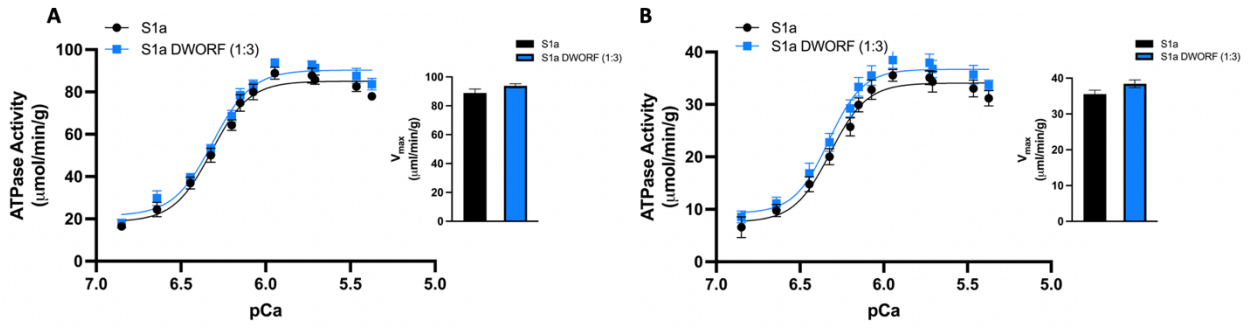


Fig. 4.3.3.1: DWORF did not alter SERCA1a kinetics under Physiological nor Maximal Conditions. Ca^{2+} - ATPase activity was assessed on crude cell homogenates isolated from HEK-293 cells transfected with either SERCA2a alone or cotransfected with SERCA1a and DWORF at a 1:3 ratio (n = 3 per group) over [Ca^{2+}] ranging from *p*Ca 6.80 to *p*Ca 4.80 to obtain V_{max} and K_{Ca}., and demonstrated no differences in these measures between the two experimental groups, in both the presence **(A)** and absence of ionphore **(B)**. * indicates a significant difference from S1a alone ($p < 0.05$)

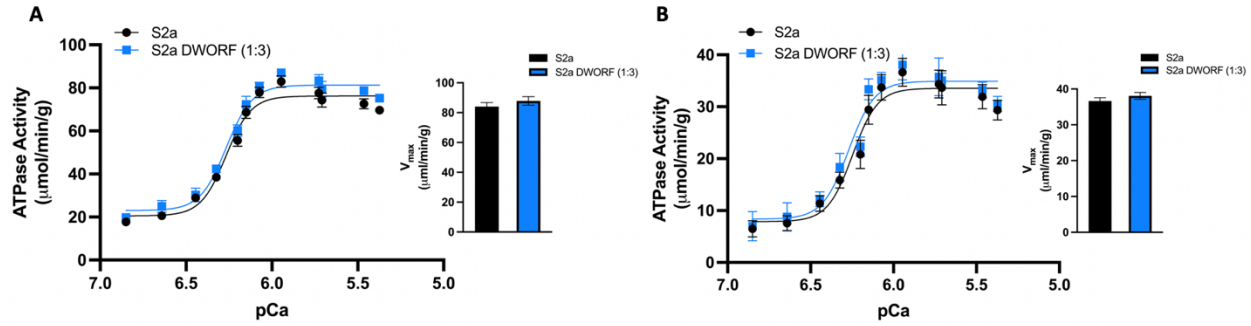


Fig. 4.3.3.2: DWORF did not alter SERCA2a kinetics under Physiological nor Maximal Conditions. Ca^{2+} - ATPase activity was assessed on crude cell homogenates isolated from HEK-293 cells transfected with either SERCA2a alone or cotransfected with SERCA2a and DWORF at a 1:3 ratio (n = 3 per group) over [Ca^{2+}] ranging from *p*Ca 6.80 to *p*Ca 4.80 to obtain V_{max} and K_{Ca}., and demonstrated no differences in these measures between the two experimental groups, in both the presence **(A)** and absence of ionphore **(B)**. * indicates a significant difference from S2a alone ($p < 0.05$)

Subsequently, HEK-293 cells were transfected for cDNA encoding SERCA1a or SERCA2a alone (20 ug) and co-transfected for cDNA encoding SERCA1a or SERCA2a (3.4 ug) at a molar ratio of 1:5 to those encoding DWORF (16.6 ug) with a total plasmid DNA of 20 µg. Successful transfection of each isoform individually and in combination with DWORF was validated via western blotting for the expression of SERCA1a, SERCA2a and DWORF (Fig. 4.3.3.7).

When Ca^{2+}-ATPase activity was assessed in crude cell homogenates in the both the presence (Fig. 4.3.3.4 A, $p = 0.033$) and absence (Fig. 4.3.3.3 A, $p = 0.029$) of a Ca^{2+} gradient, there was a significant increase in the apparent affinity of SERCA1a for Ca^{2+} in the cells co-transfected with SERCA1a and DWORF (1:5) compared to cells transfected with SERCA1a only. This was accompanied by a significant increase in the pCa_{50} (Table 4.3.3.1) and a corresponding leftward shift in plots of the Ca^{2+} dependence of Ca^{2+}-ATPase activity. Furthermore, in the both presence ($p = 0.0458$) and absence ($p = 0.0280$) of the Ca^{2+} ionophore, maximal SERCA1a activity was significantly elevated in cells co-transfected with SERCA1a and DWORF (1:5) compared to cells transfected with SERCA1a only. When examining the rate of SERCA-mediated Ca^{2+} uptake in the both the presence (Fig. 4.3.3.4 B, 0.021) and absence (Fig. 4.3.3.3 B, $p = 0.036$) of a Ca^{2+} gradient, there was a significant increase in the rate of Ca^{2+} transport in cells co-transfected with SERCA1a and DWORF (1:5) compared to cells transfected with SERCA1a only. However, despite the activation of SERCA1a observed with a five-fold overexpression of DWORF, the apparent coupling ratio and ionophore ratio remained unaltered. The Ca^{2+} transport efficiency of the SERCA1a pump was evaluated in the absence of oxalate and ionophore at a pCa of 6.00 (Fig. 4.3.3.3 C, $p = 0.598$) and in the presence of oxalate and ionophore at pCa 6.00 and 6.30 (Fig. 4.3.3.4 C, $p = 0.471$). No differences in the apparent coupling ratio were identified across pCa

values or assay conditions in cells transfected with SERCA1a alone and in those co-transfected with SERCA1a and DWORF (1:5).

Measurements of Ca^{2+}-ATPase activity and SERCA-mediated Ca^{2+} uptake in crude cell homogenates were subsequently repeated to evaluate the effect of the 1:5 transfection ratio on SERCA2a kinetics and transport efficiency. As expected, the results were consistent between the SERCA isoforms. When assessed in the both the presence (Fig. 4.3.3.6 A, $p = 0.041$) and absence (Fig. 4.3.3.5 A, $p = 0.037$) of a Ca^{2+} gradient, there was a significant increase in the apparent affinity of SERCA2a for Ca^{2+} in the cells co-transfected with SERCA2a and DWORF (1:5) compared to cells transfected with SERCA2a only. Again, this was accompanied by a significant increase in the pCa_{50} (Table 4.3.3.1) and a corresponding leftward shift in plots of the Ca^{2+} dependence of Ca^{2+}-ATPase activity. Moreover, in both the presence ($p = 0.029$) and absence ($p = 0.019$) of the Ca^{2+} ionophore, maximal SERCA2a activity was significantly higher in cells co-transfected with SERCA2a and DWORF (1:5) compared to cells transfected with SERCA2a only. The rate of SERCA-mediated Ca^{2+} uptake determined both in the presence (Fig. 4.3.3.6 B, $p = 0.023$) and absence (Fig. 4.3.3.5 B, $p = 0.031$) of oxalate showed a significant elevation in the rate of Ca^{2+} uptake in the cells co-transfected with SERCA2a and DWORF (1:5) compared to cells transfected with SERCA2a only. Lastly, the apparent coupling ratio was evaluated in the absence of oxalate and ionophore at a pCa of 6.00 (Fig. 4.3.3.5 C, $p = 0.279$) and in the presence of oxalate and ionophore at pCa 6.00 and 6.30 (Fig. 4.3.3.6 C, $p = 0.344$). No differences in the apparent coupling ratio nor ionophore ratio were identified across pCa values or assay conditions in cells transfected with SERCA2a alone and in those co-transfected with SERCA2a and DWORF (1:5).

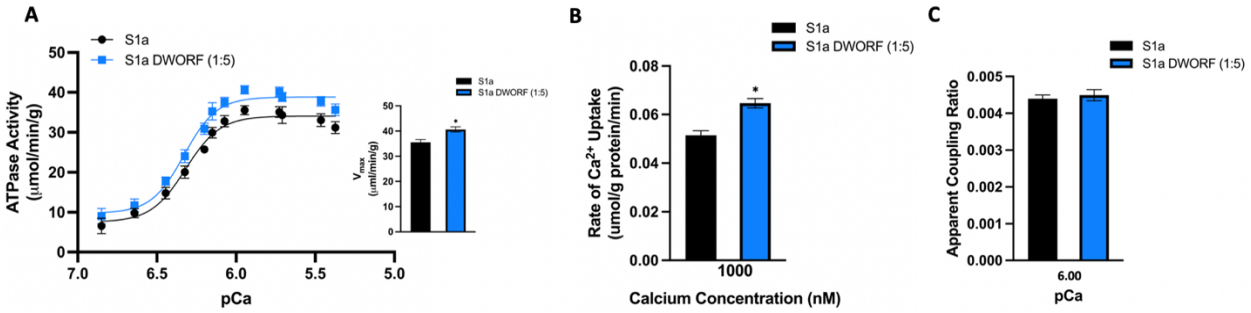


Fig. 4.3.3.3: DWORF directly activated SERCA1a but did not alter Ca^{2+} pumping efficiency under Physiological Conditions. Ca^{2+} - ATPase activity **(A)** was assessed on crude cell homogenates isolated from HEK-293 cells transfected with either SERCA1a alone or cotransfected with SERCA1a and DWORF at a ratio of 1:5 (n = 3 per group) over [Ca^{2+}] ranging from *p*Ca 6.80 to *p*Ca 4.80 to obtain V_{max} and $K_{Ca.}$, and demonstrated significant differences in these measures between the two experimental groups. The rate of Ca^{2+} - uptake **(B)** was assessed on crude cell homogenates isolated from HEK-293 cells transfected with either SERCA1a alone or cotransfected with SERCA1a and DWORF at a ratio of 1:5 (n = 3 per group) and was significantly increased in the presence of DWORF compared to SERCA1a alone at a [Ca^{2+}] of 1000 nM. SERCA efficiency **(C)** was calculated by dividing Ca^{2+} uptake rates by Ca^{2+} ATPase rates and defined as an apparent coupling ratio, measured in the absence of oxalate and the Ca^{2+} specific ionophore A23187 during Ca^{2+} uptake and Ca^{2+} ATPase measurements, it showed no differences between groups. * indicates a significant difference from S1a alone ($p < 0.05$)

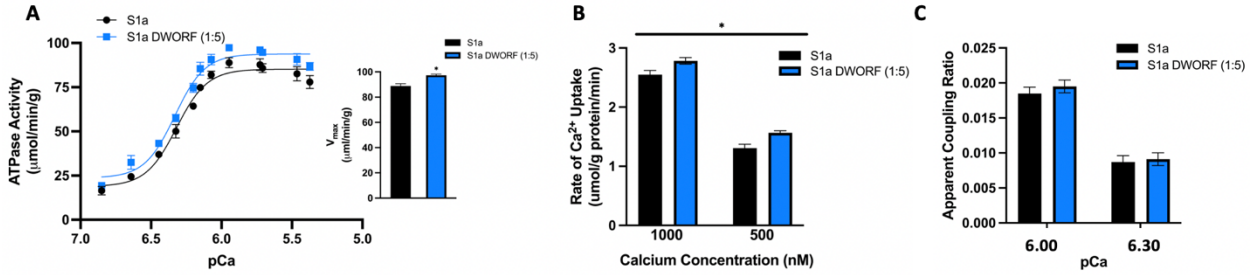


Fig. 4.3.3.4: DWORF directly activated SERCA1a but did not alter Ca^{2+} pumping efficiency under Maximal Conditions. Ca^{2+} - ATPase activity **(A)** was assessed on crude cell homogenates isolated from HEK-293 cells transfected with either SERCA1a alone or cotransfected with SERCA1a and DWORF at a ratio of 1:5 (n = 3 per group) over [Ca^{2+}] ranging from *p*Ca 6.80 to *p*Ca 4.80 to obtain V_{max} and $K_{Ca.}$, and demonstrated significant differences in these measures between the two experimental groups. The rate of Ca^{2+} - uptake **(B)** was assessed on crude cell homogenates isolated from HEK-293 cells transfected with either SERCA1a alone or cotransfected with SERCA1a and DWORF at a ratio of 1:5 (n = 3 per group) and was significantly increased in the presence of DWORF compared to SERCA1a alone at a [Ca^{2+}] of 500 nM and 1000 nM. SERCA efficiency **(C)** was calculated by dividing Ca^{2+} uptake rates by Ca^{2+} ATPase rates and defined as an apparent coupling ratio, measured in the presence of oxalate and the Ca^{2+} specific ionophore A23187 during Ca^{2+} uptake and Ca^{2+} ATPase measurements, it showed no differences between groups. * indicates a significant difference from S1a alone ($p < 0.05$)

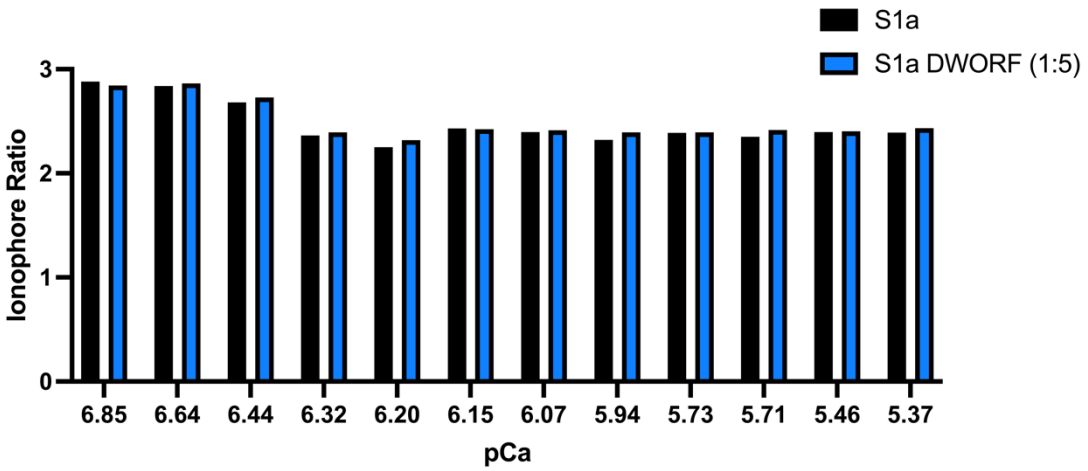


Fig. 4.3.3.5: Ionophore ratios of cells transfected with S1a and co-transfected with S1a and DWORF (1:5). Ionophore ratios were calculated at each pCa to provide an additional method of assessing SERCA efficiency and were calculated by dividing SERCA activity measured in the presence of the ionophore by SERCA activity measured in the absence of the ionophore.

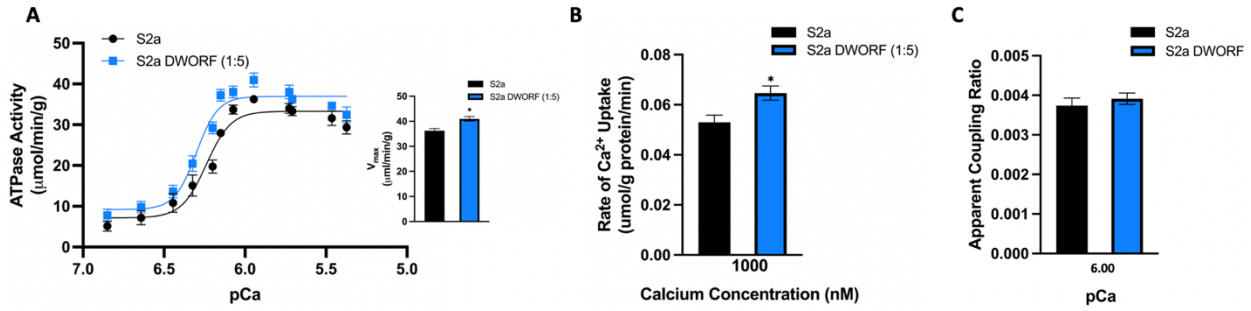


Fig. 4.3.3.6: DWORF directly activated SERCA2a but did not alter Ca^{2+} pumping efficiency under Physiological Conditions. Ca^{2+} - ATPase activity **(A)** was assessed on crude cell homogenates isolated from HEK-293 cells transfected with either SERCA2a alone or cotransfected with SERCA2a and DWORF at a ratio of 1:5 (n = 3 per group) over [Ca^{2+}] ranging from *p*Ca 6.80 to *p*Ca 4.80 to obtain V_{max} and K_{Ca}., and demonstrated significant differences in these measures between the two experimental groups. The rate of Ca^{2+} - uptake **(B)** was assessed on crude cell homogenates isolated from HEK-293 cells transfected with either SERCA2a alone or cotransfected with SERCA2a and DWORF at a ratio of 1:5 (n = 3 per group) and was significantly increased in the presence of DWORF compared to SERCA2a alone at a [Ca^{2+}] of 1000 nM. SERCA efficiency **(C)** was calculated by dividing Ca^{2+} uptake rates by Ca^{2+} ATPase rates and defined as an apparent coupling ratio, measured in the absence of oxalate and the Ca^{2+} specific ionophore A23187 during Ca^{2+} uptake and Ca^{2+} ATPase measurements, it showed no differences between groups. * indicates a significant difference from S1a alone ($p < 0.05$)

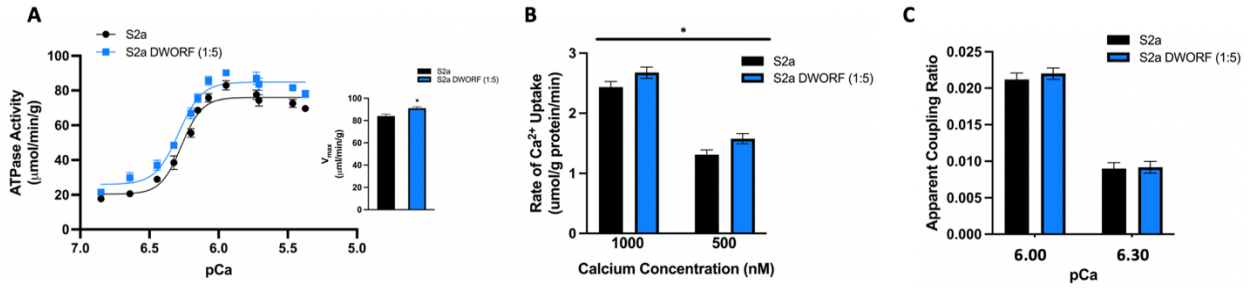


Fig. 4.3.3.7: DWORF directly activated SERCA1a but did not alter Ca^{2+} pumping efficiency under Maximal Conditions. Ca^{2+} - ATPase activity **(A)** was assessed on crude cell homogenates isolated from HEK-293 cells transfected with either SERCA2a alone or cotransfected with SERCA2a and DWORF at a ratio of 1:5 (n = 3 per group) over [Ca^{2+}] ranging from *p*Ca 6.80 to *p*Ca 4.80 to obtain V_{max} and $K_{Ca.}$, and demonstrated significant differences in these measures between the two experimental groups. The rate of Ca^{2+} - uptake **(B)** was assessed on crude cell homogenates isolated from HEK-293 cells transfected with either SERCA2a alone or cotransfected with SERCA2a and DWORF at a ratio of 1:5 (n = 3 per group) and was significantly increased in the presence of DWORF compared to SERCA2a alone at a [Ca^{2+}] of 500 nM and 1000 nM. SERCA efficiency **(C)** was calculated by dividing Ca^{2+} uptake rates by Ca^{2+} ATPase rates and defined as an apparent coupling ratio, measured in the presence of oxalate and the Ca^{2+} specific ionophore A23187 during Ca^{2+} uptake and Ca^{2+} ATPase measurements, it showed no differences between groups. * indicates a significant difference from S1a alone ($p < 0.05$)

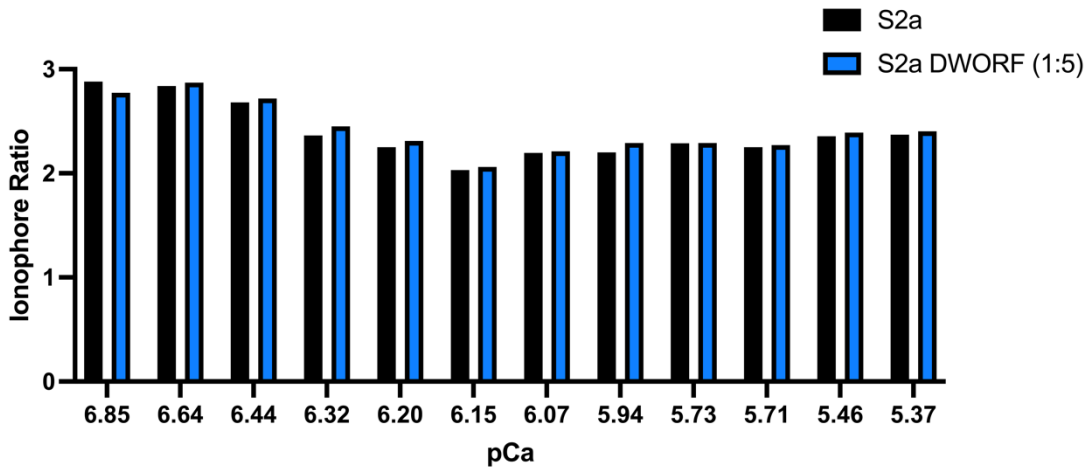


Fig. 4.3.3.8: Ionophore ratios of cells transfected with S2a and co-transfected with S2a and DWORF (1:5). Ionophore ratios were calculated at each pCa to provide an additional method of assessing SERCA efficiency and were calculated by dividing SERCA activity measured in the presence of the ionophore by SERCA activity measured in the absence of the ionophore.

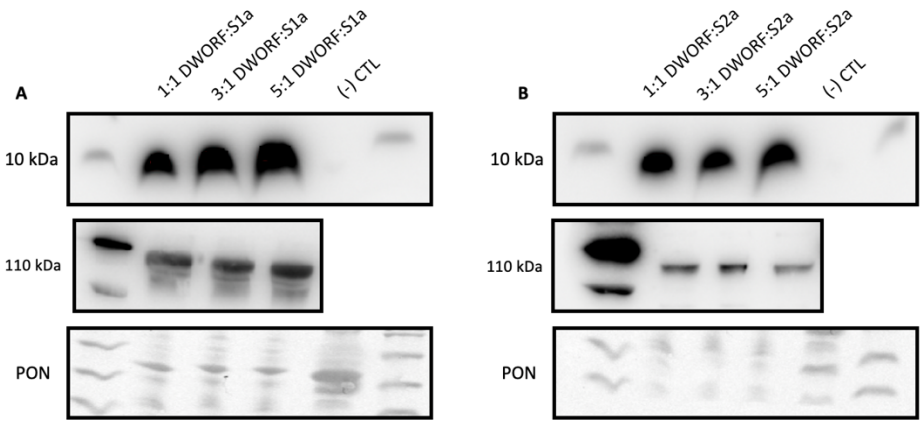


Fig. 4.3.3.9: SERCA1a/2a and DWORF protein expression in HEK-293 crude homogenate. Western blotting was performed on crude cell homogenates isolated from HEK-293 cells transfected with either SERCA1a/2a alone or cotransfected with SERCA1a/2a and DWORF (n = 3 per group)

Table 4.3.3.1. Ca^{2+} affinity (i.e. pCa_{50}: pCa at half maximal ATPase activity) of cells transfected with SERCA alone and of cells co-transfected with DWORF (n = 3/group) measured in the presence (i.e. maximal conditions) and absence (i.e. physiological conditions) of the Ca^{2+}-specific ionophore A23187.

SERCA1a		
	pCa_{50}	
Condition	SERCA1a alone	SERCA1a:DWORF
Maximal	6.225 ± 0.05	6.219 ± 0.04 (1:1)
	6.320 ± 0.03	6.327 ± 0.02 (1:3)
	6.311 ± 0.02	6.341 ± 0.03 (1:5)*
Physiological		
	6.334 ± 0.05	6.331 ± 0.06 (1:1)
	6.319 ± 0.04	6.329 ± 0.03 (1:3)
	6.309 ± 0.02	6.337 ± 0.01 (1:5)*
SERCA2a		
	pCa_{50}	
Condition	SERCA2a alone	SERCA2a:DWORF
Maximal	6.268 ± 0.08	6.270 ± 0.06 (1:1)
	6.251 ± 0.05	6.259 ± 0.04 (1:3)
	6.265 ± 0.01	6.292 ± 0.01 (1:5)*
Physiological	6.247 ± 0.01	6.249 ± 0.02 (1:1)
	6.249 ± 0.02	6.260 ± 0.03(1:3)
	6.239 ± 0.01	6.301 ± 0.02(1:5)*

*, $p < 0.05$ *versus* SERCA1a/2a alone

4.4 Discussion

The objective of this thesis was to determine if MLN and DWORF could alter SERCA transport efficiency, in a manner similar to SLN. Previous *in vitro* and *in vivo* experiments have solidified SLN as a major mediator of skeletal muscle metabolism because of its unique ability to induce slippage of Ca^{2+} ions during the reaction cycle of SERCA pumps and in doing so uncouple SERCA Ca^{2+} transport from ATP hydrolysis to increase the energy required by SERCAs to pump Ca^{2+} ions. To this end, it is of interest to examine whether SR proteins that bare structural resemblance to SLN and physically interact with the pump can exert a similar ability to regulate skeletal muscle energy metabolism. Previous work by our lab has shown that physiological levels of PLN protein within oxidative skeletal muscle do not uncouple SERCA function [84]. This finding is consistent with *in vitro* reconstitution experiments that have shown that SLN's unique cytosolic domain is responsible for conferring its uncoupling properties [92]. Deletion of this domain caused SLN to lose sensitivity to changes in $[Ca^{2+}]_i$ and negated SLN's effect on SERCA function while replacement of the SLN's cytosolic domain with that of PLN allowed the chimeric SLN protein to retain its regulatory role but abolished the ability to uncouple ATP hydrolysis from Ca^{2+} transport [92].

Given that MLN is more structurally similar to PLN and lacks SLN's signature cytosolic domain, it was hypothesized that it would be unlikely for MLN to serve as an uncoupler of SERCA. Indeed, this hypothesis held true as MLN did not alter the coupling ratio nor the ionophore ratio of either SERCA isoform under maximal and physiological conditions. Expectedly, MLN reduced SERCA1a and SERCA2a affinity for Ca^{2+} which was observed as a rightward shift in the Ca^{2+} curve of enzyme activation (representative of an increased Ca^{2+} requirement to reach half-maximal rates of SERCA Ca^{2+} uptake) and decreased the rate of SERCA-mediated Ca^{2+} uptake of both

isoforms. In a novel finding, this study revealed that in addition to altering SERCA affinity for Ca^{2+}, MLN reduced the V_{max} of Ca^{2+}-uptake of both isoforms under maximal and physiological conditions. While MLN can form stable complexes both SERCA isoforms, the fact that it has been shown to co-localize with SERCA1a has limited studies to only examine the interaction between MLN and SERCA1a or to not specify which isoform is being examined. Here, in this study, it is conclusively shown that MLN reduced SERCA1a V_{max} by ~13% under maximal conditions and ~17% under physiological conditions, likewise, MLN decreased SERCA2a V_{max} by ~15% under maximal conditions and ~17% under physiological conditions.

In similar fashion to the cell based studies that investigated SLN and PLN inhibitory function, discrepancies concerning the mechanism by which MLN exerts an inhibitory role are present in the literature. Section 1.5.3 gives a detailed account of the initial discovery paper by Anderson *et al* which showed that MLN reduces SERCA affinity for Ca^{2+} and depresses the rate of Ca^{2+} uptake without altering SERCA maximal activity [12]. In contrast, a recent study by Rathod *et al* found that MLN did not alter SERCA Ca^{2+} affinity but did lower SERCA V_{max}. Interestingly, this study additionally showed that SLN reduced both SERCA Ca^{2+} affinity and SERCA V_{max} while PLN decreased SERCA Ca^{2+} affinity while increasing SERCA V_{max} when overexpressed at levels not physiologically observed [145]. However, a criticism of the Rathod *et al* study is that SERCA activity was not measured at physiological temperature (37°C) but was instead measured at 30°C. Furthermore, the [Ca^{2+}]s across which activity was evaluated were not stated; and neither was whether the assay was performed in the presence or absence of back inhibition – therefore, it is not known if the results are representative of maximal or physiological conditions. An important characteristic that distinguishes the study described in this thesis from both of the above studies, is that we are the first to conclusively confirm the direct presence (and

absence) of the MLN protein in our cell model via western blotting. The work conducted by Anderson *et al* relied on N-terminal HA-tagged MLN fusion protein (HA-MLN) and a C-terminal FLAG-tagged MLN fusion protein (FLAG-MLN) while Rathod *et al* did not include a direct verification of successful transfection.

DWORF exhibits the most promise in possessing the ability to uncouple SERCAs because of the distinct way in which it interacts with the pump. While all four regulatory proteins can interact with SERCA's M2, M4, M6, M9 Ca^{2+} binding groove, DWORF and SLN are special in that: i) SLN can remain bound to SERCA in the presence of high Ca^{2+} while DWORF exhibits the highest affinity for conformations of SERCA that prevail at high Ca^{2+} and ii) SLN remains bound to SERCA throughout its catalytic cycle while DWORF specifically interacts with the helix of the Ca^{2+} binding groove that undergoes the largest structural changes throughout the catalytic cycle. However, DWORF shares the least sequence homology, including lacking similarity with SLN's cytosolic domain, therefore it was hypothesized that it too, would not be able to uncouple the SERCAs. This was proven correct, as DWORF did not alter coupling nor ionophore ratio. In fact, when expressed in a 1:1 molar ratio, DWORF had negligible bearing on SERCA1a/2a Ca^{2+} affinity, activity and uptake. This is consistent with the initial discovery paper published by Nelson *et al* [13], that reported MLN exhibiting no bearing on SERCA's apparent affinity for Ca^{2+} and overall SERCA function. Unfortunately, due to constraints in the transfection method, we were unable to validate whether DWORF acts as a non-inhibitory competitor to re-establish basal SERCA's Ca^{2+} affinity. With the emergent discrepancies in the literature surrounding DWORF, especially the revelations that it could directly stimulate SERCA through augmented Ca^{2+} affinity or improved maximal activity, we sought to examine whether the overexpression of DWORF affected SERCA function.

To that end, DWORF was overexpressed at 3:1 and 5:1 ratios relative to SERCA1a/2a and the results were very interesting. Under both maximal and physiological conditions, three-fold overexpression of DWORF did not significantly change SERCA kinetics, it did however, shift the Ca^{2+} curve of enzyme activation leftward (representative of a decreased Ca^{2+} requirement to reach half-maximal rates of SERCA Ca^{2+} uptake). An exciting, novel finding of this study was that five-fold overexpression of DWORF enhanced SERCA1a/2a Ca^{2+} affinity, activity and uptake without altering transport efficiency. Referring to **Table A.2** in **Appendix A**, these results diverge from Nelson *et al* [13] and corroborate the observation from Li *et al* [127] that DWORF increases SERCA Ca^{2+} affinity and the observation from the Fisher *et al* [123] that DWORF increases SERCA maximal activity.

Moreover, this thesis study contrasts with Fisher *et al* in two important aspects. First, Fisher *et al* determined that DWORF did not act to alter SERCA Ca^{2+} affinity [123], whereas, we observed a significant leftward shift the Ca^{2+} curve of enzyme activation that corresponded with a higher pCa (decreased Ca^{2+} requirement to reach half-maximal rates of SERCA Ca^{2+} uptake) and increased rates of SERCA-mediated Ca^{2+} uptake of both isoforms. Secondly, Fisher *et al* showed DWORF to starkly elevate SERCA maximal activity by ~ 1.7-fold when expressed at near equimolar ratio (~1–2 DWORF per SERCA) [123]. The magnitude of this increase in V_{max} is comparable to that of the small-molecule activator of SERCA, CDN1163, which can increase maximal activity by ~1.5-fold; [128]. We found the 1:1 and 3:1 (DWORF per SERCA) molar ratios to be insufficient for the activation of SERCA and while the 5:1 molar ratio did significantly increase maximal activity, it did so to a lower degree. Five-fold DWORF overexpression served to increase SERCA1a maximal activity by ~1.09-fold under maximal conditions and ~1.14 fold under physiological conditions, while, increasing SERCA2a maximal activity by ~1.08-fold under

maximal conditions and ~1.13-fold under physiological conditions. Discrepancies between studies can be attributed to multiple factors including differences in DWORF:SERCA stoichiometry, whether an animal-based, cell-based or reconstituted lipid system had been employed, the cell lines used, the presence of protein tags, and/or variations in reconstitution protocols which could affect lipid:protein ratios [13, 122, 123, 127].

The ability of DWORF to directly regulate SERCA function does raise the question of physiological relevance and highlights the importance of supplementing the knowledge gained from cell based models with physiological changes observed in transgenic animal models. Expression of DWORF protein overlaps with the expression of PLN in murine oxidative skeletal muscle and cardiac muscle. Moreover, in oxidative skeletal muscle, DWORF expression can be hypothesized to additionally overlap with both MLN and SLN expression. Without single fibre western blotting to confirm co-expression of DWORF with the regulatory other proteins across fibre-types, this suggests that DWORF is normally competing with one or more regulatory proteins for interaction with the pump. Even though SERCA shows a greater affinity for DWORF, three-fold overexpression of DWORF is required to displace the other regulatory proteins from the pump and alleviate their inhibition. Therefore, regardless of the molar ratio of DWORF per SERCA needed to activate the pump, the opportunity for DWORF to interact with SERCA directly and independently of the other regulators doesn't seem likely.

Investigating whether DWORF can increase apparent Ca^{2+} affinity and maximal activity of the pump in a physiological setting may prove difficult, as to do so, the other regulatory proteins would need to be absent to allow for an independent assessment of DWORF function. However, examining DWORF's function as a non-inhibitory competitor in a physiological setting has proven attainable. Interestingly, soleus tissue from a murine model of DWORF ablation showed no

differences in contractile function despite a decrease in apparent affinity of SERCA for Ca^{2+} [13]. This change in SERCA Ca^{2+} affinity could be indicative of greater binding of the other regulatory proteins and thus greater SERCA inhibition, in the absence of DWORF-mediated regulation [13]. On the other hand, the overexpression of DWORF protein in adult cardiomyocytes improved cardiac function and caused a cellular phenotype that was analogous to that observed in *Pln*$^{-/-}$ mice (described in greater detail in Section 1.5.6) [129]. In fact, as highlighted previously, DWORF overexpression completely reversed the impairments in Ca^{2+} handling associated with PLN overexpression [129]. Collectively, this strongly suggests that DWORF acts on SERCA activity by competing for and displacing PLN from the pump in order to relieve the inhibitory effects.

Touched on in Section 1.4.1, in an effort to discern structure and function, as well as, the divergences that allow for their distinct physiological roles, PLN and SLN have been the subjects of extensive mutagenesis studies. Future mutagenesis studies with the aim of teasing apart the residues responsible for i) facilitating the interaction between MLN/DWORF and the SERCAs, ii) imparting MLN's inhibitory function and DWORF's stimulatory function, and iii) conferring thermal stability under conditions of HS; would serve to further our mechanistic understanding of SERCA protection and regulation. To date, studies investigating the structure and function of MLN have been sparse. Molecular modeling and molecular dynamics simulations by Rathod and colleagues have proposed that the key interactions between MLN and SERCA are as follows: Lys^{27} of MLN with Gln^{108} of M2, Arg^{24} of MLN with Thr^{805} of M6, and Tyr^{41} of MLN with Phe^{88} and Phe^{92} of M2 [145]. However, while these simulations provide us with a starting point, mutagenesis studies evaluating mutant variants are needed to validate that these are indeed the residues forming critical contacts with SERCA and possibly conferring a regulatory and/or protective function. The initial discovery paper by Anderson *et al* revealed that alanine mutagenesis of MLN residues

shared with PLN and SLN (Leu^{29} (L29A), Phe^{30} (F30A), and Phe^{33} (F33A)) abolished the ability of MLN to interact with SERCA1, whereas, mutation of residues Lys^{27} (K27A) and Asp^{35} (D35A) did not alter this interaction [12]. Subsequent studies by Liu *et al* and Rathod *et al*, confirmed that mutation of Asp^{35} did not alter MLN's ability to interact with SERCA nor impede MLN's inhibition of SERCA Ca^{2+} affinity [154] and demonstrated that while replacement of Lys^{27} with Asn did not affect MLN's interaction with SERCA nor inhibition of SERCA Ca^{2+} affinity, it did cause a significant depression in maximal activity of the pump [155]. Moreover, Anderson *et al* postulated that the N-terminal sequence of MLN could serve as a regulatory domain through phosphorylation, as this sequence contains multiple serine and threonine residues [12], however, it is yet to be evaluated if MLN can be phosphorylated and what cellular conditions would promote this phosphorylation. Recall from Section 1.3.1, that PLN is subjected to phosphorylation under conditions of elevated $[Ca^{2+}]_i$ and adrenergic stimulation. Given the similarities between PLN and MLN, it could be hypothesized that rising $[Ca^{2+}]_i$ could also result in MLN phosphorylation to allow to unimpeded SERCA function to restore $[Ca^{2+}]_i$ homeostasis.

Meanwhile, as the only regulatory protein with the capability to displace the other regulators and positively regulate the SERCA pump, investigations into the structure and function of DWORF have been much more extensive. Recall from Section 1.5.4 that DWORF exhibits a discontinuous transmembrane domain, with a kink induced by Pro^{15}, separating the two helical domains [122, 123]. Multiple structural and functional studies have shown that that Pro^{15} (and the induced kink) are critical for DWORF's interaction with SERCA's M4 helix and for DWORF's activating effect on SERCA (both indirectly and directly) [122, 123, 127]. With M4 undergoing the most substantial movements throughout SERCA's catalytic cycle [125, 126], it is speculated that the kink permits DWORF to better accommodate the structural transitions of the complex.

Furthermore, molecular modeling by Rathod and colleagues have proposed additional residues of critical contact between DWORF and SERCA, including His^{10} on DWORF and Ser^{936} of SERCA and Val^{14} and Ile^{16} on DWORF with Trp^{107} on SERCA [145]. However, this modelling failed to identify Pro^{15} as a point of contact and in fact, did not determine any points of contact between DWORF and SERCA's M4 helix which has been reported by others to form an extensive interaction. Again, further validation of the residues identified by molecular modelling must be conducted using mutagenesis studies.

A caveat to the coupling ratio data described in thesis is that we were only able to assess coupling ratio at $[Ca^{2+}]_f$: 1000 nM (pCa 6.0) and 500 nM (pCa 6.3). Recall from Section 1.1 that $[Ca^{2+}]_f$ of resting skeletal muscle is maintained below 100 nM and that an elevation in this concentration to 1000 nM (or greater) triggers cellular activation via the induction of downstream pathways [14, 15]. The seminal *in vitro* studies that employed reconstituted liposomes to investigate SERCA uncoupling [4] and heat production [5] in the presence of SLN were able to evaluate SERCA uncoupling or heat production at $[Ca^{2+}]_f$ levels as low as 80um [5]. Moreover, *in vivo* investigations into the impact of PLN [84] and SLN [3] on SERCA pumping efficiency evaluated uncoupling at Ca^{2+} levels resembling physiological $[Ca^{2+}]_f$ in resting skeletal muscle. This is of particular importance due to the fact that the impact of SLN on SERCA pumping efficiency has been shown to be Ca^{2+}-dependent, with greater uncoupling of SERCA in WT compared to $Sln^{-/-}$ soleus at low free $[Ca^{2+}]$ (i.e. pCa 6.9, which is close to the physiological $[Ca^{2+}]_f$ in resting skeletal muscle) [3]. We did however, obtain ionophore ratio as a secondary measure of SERCA transport efficiency, which unanimously showed no change across a wide range of pCas, including those representative of $[Ca^{2+}]_f$ near that of resting skeletal muscle.

4.5 Conclusion

Prior studies have established SLN as a crucial mediator of skeletal muscle metabolism by modulating SERCA activity through the promotion Ca^{2+} ion slippage during its reaction cycle [1-3, 31]. Here, we show that MLN, structurally more akin to PLN and lacking SLN's characteristic cytosolic domain, did not demonstrate the capacity to uncouple SERCA, contrary to SLN. Instead, MLN lowered the Ca^{2+} affinity and maximal activity of both SERCA1a and SERCA2a under maximal and physiological conditions without altering the pump's transport efficiency. Conversely, DWORF, distinct in its interaction with SERCA compared to other regulatory proteins, exhibited negligible impact on SERCA1a and SERCA2a Ca^{2+} affinity, maximal activity, and rate of uptake when expressed in a 1:1 molar ratio. However, higher DWORF overexpression ratios led to enhanced Ca^{2+} affinity and maximal activity of both SERCA isoforms under maximal and physiological conditions, though no effect on transport efficiency was observed. Where Study I showcased a similar capability of all four regulatory proteins to preserve SERCA structure and function during thermal stress, Study II contributes to the growing body of evidence showing that these regulatory proteins serve functionally distinct roles in the maintenance of $[Ca^{2+}]_i$ homeostasis.

Chapter 5

Thesis Study III: Assessing Potential Compensatory Changes in SERCA Regulatory Expression

5.1 Study Objectives and Hypotheses

Study III aimed to evaluate potential compensatory changes in SERCA regulatory protein expression. To do so, quantitative RT-PCR for mRNA expression and Western blotting for protein expression were performed on soleus, left ventricle and atrial muscle isolated from male and female wild type compared to single knockout ($Sln^{-/-}$ and $Pln^{-/-}$) mice and double knockout ($Sln^{-/-}/Pln^{-/-}$) mice to examine if ablation of one or two SERCA regulatory protein(s) would result in compensatory changes in the expression of other SERCA regulatory proteins. Analyses were made in mice aged 4-6 months.

Objectives:

1. To determine if the ablation of SLN alters the expression of MLN and DWORF in soleus and atria
2. To determine if the ablation of PLN alters the expression of MLN and DWORF in soleus and left ventricle
3. To determine if the ablation of both SLN and PLN alters the expression of MLN and DWORF in soleus, left ventricle and atria

Hypotheses:

1. Based on the body of literature examining SLN and PLN ablation, respectfully, it is hypothesized that MLN expression will not change in soleus in the absence of either protein nor will it change in the atria in the absence of SLN or in the left ventricle in the absence of PLN.
2. Based on research highlighting a stronger association of DWORF with PLN in both soleus and left ventricle, it is hypothesized that the ablation of PLN will alter DWORF expression.

SLN ablation is hypothesized to have no bearing on DWORF expression in either soleus or atria

3. In the absence of both SLN and PLN, it is hypothesized that MLN expression will be altered to compensate for the loss of both SLN and PLN in soleus; however, expression of MLN will not change in left ventricle and atria
4. In the absence of both SLN and PLN, it is hypothesized that DWORF expression will be altered to compensate for the loss of both SLN and PLN in all muscles examined

5.2 Study Design

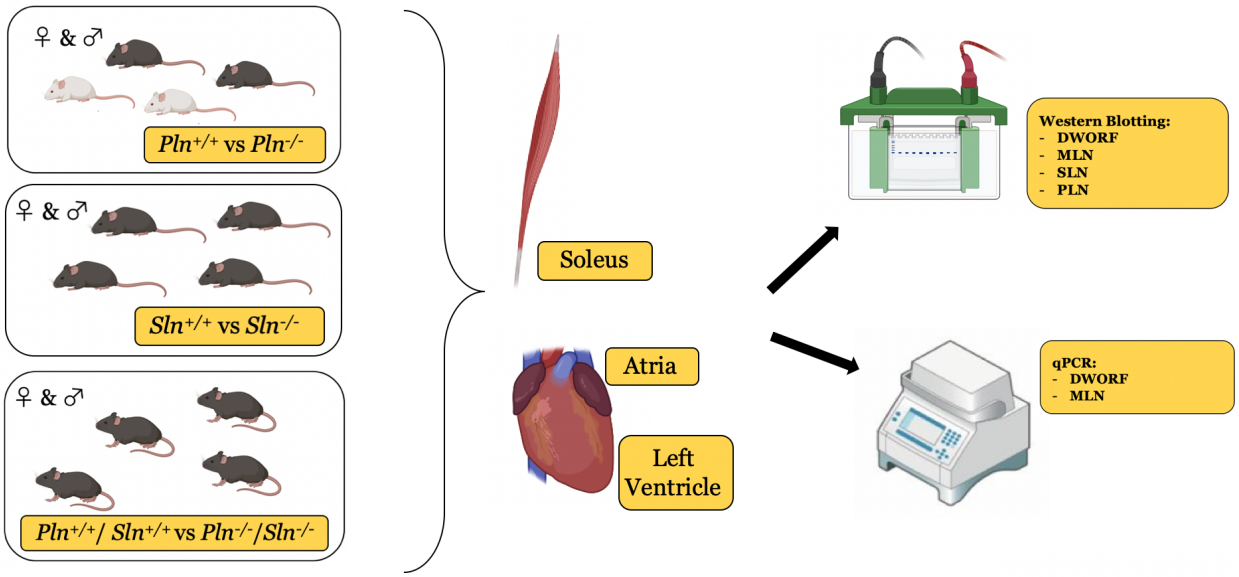


Fig. 5.2.1: Schematic of Study Design for Thesis Study III

5.3 Results

5.3.1 MLN and DWORF protein expression is not altered by the absence of PLN while *Dworf* mRNA expression shows differences with PLN ablation

Given the abundant expression of PLN in cardiac LV, prior to evaluating compensatory changes in protein expression, western blotting was conducted on LV to verify the ablation of PLN in $Pln^{-/-}$ male mice compared to WT ($Pln^{+/+}$) male controls. Indeed, PLN protein was robustly expressed in male WT LV but was undetected in LV of $Pln^{-/-}$ male mice. Subsequently, western blotting for MLN and DWORF was conducted on SOL and LV muscles from WT and $Pln^{-/-}$ male mice to investigate potential compensatory changes in the level of expression of these proteins in the absence of PLN. No significant change in MLN ($p = 0.486$) or DWORF ($p = 0.381$) protein expression was detected with the ablation of PLN in either muscle examined (Fig. 5.3.1.1).

Validation of PLN protein ablation in $Pln^{-/-}$ female mice was determined in the same fashion as for the $Pln^{-/-}$ male mice. Evaluation of MLN and DWORF protein expression in SOL and LV muscles from WT and $Pln^{-/-}$ female mice yielded similar results to those observed in the male littermates, with no significant difference in the expression of MLN ($p = 0.451$) or DWORF ($p = 0.279$) observed in either muscle in the absence of PLN (Fig. 5.3.1.2).

To compliment the protein expression analysis, real-time PCR (qPCR) was performed on SOL and LV muscles from the same WT and $Pln^{-/-}$ male and female mice to investigate potential changes in *Mln* and *Dworf* gene expression in the presence and absence of *Pln* expression. In accordance with the protein content data, gene expression of both *Mln* (SOL $p = 0.110$; LV $p = 0.958$) and *Dworf* (SOL $p = 0.283$) was unaltered with the ablation of *Pln* in both muscles examined in male mice, with the only difference being a trending increase ($p = 0.0708$) in *Dworf* gene expression in $Pln^{-/-}$ male LV tissue (Fig. 5.3.1.3). The same pattern was observed in female mice, as there was no change in gene expression of *Mln* in both SOL ($p = 0.705$) and LV ($p =$

0.106) tissue. Again, no change in *Dworf* expression was observed in female SOL tissue ($p = 0.983$), however, while male LV only showed a trending increase in *Dworf* expression in the absence of *Pln*, female LV showed a significant elevation in *Dworf* expression ($p = 0.0006$) with *Pln* ablation (Fig. 5.3.1.4).

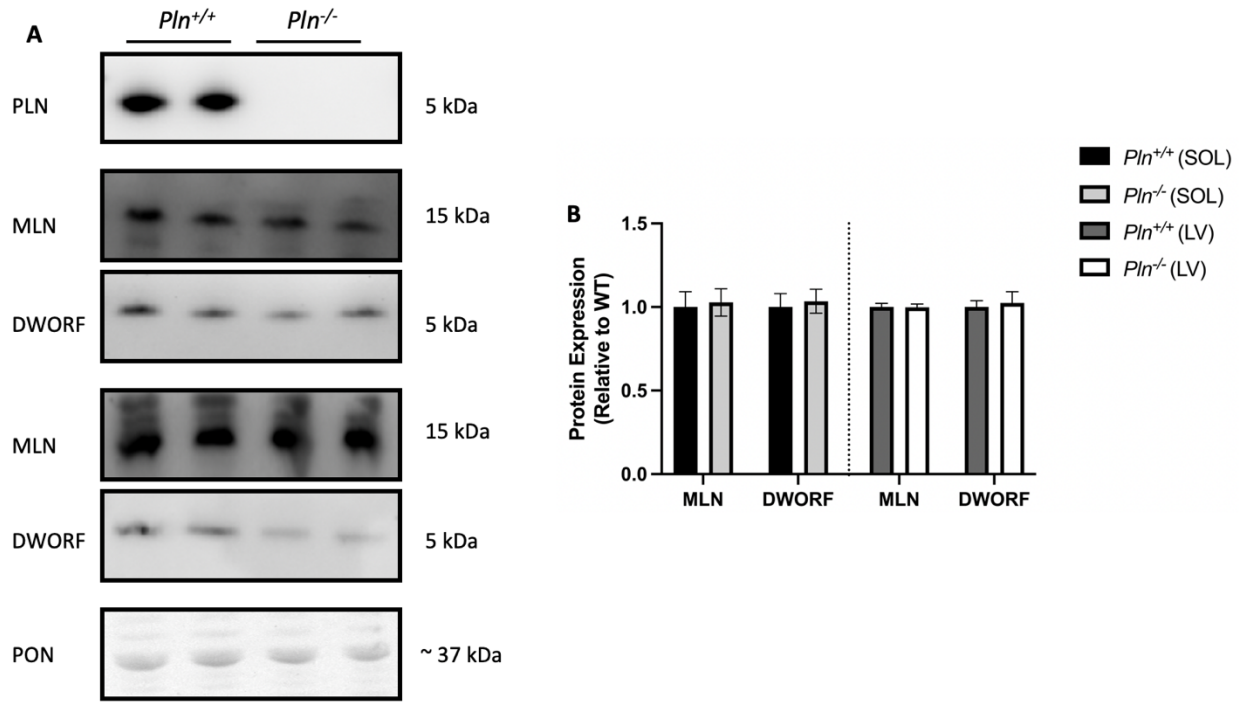


Fig. 5.3.1.1: MLN and DWORF protein expression in *Pln*$^{+/+}$ and *Pln*$^{-/-}$ male mice. MLN and DWORF protein expression is unaltered by PLN ablation in SOL and LV. **A)** Representative Western blots of 5-6 mo old male *Pln*$^{+/+}$ and *Pln*$^{-/-}$ mice (n = 6/group). Equal protein load was confirmed using Ponceau S staining. **B)** Protein expression relative to *Pln*$^{+/+}$ mice. Values are mean ± S.E.

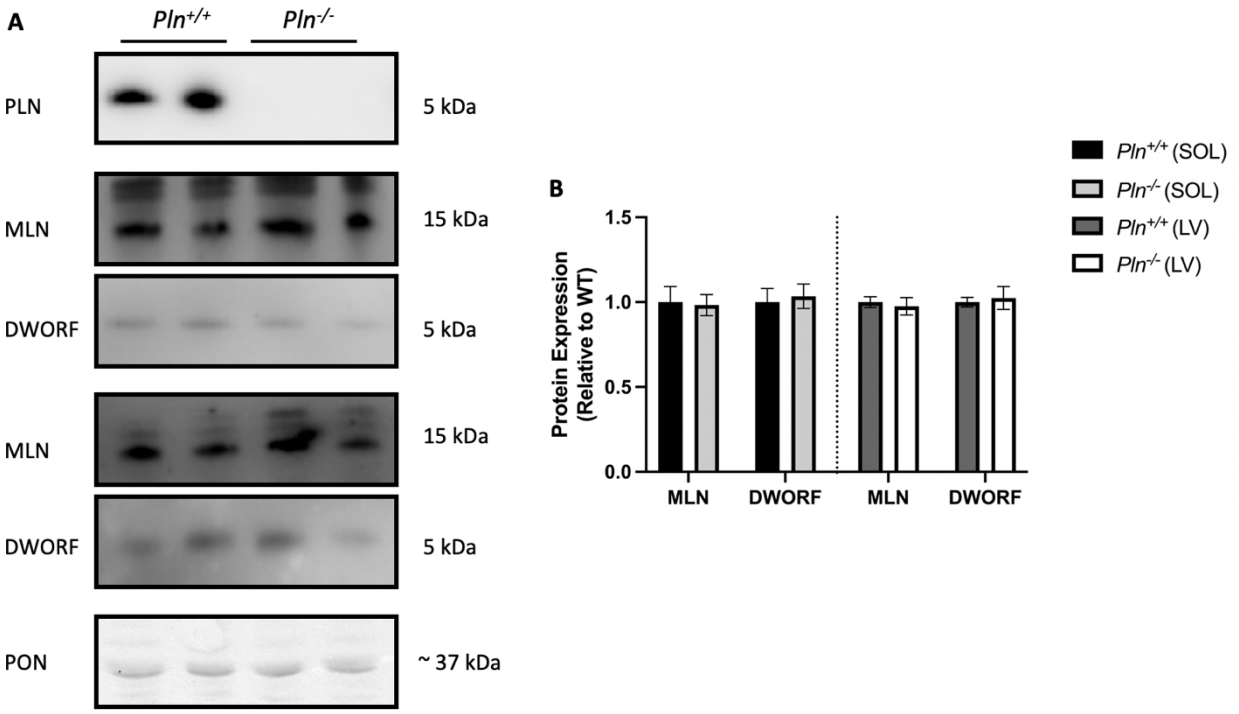


Fig. 5.3.1.2: MLN and DWORF protein expression in *Pln*$^{+/+}$ and *Pln*$^{-/-}$ female mice. MLN and DWORF protein expression is unaltered by PLN ablation in SOL and LV. **A)** Representative Western blots of 5-6 mo old female *Pln*$^{+/+}$ and *Pln*$^{-/-}$ mice (n = 6/group). Equal protein load was confirmed using Ponceau S staining. **B)** Protein expression relative to *Pln*$^{+/+}$ mice. Values are mean ± S.E.

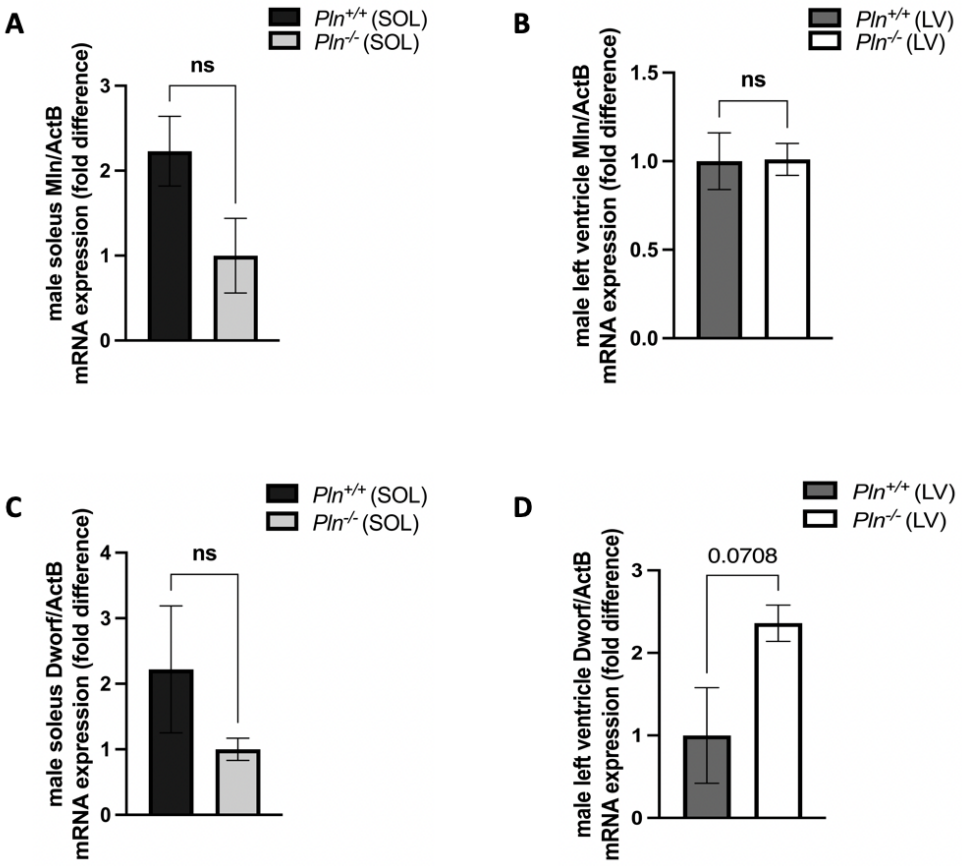


Fig. 5.3.1.3: *Mln* and *Dworf* mRNA expression in *Pln*$^{+/+}$ and *Pln*$^{-/-}$ male mice. *Mln* mRNA expression is unaltered by *Pln* ablation in **A)** SOL (n = 3/group) and **B)** LV (n = 4/group). Similarly, *Dworf* mRNA expression is not effected by *Pln* ablation in **C)** SOL (n = 4/group) and **D)** LV (n = 4/group). Values are mean ± S.E. * indicates a significant difference from WT ($p < 0.05$).

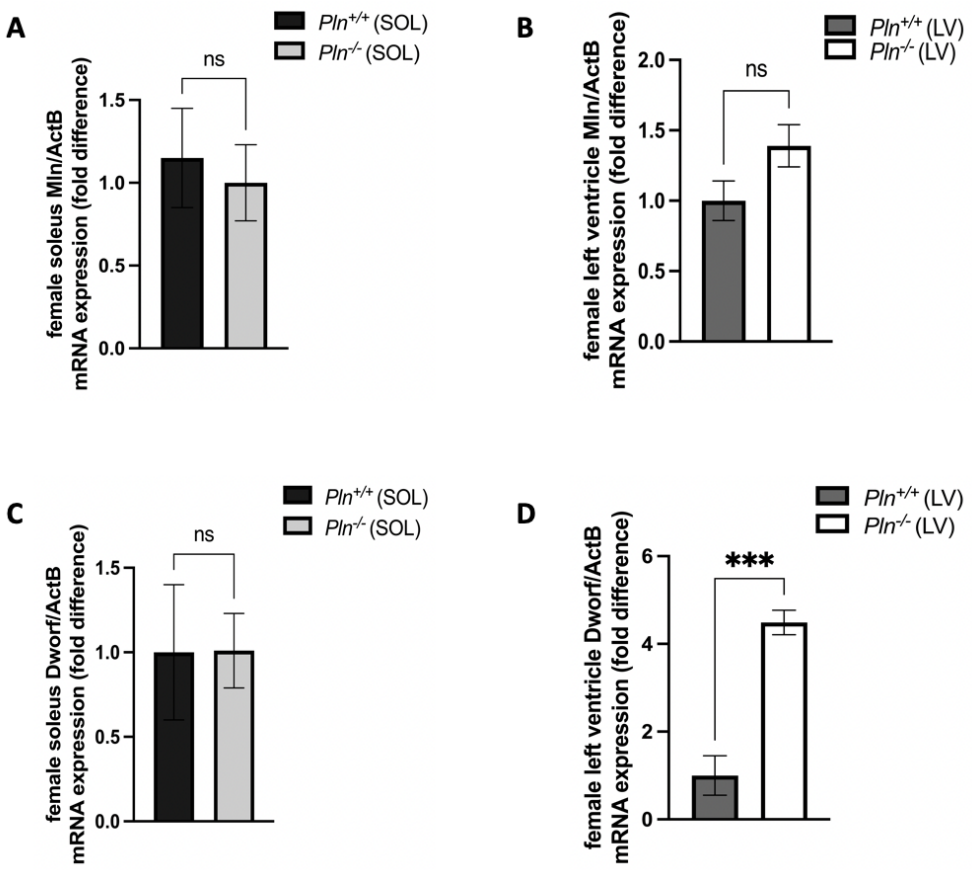


Fig. 5.3.1.4: *Mln* and *Dworf* mRNA expression in *Pln*$^{+/+}$ and *Pln*$^{-/-}$ female mice. *Mln* mRNA expression is unaltered by *Pln* ablation in **A)** SOL (n = 4/group) and **B)** LV (n = 4/group). *Dworf* mRNA expression in **C)** SOL (n = 4/group) is not effected by *Pln* ablation, however, *Dworf* expression is significantly elevated in **D)** LV in the absence of *Pln* (n = 4/group). Values are mean ± S.E. * indicates a significant difference from WT ($p < 0.05$). *** indicates a significant difference from WT ($p < 0.0005$).

5.3.2. Ablation of SLN does not affect MLN and DWORF protein content but does alter mRNA expression

Western blotting on the atria of *Sln*$^{-/-}$ and WT (*Sln*$^{+/+}$) male mice was performed validate the absence of the SLN protein in the knockout genotype, as SLN is readily detectable in this tissue. Expectedly, male WT atria exhibited robust SLN protein expression, whereas, SLN was undetectable in the atria of *Sln*$^{-/-}$ male mice. Following this, western blotting for MLN and DWORF protein expression was carried out on SOL and atrial muscles from WT and *Sln*$^{-/-}$ male mice to explore potential compensatory changes in the expression levels of these proteins in the absence of SLN. Our analysis revealed no significant changes in the expression of either MLN ($p = 0.214$) or DWORF ($p = 0.384$) proteins upon SLN ablation in the examined muscle tissues (Fig. 5.3.2.1).

For *Sln*$^{-/-}$ female mice, we employed the same methodology to ensure the genetic deletion of the SLN protein. The evaluation of MLN and DWORF protein expression in SOL and atrial muscles from WT and *Sln*$^{-/-}$ female mice showed results consistent with those observed in their male counterparts, with no significant differences in the expression of either protein (MLN, $p = 0.279$, DWORF, $p = 0.310$) detected in either muscle in the absence of SLN (Fig. 5.3.2.2).

Complimentary changes in expression at the gene level were assessed via qPCR analysis of SOL and atrial muscles from the same WT and *Sln*$^{-/-}$ male and female mice. The expression of *Mln* was unaltered with the ablation of *Sln* in both muscles examined from both sexes (Male SOL: $p = 0.425$, Atria: $p = 0.180$; Female SOL: $p = 0.619$, Atria: $p = 0.635$) (Fig. 5.3.2.3 and Fig. 5.3.2.4). However, we observed greater *Dworf* expression in SOL of *Sln*$^{-/-}$ male mice ($p = 0.0046$) and a trend towards higher expression in male *Sln*$^{-/-}$ atria ($p = 0.0527$) compared to WT (Fig. 5.3.2.3). Interestingly, female *Sln*$^{-/-}$ SOL showed no differences in *Dworf* expression ($p = 0.542$), while, *Sln*$^{-/-}$ atria showed the opposite result relative to the male data, with a significant decline in *Dworf* expression compared to WT ($p = 0.0024$) (Fig. 5.3.2.4).

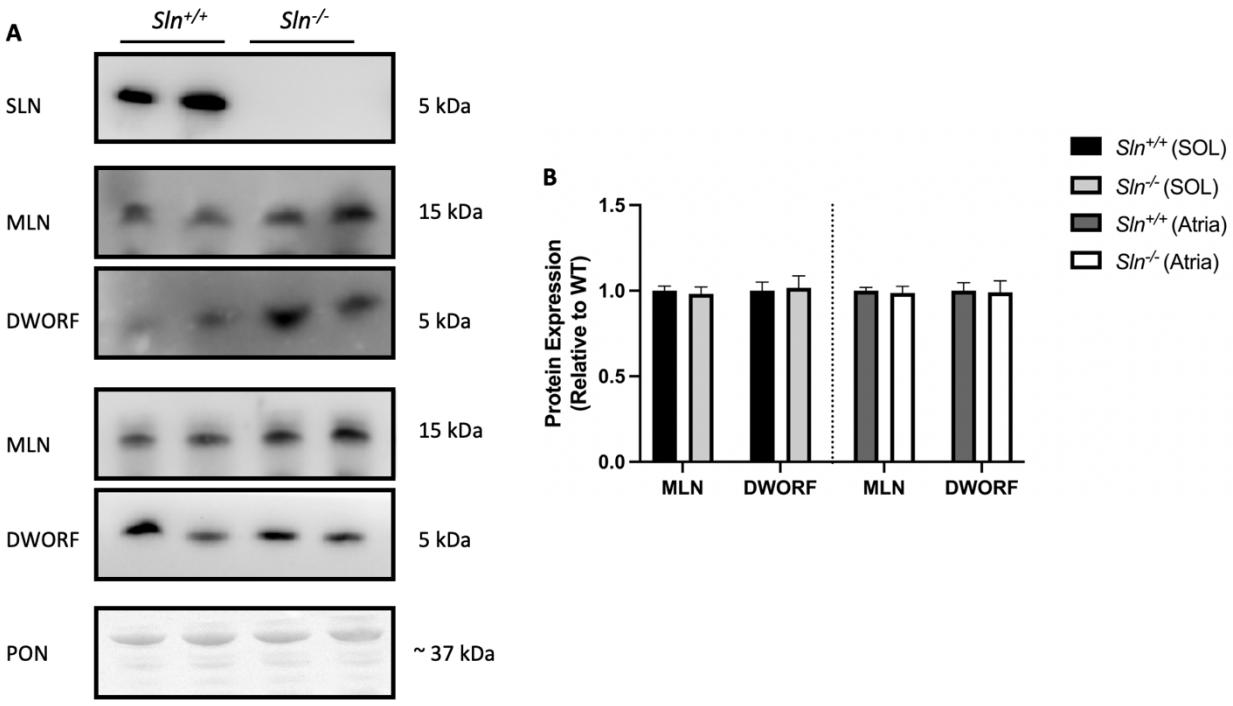


Fig. 5.3.2.1: MLN and DWORF protein expression in *Sln*$^{+/+}$ and *Sln*$^{-/-}$ male mice. MLN and DWORF protein expression is unaltered by SLN ablation in SOL and atria. **A)** Representative Western blots of 5-6 mo old male *Sln*$^{+/+}$ and *Sln*$^{-/-}$ mice (n = 6/group). Equal protein load was confirmed using Ponceau S staining. **B)** Protein expression relative to *Sln*$^{+/+}$ mice. Values are mean ± S.E.

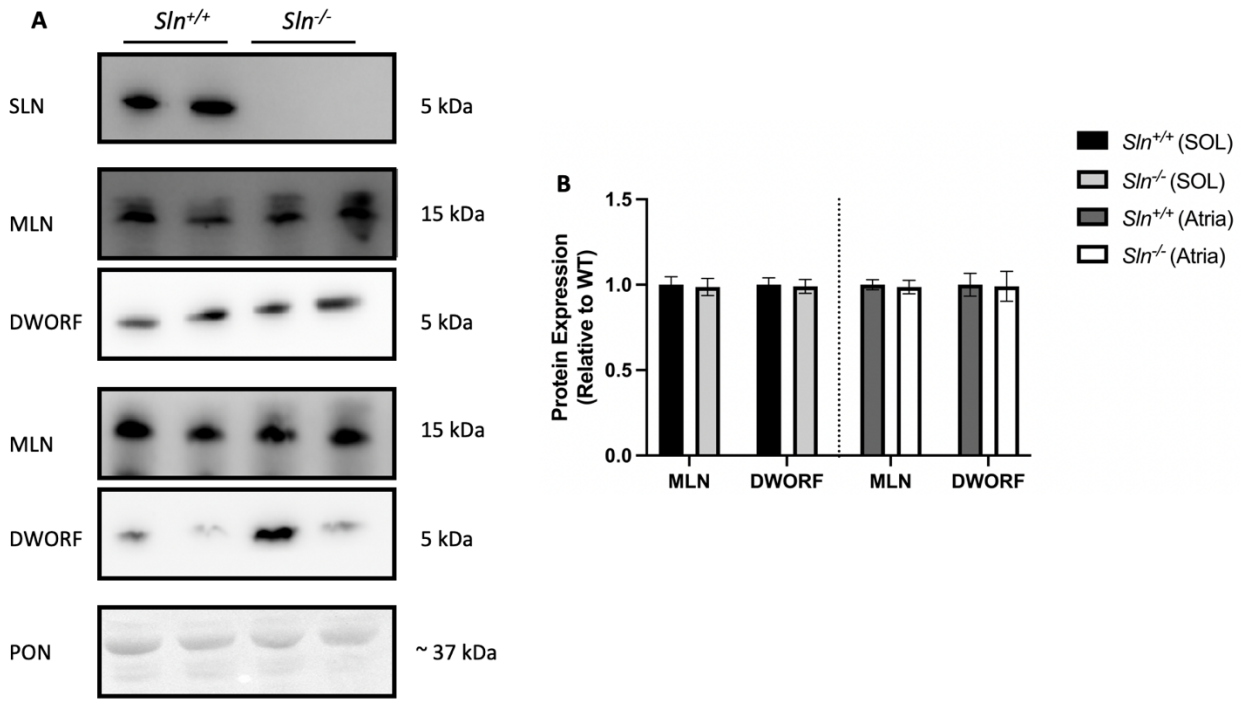


Fig. 5.3.2.2: MLN and DWORF protein expression in *Sln*$^{+/+}$ and *Sln*$^{-/-}$ female mice. MLN and DWORF protein expression is unaltered by SLN ablation in SOL and atria. **A)** Representative Western blots of 5-6 mo old female *Sln*$^{+/+}$ and *Sln*$^{-/-}$ mice (n = 6/group). Equal protein load was confirmed using Ponceau S staining. **B)** Protein expression relative to *Sln*$^{+/+}$ mice. Values are mean ± S.E.

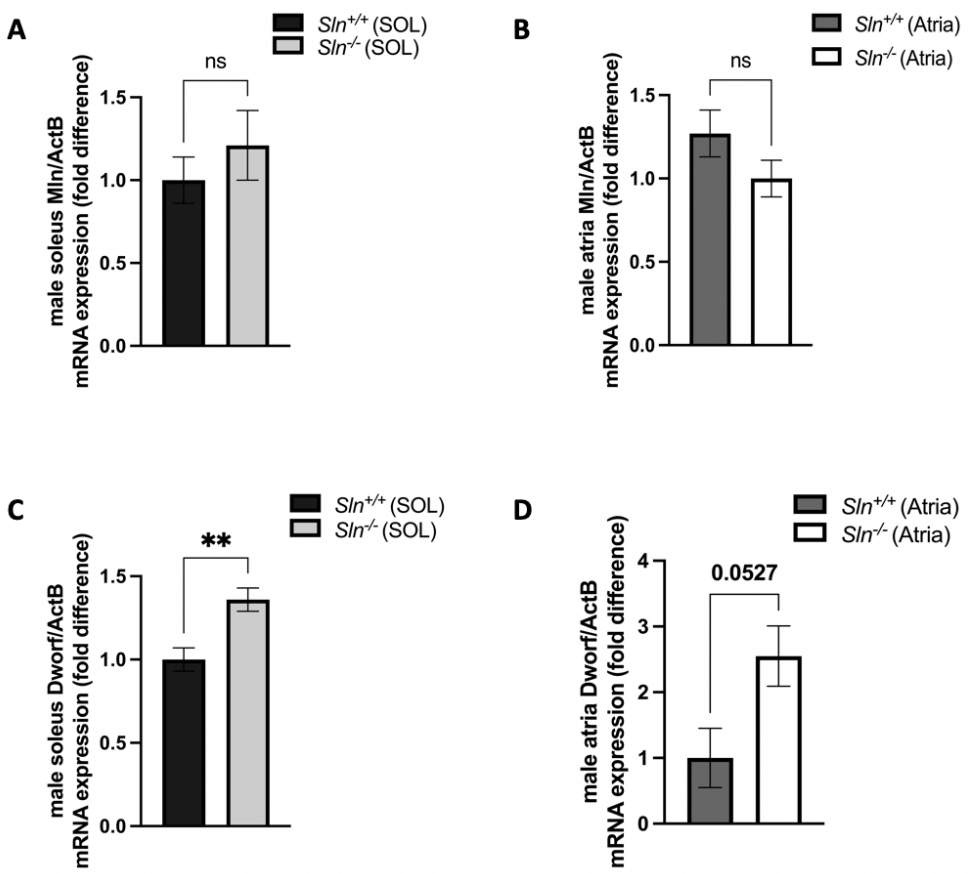


Fig. 5.3.2.3: *Mln* and *Dworf* mRNA expression in *Sln*$^{+/+}$ and *Sln*$^{-/-}$ male mice. *Mln* mRNA expression is unaltered by *Sln* ablation in **A)** SOL (n = 6/group) and **B)** Atria (n = 4/group). Meanwhile, *Dworf* mRNA expression in **C)** SOL is greater in the absence of *Sln* (n = 6/group) and is trending higher in **D)** Atria with *Sln* ablation (n = 4/group). Values are mean ± S.E. * indicates a significant difference from WT ($p < 0.05$). ** indicates a significant difference from WT ($p < 0.005$).

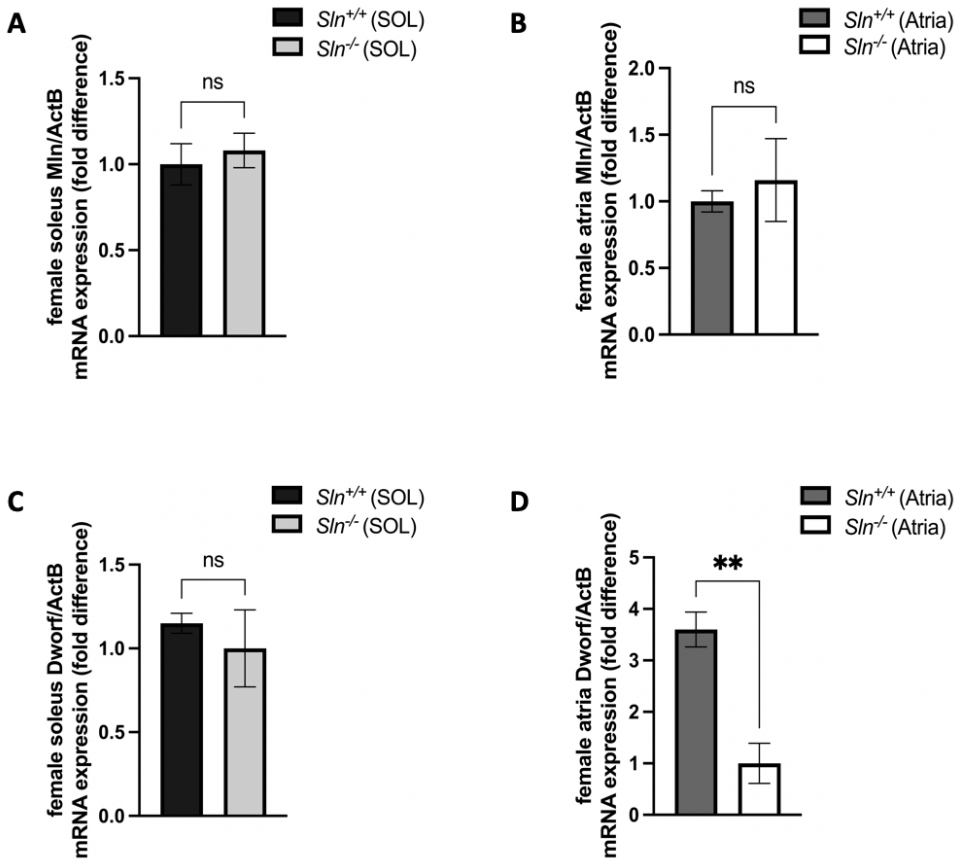


Fig. 5.3.2.4: *Mln* and *Dworf* mRNA expression in $Sln^{+/+}$ and $Sln^{-/-}$ female mice. *Mln* mRNA expression is unaltered by *Sln* ablation in **A)** SOL (n = 6/group) and **B)** Atria (n = 4/group). Likewise, *Dworf* mRNA expression in **C)** SOL is not changed in the absence of *Sln* (n = 6/group) but is decreased in **D)** Atria (n = 4/group) with *Sln* ablation. Values are mean ± S.E. * indicates a significant difference from WT ($p < 0.05$). ** indicates a significant difference from WT ($p < 0.005$).

5.3.3. Knock-Out of both PLN and SLN had no bearing on MLN and DWORF protein content but did alter mRNA expression

In order to establish that the *Sln*$^{-/-}$/*Pln*$^{-/-}$ (DKO) male and female mice were in fact devoid of SLN and PLN protein expression, western blotting for the PLN protein was conducted on LV tissue and western blotting for the SLN protein was performed on atrial tissue from male and female DKO mice and compared to *Sln*$^{+/+}$/*Pln*$^{+/+}$ (DWT) litermates. The DKO genotype was verified for both sexes. Subsequently, protein expression levels of MLN and DWORF were evaluated in both sexes to investigate if the genetic deletion of both SLN and PLN had an effect on MLN and DWORF protein expression, respectfully. Again, the results for both proteins in both sexes (Male: MLN $p = 0.357$, DWORF $p = 0.297$; Female: MLN $p = 0.443$, DWORF $p = 0.308$) matched what was observed in the single knockout models, as the ablation of both SLN and PLN did not result in any significant changes in the expression of MLN and DWORF (Male, Fig. 5.3.3.1 and Female, Fig. 5.3.3.2)

Gene expression of *Mln* and *Dworf* were investigated in SOL, atrial and LV muscles from the same WT and DKO male and female mice to determine potential changes gene expression in the dual absence of both *Pln* and *Sln*. We did not observe a significant change in the level of *Mln* expression in male SOL ($p = 0.190$), atrial ($p = 0.669$) and LV tissue ($p = 0.302$). Likewise, there was no change in *Dworf* expression in male SOL ($p = 0.883$), however, a significant decline in *Dworf* expression was observed in LV ($p = 0.0015$) and atrial ($p < 0.0001$) DKO tissue (Fig. 5.3.3.3). Again, *Mln* expression remained unchanged in female SOL ($p = 0.970$) and atrial ($p = 0.506$) tissue, but was found to be significantly greater in DKO LV compared to WT ($p = 0.0418$). Interestingly, the pattern of *Dworf* expression was the same in female mice relative to male, as no change in was observed in SOL tissue ($p = 0.291$), while a significant decline in *Dworf* expression was observed in LV ($p = 0.0300$) and atrial ($p < 0.0001$) DKO tissue (Fig. 5.3.3.4).

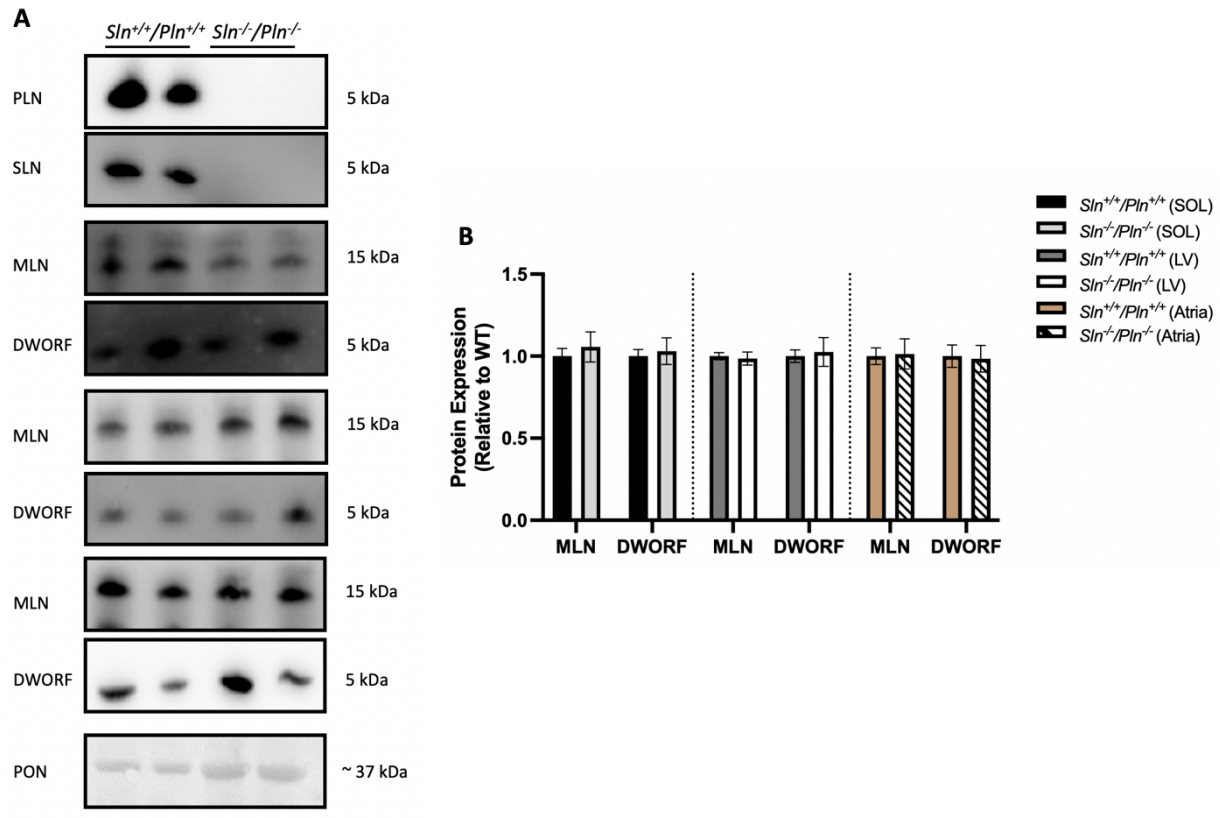


Fig. 5.3.3.1: MLN and DWORF protein expression in *Sln*$^{+/+}$/*Pln*$^{+/+}$ and *Sln*$^{-/-}$/*Pln*$^{-/-}$ male mice. MLN and DWORF protein expression is unaltered by SLN and PLN ablation in SOL, LV and atria. **A)** Representative Western blots of 5-6 mo old male *Sln*$^{+/+}$/*Pln*$^{+/+}$ and *Sln*$^{-/-}$/*Pln*$^{-/-}$ mice (n = 6/group). Equal protein load was confirmed using Ponceau S staining. **B)** Protein expression relative to *Sln*$^{+/+}$/*Pln*$^{+/+}$ mice. Values are mean ± S.E

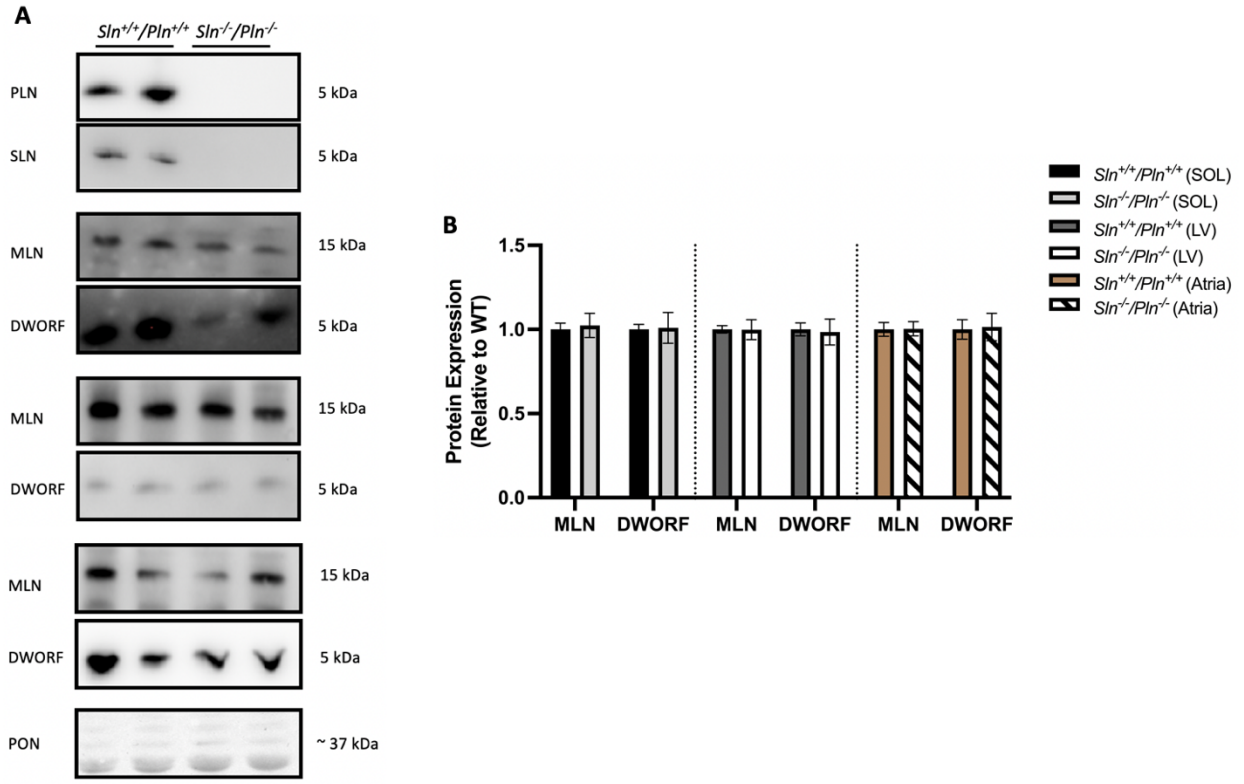


Fig. 5.3.3.2: MLN and DWORF protein expression in *Sln*$^{+/+}$*/Pln*$^{+/+}$ and *Sln*$^{-/-}$*/Pln*$^{-/-}$ female mice. MLN and DWORF protein expression is unaltered by SLN and PLN ablation in SOL, LV and atria. **A)** Representative Western blots of 5-6 mo old female *Sln*$^{+/+}$*/Pln*$^{+/+}$ and *Sln*$^{-/-}$*/Pln*$^{-/-}$ mice (n = 6/group). Equal protein load was confirmed using Ponceau S staining. **B)** Protein expression relative to *Sln*$^{+/+}$*/Pln*$^{+/+}$ mice. Values are mean ± S.E

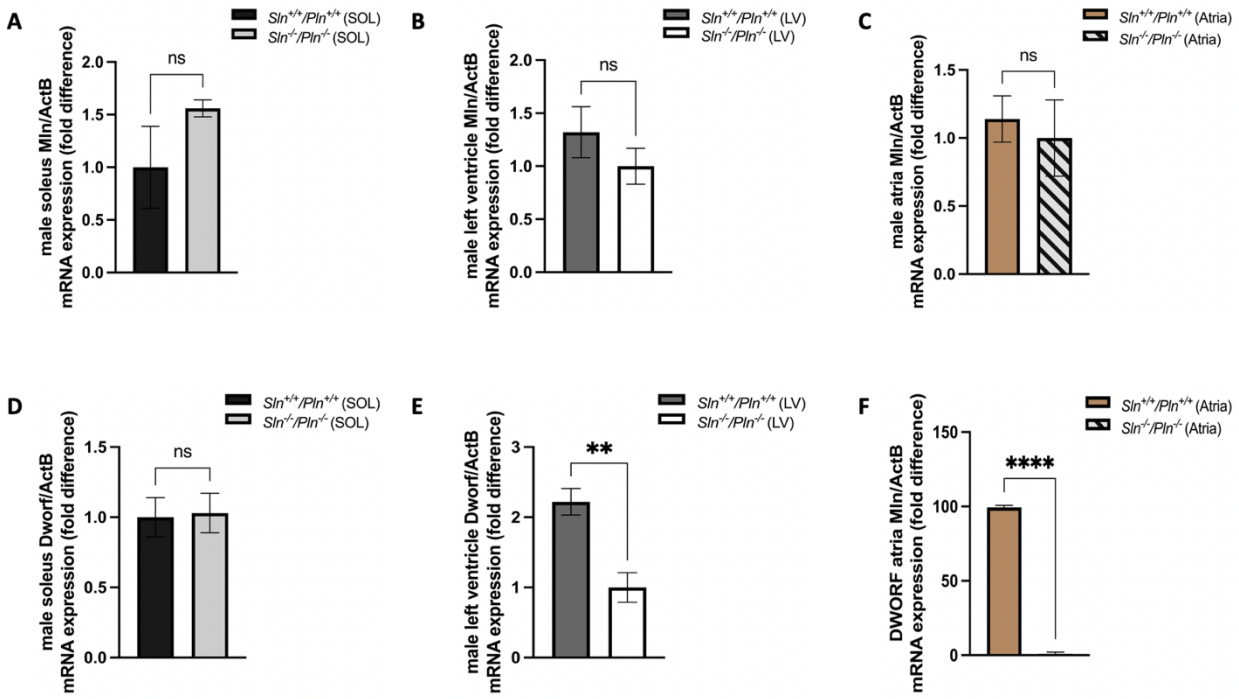


Fig. 5.3.3.3: *Mln* and *Dworf* mRNA expression in $Sln^{+/+}/Pln^{+/+}$ and $Sln^{-/-}/Pln^{-/-}$ male mice. *Mln* gene expression is unaltered by *Sln* and *Pln* ablation in SOL (n = 6/group), LV (n = 6/group) and Atria (n = 3/group). While *Dworf* gene expression was unchanged by the dual absence of *Sln* and *Pln* in SOL (n = 6/group), it was depressed in LV (n = 6/group) and Atria (n = 3/group). Values are mean ± S.E. * indicates a significant difference from WT ($p < 0.05$). ** indicates a significant difference from WT ($p < 0.005$). **** indicates a significant difference from WT ($p < 0.0001$).

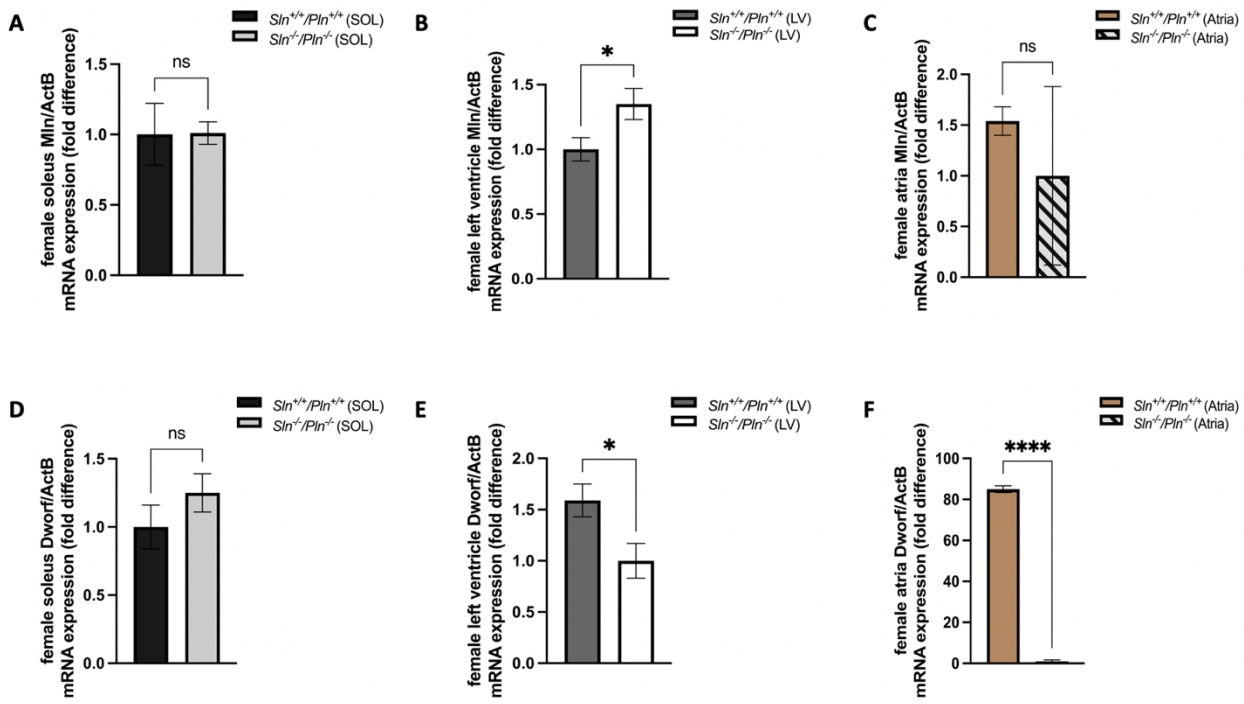


Fig. 5.3.3.4: *Mln* and *Dworf* mRNA expression in $Sln^{+/+}/Pln^{+/+}$ and $Sln^{-/-}/Pln^{-/-}$ female mice. *Mln* gene expression is unaltered by *Sln* and *Pln* ablation in SOL (n = 4/group and Atria (n = 3/group) but was elevated in LV (n = 6/group). While *Dworf* gene expression was unchanged by the dual absence of *Sln* and *Pln* in SOL (n = 4/group), it was depressed in LV (n = 6/group) and Atria (n = 3/group). Values are mean ± S.E. * indicates a significant difference from WT ($p < 0.05$). ** indicates a significant difference from WT ($p < 0.005$). **** indicates a significant difference from WT ($p < 0.0001$).

5.4 Discussion

The final study of this thesis evaluated mRNA and protein expression of MLN and DWORF in soleus, left ventricle and atrial muscle isolated from male and female wild type compared to single knockout (*Sln*$^{-/-}$ and *Pln*$^{-/-}$) and double knockout (*Sln*$^{-/-}$/*Pln*$^{-/-}$) mice. Previous work showed that SR protein expression was unaltered in *Pln*$^{-/-}$ [84] and *Sln*$^{-/-}$ [6, 100] mice and that more specifically, there were no compensatory changes in regulatory protein expression, suggesting that the capacity for Ca^{2+}-uptake, storage, and release is unaltered within oxidative muscle by PLN and SLN ablation. Therefore, it was hypothesized that the protein expression of MLN and DWORF would also not be changed in the single knockout models. Expectedly, the content of neither protein was altered in cardiac muscle and oxidative skeletal muscle of *Sln*$^{-/-}$ and *Pln*$^{-/-}$ male and female mice. In accordance with prior reports, DWORF was readily detected in soleus and left ventricle tissue [129], while a greater protein load was needed to assess its expression in atria. Conversely, MLN posed a challenge to detect and a greater protein load was required to determine expression in all three tissues.

While single gene knock-out studies show that loss endogenous levels of either SLN and PLN do not drastically alter the morphology or phenotype of muscular tissues, dual SLN/PLN ablation does. DKO mice present with left ventricular hypertrophy and aged mice are predisposed to cardiac dysfunction, this despite improved SERCA function [156]. Moreover, soleus muscle of DKO mice experienced a fast-to-slow fibre type shift and hypertrophy of both type I and IIA fibres. The fibre-type change was accompanied by an increase in SERCA2a expression and a decline in SERCA1a expression, however, DHPR, RyR, and CSQ protein content remained unchanged. Surprisingly, despite the loss of two well-described inhibitors of the Ca^{2+}-pump, SERCA maximal activity was paradoxically reduced in DKO soleus and apparent Ca^{2+} affinity was unaltered [156].

While it was speculated that the decline in SERCA function could simply reflect a lower SERCA protein density that would complement the fast-to-slow fibre-type shift in these mice, the discovery of additional regulatory proteins may provide the mechanistic explanation. To this end, it was hypothesized that MLN and DWORF expression would be altered to compensate for the combined loss of both SLN and PLN. Unexpectedly, again, protein content of both DWORF and MLN was not altered in cardiac muscle and oxidative skeletal muscle of *Sln*$^{-/-}$/*Pln*$^{-/-}$ male and female mice.

Given the dramatic impairments in cardiac function in DKO mice, perhaps it is not surprising that there is not a compensatory change in DWORF expression in left ventricle tissue. Moreover, it would seem that endogenous DWORF content is insufficient to prevent the cardiac dysfunction observed in this model. Given the proven ability of DWORF overexpression to ameliorate a model dilated cardiomyopathy [129], it is surprising that DWORF would not be naturally upregulated to combat the onset and progression of cardiac impairment. We are unable to discern whether the increase in SERCA maximal activity can be attributed to the loss of SLN/PLN, the presence of DWORF or a combination of the two factors. Nor are we able to provide a mechanistic explanation for the lack of change in the apparent Ca^{2+} affinity, though, perhaps this could be attributed to the expression of MLN. While MLN was detected in left ventricle tissue, the protein load (16 ug) required for its detection was much greater than PLN (1 ug) and DWORF (4 ug) detection, in fact, the same can also be said for the detection of MLN in murine soleus as well. Therefore, it is unknown how much of an inhibitory role MLN exerts in these two tissues.

The loss of MLN did not alter morphology or phenotype in murine soleus muscle, though it did increase the capacity for Ca^{2+} SR storage and enhanced exercise capacity as observed by a significant increase in running distance [12]. While the expression of RYR1 and SERCA1a were unaltered, the expression of PLN, SLN and DWORF were not evaluated. Furthermore, the

transgenic *Mln*$^{-/-}$ mouse model was not confirmed via western blotting to directly detect the of presence vs absence of MLN protein expression [12]. In comparison, transgenic deletion of DWORF caused a decline in apparent affinity of SERCA for Ca^{2+} [13] but did not alter contractile function. Unfortunately, SR protein expression, including regulator expression, was not evaluated. These studies indicate that single ablation of either regulatory protein does not result in skeletal muscle SR remodeling, whereas, dual ablation alters the morphology or phenotype of muscular tissues. Importantly, this is the first study to i) directly detect MLN protein in cardiac and skeletal muscle, ii) investigate endogenous MLN and DWORF content in male and female adult mice, and iii) examine the impact of single knockout and double knockout deletion of SLN and PLN on MLN and DWORF protein expression within cardiac and oxidative skeletal muscle, which we show to be unchanged regardless of sex and genotype. While this may suggest that MLN and DWORF protein expression does not compensate for the loss of PLN/SLN, we cannot rule out an enhancement in the physical interaction of MLN and/or DWORF with SERCA in the absence of PLN/SLN.

An important novel contribution of this study is the direct detection of the presence of MLN protein in murine skeletal and cardiac muscle. Though quantifying MLN expression posed considerable difficulty, preliminary tissue expression data shown here (**Appendix B**: **Figure B.3**) does confirm the expression of endogenous MLN in both oxidative (soleus and plantaris) and glycolytic (extensor digitorum longus and white gastrocnemius) murine skeletal muscle. Moreover, preliminary work confirms endogenous expression of DWORF in cardiac and oxidative skeletal muscle (soleus and plantaris, specifically) only, as it was undetectable in glycolytic skeletal muscle (specifically, extensor digitorum longus and white gastrocnemius) (**Appendix B**: **Figure B.4**). It is clear from these supplementary figures that DWORF is readily detectable in

tissues that endogenously express it, requiring protein loads and antibody concentrations that are comparable to PLN [84]. On the other hand, much greater protein loads were needed for MLN protein detection, and even for protein loads comparable to PLN [84] and SLN [156], greater concentrations of primary and secondary antibody were required. Future studies should consider investigating expression of MLN and DWORF in human skeletal muscle and furthermore, determining the muscle fibre expression profile which would also shed light on the co-expression of MLN and DWORF with the other regulatory proteins and with the SERCA isoforms. Single fiber Western blotting and immunohisto/fluorescence staining techniques have revealed that fast-twitch Type II fibers contain relatively high levels of SLN and SERCA1a proteins and relatively low levels of PLN protein and SERCA2a protein [9]. Conversely, slow-twitch Type I fibers were shown to exhibit relatively high levels of PLN and SERCA2a proteins, while relatively low levels of SLN and SERCA1a proteins were detected in > 22% of Type I fibers. Given that PLN protein was detected in every fiber, SLN and PLN were shown to be co-expressed in 81% of fibers. Moreover, although SLN and PLN exhibit isoform preferences in their regulation of the pump, physiologically they both may regulate either SERCA isoform [9]. It will be important to establish where MLN and DWORF fit in the dynamic and complex regulation of SERCA function and Ca^{2+} homeostasis.

While the protein content discussed here was evaluated under basal conditions, it would be of interest to investigate whether high fat feeding or conditions of disease, disuse or atrophy induce changes in MLN and DWORF expression as they have been proven to change expression of SLN [1, 2] (**Appendix A, Table A.1**) and PLN [84, 85]. As previously discussed, DWORF protein content does shown a responsiveness to the overexpression of PLN (**Appendix B**: **Figure B.1**), therefore it will be important to determine the conditions that promote this response. Another

consideration that could alter MLN and DWORF protein content is strain-specific differences in SLN expression. Interestingly, in our hands, endogenous levels of SLN protein expression within the soleus appear to be lowest in C57BL/6J WT mice compared to mice of other strains (FVB/N, 129S; **Appendix B**: **Figure B.2**) [156]. In contrast, Singh and colleagues observed a 2-fold increase in diaphragm and soleus SLN content in C57BL/6 mice relative to FVB/N mice [157]. Moreover, mouse strain-specific differences were identified in the relative expression of proteins involved in mitochondrial metabolism. This discrepancy could partially be explained by the degree of difficulty in quantifying SLN expression because it is relatively small and highly hydrophobic, and there are limited commercial antibodies that are proven to work in western blotting [157]. The strain that exhibits a lower expression of SLN would theoretically be prone to diet induced obesity because it would have a higher SERCA/SLN ratio, suggesting that there would be a lesser degree of uncoupling of SERCA-mediated Ca^{2+} uptake in these mice. On the other hand, strains that exhibit higher expression of SLN would, in turn, be more resistant. This is precisely what has been reported in the literature [1-3, 31]. Unfortunately, strain differences in PLN content have not yet been evaluated and nor have differences in SERCA isoform expression. This is of particular importance because the three transgenic models employed in this thesis are all on a different genetic background and have been inbred for several generations, causing further genetic drift. They are listed below:

i) $Pln^{+/-}$, strain genetic background: mix of C57BL/6, C3H, and 129S2/SvPas

ii) $Sln^{+/-}$, strain genetic background: C57BL/6J

iii) $Sln^{+/-}/Pln^{+/-}$, strain genetic background: mix of C57BL/6, C3H, and 129S2/SvPas (cross of $Sln^{+/-}$ and $Pln^{+/-}$)

Though this thesis did not compare the expression of SR Ca^{2+} handling proteins, including levels of MLN and DWORF expression, between single knockout and double knockout models, it would

be of interest to do so, to ensure that the results observed here are not due to strain-specific differences, especially with the potential for 2-fold changes in SLN expression. Furthermore, compensatory change in DWORF expression relative to PLN expression was detected in WT vs Pln^{OE} mice on a FVB/N genetic background. Therefore, in addition to endogenous basal protein expression, responsiveness to changes in expression of other regulatory proteins should also be evaluated across strains.

Skeletal muscle displays sexually dimorphic features, including major differences in structure, metabolism, and function that persist across species. In fact, total mass of muscle fibers and their individual sizes, fiber type composition, and skeletal muscle energy metabolism, contractile strength, and fatigability were all found to be different between the two sexes [158-161]. Accordingly, the preferred fuels for energy metabolism also differ and have been shown to be glucose and fatty acids in the muscles of males and females, respectively [158, 162, 163]. In accordance with prior studies in humans and rodents, we have found that females and males tended toward greater proportions of type I and type II fibres, respectively, in mouse solei (data unpublished). Moreover, we have also uncovered sexual dimorphism in the expression of SLN, as female mice show elevated SLN protein content compared to males in soleus (data unpublished). This thesis only compared the expression of MLN and DWORF between WT and their single knockout/double knockout counterparts. In this comparison, there was no difference in the expression of either protein, regardless of sex and tissue. However, it would be of interest for future studies to compare expression of PLN, MLN and DWORF between sexes to investigate potential differences in protein content.

Interestingly, while differences in protein content were not observed with single or double ablation of SLN and PLN, mRNA expression of *Mln* and *Dworf* were responsive to both the single knockout and dual knockout conditions. Gene expression of *Mln* was only altered in left ventricle tissue of female DKO, showing an elevation relative to WT. In comparison, the changes in *Dworf* gene expression were inconsistent in direction. The change in gene expression was generally unaltered in skeletal muscle tissue, with only soleus of male $Sln^{-/-}$ mice showing a significant elevation in *Dworf* expression. In contrast, cardiac tissue exhibited a more complicated story: left ventricle tissue of male and female $Pln^{-/-}$ mice showed either a trending increase or significant increase, respectively. Similarly, atria of $Sln^{-/-}$ male mice exhibited a trending increase in *Dworf* expression, whereas, atria of $Sln^{-/-}$ female mice exhibited a significant decrease. Finally, left ventricle and atrial tissue of both male and female $Sln^{-/-}/Pln^{-/-}$ mice displayed a significant decline in *Dworf* expression. It could be speculated that *Dworf* expression would show greater responsiveness to changes in expression of the other regulators due to DWORF's ability as a non-inhibitory competitor to interact with and displace the other regulatory proteins to re-establish basal SERCA's Ca^{2+} affinity. However, the changes in expression at the gene level did not translate to changes in expression at the protein level for either protein and this is consistent with what has been reported in the literature regarding gene and protein expression patterns of PLN. Several studies have shown that the expression of PLN must be strongly controlled at the protein level [10, 164, 165], as expression of PLN protein has been reported to increase two-fold without a change in gene expression [164]. Moreover, *Pln* mRNA has been detected in mouse EDL tissue [10], however, our group has been unable to detect PLN protein in EDL regardless of protein load and blotting conditions [84]. A similar post-translational control of MLN and DWORF expression might exist and would be of great interest to investigate. Contrastingly, gene and protein

expression patterns of SLN appear to be more consistent in the literature, showing complimentary upregulation and downregulation [10]. Perhaps SLN requires a need for tighter control of expression due to its importance in muscle energy metabolism and Ca^{2+} signalling pathways that contribute to muscle structure and composition. However, in our hands mRNA and protein expression of SLN did not necessarily correlate. Recall the study mentioned in Chapter 3 concerning inducibility of PLN and SLN expression during cellular stress. We found that female soleus had significantly greater SLN mRNA expression in comparison to males across all HS conditions, but, males expressed higher SLN protein than females in the heat stressed conditions [153]. These results further strengthen the importance of the development of our MLN western blotting protocol, as previous reports relied on mRNA expression in lieu of protein expression which may not be appropriate considering the discrepancies in expression shown here. It should also be of note, that because of extenuating circumstances the sample size differed between genotypes and muscle tissue for the mRNA analysis. Not to mention that that atrial tissue needed to be pooled due to its small size, further lowering in the sample size compared to other tissues. Therefore, the variability associated with small sample size could mask differences that would be observed with a more appropriate number of samples.

5.5 Conclusions

Studies I & II examined the protective and regulatory effects of MLN and DWORF in a cell model, and in doing so, were the first to showcase a protocol developed to precisely identify the MLN protein. Study III built upon this by validating the protocol in murine cardiac and skeletal muscle, in addition to, quantifying MLN and DWORF expression in single ablation and dual ablation of SLN and PLN. MLN and DWORF expression was not altered in the absence of PLN in both muscles examined and in both sexes, this is consistent with a prior study revealing similar lack of change in SLN expression in the same model [84]. Furthermore, the expression of these newly discovered regulatory proteins was unaltered in the absence of SLN nor was it altered in the ablation of both SLN/PLN in all muscles examined and in both sexes. Though quantification of MLN expression posed considerable difficulty, endogenous expression was confirmed in cardiac muscle and in both oxidative and glycolytic skeletal muscle. On the other hand, endogenous expression of DWORF was readily detectable in cardiac muscle and oxidative skeletal muscle. Contrastingly, mRNA qPCR analysis showed stark differences in gene expression of *Dworf*, particularly in cardiac tissue, that varied in direction depending on genotype and sex. However, the changes in expression at the gene level did not translate to changes in expression at the protein level for either protein. This is consistent with what has been reported in the literature regarding gene and protein expression patterns of PLN [10, 164, 165] and may suggest that MLN and DWORF undergo similar post-translational control of expression.

Chapter Six

Thesis Summary, Integrated Discussion, and Future Perspectives

6.1 Thesis Summary

There were several major novel contributions of this thesis, all of which are highlighted in Table 6.1.1 and graphically represented in Fig. 6.1.1 (MLN) and Fig. 6.1.2 (DWORF). In light of MLN and DWORF's sequence homology and similar biochemical action on SERCA function as SLN and PLN, we wanted to determine i) whether MLN and DWORF could stabilize the pump during exposure to cellular stress, ii) whether like SLN, these two newly discovered proteins could uncouple Ca^{2+} transport from ATP hydrolysis, and iii) whether endogenous physiological levels of MLN and DWORF gene and protein expression were altered in the absence of either or both SLN and PLN.

The research detailed in Thesis Study I significantly contributes to our understanding of SERCA regulation under oxidative stress conditions. SERCAs, being redox-sensitive proteins due to the presence of numerous cysteine residues in their structure, exhibit high susceptibility to oxidative damage, which causes functional impairments and loss of SERCA activity [18, 44-46]. Notably, HSP70 has been identified as a protective factor against oxidative damage to SERCAs, maintaining maximal SERCA activity and preventing damaging modifications induced by oxidative stress [44]. However, there are limitations to the protection offered by HSP70, as functional protection of SERCA is lost with progressively greater severity of HS and exposure time [44]. Suggesting that another region on SERCAs may not be able to form an interaction with HSP70, and is exposed to modification under conditions of heightened HS, resulting in inactivation [44]. Previous studies have highlighted the protective role of SLN and PLN in stabilizing SERCA structure and function under conditions of cellular stress [11]. This thesis investigated the protective effects of two regulatory proteins – MLN and DWORF, that structurally resemble SLN and PLN. Both MLN and DWORF interact with SERCA1a and SERCA2a, respectively,

demonstrating a protective mechanism against thermal inactivation and oxidative modifications under cellular stress induced by heat shock. MLN showed non-isoform-specific stabilization but did inhibit maximal SERCA activity, while DWORF preserved maximal activity without isoform preference. Future research avenues could explore mutagenesis studies targeting specific residues involved in the interaction between SERCA and regulatory proteins. Evaluating endogenous expression levels and stress-induced responses of MLN and DWORF could provide insights into their physiological relevance. Moreover, the development of a MLN antibody and Western blotting protocol represents a significant advancement in detecting and understanding MLN distribution in skeletal and cardiac muscle tissues. In summary, Thesis Study I furthers our understanding of how regulatory proteins such as MLN and DWORF exert protective effects on SERCA function under conditions of cellular stress. These findings pave the way for potential therapeutic targets to mitigate SERCA dysfunction observed in various myopathies.

While Thesis Study I illustrated the shared ability of all four regulatory proteins to maintain SERCA structure and function during thermal stress, Thesis Study II added to evidence revealing distinct functional roles of these proteins in preserving cellular Ca^{2+} homeostasis. Previous research has firmly established the role of SLN in regulating skeletal muscle energy metabolism by lowering the transport efficiency of the SERCA pumps through Ca^{2+} ion slippage during its reaction cycle [1-3, 31]. Our study reveals that MLN does not possess the ability to uncouple SERCA Ca^{2+} transport from ATP hydrolysis. Instead, MLN reduced the Ca^{2+} affinity and maximal activity of both SERCA1a and SERCA2a under maximal and physiological conditions, without impacting the pump's transport efficiency. In contrast, DWORF demonstrated minimal influence on Ca^{2+} affinity, maximal activity, and rate of uptake of SERCA1a and SERCA2a when expressed in a 1:1 molar ratio. However, higher levels of DWORF overexpression (5:1) led to augmented

Ca^{2+} affinity and maximal activity for both SERCA isoforms under maximal and physiological conditions, again while transport efficiency remained unaffected. Notably, this study's observation of reduced V_{max} contrasts with some previous reports, highlighting existing discrepancies in understanding MLN's inhibitory function. Moreover, the direct effect of DWORF overexpression on Ca^{2+} affinity, maximal activity, and rate of uptake also conflicts with previous reports. The divergent findings across studies investigating MLN and DWORF's effects on SERCA function likely stem from several factors, including differences in protein ratios, diverse experimental setups utilizing cell-based or animal models, variations in reconstitution protocols, and the utilization of different cell lines. In summary, Thesis Study II presents significant insights into understanding the intricate regulatory mechanisms that govern SERCA function by exploring the roles of MLN and DWORF. The findings underscore the complexity of these regulatory proteins' actions on SERCA and emphasize the need for further investigations to unravel their precise mechanisms and physiological implications in skeletal and cardiac muscle function.

Finally, Thesis Study III built upon the cellular-based, mechanistic investigations into the protective and regulatory roles of MLN and DWORF to determine gene and protein expression patterns of both regulators in the in the context of single and double knockout models of SLN and PLN. Contrary to the initial hypothesis, the loss of either SLN or PLN did not alter the protein content of MLN or DWORF in cardiac or skeletal muscle, suggesting a lack of compensatory changes in these proteins upon the ablation of SLN or PLN. Remarkably, even in the case of dual SLN/PLN ablation, the protein content of MLN and DWORF remained unaltered, despite evident morphological and phenotypic changes in muscular tissues, indicating a dissociation between the protein expression of these regulators and the observed alterations in muscle structure and function. Though quantification of MLN expression posed considerable difficulty, endogenous

expression was confirmed in cardiac muscle and in both oxidative and glycolytic skeletal muscle. On the other hand, endogenous expression of DWORF was readily detectable in cardiac muscle and oxidative skeletal muscle. However, while protein levels remained unaltered, mRNA expression was significantly impacted by the loss of SLN or PLN, respectfully, and the dual loss of both SLN/PLN. The differences observed between mRNA and protein expression levels of MLN and DWORF highlight the need for comprehensive investigations into post-translational control mechanisms of all four SERCA regulatory proteins. The study's novel contributions, such as directly detecting MLN protein in murine cardiac and skeletal muscle and exploring the gene and protein expression patterns of MLN and DWORF across knockout models in both sexes, pave the way for future investigations to uncover the complex regulatory network governing SR-mediated control of cellular Ca^{2+} homeostasis and to determine the factors underlying the protein expression of these regulators and their implications in muscular physiology and disease conditions.

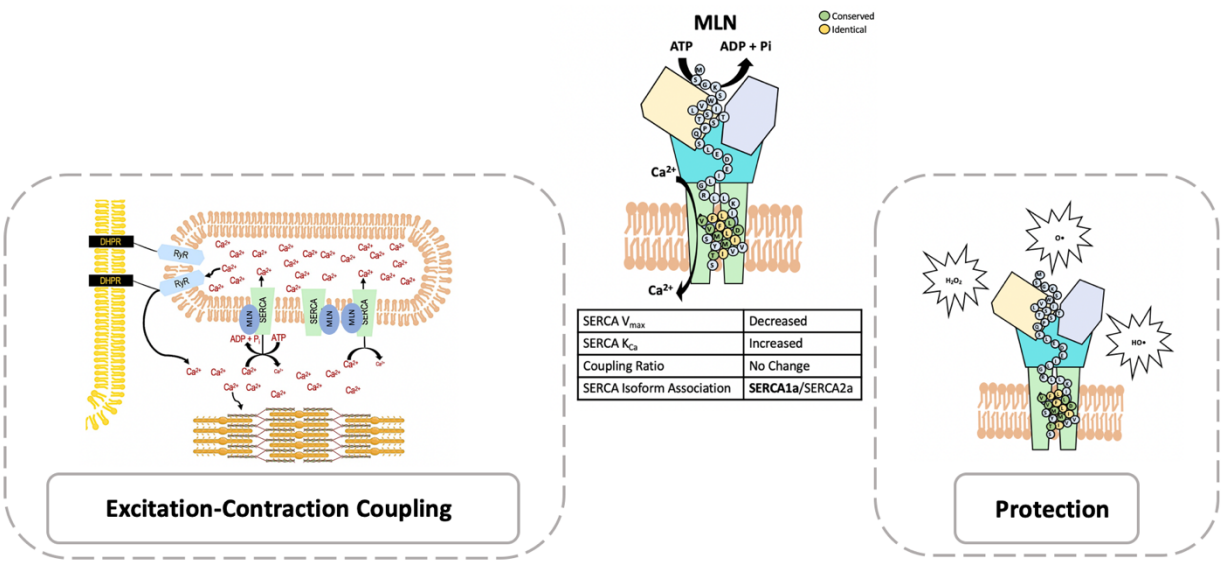


Fig. 6.1.1: Visual Summary of the Different Roles Exerted by the Interaction between MLN and SERCA
A graphical summary of the text above, showing the role of MLN in acting to inhibit SERCA function during basal/resting conditions (when the transport of Ca^{2+} to the SR lumen is not required), in addition to protecting the pump from damage incurred by cellular stress pathways and preserving maximal activity of the pump.

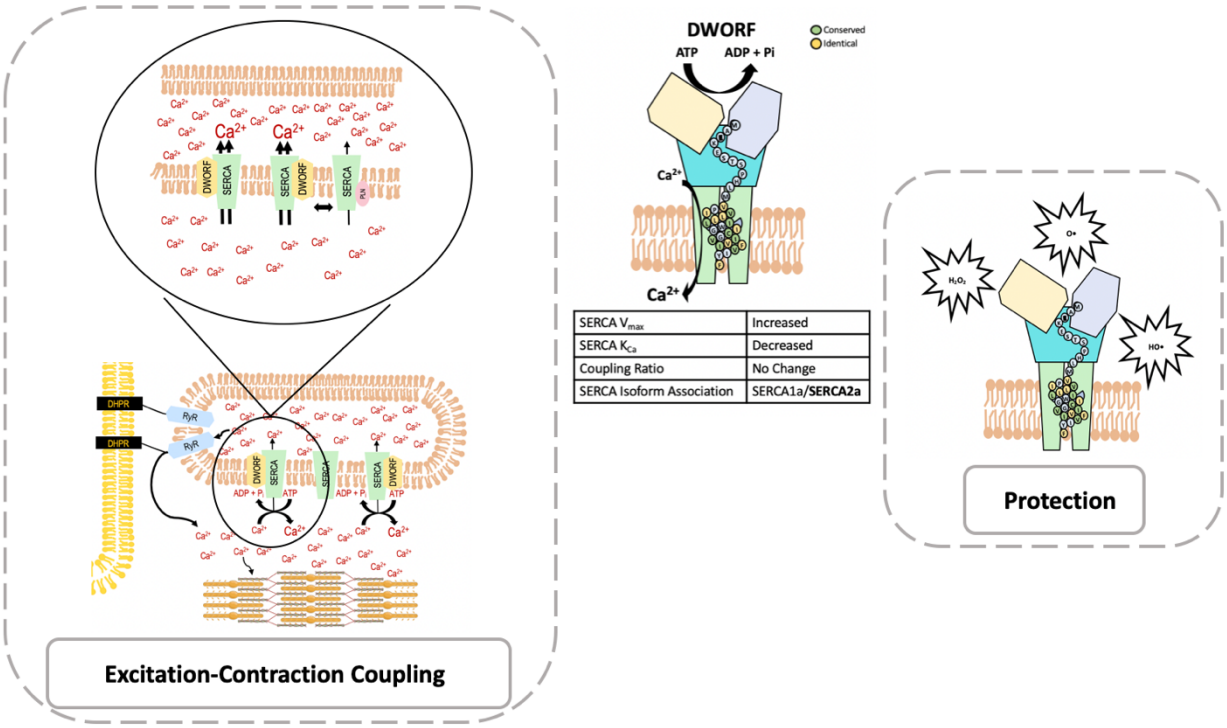


Fig. 6.1.2: Visual Summary of the Different Roles Exerted by the Interaction between DWORF and SERCA
A graphical summary of the text above, illustrating the biological roles of DWORF in acting as a protector of the pump during times of cellular stress, as well as, a key regulator of muscle contraction and relaxation by serving as a competitive non-inhibitor of the pump to interact with and displace the other regulators to return SERCA activity to basal levels and in directly stimulating the pump by increasing Ca^{2+} affinity and maximal activity.

Table 6.1.1: Summary of key findings and novel contributions

Thesis Study I: Investigating if the Interaction between MLN:SERCA and DWORF:SERCA Can Protect the SERCA pump from Oxidative/Thermal Damage	
Key Findings	• Following exposure to heat shock, SERCA activity levels are maintained in HEK293 cells co-expressed with SERCA1a/2a and MLN compared to control • Co-expression of MLN with SERCA prevented carbonyl and nitrotyrosine formation when exposed to HS • Following exposure to heat shock, SERCA activity levels are maintained in HEK293 cells co-expressed with SERCA1a/2a and DWORF compared to control • Co-expression of DWORF with SERCA prevented carbonyl and nitrotyrosine formation when exposed to HS
Conclusions & **Novel Contributions**	• Both MLN and DWORF prevent oxidation and nitrosylation of SERCA and preserve pump function in the face of heat stress • Direct detection of MLN protein and validation of western blotting protocol
Thesis Study II: Assessing if the Interaction Between MLN:SERCA and DWORF:SERCA Can Alter the SERCA Coupling Ratio	
Key Findings	• MLN reduced SERCA affinity for Ca^{2+}, maximal activity and rate of uptake of both isoforms under physiological and maximal conditions • MLN did not uncouple SERCA ATP hydrolysis and Ca^{2+} transport under neither condition • DWORF did not alter SERCA kinetics nor transport efficiency when expressed in a 1:1 ratio with both isoforms • Five-fold overexpression of DWORF increased SERCA affinity for Ca^{2+}, maximal activity and rate of uptake of both isoforms under physiological and maximal conditions • DWORF did not uncouple SERCA ATP hydrolysis and Ca^{2+} transport under neither condition
Conclusions & **Novel Contributions**	• MLN is a negative regulator of SERCA activity but is not an uncoupler • DWORF is a positive regulatory of SERCA activity and is not an uncoupler of the pump

Thesis Study III: Assessing Potential Compensatory Changes in SERCA Regulatory Protein Expression	
Key Findings	• Expression of MLN protein is not changed in SOL, LV and Atria from single and double knock SLN/PLN male and female mice • Endogenous MLN protein expression was confirmed in both oxidative and glycolytic murine skeletal muscle and murine cardiac muscle • Expression of *Mln* mRNA was only changed in left ventricle tissue of female DKO, showing an elevation relative to WT • Expression of DWORF protein is not changed in SOL, LV and Atria from single and double knock SLN/PLN male and female mice • Endogenous expression of DWORF protein was confirmed in in cardiac and oxidative skeletal muscle only • Expression of *Dworf* mRNA was elevated in soleus of male $Sln^{-/-}$ mice • Expression of *Dworf* mRNA was variable in cardiac tissue: o Left ventricle tissue of male and female $Pln^{-/-}$ mice showed either a trending increase or significant increase, respectively o Atria of $Sln^{-/-}$ male mice exhibited a trending increase in *Dworf* expression, whereas, atria of $Sln^{-/-}$ female mice exhibited a significant decrease o Left ventricle and atrial tissue of both male and female $Sln^{-/-}/Pln^{-/-}$ mice displayed a significant decline
Conclusions & Novel Contributions	• There is no compensatory change in protein expression of MLN and DWORF in the absence of either or both SLN and PLN • Like PLN, expression of MLN and DWORF might be controlled at the protein level • Validation of MLN western blotting protocol in murine skeletal and cardiac muscle and determination of MLN and DWORF protein tissue distribution

6.2 Integrated Discussion and Future Directions

The conclusions drawn from this thesis present important and novel insights into the intricate regulatory mechanisms governing Ca^{2+} handling within skeletal and cardiac muscles. Previous studies expressing SERCA1a and SERCA2a in COS-1 cells found similar kinetic properties between the two isoforms [166, 167], which is consistently shown here in Studies I and II. Furthermore, MLN's inhibitory reduction in SERCA V_{max} was proven to be consistent between the first two studies.

It has been well documented that PLN is a component of a multimeric complex in cardiac tissue, interacting with proteins including protein phosphatase 1 (PP1), HSP20 and HAX-1, and that this complex exerts an effect on both SERCA and Ca^{2+} homeostasis [65, 149]. It could very well be the case that the regulatory proteins discussed in this thesis are involved in a similar complex in skeletal muscle as well. This is supported by the dynamic relationship exhibited by PLN and DWORF to inhibit SERCA at low cytoplasmic [Ca^{2+}] and stimulate SERCA during elevations in cytoplasmic [Ca^{2+}] [123]. With PLN showing the highest affinity for SERCA in its E1-ATP state, which prevails at low [Ca^{2+}], and DWORF showing the highest affinity for SERCA in its E1P and E2P states, which dominate at high [Ca^{2+}] [124], these two regulatory proteins work together to modulate SERCA activity and by extension, Ca^{2+} homeostasis. Investigating the dynamic relationships DWORF engages in with SLN and MLN would also be of great interest. With MLN and PLN sharing structural and functional homology, it would be expected that MLN would share a similar interaction with DWORF, however, this is reliant on the ability of MLN to be phosphorylated by physiological stimuli and displaced from the pump as PLN is to allow DWORF to stimulate SERCA during elevations in cytoplasmic [Ca^{2+}]. The interaction between SLN and DWORF would be expected to be more complex as both proteins preferentially interact

with SERCA under conditions of greater $[Ca^{2+}]_i$ [93]. Therefore, it would be important to determine which regulator SERCA exhibits the most affinity for and how the presence of DWORF affects SLN's induction of Ca^{2+} ion slippage. Moreover, determining the muscle fibre expression profile which would also shed light on the extent of overlap between expression of DWORF and the other regulatory proteins *in vivo*. This analysis would additionally reveal the overlap between MLN with SLN and PLN, and could shed light on potential superinhibition of SERCA activity. Specific amino acids found in SLN (V19, I22) and PLN (I47, I48) enable these regulators to physically bind with each other to form a binary complex [168] that interacts with the SERCA groove formed by transmembrane helices M2, M4, M6 and M9, where individual PLN and SLN molecules normally bind [62]. Functionally, when SLN and PLN are expressed together with SERCA in HEK-293 cells [103] or proteoliposomes [63], superinhibition occurs and leads to drastic reductions in SERCA affinity for Ca^{2+} and maximal rates of ATP hydrolysis and Ca^{2+}-uptake. Interestingly, it has been proposed that by binding to PLN, SLN prevents the formation of non-inhibitory PLN pentamers, maintaining it in its inhibitory momomeric form [89]. It would be important to investigate if MLN can too physically interact with SLN and/or PLN to form a similar complex, especially considering that both MLN and SLN preferentially interact with SERCA1a.

It would be imperative to investigate the factors governing regulator expression, as well as, the proteins and pathways that are influenced by said expression. SLN's ability to inhibit SERCA in the face of greater $[Ca^{2+}]_i$ may make SLN more suitable for cellular signaling and mediating necessary adaptations, and may explain why it is consistently elevated across many skeletal muscle diseases and also during muscle growth and development. As speculated by Fajardo *et al,* regulation of SLN expression could be occurring via a Ca^{2+} dependent positive feedback mechanism which involves calcineurin, NFAT and the transcription factor myocyte enhancer

factor 2 (MEF2) [8]. The proposed mechanism hypothesizes that an elevation in $[Ca^{2+}]_i$ activates calcineurin and enables the dephosphorylation of NFAT (to induce translocation into the nucleus), as well as, dephosphorylation of nuclear MEF2 [8]. Activation of MEF2 and NFAT acts to promotes *Sln* transcription and consequently the SLN protein interacts with SERCA to inhibit its function and maintain the higher level of $[Ca^{2+}]_i$ [8]. The mechanisms regulating PLN, MLN and DWORF expression remain unknown, however, investigating the regulation of protein expression and the subsequent proteins and pathways of interaction represent crucial research questions that must be addressed. Moreover, it is interesting to note the differences in the pattern of expression in response to these various stressors. In mechanical overload experiments, the endogenous expression of PLN in plantaris muscles was not different in the overloaded condition compared to sham [6]. Furthermore, PLN expression in soleus muscles was found to be significantly elevated in *mdx* muscles compared with WT [85], as well as in the tenotomized soleus [6], whereas, in response to high fat feeding PLN content was significantly decreased [84]. Altogether, these data suggest that, unlike SLN which is consistently upregulated across these models PLN's response is variable, and this may precede their different roles in muscle physiology, therefore, it would of value to investigate the expression MLN and DWORF in response to various stressors.

In addition to examining the differences in the pattern of expression in response to physiological stressors and disease, differences across the lifespan should also be investigated. It is well known that SLN is naturally upregulated several-fold during muscle development in both fast and slow twitch muscles [108]. This upregulation is witnessed in neonatal muscle and peaks around birth, after which SLN remains present only in slower twitch oxidative muscles [109]. The purpose of this development upregulation in SLN content seems multifaceted. It has been proposed that this upregulation may serve to i) prevent Ca^{2+} overload and delay differentiation in premature

myotubes [169], ii) as a protective mechanism promoting thermogenesis as neonates are especially susceptible to the cold [109], and iii) to play a role in adaptive remodeling and establishment of an oxidative phenotype [110]. Investigations into the role of SLN and PLN in mediating Ca^{2+} homeostasis in aged skeletal muscle are currently underway in the Tupling lab. Future investigations into the roles of MLN and DWORF should consider endogenous expression of these regulators across the lifespan, as well as, in response to physiological stressors such as diet, heat shock and cold-exposure, in addition to disease, disuse and atrophy.

Areas of future direction are discussed throughout this document, however, the two most discussed are rodent studies to investigate the physiological effects of endogenous and induced expression (as discussed above) and mutagenesis studies. Elaborated upon in Section 1.4.1 and in the Discussions of Chapters 3 & 4, in an effort to discern structure and function, as well as, the divergences that allow for their distinct physiological roles, PLN and SLN have been the subjects of extensive mutagenesis studies. Future mutagenesis studies with the aim of determining the residues responsible for i) facilitating the interaction between MLN/DWORF and the SERCAs, ii) imparting MLN's inhibitory function and DWORF's stimulatory function, and iii) conferring thermal stability under conditions of HS; would serve to further our mechanistic understanding of SERCA protection and regulation. To date, studies investigating the structure and function of MLN have been sparse and have relied on molecular modeling and molecular dynamics simulations to propose residues responsible for facilitating the key interactions between MLN and SERCA [145]. Whereas, multiple structural and functional studies have focused on establishing Pro^{15} (and the induced kink) as crucial for DWORF's interaction with SERCA's M4 helix and for DWORF's activating effect on SERCA (both indirectly and directly) [122, 123, 127]. With these molecular modeling and molecular dynamics simulations serving to provide a starting point, mutagenesis

studies evaluating mutant variants are needed to investigate the residues forming critical contacts with SERCA and possibly conferring a regulatory and/or protective function, as well as, delineations in the respective interactions between the regulatory proteins and the pump and the subsequent effect on physiological function. Such future investigations promise to elucidate the complex mechanisms governing SERCA regulation/protection and provide crucial advancements in our understanding of Ca^{2+} handling in muscle.

The knockout models of MLN [12] and DWORF [13], respectfully, discussed in this thesis clearly demonstrate that these proteins exhibit distinct roles. Contributing to the growing body of literature examining these two regulatory proteins, this thesis has revealed that i) similar to SLN and PLN, MLN and DWORF protect SERCA structure and function during cellular stress; ii) like PLN, MLN negatively regulates SERCA kinetics without altering transport efficiency; iii) unlike any other known regulator, DWORF positively modulates the pump by enhancing SERCA apparent Ca^{2+} affinity, maximal activity and the rate of Ca^{2+} uptake without changing SERCA pumping efficiency; iv) under basal conditions, the protein expression levels of MLN and DWORF are not altered by the presence/absence of either PLN and SLN alone or the presence/absence of both PLN and SLN together; and v) like PLN, MLN and DWORF might undergo similar post-translational control of expression. Future work that will continue to examine the roles of MLN and DWORF in the context of SR function will surely reveal notable findings that will delineate the interplay between these proteins in the broader landscape of Ca^{2+} regulation.

References:

1. Bal, N.C., et al., *Sarcolipin is a newly identified regulator of muscle-based thermogenesis in mammals.* Nat Med, 2012. **18**(10): p. 1575-9.
2. Bombardier, E., et al., *Sarcolipin trumps beta-adrenergic receptor signaling as the favored mechanism for muscle-based diet-induced thermogenesis.* FASEB J, 2013. **27**(9): p. 3871-8.
3. Bombardier, E., et al., *Ablation of sarcolipin decreases the energy requirements for Ca2+ transport by sarco(endo)plasmic reticulum Ca2+-ATPases in resting skeletal muscle.* FEBS Lett, 2013. **587**(11): p. 1687-92.
4. Smith, W.S., et al., *Sarcolipin uncouples hydrolysis of ATP from accumulation of Ca2+ by the Ca2+-ATPase of skeletal-muscle sarcoplasmic reticulum.* Biochem J, 2002. **361**(Pt 2): p. 277-86.
5. Mall, S., et al., *The presence of sarcolipin results in increased heat production by Ca(2+)-ATPase.* J Biol Chem, 2006. **281**(48): p. 36597-602.
6. Fajardo, V.A., et al., *Effects of sarcolipin deletion on skeletal muscle adaptive responses to functional overload and unload.* Am J Physiol Cell Physiol, 2017. **313**(2): p. C154-C161.
7. Fajardo, V.A., et al., *Sarcolipin deletion exacerbates soleus muscle atrophy and weakness in phospholamban overexpressing mice.* PLoS One, 2017. **12**(3): p. e0173708.
8. Fajardo, V.A., et al., *Sarcolipin deletion in mdx mice impairs calcineurin signalling and worsens dystrophic pathology.* Hum Mol Genet, 2018. **27**(23): p. 4094-4102.
9. Fajardo, V.A., et al., *Co-expression of SERCA isoforms, phospholamban and sarcolipin in human skeletal muscle fibers.* PLoS One, 2013. **8**(12): p. e84304.
10. Vangheluwe, P., et al., *Sarcolipin and phospholamban mRNA and protein expression in cardiac and skeletal muscle of different species.* Biochem J, 2005. **389**(Pt 1): p. 151-9.
11. Fu, M., et al., *Phospholamban and sarcolipin prevent thermal inactivation of sarco(endo)plasmic reticulum Ca2+-ATPases.* Biochem J, 2020. **477**(21): p. 4281-4294.
12. Anderson, D.M., et al., *A micropeptide encoded by a putative long noncoding RNA regulates muscle performance.* Cell, 2015. **160**(4): p. 595-606.
13. Nelson, B.R., et al., *A peptide encoded by a transcript annotated as long noncoding RNA enhances SERCA activity in muscle.* Science, 2016. **351**(6270): p. 271-5.
14. Berridge, M.J., P. Lipp, and M.D. Bootman, *The versatility and universality of calcium signalling.* Nat Rev Mol Cell Biol, 2000. **1**(1): p. 11-21.
15. Clapham, D.E., *Calcium signaling.* Cell, 2007. **131**(6): p. 1047-58.
16. Brini, M., et al., *Calcium in health and disease.* Met Ions Life Sci, 2013. **13**: p. 81-137.
17. Rossi, A.E. and R.T. Dirksen, *Sarcoplasmic reticulum: the dynamic calcium governor of muscle.* Muscle Nerve, 2006. **33**(6): p. 715-31.
18. Periasamy, M. and A. Kalyanasundaram, *SERCA pump isoforms: their role in calcium transport and disease.* Muscle Nerve, 2007. **35**(4): p. 430-42.
19. Mekahli, D., et al., *Endoplasmic-reticulum calcium depletion and disease.* Cold Spring Harb Perspect Biol, 2011. **3**(6).
20. Berchtold, M.W., H. Brinkmeier, and M. Muntener, *Calcium ion in skeletal muscle: its crucial role for muscle function, plasticity, and disease.* Physiol Rev, 2000. **80**(3): p. 1215-65.

21. Calderon, J.C., P. Bolanos, and C. Caputo, *The excitation-contraction coupling mechanism in skeletal muscle.* Biophys Rev, 2014. **6**(1): p. 133-160.
22. Fryer, M.W. and D.G. Stephenson, *Total and sarcoplasmic reticulum calcium contents of skinned fibres from rat skeletal muscle.* J Physiol, 1996. **493 (Pt 2)**: p. 357-70.
23. Inesi, G. and L. de Meis, *Regulation of steady state filling in sarcoplasmic reticulum. Roles of back-inhibition, leakage, and slippage of the calcium pump.* J Biol Chem, 1989. **264**(10): p. 5929-36.
24. Reggiani, C. and T. te Kronnie, *RyR isoforms and fibre type-specific expression of proteins controlling intracellular calcium concentration in skeletal muscles.* J Muscle Res Cell Motil, 2006. **27**(5-7): p. 327-35.
25. Gailly, P., et al., *Critical evaluation of cytosolic calcium determination in resting muscle fibres from normal and dystrophic (mdx) mice.* Cell Calcium, 1993. **14**(6): p. 473-83.
26. Carroll, S.L., M.G. Klein, and M.F. Schneider, *Decay of calcium transients after electrical stimulation in rat fast- and slow-twitch skeletal muscle fibres.* J Physiol, 1997. **501 (Pt 3)**: p. 573-88.
27. Renganathan, M., M.L. Messi, and O. Delbono, *Overexpression of IGF-1 exclusively in skeletal muscle prevents age-related decline in the number of dihydropyridine receptors.* J Biol Chem, 1998. **273**(44): p. 28845-51.
28. Leberer, E. and D. Pette, *Immunochemical quantification of sarcoplasmic reticulum Ca-ATPase, of calsequestrin and of parvalbumin in rabbit skeletal muscles of defined fiber composition.* Eur J Biochem, 1986. **156**(3): p. 489-96.
29. Leberer, E., K.T. Hartner, and D. Pette, *Postnatal development of Ca2+-sequestration by the sarcoplasmic reticulum of fast and slow muscles in normal and dystrophic mice.* Eur J Biochem, 1988. **174**(2): p. 247-53.
30. Shaikh, S.A., S.K. Sahoo, and M. Periasamy, *Phospholamban and sarcolipin: Are they functionally redundant or distinct regulators of the Sarco(Endo)Plasmic Reticulum Calcium ATPase?* Journal of Molecular and Cellular Cardiology, 2016. **91**: p. 81-91.
31. Gamu, D., et al., *Sarcolipin provides a novel muscle-based mechanism for adaptive thermogenesis.* Exerc Sport Sci Rev, 2014. **42**(3): p. 136-42.
32. Clarke, D.M., et al., *Location of high affinity Ca2+-binding sites within the predicted transmembrane domain of the sarcoplasmic reticulum Ca2+-ATPase.* Nature, 1989. **339**(6224): p. 476-8.
33. Chemaly, E.R., Bobe, R., Adnot, S., Hajjar, R. J., & Lipskaia, L. , *Sarco (Endo) Plasmic Reticulum Calcium ATPases (SERCA) Isoforms in the Normal and Diseased Cardiac, Vascular and Skeletal muscle.* . Journal of Cardiovascular Diseases & Diagnosis, 2013. **1**(113): p. 2.
34. Tupling, A.R., *The sarcoplasmic reticulum in muscle fatigue and disease: role of the sarco (endo) plasmic reticulum Ca2+-ATPase.* Canadian Journal of Applied Physiology, 2004. **29**(3): p. 308-329.
35. Lee, A.G., *Ca2+ -ATPase structure in the E1 and E2 conformations: mechanism, helix-helix and helix-lipid interactions.* Biochim Biophys Acta, 2002. **1565**(2): p. 246-66.
36. MacLennan, D.H., W.J. Rice, and N.M. Green, *The mechanism of Ca2+ transport by sarco(endo)plasmic reticulum Ca2+-ATPases.* J Biol Chem, 1997. **272**(46): p. 28815-8.
37. Toyoshima, C., *Ion pumping by calcium ATPase of sarcoplasmic reticulum.* Adv Exp Med Biol, 2007. **592**: p. 295-303.

38. Berman, M.C., *Slippage and uncoupling in P-type cation pumps; implications for energy transduction mechanisms and regulation of metabolism.* Biochim Biophys Acta, 2001. **1513**(2): p. 95-121.
39. de Meis, L., *Role of the sarcoplasmic reticulum Ca2+-ATPase on heat production and thermogenesis.* Biosci Rep, 2001. **21**(2): p. 113-37.
40. Chinet, A., A. Decrouy, and P.C. Even, *Ca(2+)-dependent heat production under basal and near-basal conditions in the mouse soleus muscle.* J Physiol, 1992. **455**: p. 663-78.
41. Decrouy, A., P.C. Even, and A. Chinet, *Decreased rates of Ca(2+)-dependent heat production in slow- and fast-twitch muscles from the dystrophic (mdx) mouse.* Experientia, 1993. **49**(10): p. 843-9.
42. Dulloo, A.G., A. Decrouy, and A. Chinet, *Suppression of Ca(2+)-dependent heat production in mouse skeletal muscle by high fish oil consumption.* Metabolism, 1994. **43**(8): p. 931-4.
43. Smith, I.C., et al., *ATP consumption by sarcoplasmic reticulum Ca(2)(+) pumps accounts for 40-50% of resting metabolic rate in mouse fast and slow twitch skeletal muscle.* PLoS One, 2013. **8**(7): p. e68924.
44. Tupling, A.R., et al., *HSP70 binds to the fast-twitch skeletal muscle sarco(endo)plasmic reticulum Ca2+ -ATPase (SERCA1a) and prevents thermal inactivation.* J Biol Chem, 2004. **279**(50): p. 52382-9.
45. Adachi, T., et al., *S-Glutathiolation by peroxynitrite activates SERCA during arterial relaxation by nitric oxide.* Nat Med, 2004. **10**(11): p. 1200-7.
46. Knyushko, T.V., et al., *3-Nitrotyrosine modification of SERCA2a in the aging heart: a distinct signature of the cellular redox environment.* Biochemistry, 2005. **44**(39): p. 13071-81.
47. Senisterra, G.A., et al., *Destabilization of the Ca2+-ATPase of sarcoplasmic reticulum by thiol-specific, heat shock inducers results in thermal denaturation at 37 degrees C.* Biochemistry, 1997. **36**(36): p. 11002-11.
48. Viner, R.I., T.D. Williams, and C. Schoneich, *Peroxynitrite modification of protein thiols: oxidation, nitrosylation, and S-glutathiolation of functionally important cysteine residue(s) in the sarcoplasmic reticulum Ca-ATPase.* Biochemistry, 1999. **38**(38): p. 12408-15.
49. Gutierrez-Martin, Y., et al., *Modulation of sarcoplasmic reticulum Ca(2+)-ATPase by chronic and acute exposure to peroxynitrite.* Eur J Biochem, 2004. **271**(13): p. 2647-57.
50. Klebl, B.M., A.T. Ayoub, and D. Pette, *Protein oxidation, tyrosine nitration, and inactivation of sarcoplasmic reticulum Ca2+-ATPase in low-frequency stimulated rabbit muscle.* FEBS Lett, 1998. **422**(3): p. 381-4.
51. Gehrig, S.M., et al., *Hsp72 preserves muscle function and slows progression of severe muscular dystrophy.* Nature, 2012. **484**(7394): p. 394-8.
52. Schneider, J.S., et al., *Increased sarcolipin expression and decreased sarco(endo)plasmic reticulum Ca2+ uptake in skeletal muscles of mouse models of Duchenne muscular dystrophy.* J Muscle Res Cell Motil, 2013. **34**(5-6): p. 349-56.
53. Voit, A., et al., *Reducing sarcolipin expression mitigates Duchenne muscular dystrophy and associated cardiomyopathy in mice.* Nat Commun, 2017. **8**(1): p. 1068.
54. Goonasekera, S.A., et al., *Mitigation of muscular dystrophy in mice by SERCA overexpression in skeletal muscle.* Journal of Clinical Investigation, 2011. **121**(3): p. 1044-1052.

55. Fajardo, V.A., et al., *Phospholamban overexpression in mice causes a centronuclear myopathy-like phenotype.* Dis Model Mech, 2015. **8**(8): p. 999-1009.
56. Mazala, D.A., et al., *SERCA1 overexpression minimizes skeletal muscle damage in dystrophic mouse models.* Am J Physiol Cell Physiol, 2015. **308**(9): p. C699-709.
57. Cleverdon, R.E.G., et al., *Sarco(endo)plasmic reticulum Ca(2+)-ATPase function is impaired in skeletal and cardiac muscles from young DBA/2J mdx mice.* iScience, 2022. **25**(9): p. 104972.
58. Kargacin, M.E. and G.J. Kargacin, *The sarcoplasmic reticulum calcium pump is functionally altered in dystrophic muscle.* Biochim Biophys Acta, 1996. **1290**(1): p. 4-8.
59. Chambers, P.J., et al., *Role of SERCA and sarcolipin in adaptive muscle remodeling.* Am J Physiol Cell Physiol, 2022. **322**(3): p. C382-C394.
60. Ulrich, K. and U. Jakob, *The role of thiols in antioxidant systems.* Free Radic Biol Med, 2019. **140**: p. 14-27.
61. Fu, M.H. and A.R. Tupling, *Protective effects of Hsp70 on the structure and function of SERCA2a expressed in HEK-293 cells during heat stress.* Am J Physiol Heart Circ Physiol, 2009. **296**(4): p. H1175-83.
62. Asahi, M., et al., *Sarcolipin regulates sarco(endo)plasmic reticulum Ca2+-ATPase (SERCA) by binding to transmembrane helices alone or in association with phospholamban.* Proceedings of the National Academy of Sciences, 2003. **100**(9): p. 5040-5045.
63. Gorski, P.A., et al., *Sarco (endo) plasmic reticulum calcium ATPase (SERCA) inhibition by sarcolipin is encoded in its luminal tail.* Journal of Biological Chemistry, 2013. **288**(12): p. 8456-8467.
64. Toyofuku, T., et al., *Identification of regions in the Ca(2+)-ATPase of sarcoplasmic reticulum that affect functional association with phospholamban.* J Biol Chem, 1993. **268**(4): p. 2809-15.
65. MacLennan, D.H. and E.G. Kranias, *Phospholamban: a crucial regulator of cardiac contractility.* Nat Rev Mol Cell Biol, 2003. **4**(7): p. 566-77.
66. Akin, B.L. and L.R. Jones, *Characterizing phospholamban to sarco(endo)plasmic reticulum Ca2+-ATPase 2a (SERCA2a) protein binding interactions in human cardiac sarcoplasmic reticulum vesicles using chemical cross-linking.* J Biol Chem, 2012. **287**(10): p. 7582-93.
67. MacLennan, D.H., M. Asahi, and A.R. Tupling, *The regulation of SERCA-type pumps by phospholamban and sarcolipin.* Ann N Y Acad Sci, 2003. **986**: p. 472-80.
68. Toyoshima, C., et al., *Modeling of the inhibitory interaction of phospholamban with the Ca2+ ATPase.* Proc Natl Acad Sci U S A, 2003. **100**(2): p. 467-72.
69. Traaseth, N.J., et al., *Structural and dynamic basis of phospholamban and sarcolipin inhibition of Ca(2+)-ATPase.* Biochemistry, 2008. **47**(1): p. 3-13.
70. Gustavsson, M., et al., *Allosteric regulation of SERCA by phosphorylation-mediated conformational shift of phospholamban.* Proc Natl Acad Sci U S A, 2013. **110**(43): p. 17338-43.
71. Asahi, M., et al., *Physical interactions between phospholamban and sarco(endo)plasmic reticulum Ca2+-ATPases are dissociated by elevated Ca2+, but not by phospholamban phosphorylation, vanadate, or thapsigargin, and are enhanced by ATP.* J Biol Chem, 2000. **275**(20): p. 15034-8.

72. Jones, L.R., R.L. Cornea, and Z. Chen, *Close proximity between residue 30 of phospholamban and cysteine 318 of the cardiac Ca2+ pump revealed by intermolecular thiol cross-linking.* J Biol Chem, 2002. **277**(31): p. 28319-29.
73. James, P., et al., *Nature and site of phospholamban regulation of the Ca2+ pump of sarcoplasmic reticulum.* Nature, 1989. **342**(6245): p. 90-2.
74. Bidwell, P., et al., *Phospholamban binds with differential affinity to calcium pump conformers.* J Biol Chem, 2011. **286**(40): p. 35044-50.
75. Mueller, B., et al., *Direct detection of phospholamban and sarcoplasmic reticulum Ca-ATPase interaction in membranes using fluorescence resonance energy transfer.* Biochemistry, 2004. **43**(27): p. 8754-65.
76. Li, J., D.J. Bigelow, and T.C. Squier, *Conformational changes within the cytosolic portion of phospholamban upon release of Ca-ATPase inhibition.* Biochemistry, 2004. **43**(13): p. 3870-9.
77. Primeau, J.O., et al., *The SarcoEndoplasmic Reticulum Calcium ATPase.* Subcell Biochem, 2018. **87**: p. 229-258.
78. Toyoshima, C., et al., *Crystal structures of the calcium pump and sarcolipin in the Mg2+-bound E1 state.* Nature, 2013. **495**(7440): p. 260-4.
79. Akin, B.L., et al., *The structural basis for phospholamban inhibition of the calcium pump in sarcoplasmic reticulum.* J Biol Chem, 2013. **288**(42): p. 30181-91.
80. Kimura, Y., et al., *Phospholamban inhibitory function is activated by depolymerization.* J Biol Chem, 1997. **272**(24): p. 15061-4.
81. Slack, J.P., et al., *Phospholamban ablation enhances relaxation in the murine soleus.* Am J Physiol, 1997. **273**(1 Pt 1): p. C1-6.
82. Kranias, E.G. and R.J. Hajjar, *Modulation of cardiac contractility by the phospholamban/SERCA2a regulatome.* Circ Res, 2012. **110**(12): p. 1646-60.
83. Bluhm, W.F., et al., *Phospholamban: a major determinant of the cardiac force-frequency relationship.* Am J Physiol Heart Circ Physiol, 2000. **278**(1): p. H249-55.
84. Gamu, D., et al., *Phospholamban deficiency does not alter skeletal muscle SERCA pumping efficiency or predispose mice to diet-induced obesity.* Am J Physiol Endocrinol Metab, 2019. **316**(3): p. E432-E442.
85. Juracic, E.S., *Characterizing the Role of Phospholamban in Duchenne Muscular Dystrophy*. 2018, UWSpace.
86. Mercuri, E. and F. Muntoni, *Muscular dystrophies.* Lancet, 2013. **381**(9869): p. 845-60.
87. Cooper, S.T. and S.I. Head, *Membrane Injury and Repair in the Muscular Dystrophies.* Neuroscientist, 2015. **21**(6): p. 653-68.
88. Whitehead, N.P., E.W. Yeung, and D.G. Allen, *Muscle damage in mdx (dystrophic) mice: role of calcium and reactive oxygen species.* Clin Exp Pharmacol Physiol, 2006. **33**(7): p. 657-62.
89. Allen, D.G., et al., *Calcium and the damage pathways in muscular dystrophy.* Can J Physiol Pharmacol, 2010. **88**(2): p. 83-91.
90. Allen, D.G., N.P. Whitehead, and S.C. Froehner, *Absence of Dystrophin Disrupts Skeletal Muscle Signaling: Roles of Ca2+, Reactive Oxygen Species, and Nitric Oxide in the Development of Muscular Dystrophy.* Physiol Rev, 2016. **96**(1): p. 253-305.
91. Hopf, F.W., P.R. Turner, and R.A. Steinhardt, *Calcium misregulation and the pathogenesis of muscular dystrophy.* Subcell Biochem, 2007. **45**: p. 429-64.

92. Sahoo, S.K., et al., *The N Terminus of Sarcolipin Plays an Important Role in Uncoupling Sarco-endoplasmic Reticulum Ca2+-ATPase (SERCA) ATP Hydrolysis from Ca2+ Transport.* J Biol Chem, 2015. **290**(22): p. 14057-67.
93. Sahoo, S.K., et al., *Sarcolipin protein interaction with sarco(endo)plasmic reticulum Ca2+ ATPase (SERCA) is distinct from phospholamban protein, and only sarcolipin can promote uncoupling of the SERCA pump.* J Biol Chem, 2013. **288**(10): p. 6881-9.
94. Gramolini, A.O., et al., *Cardiac-specific overexpression of sarcolipin in phospholamban null mice impairs myocyte function that is restored by phosphorylation.* Proc Natl Acad Sci U S A, 2006. **103**(7): p. 2446-51.
95. Bhupathy, P., et al., *Threonine-5 at the N-terminus can modulate sarcolipin function in cardiac myocytes.* J Mol Cell Cardiol, 2009. **47**(5): p. 723-9.
96. Gramolini, A.O., et al., *Sarcolipin retention in the endoplasmic reticulum depends on its C-terminal RSYQY sequence and its interaction with sarco(endo)plasmic Ca(2+)-ATPases.* Proc Natl Acad Sci U S A, 2004. **101**(48): p. 16807-12.
97. Odermatt, A., et al., *Sarcolipin regulates the activity of SERCA1, the fast-twitch skeletal muscle sarcoplasmic reticulum Ca2+-ATPase.* J Biol Chem, 1998. **273**(20): p. 12360-9.
98. Hughes, E., et al., *Solid-state NMR and functional measurements indicate that the conserved tyrosine residues of sarcolipin are involved directly in the inhibition of SERCA1.* J Biol Chem, 2007. **282**(36): p. 26603-13.
99. Luo, W., et al., *Targeted ablation of the phospholamban gene is associated with markedly enhanced myocardial contractility and loss of beta-agonist stimulation.* Circ Res, 1994. **75**(3): p. 401-9.
100. Tupling, A.R., et al., *Enhanced Ca2+ transport and muscle relaxation in skeletal muscle from sarcolipin-null mice.* Am J Physiol Cell Physiol, 2011. **301**(4): p. C841-9.
101. Kadambi, V.J., et al., *Cardiac-specific overexpression of phospholamban alters calcium kinetics and resultant cardiomyocyte mechanics in transgenic mice.* J Clin Invest, 1996. **97**(2): p. 533-9.
102. Pattison, J.S., et al., *Phospholamban overexpression in transgenic rabbits.* Transgenic Res, 2008. **17**(2): p. 157-70.
103. Asahi, M., et al., *Sarcolipin inhibits polymerization of phospholamban to induce superinhibition of sarco(endo)plasmic reticulum Ca2+-ATPases (SERCAs).* J Biol Chem, 2002. **277**(30): p. 26725-8.
104. Babu, G.J., et al., *Ablation of sarcolipin enhances sarcoplasmic reticulum calcium transport and atrial contractility.* Proc Natl Acad Sci U S A, 2007. **104**(45): p. 17867-72.
105. Babu, G.J., et al., *Targeted overexpression of sarcolipin in the mouse heart decreases sarcoplasmic reticulum calcium transport and cardiac contractility.* J Biol Chem, 2006. **281**(7): p. 3972-9.
106. Asahi, M., et al., *Cardiac-specific overexpression of sarcolipin inhibits sarco(endo)plasmic reticulum Ca2+ ATPase (SERCA2a) activity and impairs cardiac function in mice.* Proc Natl Acad Sci U S A, 2004. **101**(25): p. 9199-204.
107. Tupling, A.R., M. Asahi, and D.H. MacLennan, *Sarcolipin overexpression in rat slow twitch muscle inhibits sarcoplasmic reticulum Ca2+ uptake and impairs contractile function.* J Biol Chem, 2002. **277**(47): p. 44740-6.
108. Babu, G.J., et al., *Differential expression of sarcolipin protein during muscle development and cardiac pathophysiology.* J Mol Cell Cardiol, 2007. **43**(2): p. 215-22.

109. Pant, M., N.C. Bal, and M. Periasamy, *Cold adaptation overrides developmental regulation of sarcolipin expression in mice skeletal muscle: SOS for muscle-based thermogenesis?* J Exp Biol, 2015. **218**(Pt 15): p. 2321-5.
110. Maurya, S.K., et al., *Sarcolipin Signaling Promotes Mitochondrial Biogenesis and Oxidative Metabolism in Skeletal Muscle.* Cell Rep, 2018. **24**(11): p. 2919-2931.
111. Bal, N.C., et al., *Is Upregulation of Sarcolipin Beneficial or Detrimental to Muscle Function?* Front Physiol, 2021. **12**: p. 633058.
112. Pant, M., N.C. Bal, and M. Periasamy, *Sarcolipin: A Key Thermogenic and Metabolic Regulator in Skeletal Muscle.* Trends Endocrinol Metab, 2016. **27**(12): p. 881-892.
113. Chin, E.R., et al., *A calcineurin-dependent transcriptional pathway controls skeletal muscle fiber type.* Genes Dev, 1998. **12**(16): p. 2499-509.
114. Michel, R.N., S.E. Dunn, and E.R. Chin, *Calcineurin and skeletal muscle growth.* Proc Nutr Soc, 2004. **63**(2): p. 341-9.
115. Chakkalakal, J.V., et al., *Stimulation of calcineurin signaling attenuates the dystrophic pathology in mdx mice.* Hum Mol Genet, 2004. **13**(4): p. 379-88.
116. Chakkalakal, J.V., et al., *Expression of utrophin A mRNA correlates with the oxidative capacity of skeletal muscle fiber types and is regulated by calcineurin/NFAT signaling.* Proc Natl Acad Sci U S A, 2003. **100**(13): p. 7791-6.
117. Chakkalakal, J.V., et al., *Targeted inhibition of Ca2+ /calmodulin signaling exacerbates the dystrophic phenotype in mdx mouse muscle.* Hum Mol Genet, 2006. **15**(9): p. 1423-35.
118. Gamu, D., et al., *Persistence of diet-induced obesity despite access to voluntary activity in mice lacking sarcolipin.* Physiol Rep, 2015. **3**(9).
119. MacPherson, R.E., et al., *Sarcolipin knockout mice fed a high-fat diet exhibit altered indices of adipose tissue inflammation and remodeling.* Obesity (Silver Spring), 2016. **24**(7): p. 1499-505.
120. Rowland, L.A., et al., *Sarcolipin and uncoupling protein 1 play distinct roles in diet-induced thermogenesis and do not compensate for one another.* Obesity (Silver Spring), 2016. **24**(7): p. 1430-3.
121. Maurya, S.K., et al., *Sarcolipin Is a Key Determinant of the Basal Metabolic Rate, and Its Overexpression Enhances Energy Expenditure and Resistance against Diet-induced Obesity.* J Biol Chem, 2015. **290**(17): p. 10840-9.
122. Reddy, U.V., et al., *A kink in DWORF helical structure controls the activation of the sarcoplasmic reticulum Ca(2+)-ATPase.* Structure, 2022. **30**(3): p. 360-370 e6.
123. Fisher, M.E., et al., *Dwarf open reading frame (DWORF) is a direct activator of the sarcoplasmic reticulum calcium pump SERCA.* Elife, 2021. **10**.
124. Cleary, S.R., et al., *Inhibitory and stimulatory micropeptides preferentially bind to different conformations of the cardiac calcium pump.* J Biol Chem, 2022. **298**(7): p. 102060.
125. Dyla, M., et al., *Structure and Mechanism of P-Type ATPase Ion Pumps.* Annu Rev Biochem, 2020. **89**: p. 583-603.
126. Toyoshima, C., *Structural aspects of ion pumping by Ca2+-ATPase of sarcoplasmic reticulum.* Arch Biochem Biophys, 2008. **476**(1): p. 3-11.
127. Li, A., et al., *The transmembrane peptide DWORF activates SERCA2a via dual mechanisms.* J Biol Chem, 2021. **296**: p. 100412.

128. Kang, S., et al., *Small Molecular Allosteric Activator of the Sarco/Endoplasmic Reticulum Ca2+-ATPase (SERCA) Attenuates Diabetes and Metabolic Disorders.* J Biol Chem, 2016. **291**(10): p. 5185-98.
129. Makarewich, C.A., et al., *The DWORF micropeptide enhances contractility and prevents heart failure in a mouse model of dilated cardiomyopathy.* Elife, 2018. **7**.
130. Makarewich, C.A., et al., *Gene Therapy With the DWORF Micropeptide Attenuates Cardiomyopathy in Mice.* Circ Res, 2020. **127**(10): p. 1340-1342.
131. Jones, D.H., et al., *Na,K-ATPase from mice lacking the gamma subunit (FXYD2) exhibits altered Na+ affinity and decreased thermal stability.* J Biol Chem, 2005. **280**(19): p. 19003-11.
132. Sweadner, K.J. and C. Donnet, *Structural similarities of Na,K-ATPase and SERCA, the Ca(2+)-ATPase of the sarcoplasmic reticulum.* Biochem J, 2001. **356**(Pt 3): p. 685-704.
133. Fu, M. and A.R. Tupling, *Protective effects of Hsp70 on the structure and function of SERCA2a expressed in HEK-293 cells during heat stress.* Am J Physiol Heart Circ Physiol, 2009. **296**(4): p. H1175-83.
134. Asahi, M., et al., *Transmembrane helix M6 in sarco(endo)plasmic reticulum Ca(2+)-ATPase forms a functional interaction site with phospholamban. Evidence for physical interactions at other sites.* J. Biol. Chem., 1999. **274**(46): p. 32855-32862.
135. Braun, J.L., et al., *Neuronatin promotes SERCA uncoupling and its expression is altered in skeletal muscles of high-fat diet-fed mice.* FEBS Lett, 2021. **595**(22): p. 2756-2767.
136. Hakem Zadeh, F., et al., *AKAP6 and phospholamban colocalize and interact in HEK-293T cells and primary murine cardiomyocytes.* Physiol Rep, 2019. **7**(14): p. e14144.
137. Schacterle, G.R. and R.L. Pollack, *A simplified method for the quantitative assay of small amounts of protein in biologic material.* Anal Biochem, 1973. **51**(2): p. 654-5.
138. Duhamel, T.A., et al., *Muscle metabolic, SR Ca(2+) -cycling responses to prolonged cycling, with and without glucose supplementation.* J Appl Physiol (1985), 2007. **103**(6): p. 1986-98.
139. Geromella, M.S., J.L. Braun, and V.A. Fajardo, *Measuring SERCA-mediated calcium uptake in mouse muscle homogenates.* STAR Protoc, 2023. **4**(1): p. 101987.
140. Li, S.Y., et al., *Cardiac contractile dysfunction in Lep/Lep obesity is accompanied by NADPH oxidase activation, oxidative modification of sarco(endo)plasmic reticulum Ca2+-ATPase and myosin heavy chain isozyme switch.* Diabetologia, 2006. **49**(6): p. 1434-46.
141. Yan, L.J., W.C. Orr, and R.S. Sohal, *Identification of oxidized proteins based on sodium dodecyl sulfate-polyacrylamide gel electrophoresis, immunochemical detection, isoelectric focusing, and microsequencing.* Anal Biochem, 1998. **263**(1): p. 67-71.
142. Divet, A. and C. Huchet-Cadiou, *Sarcoplasmic reticulum function in slow- and fast-twitch skeletal muscles from mdx mice.* Pflugers Arch, 2002. **444**(5): p. 634-43.
143. Schertzer, J.D., H.J. Green, and A.R. Tupling, *Thermal instability of rat muscle sarcoplasmic reticulum Ca(2+)-ATPase function.* Am J Physiol Endocrinol Metab, 2002. **283**(4): p. E722-8.
144. Lepock, J.R., et al., *Thermal denaturation of the Ca2(+)-ATPase of sarcoplasmic reticulum reveals two thermodynamically independent domains.* Biochemistry, 1990. **29**(3): p. 681-9.
145. Rathod, N., et al., *Nothing Regular about the Regulins: Distinct Functional Properties of SERCA Transmembrane Peptide Regulatory Subunits.* Int J Mol Sci, 2021. **22**(16).

146. Babu, G.J., et al., *Differential expression of sarcolipin protein during muscle development and cardiac pathophysiology.* J. Mol. Cell. Cardiol., 2007. **42**: p. 215-22.
147. Schertzer, J.D., H.J. Green, and A.R. Tupling, *Thermal instability of rat muscle sarcoplasmic reticulum Ca^{2+}-ATPase function.* Am J Physiol, 2002. **283**: p. E722-E728.
148. Tupling, A.R., et al., *HSP70 binds to the fast-twitch skeletal muscle Sarco (endo)plasmic reticulum Ca2+-ATPase (SERCA1a) and prevents thermal inactivation.* J Biol Chem, 2004. **279**(50): p. 52382 - 52389.
149. Yap, S.V., et al., *HAX-1: a multifaceted antiapoptotic protein localizing in the mitochondria and the sarcoplasmic reticulum of striated muscle cells.* J Mol Cell Cardiol, 2010. **48**(6): p. 1266-79.
150. Kalmar, B. and L. Greensmith, *Induction of heat shock proteins for protection against oxidative stress.* Adv Drug Deliv Rev, 2009. **61**(4): p. 310-8.
151. Larkins, N.T., R.M. Murphy, and G.D. Lamb, *Influences of temperature, oxidative stress, and phosphorylation on binding of heat shock proteins in skeletal muscle fibers.* Am J Physiol Cell Physiol, 2012. **303**(6): p. C654-65.
152. Liu, Y. and J.M. Steinacker, *Changes in skeletal muscle heat shock proteins: pathological significance.* Front Biosci, 2001. **6**: p. D12-25.
153. Brahmbhatt, A.N., *Effects of Heat Stress on Hsp70, Sarcolipin, and Phospholamban Content and SERCA*
Function in Female and Male Rat Skeletal Muscle. 2023: UWSpace.
154. Liu, A.Y., et al., *Functional Role of an Unusual Transmembrane Acidic Residue in the Calcium Pump Regulator Myoregulin.* Biochemistry, 2023. **62**(8): p. 1331-1336.
155. Rathod, N., et al., *Replacement of Lys27 by asparagine in the SERCA regulator myoregulin: A Ca(2+) affinity modulator or a catalytic activity switch?* Biochim Biophys Acta Mol Cell Res, 2024. **1871**(1): p. 119613.
156. Gamu, D., *Deletion of Sarco(endo)plasmic Reticulum Ca2+-ATPase Regulatory Proteins: Impacts on Energy Metabolism and Obesity*. 2017: UWSpace.
157. Singh, S., M. Periasamy, and N.C. Bal, *Strain-specific differences in muscle Ca(2+) transport and mitochondrial electron transport chain proteins between FVB/N and C57BL/6J mice.* J Exp Biol, 2021. **224**(Pt 2).
158. Christianto, A., et al., *Sex differences in metabolic pathways are regulated by Pfkfb3 and Pdk4 expression in rodent muscle.* Commun Biol, 2021. **4**(1): p. 1264.
159. Haizlip, K.M., B.C. Harrison, and L.A. Leinwand, *Sex-based differences in skeletal muscle kinetics and fiber-type composition.* Physiology (Bethesda), 2015. **30**(1): p. 30-9.
160. Wust, R.C., et al., *Sex differences in contractile properties and fatigue resistance of human skeletal muscle.* Exp Physiol, 2008. **93**(7): p. 843-50.
161. Hunter, S.K., *The Relevance of Sex Differences in Performance Fatigability.* Med Sci Sports Exerc, 2016. **48**(11): p. 2247-2256.
162. Green, H.J., I.G. Fraser, and D.A. Ranney, *Male and female differences in enzyme activities of energy metabolism in vastus lateralis muscle.* J Neurol Sci, 1984. **65**(3): p. 323-31.
163. Maher, A.C., et al., *Women have higher protein content of beta-oxidation enzymes in skeletal muscle than men.* PLoS One, 2010. **5**(8): p. e12025.
164. Ver Heyen, M., et al., *Replacement of the muscle-specific sarcoplasmic reticulum Ca(2+)-ATPase isoform SERCA2a by the nonmuscle SERCA2b homologue causes mild*

concentric hypertrophy and impairs contraction-relaxation of the heart. Circ Res, 2001. **89**(9): p. 838-46.
165. Braz, J.C., et al., *PKC-alpha regulates cardiac contractility and propensity toward heart failure.* Nat Med, 2004. **10**(3): p. 248-54.
166. Lytton, J., et al., *Functional comparisons between isoforms of the sarcoplasmic or endoplasmic reticulum family of calcium pumps.* J Biol Chem, 1992. **267**(20): p. 14483-9.
167. Sumbilla, C., et al., *Comparison of SERCA1 and SERCA2a expressed in COS-1 cells and cardiac myocytes.* Am J Physiol, 1999. **277**(6): p. H2381-91.
168. Morita, T., et al., *Interaction sites among phospholamban, sarcolipin, and the sarco(endo)plasmic reticulum Ca(2+)-ATPase.* Biochem Biophys Res Commun, 2008. **369**(1): p. 188-94.
169. Seth, M., et al., *Dynamic regulation of sarcoplasmic reticulum Ca(2+) stores by stromal interaction molecule 1 and sarcolipin during muscle differentiation.* Dev Dyn, 2012. **241**(4): p. 639-47.
170. Ottenheijm, C.A., et al., *Sarcoplasmic reticulum calcium uptake and speed of relaxation are depressed in nebulin-free skeletal muscle.* FASEB J, 2008. **22**(8): p. 2912-9.
171. Nakagawa, O., et al., *Centronuclear myopathy in mice lacking a novel muscle-specific protein kinase transcriptionally regulated by MEF2.* Genes Dev, 2005. **19**(17): p. 2066-77.
172. Liu, N., et al., *Mice lacking microRNA 133a develop dynamin 2-dependent centronuclear myopathy.* J Clin Invest, 2011. **121**(8): p. 3258-68.
173. Fajardo, V.A., et al., *Diaphragm assessment in mice overexpressing phospholamban in slow-twitch type I muscle fibers.* Brain Behav, 2016. **6**(6): p. e00470.
174. Tomiya, S., et al., *Cast immobilization of hindlimb upregulates sarcolipin expression in atrophied skeletal muscles and increases thermogenesis in C57BL/6J mice.* Am J Physiol Regul Integr Comp Physiol, 2019. **317**(5): p. R649-R661.
175. Calvo, A.C., et al., *Genetic biomarkers for ALS disease in transgenic SOD1(G93A) mice.* PLoS One, 2012. **7**(3): p. e32632.
176. Gayan-Ramirez, G., et al., *Corticosteroids decrease mRNA levels of SERCA pumps, whereas they increase sarcolipin mRNA in the rat diaphragm.* J Physiol, 2000. **524 Pt 2**: p. 387-97.
177. Osborne, R.J., et al., *Transcriptional and post-transcriptional impact of toxic RNA in myotonic dystrophy.* Hum Mol Genet, 2009. **18**(8): p. 1471-81.
178. Ravel-Chapuis, A., et al., *Misregulation of calcium-handling proteins promotes hyperactivation of calcineurin-NFAT signaling in skeletal muscle of DM1 mice.* Hum Mol Genet, 2017. **26**(12): p. 2192-2206.
179. Wang, W.P., et al., *Progerin in muscle leads to thermogenic and metabolic defects via impaired calcium homeostasis.* Aging Cell, 2020. **19**(2): p. e13090.
180. Campanaro, S., et al., *Gene expression profiling in dysferlinopathies using a dedicated muscle microarray.* Hum Mol Genet, 2002. **11**(26): p. 3283-98.
181. Tanihata, J., et al., *Truncated dystrophin ameliorates the dystrophic phenotype of mdx mice by reducing sarcolipin-mediated SERCA inhibition.* Biochem Biophys Res Commun, 2018. **505**(1): p. 51-59.
182. Liu, H., et al., *Skeletal muscle-specific Sidt2 knockout in mice induced muscular dystrophy-like phenotype.* Metabolism, 2018. **85**: p. 259-270.

Appendix A

Table A.1: Upregulation of SLN expression across different models of skeletal muscle disease, disuse, and injury.

Mouse Model	Muscle	mRNA/Protein	Fold Induction	Type	Ref.
Nemaline myopathy	quadriceps	protein	+20-fold	ectopic	[170]
	soleus	protein	+1.7-fold	endogenous	[170]
nebulin knockout	EDL	protein	+10-fold	endogenous	[170]
Centronuclear myopathy					
Srpk3 knockout	tibialis anterior	mRNA	+3.5-fold	ectopic	[171]
miR133a knockout	tibialis anterior	mRNA	+35-fold	ectopic	[172]
		protein	+3.5-fold	ectopic	[172]
Pln^{OE}	soleus	protein	+9-fold	endogenous	[55]
	diaphragm	protein	+2.5-fold	endogenous	[173]
Disuse					
Cast immobilization	soleus	mRNA	not quantified	endogenous	[174]
	plantaris	mRNA	not quantified	ectopic	[174]
	gastrocnemius	mRNA	not quantified	ectopic	[174]
	soleus	protein	not quantified	endogenous	[174]
	plantaris	protein	not quantified	ectopic	[174]
	gastrocnemius	protein	not quantified	ectopic	[174]
Mechanical Unload	soleus	protein	+14-fold	endogenous	[6]
Amyotrophic lateral sclerosis disease $SOD1^{G93A}$	gluteus superficialis	mRNA	+2-fold	ectopic	[175]
Corticosteroid myopathy	diaphgram	mRNA	+2-fold	endogenous	[176]
Myotonic dystrophy					
HSA^{LR}20b	quadriceps	mRNA	+98.3-fold	ectopic	[177]
HSA^{LR}41	quadriceps	mRNA	+72.8-fold	ectopic	[177]
$Mbln^{-/-}$	quadriceps	mRNA	+42.6-fold	ectopic	[177]
DM1	EDL	mRNA	+2-fold	endogenous	[178]
	EDL	protein	+4-fold	endogenous	[178]
Emery-Dreifuss dystrophy					
$Lmna^{-/-}$	soleus	mRNA	not quantified	endogenous	[179]
Facioscapulohumeral muscular dystrophy					
FRG1	tibialis anterior	protein	not quantified	ectopic	[111]
	trapezius	protein	not quantified	ectopic	[111]
Myotubular Myopathy					
MTM1-KI					
	soleus	protein	not quantified	endogenous	[111]
	quadriceps	protein	not quantified	ectopic	[111]
	gastrocnemius	protein	not quantified	ectopic	[111]
Muscular dystrophy					
human limb girdle	vastus lateralis	mRNA	d.n.s.	endogenous	[180]
human limb girdle	deltoid	mRNA	d.n.s.	ectopic	[180]
mdx	soleus	protein	+10-fold	endogenous	[52]
	soleus	protein	not quantified	endogenous	[8]
mdx	diaphragm	protein	+3-fold	endogenous	[52]
	diaphragm	protein	not quantified	endogenous	[8]
mdx	quadriceps	protein	not quantified	ectopic	[52]
mdx	tibialis anterior	mRNA	25-fold	ectopic	[181]
	tibialis anterior	protein	6-fold	ectopic	[181]
$mdx/utr^{-/-}$	soleus	protein	+20-fold	endogenous	[52]
$mdx/utr^{-/-}$	diaphragm	protein	+8-fold	endogenous	[52]
	diaphragm	protein	not quantified	endogenous	[111]
	diaphragm	protein	not quantified	endogenous	[53]
$mdx/utr^{-/-}$	quadriceps	protein	+2-fold	ectopic	[52]
	quadriceps	protein	not quantified	ectopic	[53]
$mdx/utr^{-/-}$	pectoral	protein	not quantified	ectopic	[53]
$mdx/utr^{-/-}$	EDL	protein	not quantified	endogenous	[111]
$Sidt2^{f/f}$ Cre	rectus femoris	mRNA	+20.3-fold	ectopic	[182]

d.n.s. data not shown, upregulation of *Sln* mRNA was suggested but not shown. Not quantified, upregulation of SLN protein or *Sln* mRNA was shown but not expressed as fold changes.

Table A.2: Comparison of Key Parameters in Studies Evaluating the Interaction of SERCA with DWORF and its Effect

Study	System(s) Employed	Transfection Ratio	Inhibitory Regulator Displacement	SERCA Apparent Ca^{2+} Affinity	SERCA V_{max}
Nelson et al, 2018	COS7 cells	1:1 (DWORF:SERCA) 3:1:1 (DWORF:PLN:SERCA) 3:1:1 (DWORF:SLN:SERCA) 3:1:1 (DWORF:MLN:SERCA)	Displaced PLN, SLN & MLN	No Effect	No Effect
Li et al, 2021	HEK-293 cells; Lipofectamine 300 transfection; Unlabelled & FRET tagged	Not stated	Displaced PLN	Increased	Not Determined
Fisher et al, 2021	In vitro membrane co-reconstitution system; T-Rex-293 Cell Line;	~1-2 (DWORF:SERCA)	Not Determined	No Effect	Increased
Reddy et al, 2021	Reconstituted lipid-bilayer systems	2:1 (DWORF:SERCA)	Not Determined	Decreased	Increased

Table A.3: *Mln* and *Dworf* primer sequences for qPCR analysis

Gene	Organism	Primer Name	Direction	Primer Sequence (5' → 3')
Mln	Mouse	MLN	Forward	CAACGTTGCTAGGAGAACACC
			Reverse	GCTCTTGCCACTCATGTTCA
Dworf	Mouse	DWORF	Forward	TTCTTCTCCTGGTTGGATGG
			Reverse	TCTTCTAAATGGTGTCAGATTGAAGT

High DNA Extraction Protocol

Buffers:

Mouse Ear-notch/Tail DNA Isolation Buffer

0.5% SDS

0.1M NaCl

0.05M Tris base (pH 8.0) 2-4mM EDTA

Set final pH to 8.0.

8M Potassium Acetate

4g in 200mL dH20 (autoclaved water)

1. Add Proteinase K from pureLink Genomic DNA mini kit (Invitrogen, Carslbad, CA) to mouse ear-notch/tail DNA Isolation Buffer (see recipe below) at a concentration of 1.0 mg/ml and mix.
2. Add 400ul of solution to each Eppendorf tube with sample (ear notch/tail clip). Place tubes in a conical tube.
3. Immediately place tubes in a water bath set to 63°C. Let tissue digest overnight. NOTE: The digests are freezable after.
4. Add 75ul of 8M potassium acetate to each tube.
5. Add 500ul of chloroform to each tube. Vortex for 5-10 mins. Sample can be frozen overnight if needed.
6. Spin 5-8mins at 9,000 *g*.
7. Pipetter aqueous top layer in a new Eppendorf tube. There should be approximately 400ul.
8. Add 2 volumes (if you get 400ul from step 7 then you add 800ul) of 100% ethanol at room temperature. Mix by inverting.

9. Spin at 14000 rpm for 20min at 4°C.

10. Remove the supernatant and air dry for 2-3 mins.

11. Add 30 ul of Autoclaved Water.

12. Dilute to desired concentration with autoclaved water after determining concentration in a Nanodropper 2000 (for mdx genotyping protocol dilute to 20ng/ul).

Table A.4. Primer sequences for genotyping of wild-type (WT) phopholamban (PLN), sarcolipin (SLN), or corresponding targeted knock-out sequences.

Genotype	Primer Name	Sequence
Pln$^{+/+}$	27 WT Forward	5'CACGTCAGAATCTCCAGAACC-3'
	27 WT Reverse	5'-TCCCCCTTTAACTCTCATAAGC-3'
Pln$^{-/-}$	MMRRC Line 27 HLT7	5'-TGTGGGTTGCAAAGTTAGGC-3'
	L27 NEO	5'-TCCTCGTGCTTTACGGTATC-3'
Sln$^{+/+}$	SLN-WT Forward	5'-TGTCCTCATCACCGTTCTCCT-3'
	SLN-WT Reverse	5'-GCTGGAGCATCTTGGCTAATC-3'
Sln$^{-/-}$	SLN-null Forward	5'-GTGGCCAGAGCTTTCCAATA-3'
	SLN-null Reverse	5'-CAAAACCAAATTAAGGGCCA-3'

Table A.5. Western blotting details. Samples were transferred to either polyvinylidene difluoride (PVDF) or nitrocellulose (NC) membranes. Antibody incubations occurred at room temperature (RT) or overnight (ON).

Protein	Gel % (Type)	Membrane	Blocking Agent	1° (Time/Temp)	1°	2° (Time/Temp)	2°	ECL Substrate
SERCA1a	7.5% (Glycine)	PVDF	5% Skim Milk	1:10000 (O/N 4°C)	Anti-mouse	1:20000 (1hr/RT)	Anti-mouse	Luminata Forte
SERCA2a	7.5% (Glycine)	PVDF	5% Skim Milk	1:2000 (O/N 4°C)	Anti-mouse	1:5000 (1hr/RT)	Anti-mouse	Luminata Forte
MLN	13% (Tricine)	PVDF	5% BSA	1:100 (O/N 4°C)	Anti-rabbit	1:500 (1hr/RT)	Anti-rabbit	ECL
DWORF	13% (Tricine)	PVDF	5% Skim Milk	1:1000 (O/N 4°C)	Anti-rabbit	1:2000 (1hr/RT)	Anti-rabbit	Luminata Forte
SLN	13% (Tricine)	NC	5% Skim Milk	1:100 (O/N 4°C)	Anti-rabbit	1:1000 (1hr/RT)	Anti-rabbit	ECL
PLN	13% (Tricine)	PVDF	5% Skim Milk	1:1000 (O/N 4°C)	Anti-mouse	1:2000 (1hr/RT)	Anti-mouse	Luminata Forte

Appendix B

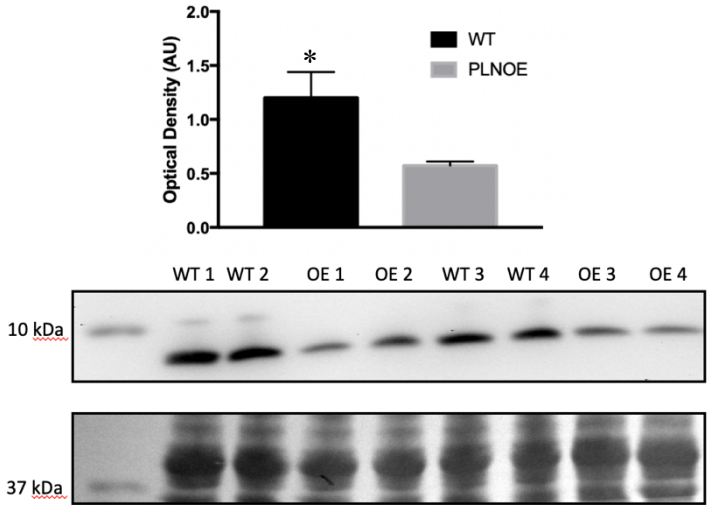


Fig. B.1: DWORF protein expression is reduced in soleus of *Pln*^{OE} male mice. Representative Western blots of 5-6 mo old male *Pln*^{OE} and WT mice (n = 4/group). Equal protein load was confirmed using Ponceau S staining. Values are mean ± S.E. * indicates a significant difference from WT ($p < 0.05$).

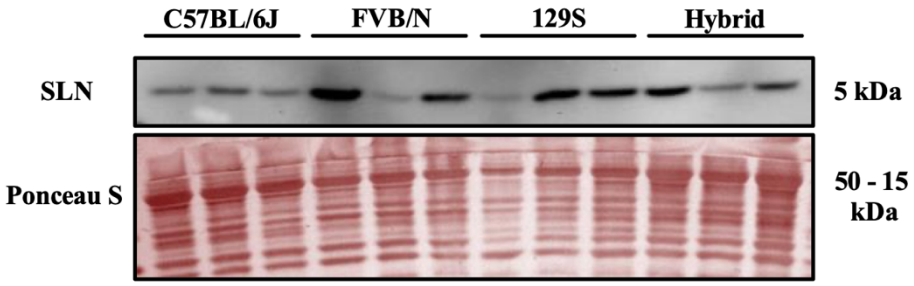


Fig. B.2: Strain differences in SLN expression in murine soleus. SOL SLN protein expression of WT mice (4-6 months old) across different strains. 20 μg of protein was resolved on a 13% tricine gel. Adapted from [156]

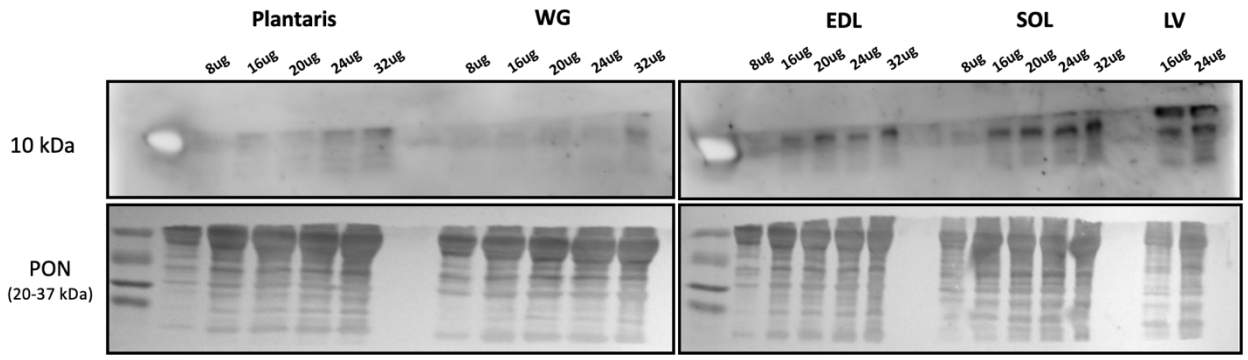


Fig. B.3: Tissue distribution of MLN protein content in *Sln*$^{+/+}$/*Pln*$^{+/+}$ male mice. MLN protein expression was evaluated in select oxidative and glycolytic muscle of WT mice (4-6 months old) to establish an optimal blotting protocol. The varying protein loads were resolved on a 13% tricine gel and transferred to a PVDF membrane, where MLN protein was detected via a polyclonal rabbit primary antibody (1:100 dilution) and a HRP-conjugated anti-rabbit secondary antibody (1:500 dilution).

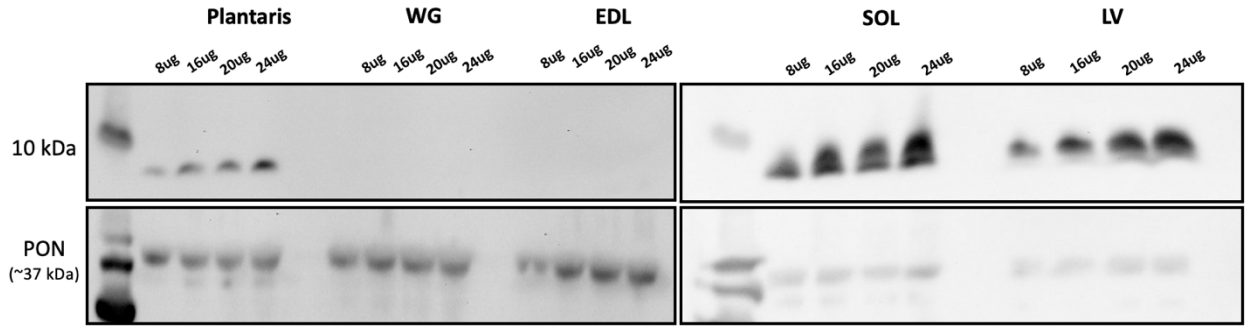


Fig. B.4: Tissue distribution of DWORF protein content in *Sln*$^{+/+}$/*Pln*$^{+/+}$ male mice. DWORF protein expression was evaluated in select oxidative and glycolytic muscle of WT mice (4-6 months old) to establish an optimal blotting protocol. The varying protein loads were resolved on a 13% tricine gel and transferred to a PVDF membrane, where DWORF protein was detected via a polyclonal rabbit primary antibody (1:1000 dilution) and a HRP-conjugated anti-rabbit secondary antibody (1:2000 dilution).